A simulation framework for enhancing natural attenuation for the remediation of subsurface organic contaminants using targeted PAT intervention.

Author:
Luther Brown
Supervisors:
Dr Domenico Baú
Professor Steve Thornton

Groundwater Protection and Restoration Group
Civil and Structural Engineering,
University of Sheffield

Dissertation submitted to the University of Sheffield in fulfilment of the requirements for the degree of

Doctor of Philosophy

April 2024

Acknowledgements

I would like to thank my supervisors, Domenico Baú, and Steve Thornton, for their guidance and support over the years. I would also like to thank James Shucksmith, Serge Brouyère, Vivek Bedekar, Harry Lee, and the creators of FloPy. A special thank you goes to my partner for their support over the years.

Contents

Nomenclature

This thesis will refer to the principles defined here throughout:

- Natural attenuation (NA) refers to the combination of physical, chemical, and biological processes which attenuate contaminant concentrations through the processes of advection, hydrodynamic or mechanical dispersion, sorption, dilution, volatilization, biodegradation, and abiotic/chemical degradation.
- Monitored natural attenuation (MNA) is an in situ remediation technology in which the process of NA is managed to ensure that the contaminant is being remediated in order to achieve site specific remediation objectives within a reasonable time frame.
- Pump and treat (PAT) refers to pump and treat is an active engineered technology which uses a submersible pump located in a borehole in order to extract contaminated groundwater, which is then routed to the next stage of the treatment train or treatment plant.
- NA and biodegradation are used interchangeably, since biodegradation is arguably the most important component of NA, as it reduces both contaminant mass and concentration.
- Biodegradation mass or mass biodegraded refers to the contaminant mass that is removed by biodegradation processes.
- *Remediation effectiveness* in this thesis is defined as how much mass is reduced by the remediation method. If a remediation method reduces more contaminant mass than another, then it has higher remediation effectiveness.
- *Remediation efficiency* is the amount of mass biodegraded per unit of effort. If a scenario degrades 100kg of contaminant mass with a pumping rate of -30 m^3/d, then it's more efficient than a scenario that degrades the same amount of mass with double the pumping rate.
- *Intrinsic biodegradation* refers to biodegradation is naturally occurring in the aquifer, as opposed to biodegradation that is occurring as a result of bioaugmentation and/or biostimulation.

Abstract

A remediation approach which uses pump and treatment (PAT) to enhance the biodegradation of organic contaminant plumes in groundwater was evaluated for a phenol-contaminated aquifer using a novel reactive transport model, which simulates kinetic reactions the groundwater. The influence of system design and operation on plume remediation to enhance contaminant mass removal by biodegradation was examined.

Increasing the distance of an extraction or injection well from the plume interior enhances biodegradation by increasing the dispersive mixing of the plume with the groundwater. An extraction well far away from the plume enhances biodegradation to a greater degree than an extraction well on the fringes. In the best performing single well scenario (injection of EAs at the fringes of the plume), biodegradation was enhanced by 128%, compared with no intervention (intrinsic NA) over the same time period.

It was discovered that wells placed too closely together do not promote mixing and often do not enhance biodegradation as much as a single well. A series of 10 increasingly complex multiwell modelling scenarios were designed to conduct a more in-depth investigation. Analysis of this phenomenon discovered a configuration of 4 injection wells which enhanced biodegradation by 520% over no intervention over 10 years.

It was hypothesized that enhancement of in situ NA could potentially reduce of the total operational cost of site remediation. Six other modelling scenarios, with the goal of remediating 90% of the contaminant over 60 years through a combination of mass removal through PAT and enhanced in situ NA. The arguably best performing scenario enhanced biodegradation by 285%, degraded 15% of total phenol mass, and reduced the cost of remediation by $66,000, but incurred $85,000 in electricity costs and $540,000 in treatment costs over 40 years. It was determined that this approach examined in this study was limited by the concentration of the contaminant, which is orders of magnitude higher than the concentration of the oxidants, in addition to the slow biodegradation kinetics. However, this framework may remediate contaminants that are more readily biodegradable under aerobic conditions, such as BTEX.

PAGE INTENTIONALLY LEFT BLANK.

Chapter 1

Introduction

1.1 Problem Statement and Motivation

Groundwater is a globally important resource. It provides an estimated 36% of global potable water and more than 42% for global irrigation, although this exact number differs among countries (Döll et al., 2011). For example, groundwater accounts for 30% of the potable water supply from the USA and England, >50% for the MENA countries, and nearly 100% for Denmark, Iceland, and Austria (European Environment Agency, 2023). However, groundwater pollution is a significant problem globally. For instance, in the USA, there are over 300,000 contaminated sites (National Research Council, 2004) and more than 60% of China's aggregate groundwater is bad quality or worse (Ministry of Environmental Protection PRC, 2015; 2016).

Groundwater pollution can arise from point or diffuse sources due to anthropogenic activities, such as industry, agriculture, transport, and sanitation. Contaminants can either be organic or inorganic. Examples of organic contaminants are aromatic hydrocarbons, oxygenated hydrocarbons, polycyclic aromatic hydrocarbons, heterocyclic aromatic hydrocarbons, fuel and petroleum hydrocarbons, chlorinated solvents, and pesticides (Federal Remediation Technologies Roundtable, 2023; Li et al., 2021; Fetter et al., 2017; US EPA, 2006). Examples of inorganic contaminants include saline intrusion, arsenic, chromium, cadmium, acid mine drainage, fluoride, nitrate, and radionuclides (Li et al., 2021). Other contaminants, to which shallow aquifers are at higher risk, include bacteria, viruses, protozoa, and parasites (Li et al., 2021).

These contaminants are all hazardous to public health and the environment (Li et al., 2021; Karunanidhi et al., 2021; Liang et al., 2020). The toxicity among contaminants varies wildly, with some contaminants taking years to produce cancerous or mutagenic effects, while some are lethal even in small doses (Li et al., 2021). Contaminants such as phenol are deadly to fish and have mutagenic effects in humans, even at low concentrations (Saha et al., 1999; Agostini et al., 2010; Gami et al., 2014). Most governments around the world take contamination via these pollutants seriously. Often government, site owners, and consultants must work together to remediate a contaminated site, which can require decades.

Remediation timeframes using current technologies are often prolonged and expensive; the US Environmental Protection Agency has estimated that the cost of soil and groundwater remediation at over 300,000 sites between 2004 and 2033 may exceed 200 billion USD (US EPA, 2004). Furthermore, the National Research Council has estimated that there are at least 126,000 sites across the US that will require 110 billion to 127 billion USD to remediate. A significant number of sites are unlikely to reach remediation targets within 50-100 years.

There are a range of remediation technologies that can be utilized to remediate contaminated sites, both ex situ or in situ, where the contaminant is treated above ground and below

ground, respectively. These treatment processes can be either physical, biological, chemical, or some combination of the three (Lemming et al., 2010). Examples of in situ technologies include: monitored natural attenuation (MNA), permeable reactive barriers (PRBs), in situ chemical oxidation (ISCO).

Natural attenuation (NA) is the combination of natural processes which attenuate contaminant concentrations through the processes of advection, hydrodynamic or mechanical dispersion, sorption, dilution, volatilization, biodegradation, and abiotic/chemical degradation (Wiedemeier 1996; 1999; NRC, 2000; Scow and Hicks, 2005; Rivett and Thornton, 2008). Monitored natural attenuation (MNA) is a remediation technology in which the processes of NA are managed to ensure that the contaminant is being remediated in order to achieve site specific remediation objectives within a reasonable time frame. MNA is often used as a final remediation technology to treat the residual contaminant mass after the primary technology has removed most contaminant mass (US EPA, 1997; Santo and Prosperi, 2022).

PRB technology on the other hand, is usually when a trench is installed in the flow path of the contaminant plume and is then filled with powdered zerovalent iron, forcing the plume to pass through and react; it is usually designed such that the contaminant solute passes through slowly and is transformed or destroyed.

Finally, ISCO remediation is where strong oxidizers such as persulfate, permanganate, and hydrogen peroxide are injected into the plume interior which react with the contaminants, causing degradation reactions which remediate the plume (O'Connor et al., 2018).

Ex situ technologies include source removal via excavation, where contaminate source is removed from the site through physical means for treatment, and pump and treat (PAT).

PAT is one of the most commonly used ex situ remediation technologies used within large and complex sites, where other remediation technologies are often ineffective. In PAT systems, the plume is removed via an extraction well using a submersible pump before it can migrate further downgradient and is transported to the next stage of the treatment train or a treatment plant.

At many contaminated sites, in addition to having exorbitant operational and capital costs, conventional PAT systems alone are often unable to remediate the plume. This is due to PAT limitations inherently linked to site complexities such as heterogeneity, anisotropy, low permeability, sorption-desorption processes, and matrix diffusion. MNA may remove these limitations when subsurface contaminants are biodegradable, with limiting factors such as low dispersive mixing of the plume with dissolved electron acceptors (EAs) in the groundwater, lack of EA presence, and lack of microbial communities that can utilize the present terminal electron acceptor processes. Therefore, the limitations of MNA may be removed with engineered solutions such as injection of microbes and amendments that contain EAs, and the enhancement of mechanical dispersion. MNA also benefits from a substantially lower cost than PAT, but suffers from longer remediation timeframes (Santo and Prosperi, 2022).

Recent studies have shown that targeted PAT at the fringes of a plume can enhance the mechanical dispersion of the plume which increases mixing of the plume interface with the EA rich uncontaminated background groundwater (Thornton et al., 2014). This method

effectively enlarges the reactive plume fringe in addition to reducing contaminant mass and concentration, which has been attributed to an approximate doubling in the rate of in situ biodegradation. Thus, if MNA and PAT are combined in this way, it might be possible to improve solute mass removal, and lower the remediation time scale as well as operational costs. A modelling study of what influence PAT has on intrinsic has never been conducted to investigate how the PAT system behaves in further detail, how it can be improved, and what its potential limitations are.

1.2 Aims and Objectives

Based on the gaps identified above, the aim of this thesis is to develop a conceptual remedial framework which integrates PAT with NA to improve remediation performance by considering operational variables and analysis of mass transport processes which limit biodegradation.

The specific objectives are to:

1. **Develop an advective-dispersive-reactive solute transport model which will act as a simulation framework to evaluate scenarios' biodegradation performance for the integrated PAT and NA system.** The framework will consist of a 3D groundwater flow and reactive solute transport model based on MODFLOW-2005 for the groundwater flow component, and MT3D-USGS for the multispecies reactive transport component (Harbaugh et al., 2005; Bedekar et al., 2016).

2. **Develop a series of modelling scenarios to assess the remediation effectiveness of NA-enhanced PAT compared with conventional PAT.** An analysis investigating the mechanisms which effect intrinsic biodegradation will be carried out with each simulation to determine how well location, well configuration, and positive or negative pumping rate influences both mass removal through extraction and biodegradation (Chapter 4). Examine multiwell scenarios, the injection of amendments, and determine their impact on mass removal and in situ biodegradation (Chapter 5). All simulations will be cross analysed to determine which well processes are having the greatest effect on mass biodegraded in situ vs. mass removal through extraction.

3. **Establish whether NA can be enhanced in situ in order to reduce the operational cost of PAT for the remediation of organic contaminants.** Design and simulate an assortment of modelling scenarios with the aim of enhancing in situ biodegradation using combinations of multiple extraction and injection wells. For each scenario, analyse the amount of mass removed via biodegradation, the time taken to reach 90% of contaminant solute mass removal, and the cost of remediation. All simulations in all scenarios will then be cross-compared and ranked by cost, remediation efficiency and effectiveness compared to a conventional PAT system (Chapter 6).

1.3 Thesis Structure

This thesis is organized as follows:

Chapter 1 – introduction, aims and objectives. This chapter broadly explains the background to this research and provides the context supporting the programme of work developed. It includes research objectives linked to research questions that are addressed in the program of work undertaken.

Chapter 2 – literature review and research questions. This is presented to summarize the current state of knowledge in the various discipline areas covered by the research (Chapter 4-6). This chapter also critically evaluates relevant studies to inform the design of the scenarios that are developed in Chapters 4-6.

Chapter 3 – development of the methodology for each experimental chapter in the entire thesis. This chapter also briefly illustrates the mechanisms by which in situ biodegradation is enhanced using PAT by considering a 2D test case.

Chapter 4 – **"Enhancing in situ biodegradation in groundwater using pump and treat remediation: a proof of concept and modelling analysis of controlling variables".** This chapter investigates the effect of PAT design and operational variables on the enhancement of in situ biodegradation. A modified version of this chapter has been prepared as a paper and has been published in the journal of Environmental Science and Pollution Research (doi: 10.1007/s11356-024-32662-x).

Chapter 5 – **"Enhancing in situ biodegradation in groundwater using pump and treat remediation: a modelling analysis of the impact of multiwell configurations on NA".** This chapter investigates the effect of multiple well configurations on mass removal through biodegradation and extraction. It also goes explores the decision space of the numerical model in more depth, to determine the optimal placements of wells; to determine the effect of plume fringe biodegradation processes vs. plume interior biodegradation processes; it explores the effect of heterogeneity on in situ biodegradation; and compares controlled release materials to injection of amendments. A modified version of this chapter is intended to be submitted to the Journal of Contaminant Hydrology or another journal with a similar scope.

Chapter 6 – **"Enhancing in situ biodegradation in groundwater using multiwell pump and treat remediation: cost analysis for longer term remediation scenarios**". Using the knowledge gained from Chapters 3, 4, and 5, the work in this chapter attempts to utilize the enhancement of in situ biodegradation by targeted PAT and injection intervention to remediate 90% of the contaminant plume. In order to effectively compare the scenarios, the simulations are protracted for 60 years. The scenarios are compared and ranked according to the operational cost of remediating the entire plume, and the cost reduction generated by in situ biodegradation. A modified version of this chapter is intended to be submitted to the Journal of Contaminant Hydrology or another journal with a similar scope.

Chapter 7 – conclusions and recommendations for further research. This chapter provides a recommendation for research to further improve the program of work and addresses knowledge gaps that have been identified.

PAGE INTENTIONALLY LEFT BLANK.

Chapter 2

2.1 Literature review

2.1.2 Problem statement

Groundwater pollution via organic contaminants is a significant problem globally. Groundwater pollution is a threat to ecosystems and public health (Li et al., 2021). Remediation timeframes using current technologies are often prolonged and expensive; the US Environmental Protection Agency has estimated that the cost of soil and groundwater remediation at over 300,000 sites between 2004 and 2033 may exceed 200 billion USD (US EPA, 2004b). Furthermore, the National Research Council (NRC) has estimated that there are at least 126,000 sites across the US that will require 110 billion to 127 billion USD to remediate. Although pump and treat (PAT) often incurs the highest cost of all the remediation approaches (Santo and Prosperi, 2022), in many cases, PAT systems are often implemented at such sites to manage the plume and remediate groundwater contamination over extended timescales (National Research Council, 2013). On average, total remediation costs are expensive, ranging from $500,000 to $1,000,000 per site with a significant number of sites unlikely to reach remediation targets within 50-100 years, warranting cheaper and more efficient strategies and technologies that can be applied to a large variety of site conditions (Bau and Mayer, 2006; Kent and Mosquera, 2014).

2.1.3 Pump and treat

According to the Federal Remediation Technologies Roundtable (FRTR), pump and treat (PAT) is an active engineered technology which uses a submersible pump located in a borehole in order to extract contaminated groundwater, which is then routed to the next stage of the treatment train or treatment plant. PAT is most often used for minimizing the flux of contaminants from the source area (source control), hydraulic containment of contaminant plumes or removal of contaminant mass in groundwater for treatment (Truex et al., 2017; Mackay and Cherry, 1989). It can be used to treat a wide range of contaminants such as coal tar distillates, phenols, polycyclic aromatic hydrocarbons, heterocyclic aromatic compounds, fuel hydrocarbons, chlorinated solvents (US EPA, 2006), and is most effective for the removal of high aqueous solubility contaminants under homogeneous, isotropic, and permeable hydrogeologic conditions, i.e., sand, gravel, and alluvial aquifers (National Research Council, 2013). Multiphase extraction is a special type of PAT that can remove LNAPLs floating the surface of the groundwater and may also be set up to simultaneously remove vapor plumes (volatilization partitions from the contaminant source which migrate to the unsaturated zone); usually specialist equipment is required, such as a submersible pump for the groundwater, vacuum pump and air filter/outlet for the volatile component, and an oil/water separator for the LNAPL-groundwater component (FRTR, 2023).

In more complex aquifers, processes such as heterogeneity, anisotropy, low permeability, non-aqueous phase liquids (NAPLs), sorption-desorption processes, and matrix diffusion, may limit the effectiveness of PAT remediation (McDade et al., 2013). Likely due to these limitations, and the high cost of installation and operation, PAT usage for mass removal at National Priorities List (Superfund) sites has declined from 56% to 22% over the past few decades (US EPA, 2007; 2013). In recent years, PAT is more commonly used for plume containment and management instead of being used to remove contaminant mass and concentration (FRTR, 2023; Truex et al., 2017). However, for more complicated sites such as deep (>30m) consolidated aquifers, and more recalcitrant contaminants such as chlorinated solvents, PAT is still one of the most commonly used and effective treatment methods (US EPA, 2005; NRC, 2013; ITRC, 2023; FRTR, 2023). This is often due to the depth of the contaminant being cost prohibitive with regards to implementing other in situ technologies, such as permeable reactive barriers (PRBs). There is one such site in Four Ashes, UK, where a PAT system was installed for plume removal and management, due to the depth of the contaminant (>60m) and diving nature of the plume (Thornton et al., 2014).

Other studies have demonstrated that PAT's effectiveness can be enhanced with a pulsed pumping technique, an in situ bioremediation approach, or surfactant enhanced remediation; however, these applications can often be site specific and are subject to limitations. While bioremediation is effective for treatment of BTEX plumes, it can result in microbial overgrowth that blocks aquifer pores and prevents groundwater flow (Hazen, 2018); and surfactants are more suitable for remediating NAPL contaminants but require highly permeable conditions, and pulsed pumping is most effective for managing rebound and tailing from sorbing contaminants, but can lead to prolonged remediation timescales (NRC, 2013; FRTR, 2023).

2.1.4 Natural attenuation

Natural attenuation (NA) is the combination of physical, chemical, and biological processes which attenuate contaminant concentrations through the processes of advection, hydrodynamic or mechanical dispersion, sorption, dilution via recharge, volatilization, biodegradation, and abiotic/chemical degradation (Wiedemeier 1996; 1999; NRC, 2000; Scow and Hicks, 2005; Rivett and Thornton, 2008).

Advection is caused by the groundwater pore velocity, which transports the contaminant along the hydraulic gradient, conserving contaminant mass and concentration. Mechanical dispersion is the mixing of a contaminant along its flowpath due to variations in velocity caused by pore size, the distance water must travel in between pores (tortuosity), and the pore friction (Fetter et al., 2017). This results in dilution of the contaminant, but conserves mass. The pore velocity is determined by the specific discharge - which is the product of the hydraulic conductivity and the hydraulic gradient - divided by the effective porosity. Mechanical dispersion occurs in the direction of the flow path, known as longitudinal dispersion, and normal to the flowpath, known as transverse dispersion, which occurs horizontally and vertically. Hydrodynamic dispersion is the combination of mechanical

dispersion and molecular diffusion. Hydrodynamic dispersion is therefore complex and affected by different variables, e.g., the greater the heterogeneity in hydraulic conductivity, the greater the dispersion will be.

Other aspects of NA, such as sorption, conserves mass by trapping (sorbing) the contaminant in the pores of the aquifer matrix but reduces concentration. The sorptability of contaminants varies, and this aspect of NA is often a hindrance to remediation, as sorbed contaminants can later desorb after the remediation has ceased, leading to a resurgence in contaminant solute concentration. Volatilization is a process which is more important for highly volatile compounds, especially in unsaturated zones. Volatilization can reduce mass and concentration, but not typically at significant levels except for unique cases, such as with the natural attenuation of MTBE (Lahvis et al., 2005).

Biodegradation is the primary component of NA which reduces both contaminant mass and concentration (Nielsen et al., 1995; Bauer et al., 2006). Biodegradation occurs as a plume migrates through the porous media and encounters the microbes present there, resulting in microbially mediated redox reactions where the contaminant serving as an electron donor (ED), is oxidized by an electron acceptor (EA), such as oxygen or nitrate, which is then reduced. This results in the production of organic or inorganic metabolites and water. Usually, these byproducts are less toxic than the original product, and they too undergo biodegradation. Eventually, the end product of biodegradation is carbon dioxide and water (Wiedemeier, 1996; Wiedemeier, 1999). However, some contaminants such as chlorinated solvents act as EAs and require a different metabolic pathway in order to be degraded (e.g., reductive dechlorination). Despite this, the state of the art is focused on aerobic respiration, as the contaminant of concern is oxidizable (Wiedemeier, 1999).

As the plume progresses, the higher Gibbs free energy terminal electron accepting processes (TEAPS) are favored by the microbial consortia first, such as aerobic respiration and denitrification. As the oxygen and nitrate become depleted, the following lower Gibbs free energy TEAPS are then utilized: iron reduction, manganese reduction, sulfate reduction, and finally methanogenesis (Christensen et al., 2000; Lovley et al., 2001; Baker et al., 2012). Methanogenesis is usually confined to the plume source whereas aerobic respiration and denitrification occur only in the reactive fringe. Aerobic respiration and denitrification degrade most organic contaminants faster than lower Gibbs free energy TEAPS, (e.g., sulfate reduction and methanogenesis), given that EAs are available. In such a case, oxygen or oxygen release compounds would be injected into the aquifer to stimulate biodegradation. However, with recalcitrant organic contaminants, methanogenesis is more important, and hydrogen gas would instead be injected, to facilitate the fermentation processes needed for methanogenesis, such as with reductive dechlorination (Wiedemeier, 1999). [LB1]

2.1.5 Monitored natural attenuation

The planned and managed utilization of natural attenuation processes to remediate contaminated aquifers is known as monitored natural attenuation (MNA). It requires comprehensive monitoring and analysis to determine if natural attenuation is occurring in the

aquifer, requiring lines of evidence such as reduced concentration along the flow path, presence of biogeochemical indicators/markers, microbiological analysis, microcosm analysis, and so on (Rivett and Thornton, 2008; Illman and Alvarez, 2009). MNA is a risk-based remediation method, wherein the combined effect of naturally occurring physical, chemical and biological processes, such as sorption, dispersion, and biodegradation, are used to treat contaminants in situ (Wiedemeier et al., 1999).

As MNA involves monitoring the processes of NA, the most important component of MNA is biodegradation. However, the effectiveness of biodegradation is commonly subject to limitations, such as low dissolved aqueous EA availability, lack of an appropriate microbial community capable of degrading the contaminant, recalcitrance of the contaminant, slow kinetics, and toxicity effects to microbial metabolism driven by the contaminant concentration (Wiedemeier et al., 1999; Thornton et al., 2001a,b).

Biodegradation of contaminant plumes is controlled by mechanical dispersion, which in turn controls the rate of mixing between the ED and the EA. For plumes that have yet to reach steady state, the front of the plume has the highest rates of biodegradation. However, for plumes at steady state, the transverse fringes of the plume have the highest rates of biodegradation. For plumes at steady state, transverse dispersion is often the most important process for controlling biodegradation (Cirpka et al., 2005; Rolle et al., 2009). Hence, even where EAs are abundant, biodegradation may still be limited by slow mixing due to low pore velocities and dispersivity (Lerner et al., 2000; Thornton et al., 2001a; Tuxen et al., 2006).

The plume fringe, at the interface between the background groundwater and plume interior has been found to be an area of higher biodegradation activity with reported values of 90% of total biodegradation (Lerner et al., 2000; Thornton et al., 2001 a,b). The higher rate of biodegradation in the reactive fringe is driven by the dispersive mixing of EAs in uncontaminated groundwater with biodegradable organic compounds in the plume (Thornton et al., 2001a,b; 2014; Tuxen et al, 2006). Biodegradation becomes limited to the plume fringe because, over time, the interior of contaminant plumes often become depleted of available aqueous EAs by microbially mediated redox reactions, and mixing between the plume and background EAs is limited by the low values of transverse dispersivity (Rolle et al., 2009). This depletion of EAs in the plume interior results in sequential redox zones in the plume, with a methanogenic core, followed by a sulfate reducing zone, an iron/manganese reducing zone, and a narrow fringe at the leading tip and sides of the plume where the flux and availability of oxygen and nitrate is favorable, and therefore aerobic degradation and denitrification can occur (Christensen et al., 2000).

However, MNA has complications and limitations. MNA is limited by pore velocity, mechanical dispersion, and kinetic biodegradation rates as influenced by the contaminant type, the EA availability, and the capability of the microbial community of using the EAs to degrade the contaminant. MNA on its own, without enhancement, is capable of biodegrading many types of organic contaminants in both aerobic and anaerobic conditions, but typically takes a substantial period of time, from >8 years to >800 years, depending on the type of

contaminant, the mass of the plume, and the attenuation rate (Santo and Prosperi, 2022; Thornton et al., 2001a; DoD, 2008; FRTR, 2023). For this reason, MNA is typically only used to remediate certain parts of a plume, certain contaminants within a mixed plume, or at the end of a treatment protocol once the primary technologies, such as source removal and PAT, have reduced the contaminant concentration to a level at which MNA is able to achieve remediation to required standards (NRC, 2013; Adamson and Newell, 2014; Truex et al., 2017).

However, some of the limitations of MNA could potentially be reduced with intervention. When EA availability is high, transport processes are more important to biodegradation (Thornton et al., 2001 a,b; Harrison et al., 2001). If mixing can be increased, then it will accelerate biodegradation rates by enhancing the respiration reactions that are already occurring at the plume fringe (Castro-Alcaca, 2012; Thornton et al., 2014). However, if EA availability is low, increasing EA availability with amendments would be more important (Kao et al., 2016). If both EA availability and dispersion are low, then both mixing, and EA concentrations would need to be enhanced (Lerner et al., 2000; Jones et al., 2002; Thornton et al., 2014).

2.1.6 In situ bioremediation and enhancement of NA

NA can be enhanced in situ by injecting amendments. Enhancing the rates of intrinsic NA by injecting chemical amendments such as EAs, EDs, or nutrients needed for microbially mediated TEAPS is a process known as biostimulation (Kao et al., 2016). Bioaugmentation is the addition of specific cultured microbes to stimulate the biodegradation of organic contaminants (Lyon et al., 2013).

In situ bioremediation is a combined technology that uses an upgradient injection well to disperse amendments, nutrients, microbes, hydrogen, enzymes, oxygen release compounds, or controlled release materials (CRMs) through the plume in order to induce biostimulation or bioaugmentation which leads to in situ biodegradation of the contaminant (NRC, 2013; Alvarez et al., 2005). Typically, a downgradient extraction well is used to promote the flow of the amendment through the plume, rather than remove mass. This increased flow promotes biodegradation to occur or enhances intrinsic biodegradation rates. Sometimes the injection and extraction system are recirculated to improve mixing (Bagtzoglou and Oates, 2007).

Due to the physical and economic limitations of PAT remediation, in situ bioremediation has become a more common approach in recent decades (Fetter et al., 2017). The technology is particularly effective at remediating BTEX, MTBE, and chlorinated solvent plumes (Wiedemeier et al., 1999; Adamson and Newell, 2014; FRTR, 2023). However, mixing between the treatment chemical and the contaminant plume is typically limited (Piscopo et al., 2013). Improving the mixing between the treatment chemical and the contaminant would be highly advantageous in reducing remediation timeframes and overall effectiveness of the bioremediation approach; however, enhancing mixing to achieve these remediation objectives is a relatively new and underexplored area of research. Another limitation of in situ

bioremediation is that excess microbial biomass can cause plugging of the aquifer around the injection site (Hazen, 2018). This limitation can possibly be overcome by using CRMs.

CRMs are a type of amendment sometimes used to support in situ bioremediation via the introduction of carbon sources (electron donors), oxygen (electron acceptors), oxidants (to facilitate in redox reactions), which can enhance in situ biodegradation. There are various types of CRMs which differ in their composition and design and thus are used for different situations. These include: "candle" type CRMs which are directly placed in a borehole and release reaction materials slowly; pellet and droplet type CRMs which come in different sizes but are generally smaller than candle type CRMs and can be dispersed in coarser aquifer materials; and gel type CRMs which are injected in liquid form and dissolve quickly, allowing their contents to be released in the groundwater (O'Connor et al., 2018). CRMs release reaction materials for prolonged periods and can be utilized without the need for injection wells and above ground storage tanks (O'Connor et al., 2018).

Combining PAT with chemical amendment injection has been shown in previous research to increase mass biodegradation in situ and thereby reducing the amount of mass that is treated ex situ (Marquis and Dineen, 1994; Park et al., 2007). However, only concentration data, rather than a full mass balance, was reported in these studies, so the contribution of NA to mass removal relative to contaminant dilution and dispersion caused by the injection is unclear. Also, intrinsic NA was not accounted for in these modelling studies - instead a first order decay rate was used which is independent of the ED and EA concentration. However, previous research has shown that PAT could also enhance in situ intrinsic NA (Jones et al., 2002; Thornton et al., 2014) by enhancing dispersive mixing (Piscopo et al., 2013; LJ Sather 2022; 2023) and mass flux of EAs into the plume.

In cases where a biodegradable plume suffers from low dispersion, amendment with CRMs may enhance mass loss from biodegradation. Since targeted PAT has been shown to enhance intrinsic NA only at the plume fringes, CRM injection with targeted PAT could potentially be combined such that biodegradation rates are enhanced in the plume interior and at the fringes simultaneously (Marquis and Dineen, 1994; Park et al., 2007; Thornton et al., 2014). To the author's knowledge, combining targeted PAT with CRM remediation to also enhance the effects of intrinsic NA has never been attempted.

2.1.7 Enhancing advective spreading and contaminant mixing

Spreading of a solute plume naturally occurs due to existing spatial and temporal variations in velocity caused by heterogeneity, recharge, and river filtration pumping (Rolle et al., 2009; Chiogna et al., 2010; RD Bauer et al., 2009; Kim et al., 1997; Zhu et al., 2018). Spreading stretches the solute plume, increasing the contaminant plume volume available for mixing and reaction. Additionally, plume stretching increases concentration gradients, which enhances transverse mixing and therefore contaminant degradation (Ou and Ranz, 1983a; Cirpka et al., 2005; Rolle et al., 2009). These processes naturally facilitate in the mixing of EAs and EDs within groundwater (Castro-Alcaca et al., 2012)

These processes of plume spreading, and mechanical mixing can also be artificially enhanced by induced transient unsteady flows from alternating injection and extraction wells or several oscillating or pulsing wells (Devlin and Barker, 1996; Bagtzoglou and Oates, 2007; Piscopo et al., 2011; Mays and Neupauer, 2012; Piscopo et al., 2013; Neupauer et al., 2014; Suk et al., 2021; LJ Sather et al., 2022, 2023). The method of utilizing oscillating wells can be used to induce chaotic advection; a random and chaotic flow field which increases the mixing of a contaminant plume with an amendment chemical, thus increasing reaction speed (Bagtzoglou and Oates, 2007; Zhang et al., 2009). In a study by Bagtzoglou and Oates (2007), three randomly oscillating wells connected by pipes and a central manhole were used to stimulate mixing between a contaminant solute and an amendment chemical, achieving complete mixing by 60 days. In this study, only the comparative separation between the two chemicals and dilution index were recorded, and no reactions between the contaminant and amendment were simulated. However, the flow field was mostly representative of alluvial aquifers, and the plume dimensions were not representative of typical contaminant sites. It was briefly proposed in this study that this method could also be appropriate for accelerating NA rates as a potentially cheaper remediation strategy as increasing the amount of contaminant that is degraded in situ, often has a lower cost than ex situ treatment but this was not addressed in the methodology (Bagtzoglou and Oates, 2007).

Previous studies have investigated active plume spreading have focused on using injection and extraction wells to increase the mixing between a contaminant solute and a treatment chemical (Piscopo et al., 2013). Piscopo et al., (2013) simulated the use of 4 injection and extraction wells which were located north, south, east, and west of the plume. By switching from injection to extraction at different times, the plume could be hydraulically stretched and folded in order to mix the contaminant and a treatment chemical. The enhancement in reactions was significant, with >60% of cumulative contaminant mass being degraded (Piscopo et al., 2013). The plume was simulated in a stationary flow field, i.e., no hydraulic gradient so that the plume could be contained by the wells. The mean hydraulic conductivity was 0.5 m/d in purely advective conditions, which indicates that this engineered injection and extraction method is not reliant on dispersion, and that plume spreading can occur due to variations in the velocity field as induced by the extraction and injection wells (LJ Sather et al., 2022; 2023).

However, the experimental setup was quite synthetic. The circular geometry, stationary flow field, and small dimensions of the plume made this method possible to execute; it would be considerably more challenging to utilize this method for the remediation of large and complex plumes. Additionally, as this study used a 2D model to run simulations, it is unknown how well this method would work in a 3D framework. Also, while it was shown engineered injection and extraction improved reaction rates by >60%, there was no mention of a detailed mass balance, i.e., how much mass of the contaminant vs. treatment chemical that was degraded, and how much mass was removed by the extraction well. However, the focus of the study was on enhancing reactions rather than chemical kinetics.

Although it has been proposed by previous research that this enhanced mixing and dispersion process could be used to enhance intrinsic NA of contaminant solutes (Bagtzoglou and Oates,

2007; Mays and Neupauer, 2012), to the author's knowledge, this phenomenon has never been investigated in detail.

2.1.8 Cost overview of groundwater remediation

PAT design and installation costs vary heavily, typically varying between $200,000 to $2,000,000, depending on site characteristics and contaminant properties (US EPA, 2001; Khan et al., 2004). Remediation with PAT systems at some sites have cost as much as $30,000,000 (NAVFAC, 2003; Khan et al., 2004; FRTR, 2023). PAT system capital costs range from $1 to $100 per 3.78 m^3 of treated groundwater, with a median value of $78 per 3.78 m^3 (US EPA, 2001; Khan et al., 2004). PAT system operational costs vary from $1 to $100 per 3.78 m^3, with a median of $16 per 3.78 m^3 (US EPA, 2001; Khan et al., 2004). Generally, the larger the system treatment volume, the lower the annual operating and capital costs per volume.

With regards to PAT, phenol for example, can be remediated by a variety of processes such as pyrolysis, distillation, separation, and adsorption. Phenol is only slightly volatile, so a stripping tower system would likely have low efficacy (Hamdaoui and Naffrechoux, 2007; FRTR, 2023). Phenol has fair sorptability on activated carbon therefore granular activated carbon system could hypothetically remediate phenol up to concentrations of 4000 mg/l (Gundogdu et al., 2012; Hamdaoui and Naffrechoux, 2007). Previously an optimization and cost framework was developed for a joint PAT and GAC treatment system (Culver et al., 1999). GAC has generally low capital, operating costs, and low labor requirements compared to other ex situ treatment methods (US EPA, 2005). The operating cost of sites that use granular activated carbon (GAC) only range between $2 to $12 per 3.78 m^3 (Khan et al., 2004). Phenol adsorption onto GAC is 0.2 kg/kg (Gundogdu et al., 2012; Hamdaoui and Naffrechoux, 2007); for example, it would take 5 kg of GAC to remove 1 kg of phenol. This contrasts with the typical cost function mentioned in optimization papers, where a stripping tower is used to treat VOCs (Bau and Mayer, 2006).

Comparatively, in situ remediation strategies tend to have a much lower cost. For example, on average, the in situ chemical oxidation remediation costs a total of $220,000. This is mirrored by similar in situ strategies such as bioremediation of MTBE contaminated sites with costs ranging from $100,000 to $700,000, with a median of $125,000 for (US EPA, 2001c; US EPA, 2005). Overall, MNA typically has one of the lowest cost technologies available with a median capital cost of $100,000 and a median operating cost of $25,000 per year (McGuire et al., 2004; DoD, 2008; Santo and Prosperi, 2022).

While in situ remediation strategies such as MNA were found to be significantly cheaper than ex situ remediation strategies such as PAT, remediation timeframes are significantly longer. Clean up time with MNA varies between 10 to 70 years (McGuire et al., 2004; DoD, 2008). There is a compromise between short remediation timeframes and incurring higher upfront costs; or remediating the site more slowly and having the costs spread over a longer period with variable savings from NA (Fetter et al, 2017). Alternatively, some studies have found that the use of an in situ bioremediation strategy using amendments may have a better balance

between a lower cost (relative to PAT) but with comparatively shorter remediation timeframes than MNA alone (Santo and Prosperi, 2022).

However, because MNA has such a low operational cost comparative to other methods of remediation, the concept of taking biodegradation into account when designing remediation systems to reduce the overall cost has been gaining momentum in research (Butler et al., 1995; NRC, 2000; NRC, 2013). For example, a study by the US Department of Defense (2008) found that a source area remediation strategy combined with MNA to remediate a TCE and naphthalene plume could lead to estimated savings of $100,000 per year. Furthermore, incorporating a combined MNA and source removal remediation strategy at >200 similar sites could result in >$20,000,000 in savings (DoD, 2008). However, the timeframe of this strategy is fairly long, requiring 50 years for the TCE plume and 70 years for the naphthalene plume to be remediated using these strategies. This contrasts to the relative short remediation timeframes of other higher-cost remediation strategies.

Using PAT to leverage the benefits of enhancing intrinsic NA in situ could potentially reduce remediation timeframes and further decrease cost by reducing the amount of mass requiring ex situ treatment by the PAT system (Thornton et al., 2014). Additionally, actively enhancing NA using amendments could possibly reduce treatment costs further, by degrading additional mass in situ, reducing the number of extraction wells and treatment instrumentation needed, or both (Marquis and Dineen, 1994; Park et al., 2007; NRC, 2013). Further research is needed which explores potential remediation cost reduction of using well configurations which utilize PAT and injection to promote mixing and further enhance NA (Marquis and Dineen, 1994; Park et al., 2007; Piscopo et al., 2013).

2.1.9 Research gaps

Gaps have been identified in the literature of the following technologies: MNA and PAT; enhanced advective spreading and contaminant mixing; and in situ bioremediation.

A field study by Thornton et al (2014) showed that PAT influenced the plume mechanical dispersion and contaminant concentrations which enhanced biodegradation of the phenolic compounds in groundwater at the field scale. In this study, the contaminant plume core/interior was depleted of EAs and biodegradation was mostly limited to the plume fringe, which is controlled by dispersive mixing between the EAs and the plume. Biodegradation was limited by low pore velocities and dispersion, despite the aquifer having an abundance of aqueous EAs. The *in-situ* biodegradation rate of phenolic compounds at the plume fringe doubled over a 3-year period during operation of the PAT system (groundwater extraction rate of 6-50 m^3/d). The location of the PAT well (at the plume fringe), combined with the low pumping rate, was critical to enhancing the dispersive mixing of the contaminant plume with the EA-rich background groundwater.
Previous research has indicated that NA can be enhanced by targeted PAT as an extraction or injection well, or a combined configuration, could actively spread the plume in order to enhance intrinsic biodegradation and thereby reduce contaminant mass and concentration in situ (Thornton et al., 2001 a,b; Thornton et al., 2014; Bagtzoglou and Oates, 2007; Mays and

Neupauer, 2012). For example, Jones et al. (2002), developed a scheme of alternating extraction and injection of groundwater at the fringe of the plume, which they termed hydraulic manipulation. They showed that this scheme enhanced NA that was already occurring in the aquifer. However, in this study, the complex processes that constitute NA were represented only with first order decay. The main limiting factor of this hydraulic manipulation strategy was the low permeability (hydraulic conductivity) of the aquifer. For an aquifer with reasonable permeability and a biodegradable contaminant with a sufficient microbial community and available aqueous EAs, this method could be more effective. The main issue with the study was that while there were units of mass biodegraded for each remediation scenario, there was no mention of what percentage of total mass these values were. The large values of biodegraded mass seem to indicate that the plume had a constant source, which would explain why the plume could not be remediated by this method. There was also no indication how much mass was being removed by the extraction wells vs. the mass removed by biodegradation. Additionally, this study was only 2D and not kinetic (first order decay rate only). It is also worth mentioning that the hydraulic manipulation used by Jones et al., (2002) also falls into this category of enhancing advective spreading, as well as the category of combining PAT and MNA technologies. However, this is the only study to date which uses the combined technologies of PAT, MNA, and active plume spreading and mixing.

However, besides the study by Thornton et al. (2014) and Jones et al., (2002), there is a lack of research that relays the effects of using PAT to enhance intrinsic biodegradation in situ or explores the mechanisms behind these enhancements in detail. While sequential injections and extractions have been simulated with the aim to enhance NA *in situ* (Jones et al., 2002), **there is no current research** investigating variables such as extraction/injection well locations, the distance between injection/extraction well pairs, pumping rate, and duration on the effects of biodegradation, which could inform the design of future remediation systems which combine PAT with NA with the aim of enhancing NA in situ.

Also, using Monod kinetic redox reactions in contaminant plumes would give a more realistic mass balance representation of the biodegradation rates and overall mass that is biodegraded. It would elucidate the relative contribution of TEAPs, as a PAT system can be used to enhance the biodegradation rate (Mayer et al., 2001; Watson et al., 2005; Thornton et al., 2014). **There is also a lack of research** investigating whether injections of dissolved EAs can be combined with a targeted PAT system with the goal of further augmenting biodegradation, combined with a detailed mass balance.

Additionally, while there are a number of studies which focus on heuristically and optimally designing well configurations for different remediation objectives, such as mass removal, enhancing mixing in situ, and enhancing in situ bioremediation (Marquis and Dineen, 1994; Guo and Brusseau, 2017), to the author's knowledge, **there are no current studies** that explore in detail the effects of how a multiwell configuration could enhance the biodegradation rate of intrinsic NA and be further enhanced through the injection of amendments.

Furthermore, if advective spreading can enhance bioremediation by locally enhancing the dispersive mixing of the plume with EAs and globally enhancing the volume of the plume fringe, this could also reduce remediation costs by reducing the amount of mass needed to be treated through PAT (Thornton et al., 2014; Bagtzoglou and Oates, 2007; Mays and Neupauer, 2012). However, there are currently no studies investigating the mechanisms involved with respect to a PAT system design that enhances mass removal through in situ biodegradation to achieve remediation at a lower economic cost and time, and the relative importance of operational factors in system deployment, despite the opportunities to reduce remediation costs and improve sustainability and remediation performance.

A modelling study of this phenomenon has never been conducted to investigate how the PAT system behaves in further detail, how it can be improved, and what its potential limitations are. A reactive 3D transport model (Chapter 4) was developed for this study, using phenol as a candidate organic contaminant (electron donor). Phenol is a common groundwater contaminant that originates from many industrial processes (e.g., wood preservation plants, organic chemical manufacturing, gasworks). The approach is evaluated at a site on a UK sandstone aquifer contaminated with a large plume of phenolic compounds, at which a PAT system has been installed for plume management (Baker et al., 2012; Thornton et al., 2014). An extensive database of groundwater quality data and aquifer properties, developed from >25 years of previous research at this site, is available to provide a unique opportunity to compare the modelling results.

PAGE INTENTIONALLY LEFT BLANK.

Chapter 3

3.0 Methodology

This chapter presents the methodology for the development and implementation of the framework from which all scenarios from each chapter in entire thesis were modelled.

Section 3.1 begins with an overview of the study site and presents the relevant data from which past research has presented.

Section 3.2 presents the flow and transport methodology which is comprised of the flow and transport equations, reactions, kinetic reaction model, and mass equations, that are used for Chapter 4, 5, and 6.

Section 3.3 then presents the cost function methodology which is used to calculate the various costs involved in the remediation of each scenario for Chapter 6.

Section 3.4 presents the foundation for the development of the conceptual model and numerical regional flow model. This section then describes how the 3D flow and transport model – that is later used for the scenario modelling – was developed.

Section 3.5 discusses the numerical accuracy of the 3D flow and transport model presented in section 3.4.

Section 3.6 presents a demonstrative proof of concept set of 2D simulations that aim at explaining how the enhancement of in situ biodegradation via targeted PAT functions. A 2D model is used because it visibly demonstrates how biodegradation is being enhanced by the PAT well very clearly. The findings from the 2D model experiments are then used to plan the scenarios for enhancing biodegradation in situ using the 3D model for chapter 4, 5, and 6.

Section 3.7 finally gives a brief overview of the general methodology for the various scenarios presented for Chapter 4, 5, and 6. More detail is provided in the methodology section for each specific chapter.

3.1 Conceptual and numerical model development

3.1 Study site

The field site considered in this thesis is a fine-grained, unconfined, fluviatile, sandstone bedrock aquifer located beneath a former coal tar distillation plant in Four Ashes, UK. The site has been extensively investigated since the late 1990s. Site characterization was undertaken at Four Ashes by the Environment Agency in cooperation with the British Geological Survey, the Institute of Freshwater Ecology, and third-party consultants. Characterization included drilling new boreholes, conducting pumping tests, water quality sampling and geochemical analysis, mapping of the contaminant plume, etc., which culminated in the development of a radial flow model and a regional flow model. Despite extensive investigation, the resolution of the hydraulic heads, hydraulic conductivity,

effective porosity, and other physical parameters is poor, in part due to the use of 5 meter well screens.

Most of the site data, such as the regional flow model, and the project reports, from Four Ashes are confidential; however, more information is available from publications based on the site data, with studies on the interpretation of groundwater contamination (Williams et al., 2001), redox processes and contaminant biodegradation (Thornton et al., 2001a; 2014; Wu et al., 2006; Baker et al., 2012;), aquifer stable isotope geochemistry (Spence et al., 2001), aquifer microbiology (Pickup et al., 2001; Elliot et al., 2010; Rizoulis et al., 2013; Mujica-Alarcon et al., 2021), plume mass balance (Thornton et al., 2001b) and reactive transport modelling (Mayer et al., 2001; Watson et al., 2005). The site history, summarised here, is described in detail in Williams et al. (2001). Data from the project reports and the regional flow model have been used in previous modelling studies on the site, such as Mayer et al., (2001) and Watson et al., (2005).

The site is contaminated with a mixed plume of phenolic compounds (primarily phenol, cresols and xylenols) which extends approximately 500 m down hydraulic gradient of the site, with an estimated width of 150 m and depth of 60 m (Williams et al., 2001; Thornton et al., 2001a,b). Groundwater flow is westerly, with a pore velocity between 4-11 m/year, consistent over the history of the plume. Vertical flow due to groundwater recharge is also present, with velocities estimated at 1-2 m/year. Previous investigations have identified a heterogeneous distribution of phenolic compounds and biogeochemical processes responsible for their biodegradation within the plume (Thornton et al, 2001a). The plume is anchored by a dense non-aqueous phase liquid (DNAPL) source, with concentrations of individual phenolic compounds (e.g., phenol) reaching 25,000 mg/l. Although this concentration may seem high, the max solubility of phenol in water is 86,000 mg/l; however, values this high have not been observed.

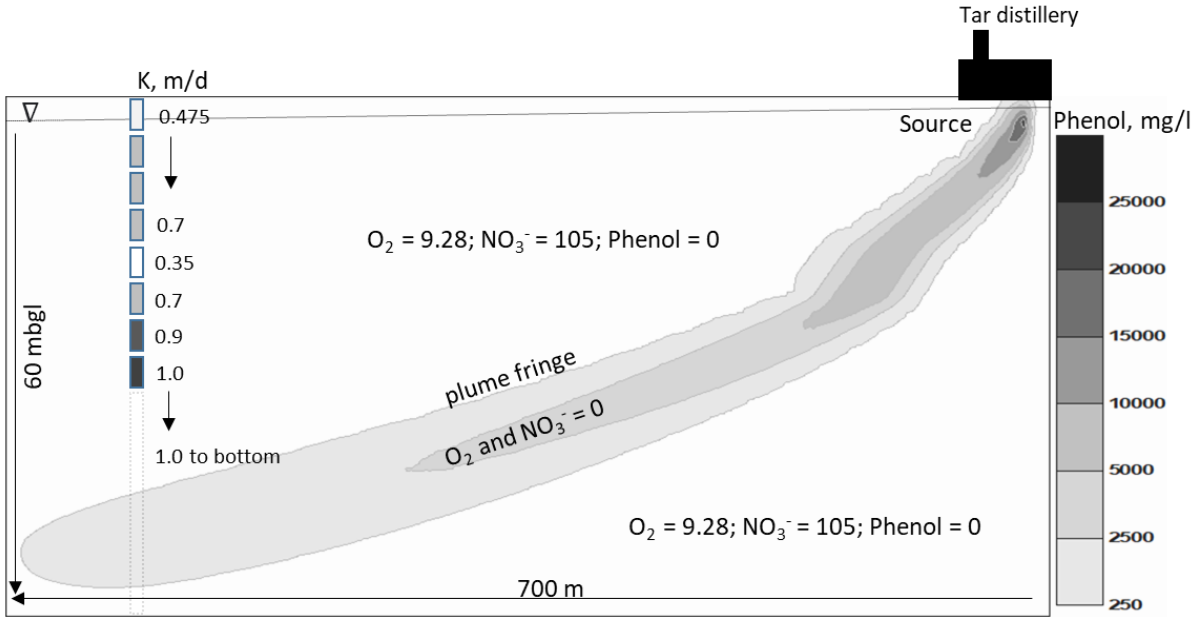

Figure 3-1. Schematic of plume concentration envelope based on groundwater chemistry and numerical simulation of site data. The concentrations shown are in mg/l. The hydraulic conductivity scale, represented by K, indicates that some layers have the same values (Thornton et al., 2001b). Note that the concentrations of oxygen and nitrate are below detection in the plume interior due to biodegradation of the phenolic compounds. Note the vertical exaggeration of the depth scale.

Table 3-1. Input parameters for all of the modelling scenarios in Chapters 4, 5, and 6.

Flow and transport parameters	**Value**			**Data source**
Effective porosity (-)	0.125[a]			Core samples/geophysical logs[a]
Hydraulic conductivity range, K (m/d)	0.35-1.0[a]			Pumping tests and RFM[c]
Recharge rate (m/d)	8.00e-04[a]			Effective infiltration estimation[b]
Longitudinal dispersivity (m)	1[b]			
Vertical transverse dispersivity (m)	4.00e-03[b]			Tracer tests and numerical
Horizontal transverse dispersivity (m)	1.00e-02[b]			modelling
Grid block size (m^3)	5			Well screen lengths are 5 meters.[a]
Model length, width, and depth (m)	1200x300x255			
	Species			
Biodegradation module parameters	*Phenol*	*Oxygen*	*Nitrate*	
Half saturation constant (mg/l)	-	0.1[b]	0.5[b]	Determined by a mesocosm
Inhibition constant (mg/l)	-	0.9[b]	0.9[b]	experiment[b]
Decay rate (1/T)	-	3.44e-05[b]	3.44e-06[b]	
Yield coefficient (-)	0	2.38[b]	3.69[b]	Reaction stoichiometry (Eq. 3)
Source concentration (mg/l)	25000	0	0	Groundwater quality monitoring[a]
Background groundwater concentration (mg/l)	0	9.28[b]	105[b]	Groundwater quality monitoring[a]

a. Unpublished data from confidential third-party consultant reports.
b. Values used in previous modelling studies on the site [Watson et al. (2005) and Mayer et al. (2001)].
c. RFM refers to Radial Flow Modelling undertaken by third party consultants.

3.2 Numerical methodology for flow and transport model

The methodology for the flow and transport model used in Chapters 4, 5, and 6 is presented in this section.

The flow and transport model was developed using Eq 1. Groundwater flow is governed by the classical PDE:

$$\frac{\partial}{\partial x}\left(K_{xx}\frac{\partial h}{\partial x}\right)+\frac{\partial}{\partial y}\left(K_{yy}\frac{\partial h}{\partial y}\right)+\frac{\partial}{\partial z}\left(K_{zz}\frac{\partial h}{\partial z}\right)+W=S_s\frac{\partial h}{\partial t} \quad \text{Eq 1}$$

where K_{xx}, K_{yy}, and K_{zz} are hydraulic conductivity along the x, y, and z coordinate axes (L/T); h is the hydraulic head (L); W is a volumetric flux per unit volume representing sources and/or sinks, such as recharge and wells (T^{-1}); S_s is the specific storage of the porous material (L^{-1}); and t is time (T). The model is isotropic ($K_{xx} = K_{yy} = K_{zz}$) and heterogeneous, with hydraulic conductivity generally increasing with depth (Figure 3-3). Based on historical data from >25

years of monitoring, the groundwater flow system was set at steady state. Eq 1 is solved using MODFLOW-2005 (Harbaugh et al., 2005; 2017), based on a finite different grid characterized by 200 rows, 60 columns, and 37 layers, with a refined grid-block size of 5m × 5m × 5m in the region of the plume. The flow model is by characterized by constant head boundary conditions on the east and west (see Figure 3-1), with groundwater recharge applied to the water table (Table 3-1). Other boundaries are set as "no flow".

After solving Eq 1., MODFLOW-2005 then calculates the pore velocity field:

$$\boldsymbol{v} = -\frac{K}{\phi} \cdot \nabla h \qquad \text{Eq 2}$$

where ϕ is the effective porosity (-), K is the hydraulic conductivity (L/T), and h is the hydraulic gradient (/).

After calculating Eq 2, the principal components and cross terms of the hydrodynamic dispersion tensor are then calculated (Burnett and Frind, 1987; Zheng and Wang, 1999):

$$D_{xx} = \alpha L \frac{v_x^2}{|v|} + \alpha_{TH} \frac{v_y^2}{|v|} + \alpha_{TV} \frac{v_z^2}{|v|} + D^* \qquad \text{Eq 3}$$

$$D_{yy} = \alpha L \frac{v_y^2}{|v|} + \alpha_{TH} \frac{v_x^2}{|v|} + \alpha_{TV} \frac{v_z^2}{|v|} + D^* \qquad \text{Eq 4}$$

$$D_{zz} = \alpha L \frac{v_z^2}{|v|} + \alpha_{TV} \frac{v_x^2}{|v|} + \alpha_{TV} \frac{v_y^2}{|v|} + D^* \qquad \text{Eq 5}$$

$$D_{xy} = D_{yx} = (\alpha_L - \alpha_{TH}) \frac{v_x v_y}{|v|} \qquad \text{Eq 6}$$

$$D_{xz} = D_{zx} = (\alpha_L - \alpha_{TV}) \frac{v_x v_z}{|v|} \qquad \text{Eq 7}$$

$$D_{yz} = D_{zy} = (\alpha_L - \alpha_{TV}) \frac{v_y v_z}{|v|} \qquad \text{Eq 8}$$

where D_{xx} ,D_{yy} ,D_{zz} = principal components of the dispersion tensor, L^2T^{-1}; D_{xy}, D_{xz}, D_{yx}, D_{yz}, D_{zx}, D_{zy} = cross terms of the dispersion tensor, L^2T^{-1}; α_L = longitudinal dispersivity coefficient, L; α_T = transverse dispersivity coefficient, L**;** α_{TV} = transverse vertical dispersivity coefficient, L**;** D* = effective molecular diffusion coefficient, L^2T^{-1}; v_x, v_y, v_z = components of the velocity vector along the x, y, and z axes, LT^{-1}; and $|v| = \sqrt{v_x^2 + v_y^2 + v_z^2}$, which is the magnitude of the velocity vector (L/T).

The velocity and dispersion tensor (Eq 2 and Eq 3-8) are then used in the multispecies reactive contaminant transport simulator MT3D-USGS (Bedekar et al., 2016) to solve a system of

coupled partial differential equations, each of which represents the mass continuity for the species simulated:

$$\nabla(\phi \cdot \mathbf{D} \cdot \nabla C_i) - \nabla(\phi \cdot \mathbf{v} \cdot C_i) + \mathrm{q}_{s,i} \cdot C_{s,i} + R_i = \frac{\partial(\phi \cdot C_i)}{\partial t} \quad \text{Eq 9}$$

where $C_i$is the concentration of species i [ML^{-3}], **D** is the hydrodynamic dispersion tensor [L^2T^{-1}], $\mathrm{q}_{s,i}$ [ML^{-3}] and $C_{s,i}$[ML^{-3}] represent specific discharge and concentration of sources for species i, R_i represents the species rate of reaction (disappearance) [$ML^{-3}T^{-1}$]. In this case, there are three species ($i = 1,2,3$), and the terms R_i depend on ongoing kinetic reactions occurring between 1 electron donor (ED) and 2 electron acceptors (EAs), simulated using a Monod kinetic model developed by Lu et al. (1999).

The stoichiometric reactions between phenol (C_6H_6O), which is the ED, and the two EAs, oxygen (O_2) and nitrate (NO_3^-), are described by the following equations:

(a) $C_6H_6O + 7O_2 \rightarrow 6CO_2 + 3H_2O$ Eq 10

(b) $C_6H_6O + \frac{28}{5}NO_3^- + \frac{28}{5}H^+ \rightarrow 6CO_2 + \frac{14}{5}N_2 + \frac{29}{5}H_2O$ Eq 11

Eq 10 and 11 are presented to illustrate the stoichiometry of the reactions which are considered in Eq 12.

The ED rate of biodegradation ($i = 1$ in Eq 9 is given by (Lu et al., 1999). The r_{ED} varies in time and space.

$$r_{ED} = \sum_{j=1}^{2} r_{ED,j} = -\left\{\frac{k_{EA_1} \cdot [EA_1]}{K_{EA_1} + [EA_1]} + \frac{k_{EA_2} \cdot [EA_2]}{K_{EA_2} + [EA_2]} \cdot \frac{K_{I,EA_1}}{K_{EA_1} + [EA_1]}\right\} \cdot [ED] \quad \text{Eq 12}$$

where $[ED]$, $[EA_1]$, and $[EA_2]$ represent the concentration of the ED and the two EAs (M/L^3), respectively; $k_{EA_1}$and k_{EA_2} are first-order decay rate constant for the EAs (T^{-1}); K_{EA_1} and K_{EA_2} are the half saturation constants for the EAs (M/L^3); K_{I,EA_1} (M/L^3) is the inhibition constant for the first EA, which is oxygen, which has the highest Gibbs free energy (Christensen et al., 2000). Correspondingly, the rates of consumption of the two EAs ($i = 2,3$ in Eq 9) are:

$$r_{EA_j} = Y_{EA_j} \cdot r_{ED} \quad \text{Eq 13}$$

where $Y_{EA_j}(j = 1,2)$ is the yield coefficient for the EA, that is, the EA mass used per ED unit mass, calculated from the stoichiometry in Eq 10 and 11 (Table 3-2). Approximately 2.38 units of oxygen is required to remove 1 unit of phenol.

The mass of the species, phenol, or oxygen, at time t is calculated with the following equation, which is a spatial integral of concentration over the pore volume across the whole aquifer system. It is calculated as follows:

$$M(t) = \sum_{k=1}^{NLAY} \sum_{i=1}^{NROW} \sum_{j=1}^{NCOL} \theta_{ijk} \cdot C_{ijkt} \cdot \Delta X_j \cdot \Delta Y_i \cdot \Delta Z_k \cdot (t) \quad \text{Eq 14}$$

where NLAY, NROW, and NCOL are the number of layers, rows, and columns in the model, respectively; and θ_{kij} (/) is the effective porosity, t (T) is the time, and $\Delta X_j \Delta Y_i \Delta Z_k$ (L) are the dimensions of the cells.

The mass biodegraded is obtained by integration of the rate of ED biodegradation r_{ED} (Eq 12) over the model domain for the remediation period T, that is:

$$M_{bio}(T) = \int_{t=0}^{T} \left[\int_{\Omega} \theta \cdot r_{ED} \cdot d\Omega \right] dt \quad \text{Eq 15}$$

where Ω represents the 3D model domain, θ (/) is the effective porosity, r_{ED} (M/L^3/T) is the biodegradation rate (Eq 5). This integral is numerically calculated over the model grid and the discretization of the time interval $[0, T]$ adopted in the flow and transport simulation.

3.3 Methodology for the operational cost model

This section presents a cost model which estimates the PAT operational cost, which is pumping electricity cost combined with GAC cost, over the remediation period *p*. The operational cost is determined by the number of wells, the screen locations, the extraction/injection schedule, the concentration extracted by the wells over time, the hydraulic head of the wells over time, and the time required to reach the remediation target. The flow and transport is used to estimate these variables required by the cost model.

The operational cost over time for each scenario in Chapter 6 is calculated using the following equation (Culver et al., 1998):

$$Cost = G_{pump,p} + G_{GAC,p} \quad \text{Eq 16}$$

where $G_{pump,p}$ is the PAT system operational electricity cost and $G_{GAC,p}$ is the operational cost for the granular activated carbon (GAC) treatment system.

As Eq 16 states, the operational cost is the sum of the electricity cost for the pumping wells and the cost of the GAC. The electricity cost is calculated as:

$$G_{pump,p} = \sum_{k=1}^{N_{tp}} \rho \cdot g \cdot Q_{ik} \cdot (Z_h - h_{ik}) \cdot \frac{S_p}{\varepsilon} \cdot \Delta t_k \quad \text{Eq 9}$$

where ρ is the density of water (M/L^3), g is acceleration due to gravity (L/T^2), Q_{ik} is the well i volumetric flow rate at time step k (L^3/T), Z_h is the elevation of the ground surface (L), h_{ik}

is the hydraulic head in the well at time step k (L), S_p is the cost of electricity per kilowatt-hour ($/M*L^2/T^2), ε is the efficiency of the submersible pump (/), and Δt_k is the length of the time period k (T).

The GAC cost is primarily determined by the amount of phenol mass that is removed by the extraction wells, the mass of carbon required to adsorb (remove) the mass of the contaminant, $CURC_p$, and the cost per unit, S_c, of the carbon. $G_{GAC,p}$ is calculated as:

$$G_{GAC,p} = \sum_{k=1}^{N_{tp}} \frac{S_c}{CURC_p} \cdot C_k \cdot Q_{Tk} \cdot \Delta t_k \qquad \text{Eq 10}$$

where S_c is the carbon cost coefficient ($/M), $CURC_p$ is the constant carbon use rate (M/M), C_k is the average influent concentration to the adsorbers (M/L^3), Q_{Tk} is the total volumetric flow rate for time step k (L^3/T), and Δt_k is the time step length at period k (T).

Q_T, the total volume extracted, is calculated as:

$$Q_{Tk} = \sum_{i=1}^{m} Q_{ik} \qquad \text{Eq 19}$$

C_k is the average influent concentration sent to the adsorbers, which varies over time and is calculated as:

$$C_k = \frac{\sum_{i=1}^{m} C_{ik} \cdot Q_i}{Q_T} \qquad \text{Eq 20}$$

where C_{ik} is the concentration of the extracted groundwater from well i (M/L^3) at time-step k.

3.4 Numerical model development

3.4.1 Regional flow model

The original flow model was created using ~20 year old data from a confidential report on the study site conducted by the Environment Agency. Data for a calibrated flow model were provided by third party consultants. The mean error and RMS errors for the calibrated model were 0.0004 and 0.44, respectively.

A 3D regional flow model was developed to understand the impact of regional flow on the plume development. The flow model domain is 6420 meters wide by 5800 meters long by 255 meters thick, which is discretized into 128x116x10 finite-difference cells with variable grid spacing. The model is heterogeneous, isotropic, and the range of hydraulic conductivity values represented by Table 3-l.

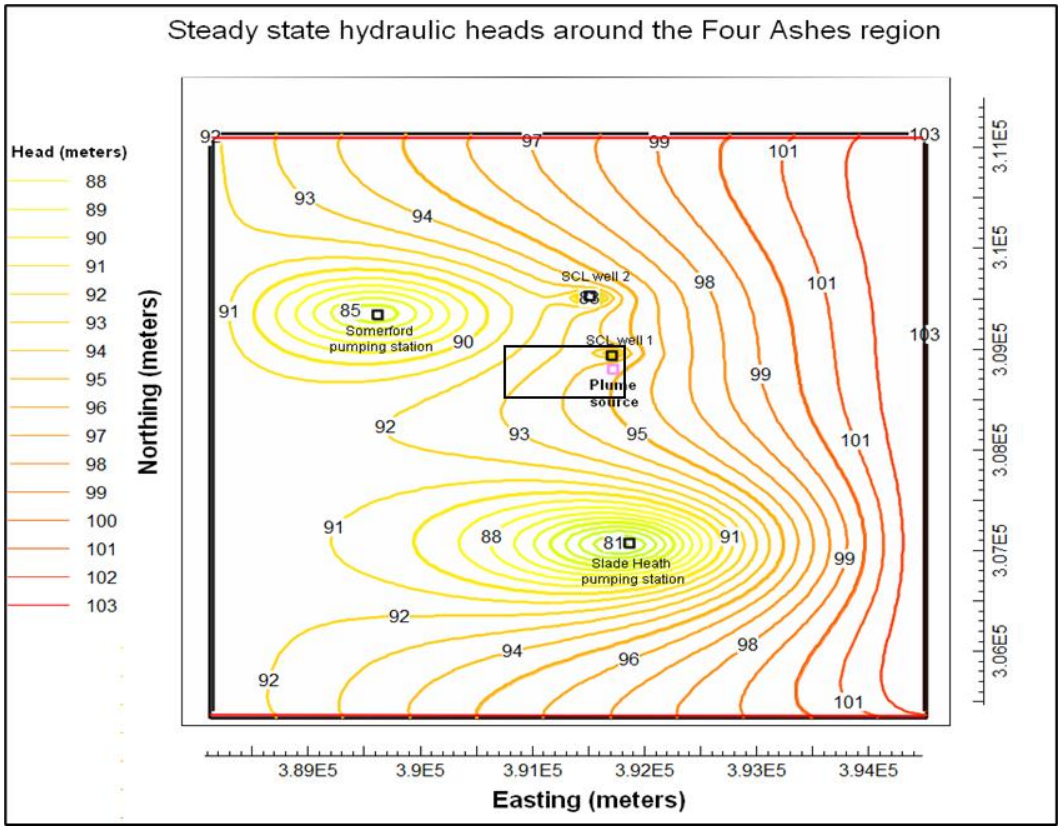

Figure 3-2. Hydraulic heads and dimensions for the Four Ashes regional model. The black box is the approximate location for the 3D flow and transport model, which is used in Chapters 4, 5, and 6.

Table 3-2. Extraction wells included in the regional flow model. PS = pumping station for public water supply. X and Y are eastings and northings. Note the large pumping rate that can be obtained when extracting from a deep unconfined aquifer.

Well ID	X location (m)	Y location (m)	Z location (m)	Duration (d)	Pumping rate (m^3/d)
SCL BH#1	391512.5	309525	70	25567	-330
SCL BH#2	391712.5	308937.5	70	25567	-165
Slade Heath PS	391862.5	307075	150	25567	-4300
Somerford PS	389625	309337.5	-150	25567	-2820

The boundary conditions are assigned as constant head values of 103 and 88 meters on the west and east boundaries, respectively. The north and south boundaries are set to linearly decreasing

constant head, from 103 to 88 meters (Figure 3-2). Recharge is estimated at 8.0e-4 and applied to the top active layer in the model. Outflows are also simulated: two major water supply wells have been included as they have a significant influence on the hydraulic plume transport (Figure 3-2 and Table 3-2).

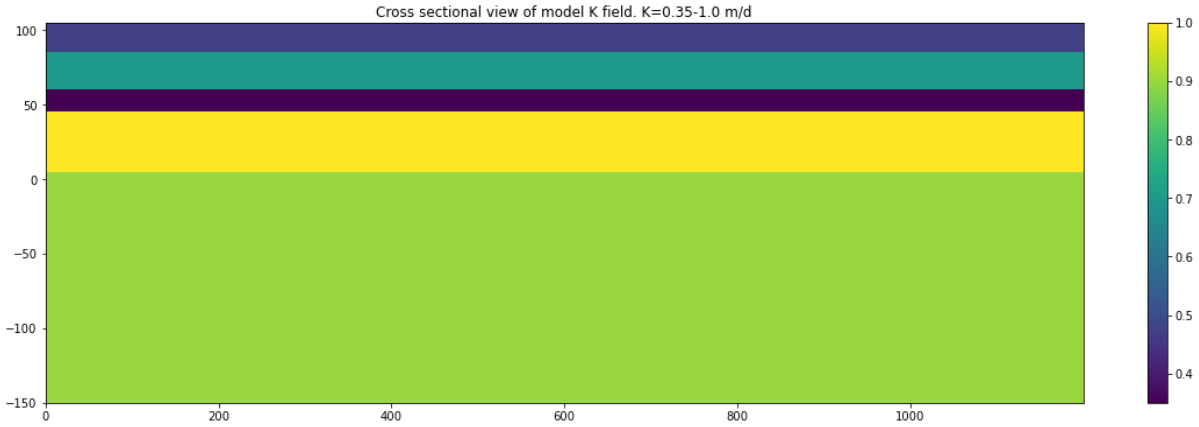

Figure 3-3. Vertical slice of the numerical model showing the hydraulic conductivity throughout the layers. The hydraulic conductivity units are in m/d.

3.4.2 New 3D flow and transport model

Although the consultant's model was precalibrated, it was too large, coarse, and generalized (i.e. it simulated regional supply wells) to be used for the purposes of this thesis. Ultimately, it was only used alongside site data to validate the development of a new smaller flow and transport model. In order to reduce computational cost and to focus on solute transport at the Four Ashes site rather than the entire region, the regional flow model was truncated to the approximate size of the black box in Figure 3-2. The regional pumping wells were excluded from the updated 3D flow and transport model.

No model verification has been attempted, as the results are intended to be qualitative rather than quantitative. The goal when creating the new flow and transport model was not to interpret the actual site conditions, but to instead use the model to develop hypothetical scenarios that explore the effect of key factors on contaminant mass removal in groundwater through the operation of the PAT system. The rationale behind using this approach was not to interpret the actual contamination conditions at the site, but to instead develop a model that is internally coherent and consistent. This enabled a hypothetical but realistic example model to be created, with results that can be extended to other sites with similar characteristics and/or contaminated with coal tar distillate plumes (e.g. Blum et al., 2011). However, the plume has been validated based on observed concentration distributions and previous modelling data (see Figure 3-1 and Table 3-1).

This new truncated 3D flow and transport model was created based on hydraulic head contours which were measured at the field site (unpublished confidential data). Head values measured at the site produced an average hydraulic gradient of 0.0042, which is consistent with the value used in other modelling studies (Mayer et al., 2001; Watson et al., 2005). The

water table in the new model fits well with a section of the water table in the regional model which corresponds to the Four Ashes site. The values of hydraulic conductivity chosen for the new model are in the range measured at the site (Figure 3-3).

The model domain that was chosen was X = 1200 m, Y = 300 m, and Z = 255 m. The plume was placed in a refined region of 5x5x5 m; the remaining grid cells are 10x5 m. The spacing on the Z axis begins to increase below the region of the plume, in order to reduce the model simulation time. There is no appreciable difference between a model with constant 5x5x5 m spacing and a model with variable spacing, but the computational gain is significant. The full thickness of the aquifer was necessary to avoid mounding. The other dimensions of the model were chosen to allow space for the plume evolution over time and for the PAT system. Low pumping rates were chosen for scenarios in the later chapters to avoid interaction with the boundaries. This resulted in a model has ~420,000 cells and requires 6-24 hours to complete a simulation, depending on the number of wells and the cumulative pumping rate.

Recharge was estimated from effective infiltration and was applied to the water table (Table 3-1). Initial simulations revealed that the most important parameters for the transport model are hydraulic conductivity, hydraulic gradient, and recharge. Eastern and western constant head boundary conditions of 103m and 98m were used along with a recharge rate of 8e-4 m/d to simulate the average horizontal hydraulic gradient for the site (0.0042). The north, south, and bottom boundaries were set to no flow. Additional simulations (not presented here) of a transient model showed that it reaches steady state quickly, so a steady state assumption was used for the flow component of the model.

It is accepted that in reality groundwater flow is transient (Suthersan et al., 2015) and that transient conditions improve plume mixing (Bagtzolgou and Oates, 2007; Piscopo et al., 2013), therefore would likely enhance biodegradation rates. This would likely be the case if time series data was available for the recharge and the hydraulic heads where the boundary conditions are located. However, based on the data available, which is not temporarily varying, the model is assumed to be at steady state. Even when run under transient conditions, the flow model resolves to steady state quickly. For a single well pumping at Q = -30 to -100 m3/d, the hydraulic heads trend to steady state after ~300 days, in the cell where the well is located and for any other location in the model domain. This is not unexpected, as the aquifer is 250 meters thick and there are two public water supply boreholes in the region pumping at -2820 m3/d and -4300 m3/d, respectively (see Table 3-2). The pumping rates used in this thesis do not even approach pumping rates of that magnitude. However, if the pumping rate is increased by 0.1 m3/d for 1800 days, the flow system never resolves to steady state.

While the values of hydraulic head used at the eastern and western boundaries are based on observed data at the field site, they are not strictly necessary for generating a valid plume. As long as the hydraulic gradient is the average value of 0.0042 (Mayer et al., 2001; Watson et al., 2005) it will produce a plume similar to that observed in Williams et al., (2001) and Thornton et al., (2001b). However, changing the hydraulic conductivity will change the values of specific discharge, which will change the velocity. The groundwater velocity at the

site varies between 4-11 m/d. Since the plume is estimated to be 50 years old and has reached an observed length of 500 meters, the length is considered to be indicative of the groundwater flow velocity, because the plume is composed of contaminants with low sorption potential, low diffusivity, and slow biodegradation rates. This indicates that the groundwater flow velocity in the vicinity of the plume is approximately 10 m/year, which equates to 0.027 m/d in the longitudinal direction. The velocities are estimated at 1-2 m/year in the Z (vertical transverse) direction. These values of velocity have been reproduced in the model.

The plume is anchored by a dense non-aqueous phase liquid (DNAPL) source, with concentrations of individual phenolic compounds (e.g., phenol) reaching 25,000 mg/l. To reduce the complexity of the numerical model, phenol was selected as a representative organic contaminant for the simulations and the concentrations of all other phenolic compounds were converted into equivalent phenol concentrations. At the site, the source term inputs are spatially and temporally variable based on the MLS profiles. However, the true source location(s) and temporally variable loading terms are unknown. This thesis does not attempt to solve an inverse problem. With that considered, the contaminant source consists of DNAPL (coal tar distillate) trapped within shallow groundwater at the site, which was simulated as a single 5x5x5 m3 cell. In order to generate a plume comparable to that observed at the site (Williams et al., 2001; Thornton et al., 2001a,b) but also accounting for the plume being 20 years older, the release of phenols from the source was simulated at 1344 mg/d over 70 years. This was determined to give the corresponding concentration distribution in the aquifer, with a maximum dissolved concentration of 25,000 mg/l (similar to the source zone) and total plume mass of 34,000 kg. The source was then assumed to be removed (as per conventional remediation practice) before PAT operations commenced (US EPA, 1997).

To develop the multispecies kinetic reaction component of the model, which is based on a Monod formulation, the EAs (oxygen and nitrate) were applied to the eastern constant head boundary and recharge (constant concentration). Note that the EA concentrations used correspond to those of the background groundwater (Table 3-1). For the kinetic reaction component of the model, Monod parameter values from previous studies were used (Mayer et al., 2001; Watson et al., 2005). Biodegradation only occurs in cells that have a non-zero concentration of an EA (oxygen and nitrate) and the ED (phenol). Based on unpublished calculations of the reaction rates, the most important parameters that are subject to change in space and time are the ED and EA concentrations. The other Monod parameters, such as the half saturation constant, inhibition constant, yield coefficients, and first order biodegradation rates are constant. Key sensitivities in the biodegradation model are hydraulic conductivity, recharge, and the dispersion coefficients, which is consistent with what was observed by Lu et al., (1999). See Table 3-1 for more detail.

Since the plume has aged by 20 years, the model was run for 70 years to establish the cumulative biodegradation mass at the end of the period. Between approximately 1-5% of the plume is degraded over 70 years, with is consistent with a study on the mass balance of the plume (Thornton et al., 2001b). The source was then removed and natural attenuation was simulated for an additional 10 years. The value of biodegradation from this 10 years is used

as a baseline control on which to qualitatively compare future modelling scenarios. It is referred to the "baseline biodegradation" in Table 1.

As the magnitude of dispersion is a function of the aquifer dispersivity (Ye et al., 2015), values of this coefficient were taken from previous modelling studies at the site (Table 1), which were of the same order as those estimated in other studies (e.g. Cirpka et. al., 1999, 2006; Cupola et al., 2015; Sather et al., 2022; 2023).

Previous studies have shown that the phenolic contaminants are biodegraded by several processes; however, most mass loss due to biodegradation (>90%) arises from consumption of oxygen and nitrate in the groundwater (Lerner et al., 2000; Thornton et al., 2001a,b; Mayer et al., 2001; Jones et al., 2002; Watson et al., 2005). For this reason, the modelling scenarios presented in the following chapters were developed to assess the contribution of these two EAs to biodegradation, as influenced by the PAT system.

3.5 Assessing model numerical accuracy

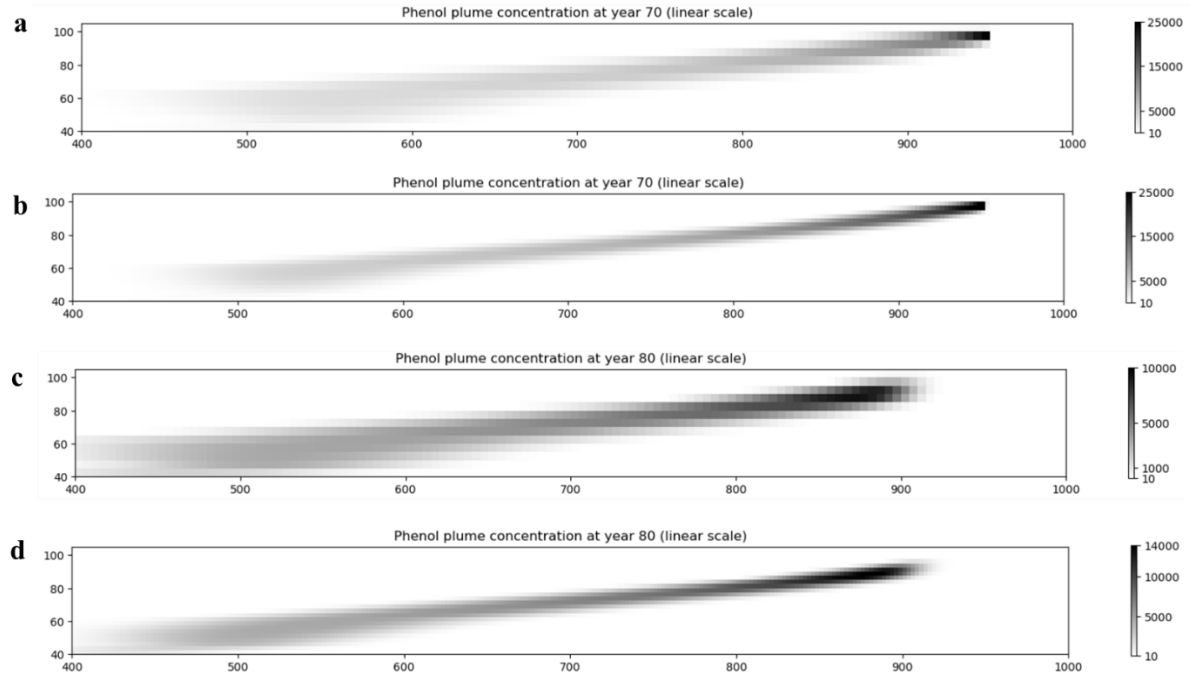

Figure 3-4. Shown above are the concentration distributions of phenol for the coarse grid (a and c) and the fine grid (b and d) for years 70 and 80. The constant concentration source was removed at the end of year 70, which results in a difference between plume concentration for the coarse and fine grid models (c and d). Note that there is no interpolation.

To assess the numerical accuracy of the 3D model, the impact of the grid cell size on numerical dispersion was analyzed. A 5x5x5 meter grid spacing – in the region where the plume flows – was used for all of the simulations in Chapters 4, 5, and 6. The TVD method was used to solve the advection term, which is claimed to significantly reduce numerical dispersion and artificial oscillation, especially when a smaller Courant number is used (Zheng and Bennett, 2002). In order to obtain a quantitative solution that is virtually free from numerical dispersion, the dimensionless Peclet number should ideally be equal to 1 but

should be no more than 2 (Zheng and Bennett, 2002). With the current 5x5x5 meter grid spacing and dispersivity values of αl=1m, αy=2cm, and αz=4mm, this would equate to required grid spacings dx, dy, dz equal to 2 m, 2 cm, and 0.8 cm, respectively. With the model domain of (X, Y, Z) 1200x300x255 meters used for the modelling, this would require 2.87e11 cells, given a constant cell spacing.

This grid spacing requirement is due to the low dispersivity of the aquifer. The magnitude of the computational requirement is compounded by the significant contribution of recharge to the unconfined aquifer, which is causing the plume to flow in 2 dimensions, so discretization and possible numerical dispersion in the Z direction becomes an issue. Furthermore, the numerical difficulty is further increased by the fact that a large aquifer thickness (255 meters) is required to be simulated in order to avoid water table mounding and to have the water table divide in the appropriate location (at the eastern boundary). Increasing dispersivity coefficients to values expected for a plume of its scale (Gelhar et al., 1992) would still result in a large numerical burden. For example, an αl=5m, αy=10cm, and αz=1cm (ay and az are generally not higher than these values) would be required to eliminate numerical dispersion, which would still require a very large model grid.

To assess the model numerical accuracy, the coarse model (5x5x5 meter grid spacings) was compared to a fine grid (2.5x2.5x2.5 meter grid spacings) model to assess whether the TVD method was eliminating numerical dispersion. A time step of 0.2 days was chosen as it produces a Courant number of 0.00112. It was determined that the coarse grid plume is approximately 20 meters longer and 10 meters thicker than the fine grid plume and the plume width is unchanged. The plume size increase that is induced by numerical dispersion results in a more concentrated plume and more mass that is biodegraded (a difference of +30%) over 70 years of plume generation (see Figure 3-4). For the fine grid model, a trial and error analysis was undertaken to determine which values of dispersivity produce a plume of similar thickness, length, concentration, and biodegradation mass as the coarse grid model. The result was that the fine grid model requires an αl of 1.4 m (+40%) and an αz of 2 cm (+400%). In conclusion, in the coarse model there is numerical dispersion which is causing the plume to be reduced in concentration and increased in size. However, this issue is not that significant, as the plume simply has higher dispersion than intended for an almost entirely advection driven plume. Despite the fact that the numerical dispersion is inflating the biodegradation mass, the values in Chapters 4 and 5 are still within the established 1-5% of total plume mass that is biodegraded over the lifetime of the plume (Thornton et al., 2001a,b; Williams et al., 2001; Mayer et al., 2001; Watson et al., 2005).

In the following chapter, there is an experiment with varying values of dispersivity coefficients which show that increasing the dispersivity coefficient significantly enhances biodegradation, as expected. While the TVD method may not be completely eliminating numerical dispersion, it is significantly reducing it considering a Peclet constraint of 2. Other methods that could be used to eliminate numerical dispersion to conduct a quantitative analysis could be parallel computing on a high performance computing cluster or particle tracking. However, the particle tracking method in MT3D-USGS, the method of characteristics, often is not mass conservative, which would lead to errors when calculating the total mass biodegraded (Zheng and Bennett, 2002). A novel particle tracking method would instead need to be used in order to include kinetic biodegradation reactions and calculate the total mass biodegraded.

3.6 Demonstration of PAT on biodegradation using a 2D model

This section aims to explain how the enhancement of biodegradation via targeted PAT works, to enable the reader to better understand and interpret the results in experimental chapters 4, 5, and 6. For this purpose, a 2D model flow and transport model was created in order to reduce the runtimes and simplify the presentation of the work for demonstrative purposes. The 2D model uses all the same parameters as the 3D model (see Table 3-1); however, there is no recharge component, there is only a single layer, and this model is confined.

The following are the initial conditions for the 2D flow and transport model (Figure 3-4). The domain is 1000 by 1000 meters, discretized into 200 columns and 200 rows with a constant grid spacing of dx, dy = 5 meters. Phenol was generated through a constant concentration of 25,000 mg/l over 70 years into a domain where oxygen was 9 mg/l everywhere. After 70 years, the source was removed, and PAT at Q = -1 m^3/d was simulated for an additional 10 years. As a result of phenol flowing through the oxygen plume, the oxygen was depleted inside the interior of the phenol plume, where the phenol concentration is high. Where the two species meet, a kinetic reaction occurs, following Eq 12. For the purposes of this simple exercise, nitrate is not included in this model. The advection term is solved using the TVD method.

The results of the baseline plume generation and the PAT experiment are shown below.

3.6.1 Presentation of 2D model results

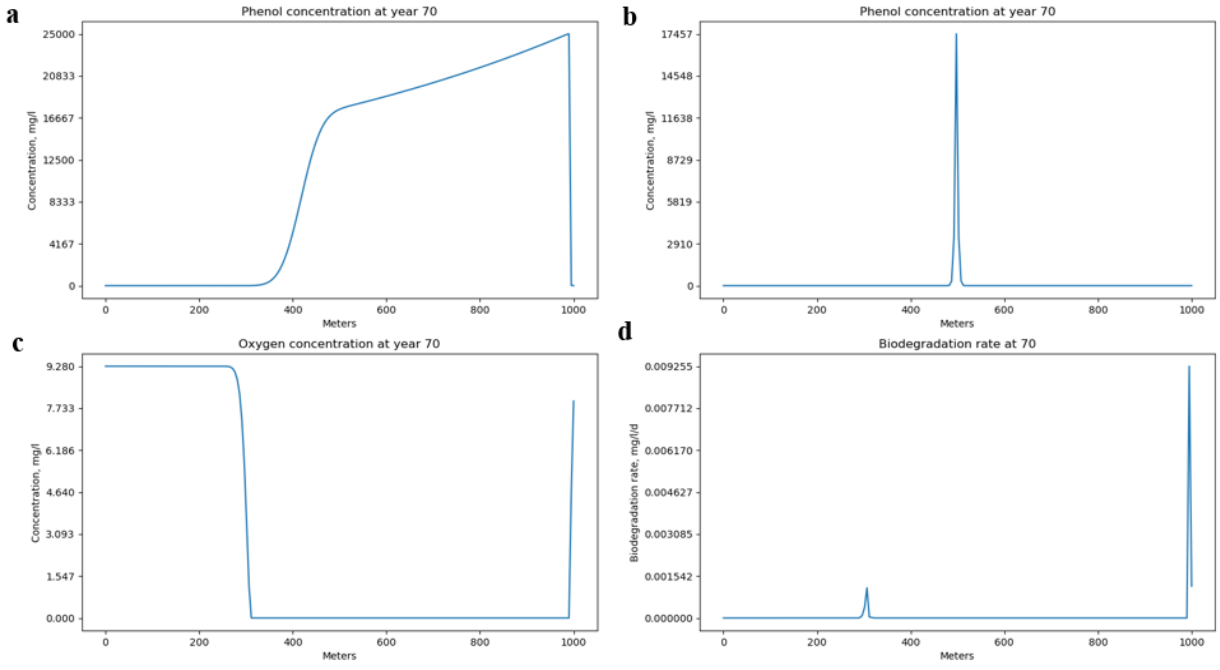

Figure 3-5. The initial conditions of the plume before PAT intervention. (a) phenol concentration in X direction, (b) phenol concentration Y direction, (c) oxygen concentration in X direction, and on the (d) biodegradation rate in the X direction.

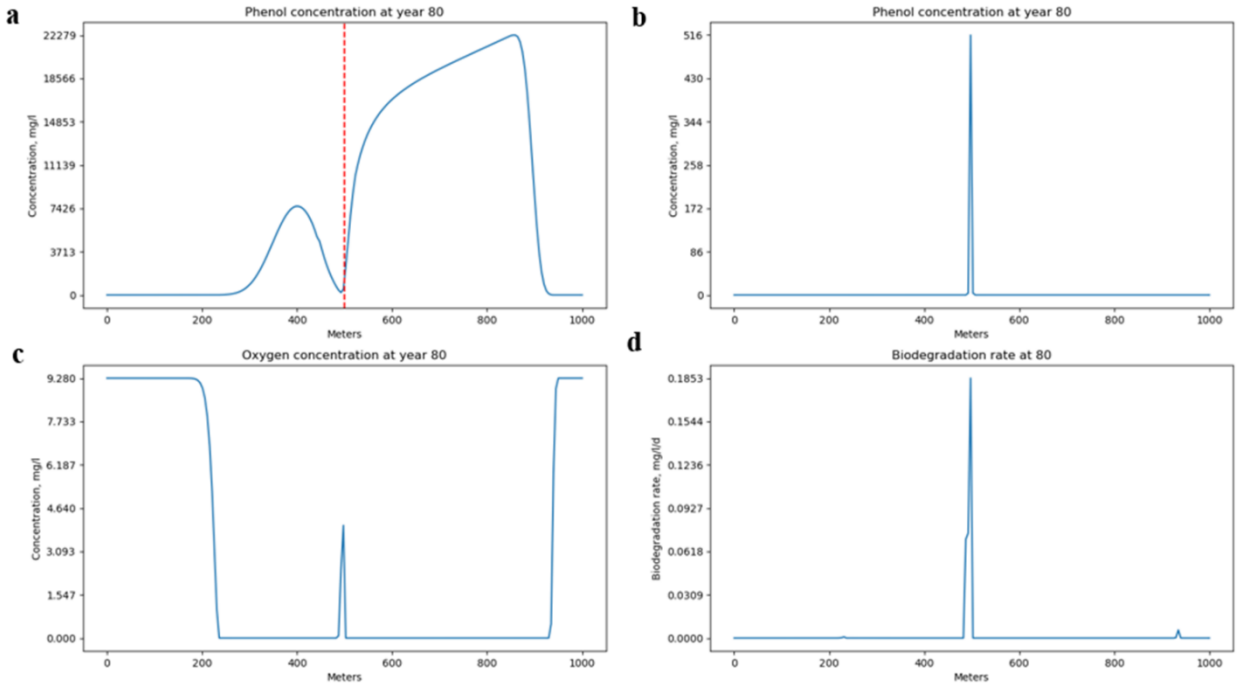

Figure 3-6. Shown above is the effect of 10 years of PAT intervention on the (a) phenol concentration in X direction, (b) phenol concentration Y direction, (c) oxygen concentration in X direction, and on the (d) biodegradation rate in the X direction. The red line indicates the location of the well.

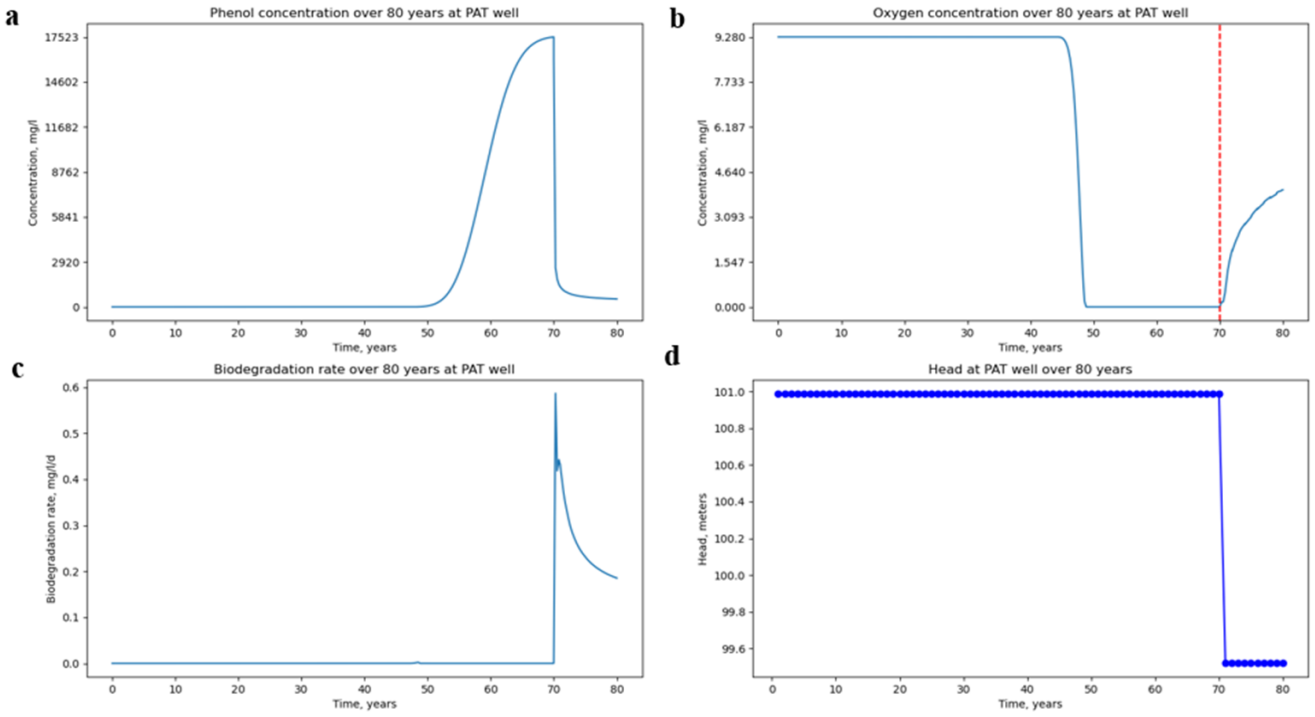

Figure 3-7. Shown above are the phenol and oxygen concentrations at the PAT well over 80 years. (a) phenol concentration, (b) oxygen concentration, (c) biodegradation rate, and (d) hydraulic head. The red line indicates the time PAT intervention begins.

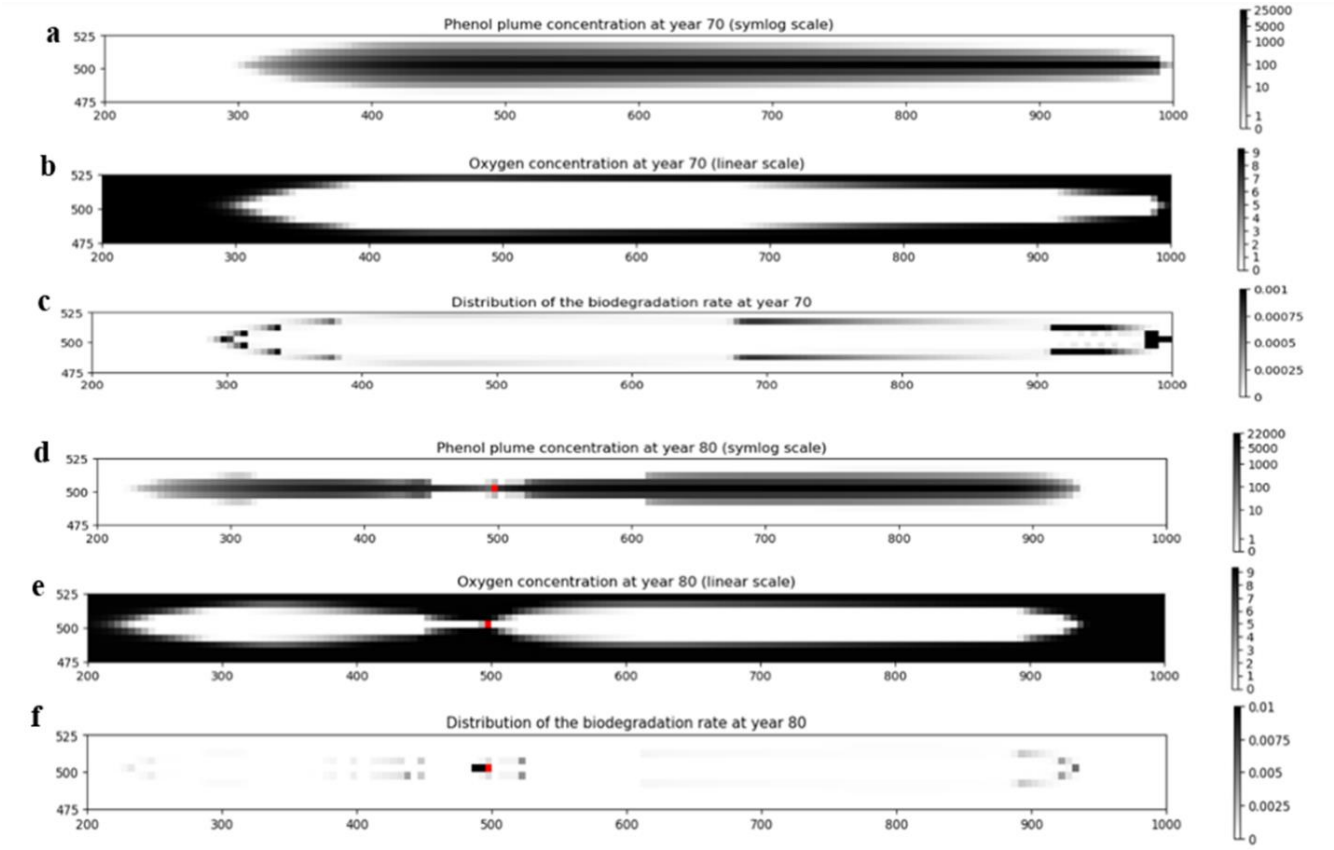

Figure 3-8. Presented above are plane view concentration plots of (a, d) phenol and (b, e) oxygen, and the (c, f) biodegradation rates before and after 10 years of PAT intervention. Note that biodegradation only occurs on the fringes of the plume, which is where mixing occurs.

3.6.2 Discussion of results

Figure 3-5 shows the results for "no intervention", i.e., the pumping well is inactive and instead used an as observation well. The PAT well is located at the center of the phenol plume, at (X = 500, Y = 500) meters. Figure 3-5a and 3-5b show the concentration of phenol in the X direction and Y direction, respectively. Figure 3-5b shows the plume is quite thin – approximately 50 meters wide. Figure 3-5c shows that the oxygen concentration is low where phenol concentration is high. Figure 3-5d shows the biodegradation rate in the X direction. Note that the biodegradation rate is zero where oxygen is depleted and is nonzero where phenol and oxygen mix (at the front and back of the plume). **The biodegradation rate at the back of the plume is higher than at the front due to the order of magnitude difference in phenol concentration.**

Figure 3-6a shows that phenol concentration decreases significantly at the well location and that the max phenol concentration is decreased. Figure 3-6b shows that phenol concentration is significantly decreased in the Y direction, as compared to Figure 3-4a. Figure 3-6c shows that the oxygen concentration is increasing at the PAT well, which indicates that the PAT well itself is increasing the flux of EAs into the plume, which was originally postulated by

Thornton et al., (2014). Figure 3-6d shows that the biodegradation rate is highest near the PAT well. Note the significant difference in biodegradation rate between Figure 3-5d and 3-6d.

Figure 3-7 shows the change in phenol and oxygen concentration and the biodegradation rate over 80 years at the PAT well. Note that at the PAT well, the biodegradation rate is zero before pumping starts, as the well is located in the plume interior where the oxygen concentration is 0. Figure 3-7a shows that the phenol concentration declines sharply when pumping begins. Figure 3-7b shows that oxygen concentration was zero at the well location (plume interior) before pumping increases the flux of oxygen into the well and therefore the plume interior. Figure 3-7c shows the change in biodegradation rate over time; it is zero at the beginning, increases sharply, and then sharply declines due to the sharp decline in the phenol concentration (Figure 3-7a). The reason for this sharp decline in phenol concentration and therefore biodegradation rate is because the plume is so thin the Y dimension. It is expected that if the plume were wider in the Y dimension, that the biodegradation rate profile (Figure 3-7c) would decrease more slowly as more mass can enter orthogonally into the cell where the well is located. Figure 3-7d shows the hydraulic head in the well over time. The drawdown is 1.4 meters and heads at the well trend to steady state quite quickly (~2 years) due to a constant low pumping rate.

Figure 3-8 shows a 2D distribution of the phenol and oxygen concentration and the biodegradation rate before and after PAT intervention. After pumping, the max phenol concentration is reduced (Figure 3-8d vs 3-8a) and most of the phenol is depleted in the vicinity of the well, as expected. Oxygen is initially depleted in the plume interior (Figure 3-8b), but pumping increases the flux of oxygen into the plume (Figure 3-8e). Before pumping, biodegradation only occurs on the fringes, which is expected (Thornton et al., 2001a,b). However, after PAT intervention, biodegradation is increased at and near the well (Figure 3-8f). The peak biodegradation is much higher during PAT intervention due to the enhanced mixing of phenol and oxygen. The total mass biodegraded is increased from 9.7 kg at year 70 to 25.6 kg at year 80, which is a significant enhancement in biodegradation. However, it is not significant in absolute terms as the mass biodegraded is less than 1% of the total phenol mass.

3.7 Scenario development for chapter 4, 5, and 6

All scenarios were developed by careful consideration of the PAT system configuration design guidance by Satkin and Bedient (1988), Marquis and Dineen, (1994), US EPA (1997), Jones et al., (2002), Bau and Mayer (2006), and Piscopo et al., (2013). Besides the guidance and studies above, trial and error was used to design the scenarios. Only the most appropriate scenarios were selected for each chapter.

As demonstrated in the results of the 2D flow and transport model in section 3.6, the PAT well gradually increases the concentration of oxygen towards the well. Due to the direction of the flow field, perfectly east to west, and the low transverse dispersivity, there is low mixing transverse horizontally to the plume. The PAT well increases the mixing by advecting uncontaminated groundwater containing EAs horizontally transverse and perpendicularly to the plume. This enhancement of biodegradation is accentuated in 3D where this mixing induced by the PAT well is enhanced, as it also occurs above and below the well, where several layers will be affected at once.

Chapter 4 investigates the effect of PAT design variables, such as flow rate, well locations, and well configuration, as a proof of concept for enhancing NA using targeted PAT. A preliminary analysis of PAT systems which combines extraction and injection is also investigated. Two types of injection are considered: injection of water without EAs, with the aim of determining the effect of divergent flows on biodegradation as a function of plume fringe processes, and injection of EA-rich water (oxygen and nitrate). The objective of this chapter is to develop a series of modelling scenarios to assess the effectiveness of remediation using NA-enhanced PAT compared with conventional PAT.

The aim is to determine the effects of well location on biodegradation mass. The biodegradation mass at this location will also depend on factors such as the hydraulic conductivity and physical heterogeneity, and the distance of the well to the plume interior. The potential limitations of this approach are the biodegradation rates, the low flow velocity, and the magnitude of aquifer dispersivity, which depends on the system heterogeneity.

Chapter 5 builds upon chapter 4 by extending the investigation of the plume space to identify the pumping locations which enhance biodegradation the most, as the plume is heterogeneous and 3D. This research attempts to find ways to reduce the "diminishing returns" incurred by having more than 1 well. The diminishing returns occurred when multiple wells were used in the same simulation, their enhancement of biodegradation was less than the sum of what each of the wells achieved in separate simulations. The goal was to find a linear or at least sub-linear relationship between numbers of wells and biodegradation, rather than logarithmic. This research also investigates the effect of amendment concentration on biodegradation mass and compares it to the fringe biodegradation processes. Since biodegradation rates are low, due to reduced bioavailability, the injection of amendments could be used to introduce EAs to the most contaminated regions of the plume in addition to spreading the plume. In other words, amendment injections may enhance biodegradation by promoting the direct contact between the phenol and the EAs, in addition to enhancing the plume fringe reactions. The objective of this chapter was to examine multiwell scenarios and determine their impact on mass removal and in situ biodegradation, in addition to comparing the impact of different amendments and terminal electron accepting processes.

Chapter 6 builds upon chapters 4 and 5 by applying the lessons learned to complete the third objective of this thesis, which is to establish whether NA can be enhanced in situ to reduce the operational cost of PAT for the remediation of organic contaminants. This chapter aims to determine whether combinations of extraction and injection wells can be used to enhance biodegradation such that the total cost of remediation can be significantly reduced. The total remediation cost, GAC combined with the pumping electricity cost, will be calculated for each scenario using Eqs 16-20. The cost model is implemented for Chapter 6 only. The objective is to remediate 90% of the plume through combinations of extraction and biodegradation within 60 years, while the residual mass can be handled by NA only. The purpose of this relatively long remediation period is to compare modelling scenarios which may reach the remediation target (90%) at different times, as it is understood from previous modelling scenarios that a PAT system which enhances biodegradation will require more time to reach the remediation target than a PAT system designed to hydraulically remove the plume as quickly as possible.

PAGE INTENTIONALLY LEFT BLANK.

Chapter 4

Enhancing *in situ* biodegradation in groundwater using pump and treat remediation: a proof of concept and modelling analysis of controlling variables.

4.0 Abstract

A remediation approach which uses pump and treatment (PAT) to enhance the biodegradation of organic contaminants by increasing dispersive mixing between plumes and groundwater was evaluated for a phenol-contaminated aquifer, using a reactive transport model which simulates kinetic reactions between an electron donor (ED) in the plume and electron acceptor (EA) in the groundwater. The influence of system design and operation was examined in six modelling scenarios. Injection or extraction of groundwater increases biodegradation above no action and the location, pumping rate and distance between well(s) are important variables which influence biodegradation. An increase in pumping rate, distance of the wells from the plume centreline and changing the flow direction increases dispersive mixing between the plume and groundwater. This increases plume spreading and the plume fringe interface, providing a greater flux of dissolved EAs for biodegradation. In general, injection of groundwater containing natural EAs enhances biodegradation more than extraction. The enhancement of biodegradation is sensitive to the relative fluxes of ED and EA, as controlled by the arrangement of the wells. In the best performing scenario, the mass biodegraded was enhanced by 128%, compared with no PAT intervention.

4.1 Introduction

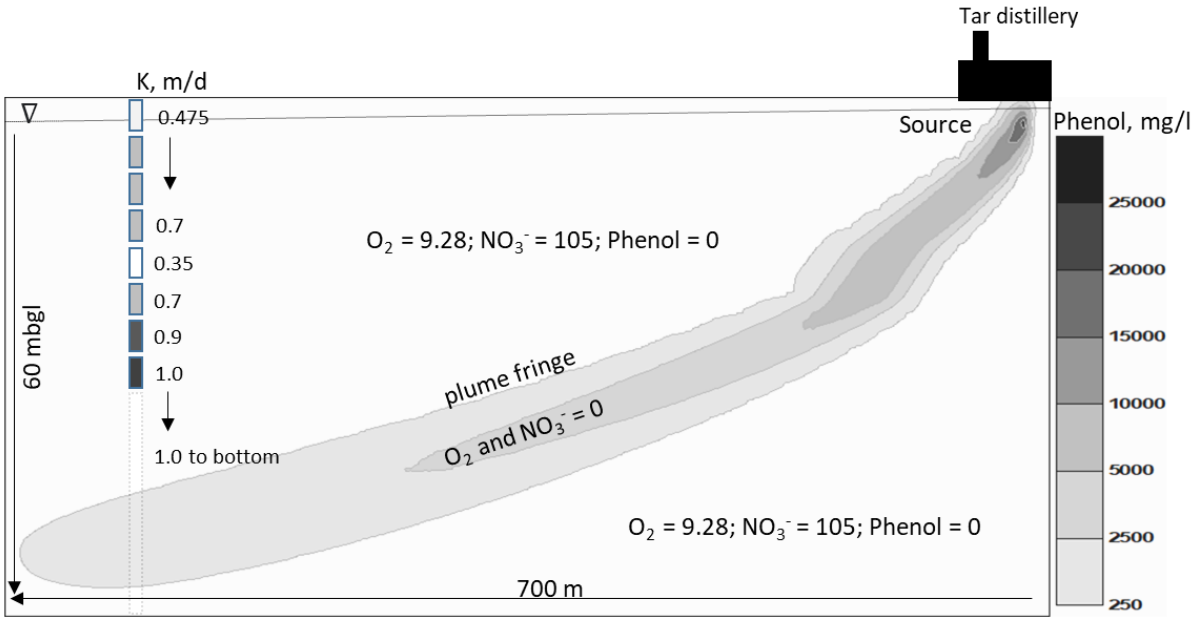

5

Figure 4-1. Schematic of plume concentration envelope based on groundwater chemistry and numerical simulation of site data. The concentrations shown are in mg/l. The hydraulic conductivity scale indicates that some values repeat throughout the layered system (Thornton et al., 2001b). Note that the concentrations of oxygen and nitrate are below detection in the plume due to biodegradation of the phenolic compounds. Note the vertical exaggeration of the depth scale.

Groundwater contamination by organic compounds is a major global problem, with at least 300,000 sites in the U.S. alone requiring remediation at an estimated cost of US$ 127B (NRC, 2013). There are a comparable number of contaminated sites in Europe that require remediation (Antelmi et al., 2020). A significant number of sites are unlikely to reach remediation targets within 50-100 years. For example, pump and treat (PAT) systems installed at US Superfund sites in the 1990s are still operating today, with current systems expected to have comparable operational timescales (USEPA, 2021).

PAT is most often used for hydraulic manipulation of contaminant plumes (source control/reduction and plume containment to prevent expansion or offsite migration), to reduce contaminant concentrations *in situ*, or to remove dissolved and mobile free-phase contaminant mass in groundwater for treatment (Mackay and Cherry, 1989; USEPA, 1990; 1996; Cohen et al., 1997; Suthersan et al., 2015; Truex et al., 2017; Speight, 2020). PAT is used to treat a wide range of contaminants, including coal tar distillates, phenols, polycyclic aromatic hydrocarbons, heterocyclic aromatic compounds, fuel hydrocarbons, and chlorinated solvents (Truex et al., 2017; Speight, 2020), and is most effective for the removal of contaminants in alluvial aquifers with relatively homogenous hydrogeological properties (USEPA, 1990; 1996; NRC, 2013). The limitations of PAT are well known and in more complex aquifers contaminant sorption-desorption hysteresis, free-phase dissolution kinetics and/or matrix diffusion may affect the effectiveness and application of this technology (Keely, 1989; USEPA, 1990; 1996; Cohen et al., 1997; McDade et al., 2013; NRC, 2013; Truex et al., 2017; Guo et al., 2019; Speight, 2020). Consequently, PAT systems are often used in combination with other remediation techniques to achieve clean-up goals at contaminated sites (USEPA, 1990; 1996; Cohen et al., 1997; Bayer et al., 2004; CRC CARE, 2019).

Natural attenuation (NA) is a risk-based remediation method, wherein the combined effect of naturally occurring physical, chemical and biological processes are used to treat contaminants *in situ* (Wiedemeier et al., 1999). Biodegradation is typically the most important process for organic contaminant attenuation (Bauer et al., 2009; Meckenstock et al., 2015). In contaminated groundwater, the plume fringe is a zone of enhanced biodegradation activity at the interface between the background groundwater and contaminant plume, driven by the dispersive mixing of electron acceptors (EA) in groundwater with biodegradable organic compounds in the plume (Thornton et al., 2001a,b; 2014; Jones et al., 2002; Tuxen et al., 2006; Bauer et al., 2009). As the length scale of dispersion is small relative to the size of a contaminant plume, reactions are limited to a narrow region at the plume fringe where the substrate and EAs mix (Reising, 2018; Sather et al., 2022; 2023). Biodegradation in plumes is limited by dissolved EA availability and aquifer dispersivity (Cirpka et al., 1999; Lerner et al., 2000; Thornton et al., 2001a; Jones et al., 2002; Tuxen et al., 2006; Sather et al., 2022; 2023), but can be increased if the supply (i.e. mass flux) of EAs into the plume can be increased by promoting mixing of the background groundwater and plume. Solute mixing in porous media can be enhanced by increasing the magnitude of dispersion, principally by controlling the flow velocity (Bagtzoglou and Oates, 2007; Werth et al., 2006; Ye et al., 2015; Neupauer et al., 2020). Furthermore, dispersive mixing of reactants can occur due to anisotropy, hydraulic conductivity contrasts between porous media, chaotic advection, flow-folding and flow

focusing in high permeability zones (Bagtzoglou and Oates, 2007; Werth et al., 2006; Eckert et al., 2012; Piscopo et al., 2013; Ye et al., 2015; 2021; Xu et al., 2018; Suk et al., 2021; Sather et al., 2023). Consequently, biodegradation can be increased under conditions which enhance the flow velocity and/or dispersion (Werth et al., 2006; Bauer et al., 2009). Hence, the PAT system may be used to address mass transport limits on *in situ* biodegradation, by suitable modification of the ambient flow field to enhance dispersive mixing of solutes.

Previously, Thornton et al. (2014) demonstrated at the field scale that the biodegradation of phenolic compounds can be increased by a PAT well pumping at the plume fringe. In that study, the *in situ* biodegradation rate of phenolic compounds at the plume fringe doubled over a 3-year period during operation of the PAT (groundwater extraction rate of 6-50 m^3/d). This was achieved by reducing the concentration of phenolic compounds in the plume which inhibit biodegradation (dilution of plume contaminants) and increasing the dispersive mass flux of dissolved EAs into the plume from the background groundwater (induced by the elevated pumping rates) and surface area of the plume fringe interface for biodegradation. This study therefore showed that it is possible to combine PAT with NA to improve remediation performance, by suitable modification of the ambient flow field to enhance dispersive mixing of solutes, although this is logically influenced by the design of the PAT system (e.g. injection/extraction well locations and spacing, pumping rate and duration).

Given the limitations of conventional PAT systems, the integration of these with other remediation techniques is recommended to enhance its effectiveness (USEPA, 1990; 1996; 2021). However, while guidelines exist for the deployment of conventional PAT systems (e.g. Cohen et al, 1997; USEPA, 1990; 1996; 2021), there is currently no technical basis to support the development of an integrated PAT and NA system (as proposed herein) for contaminated groundwater remediation. The motivation for this research is to explore the scientific basis for integrating PAT with NA as a remediation concept. The novelty of the study lies in the synergy of combining the two technical approaches of PAT with NA to increase mass biodegradation relative to mass extraction by the PAT well(s), over that possible with PAT alone. While well location, pumping rate and injection/extraction strategies are known to influence remediation performance in these separate contexts, this has not been formally considered in their combined application. The aim of this study is therefore to examine this approach as a proof of concept and to understand the influence of operational variables, such as well location, pumping strategy and rate, on PAT performance to enhance the *in situ* biodegradation of organic contaminants in groundwater for remediation and plume management. The specific objectives are to: (a) Analyze the effect of well location, pumping rate and pumping strategy on mass removal and biodegradation; (b Identify strategies which increase the mass biodegraded relative to the total contaminant mass extracted; and (c) Investigate the effectiveness of a PAT system that combines extraction and injection of groundwater.

The approach is evaluated at a site on a UK sandstone aquifer contaminated with a plume of phenolic compounds, in which a PAT system has been installed for plume management (Baker et al., 2012; Thornton et al., 2014). Phenol is a common groundwater contaminant from many industrial processes (e.g. wood preservation plants, organic chemical manufacturing, coal tar processing, gasworks) and is used as a candidate organic contaminant in this study.

4.2 Methodology

Table 4-1. Input parameters used in the scenario modelling.

Flow and transport parameters		**Value**		**Data source**
Effective porosity (-)		0.125[a]		Core samples/geophysical logs[a]
Hydraulic conductivity range, K (m/d)		0.35-1.0[a]		Pumping tests and RFM[c]
Recharge rate (m/d)		8.00e-04[a]		Effective infiltration estimation[b]
Longitudinal dispersivity (m)		1[b]		
Vertical transverse dispersivity (m)		4.00e-03[b]		Tracer tests and numerical modelling
Horizontal transverse dispersivity (m)		1.00e-02[b]		
Grid block size (m^3)		5		Well screen lengths are 5 meters.[a]
Model length, width, and depth (m)		1200x300x255		
		Species		
Biodegradation module parameters	*Phenol*	*Oxygen*	*Nitrate*	
Half saturation constant (mg/l)	-	0.1[b]	0.5[b]	Determined by a mesocosm experiment[b]
Inhibition constant (mg/l)	-	0.9[b]	0.9[b]	
Decay rate (1/T)	-	3.44e-05[b]	3.44e-06[b]	
Yield coefficient (-)	0	2.38[b]	3.69[b]	Reaction stoichiometry
Source concentration (mg/l)	25000	0	0	Groundwater quality monitoring
Background groundwater concentration (mg/l)	0	4.5-9.28[b]	91-105[b]	Groundwater quality monitoring

d. Unpublished data from confidential third-party consultant reports.
e. Values used in previous modelling studies on the site [Watson et al. (2005) and Mayer et al. (2001)].
f. RFM refers to Radial Flow Modelling undertaken by third party consultants.

4.2.1 Study site

The considered field site is a fine-grained, unconfined, fluviatile, sandstone bedrock aquifer located underneath a former coal tar distillation plant in UK. The site has been extensively investigated over 25 years, with studies on the interpretation of groundwater contamination (Williams et al., 2001), redox processes and contaminant biodegradation (Thornton et al., 2001a; 2014; Wu et al., 2006; Baker et al., 2012;), aquifer stable isotope geochemistry (Spence et al., 2001), aquifer microbiology (Pickup et al., 2001; Elliot et al., 2010; Rizoulis et al., 2013; Mujica-Alarcon et al., 2021), plume mass balance (Thornton et al., 2001b) and reactive transport modelling (Mayer et al., 2001; Watson et al., 2005). The site history, summarised here, is described in detail in Williams et al. (2001).

A mixed plume of phenolic compounds (primarily phenol, cresols and xylenols) extends approximately 700 m down hydraulic gradient of the site, with an estimated width of 150 m and depth of 60 m. Groundwater flow is westerly, with a pore velocity between 4-11 m/year, consistent over the history of the plume. Vertical flow due to groundwater recharge is also important (Table 4-1). Previous investigations have identified a heterogeneous distribution of phenolic compounds and biogeochemical processes responsible for their biodegradation within the plume (Thornton et al, 2001a). The plume is anchored by a dense non-aqueous phase liquid (DNAPL) source, with concentrations of individual phenolic compounds (e.g., phenol) reaching 25,000 mg/l. Considering this, and to reduce the complexity of the numerical model, phenol was selected as a representative organic contaminant for the simulations and the concentrations of all other phenolic compounds were converted into equivalent phenol concentrations.

Previous studies have shown that the phenolic contaminants are biodegraded by several processes, with most mass loss (>90%) arising from consumption of oxygen and nitrate in the groundwater (Lerner et al., 2000; Thornton et al., 2001a,b; Mayer et al., 2001; Jones et al., 2002; Watson et al., 2005). For this reason, the modelling scenarios were developed to assess the contribution of these two EAs to biodegradation, as influenced by the PAT system.

4.2.2 Flow and reactive transport model

A 3-D flow and transport model was developed using the input data in Table 4-1. Groundwater flow is governed by the classical PDE:

$$\frac{\partial}{\partial x}\left(K_{xx}\frac{\partial h}{\partial x}\right)+\frac{\partial}{\partial y}\left(K_{yy}\frac{\partial h}{\partial y}\right)+\frac{\partial}{\partial z}\left(K_{zz}\frac{\partial h}{\partial z}\right)+W=S_s\frac{\partial h}{\partial t} \quad \text{Eq 1}$$

where K_{xx}, K_{yy}, and K_{zz} are hydraulic conductivity along the x, y, and z coordinate axes (L/T); h is the hydraulic head (L); W is a volumetric flux per unit volume representing sources and/or sinks, such as recharge and wells (1/T); S_s is the specific storage of the porous material (1/L); and t is time (T). The model is isotropic ($K_{xx}=K_{yy}=K_{zz}$) and heterogeneous, with hydraulic conductivity generally increasing with depth (Figure 4-1). The groundwater flow system was set to steady state, as the hydraulic heads trend to steady state after ~2 years of pumping. Equation 1 is solved using MODFLOW-2005 (Harbaugh et al., 2005), based on a finite different grid characterized by 200 columns, 60 rows, and 38 layers, with a grid-block size of 5m × 5m × 5m in the region of the plume. The flow model is by characterized by a constant head boundary condition on the east and west (see Figure 4-1), with groundwater recharge applied to the water table (Table 4-1). Other boundaries are set as "no flow". MODFLOW-2005 calculates the pore velocity field ($\boldsymbol{v}=-\frac{K}{\phi}\cdot\nabla h$, where ϕ is the effective porosity), which is then used in the multispecies reactive contaminant transport simulator MT3D-USGS (Bedekar et al., 2016) to solve a system of coupled partial differential equations, each of which represents the mass continuity for the species simulated:

$$\nabla(\phi\cdot\mathbf{D}\cdot\nabla C_i)-\nabla(\phi\cdot\mathbf{v}\cdot C_i)+\mathrm{q}_{s,i}\cdot C_{s,i}+R_i=\frac{\partial(\phi\cdot C_i)}{\partial t} \quad \text{Eq 2}$$

where C_i is the concentration of species i [M/L^{-3}], **D** is the hydrodynamic dispersion tensor [L^2/T^1], $\mathrm{q}_{s,i}$ [M/L^3] represents the specific discharge for species i, $C_{s,i}$[M/L^3] represents the concentration of sources for species i, and R_i represents the reaction rate of species i [M/L^3/T^1]. In this case, there are three species ($i=1,2,3$), and the term R_i depends on ongoing kinetic reactions occurring between 1 electron donor (ED) and 2 electron acceptors (EAs), simulated using a Monod kinetic model developed by Lu et al. (1999), following approaches used in previous studies (Rolle et al., 2008).

The stoichiometric reactions between phenol (C_6H_6O), which is the ED, and the two EAs, oxygen (O_2) and nitrate (NO_3^-), are described by the following equations:

(a) $C_6H_6O + 7O_2 \rightarrow 6CO_2 + 3H_2O$ Eq 3

(b) $C_6H_6O + \frac{28}{5}NO_3^- + \frac{28}{5}H^+ \rightarrow 6CO_2 + \frac{14}{5}N_2 + \frac{29}{5}H_2O$ Eq 4

Eq 3 and 4 are presented to illustrate the stoichiometry of the reactions which are considered in Eq 6.

The rate of ED biodegradation ($i = 1$ in Eq. 2) is given by (Lu et al., 1999):

$$r_{ED} = \sum_{j=1}^{2} r_{ED,j} = -\left\{\frac{k_{EA_1} \cdot [EA_1]}{K_{EA_1} + [EA_1]} + \frac{k_{EA_2} \cdot [EA_2]}{K_{EA_2} + [EA_2]} \cdot \frac{K_{I,EA_1}}{K_{EA_1} + [EA_1]}\right\} \cdot [ED] \quad \text{Eq 5}$$

where $[ED]$, $[EA_1]$, and $[EA_2]$ represent the concentration of the ED and the two EAs (M/L^3), respectively; k_{EA_1} and k_{EA_2} are first-order decay rate constants for the EAs (1/T); K_{EA_1} and K_{EA_2} are the "half saturation" constants for the EAs (M/L^3); K_{I,EA_1} (M/L^3) is the inhibition constant for the first EA, oxygen, which has the highest Gibbs free energy (Christensen et al., 2000). Correspondingly, the rate of consumption of the two EAs, which affects the concentration of the EAs, ($i = 2, 3$ in Eq. 2) is given by:

$$r_{EA_j} = Y_{EA_j} \cdot r_{ED} \quad \text{Eq 6}$$

where $Y_{EA_j} (j = 1, 2)$ is the yield coefficient for the EA, that is, the EA mass used per ED unit mass biodegraded, calculated from the stoichiometry in Eqs. 3 and 4 (Table 4-1).

The mass biodegraded is obtained by integration of the rate of ED biodegradation r_{ED} (Eq 5) over the model domain for the remediation period T, that is:

$$M_{bio}(T) = \int_{t=0}^{T} \left[\int_{\Omega} \theta \cdot r_{ED} \cdot d\Omega\right] dt \quad \text{Eq 7}$$

where Ω represents the 3D model domain, θ (/) is the effective porosity, r_{ED} (M/L^3/T) is the biodegradation rate (Eq 5). This integral is numerically calculated over the model grid and the discretization of the time interval $[0, T]$ adopted in the flow and transport simulation.

Table 4-2. Scenarios (A-F) evaluated in 10-year modelling simulations and the respective approach followed (see text for explanation).

Scenario	Description	Injection/extraction well layout
A. Effect of extraction well distance along flow path	Extraction well is located on the plume centerline, at distances which increase by 200m in successive simulations. Well extraction rate is fixed at $\underline{Q}$=30 m^3/d.	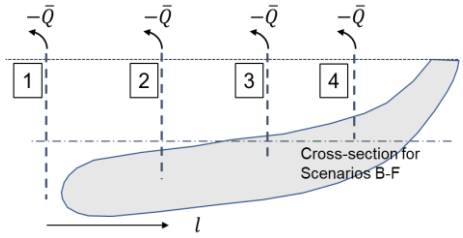
B. Effect of asynchronous injection and extraction rate	Well location is fixed ($\underline{d}$=m) and injection/extraction rate Q progressively increased. This scenario includes injection of either GWWEA or GW in separate sub-scenarios (see text).	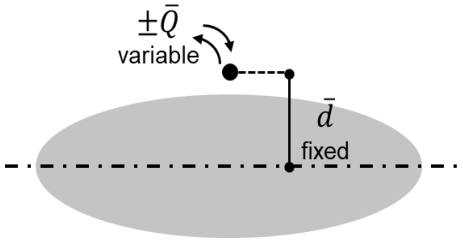
C. Effect of asynchronous extraction/injection well location lateral to flow path	Injection/extraction well is moved an increasing lateral distance from the plume centerline. Well pumping rate is fixed at $\underline{Q}$=±30 m^3/d. This scenario includes injection of either GWWEA or GW in separate sub-scenarios (see text).	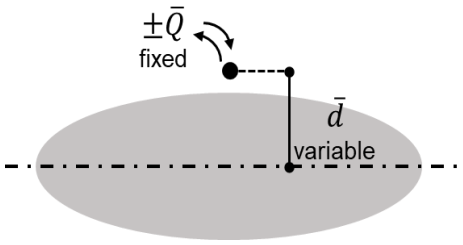
D. Effect of well pumping rate for two concurrent extraction wells	Extraction wells are placed symmetrically at a fixed lateral distance $\underline{d}$=m from the plume centerline, with $\underline{Q}$ progressively increased.	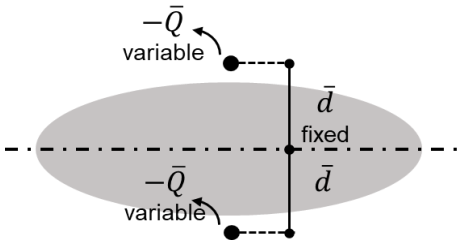
E. Effect of location for two concurrent extraction wells	Extraction wells are placed symmetrically at a progressively increasing lateral distance $\underline{d}$ from the plume centerline, with $\underline{Q}$ fixed at 60 m^3/d.	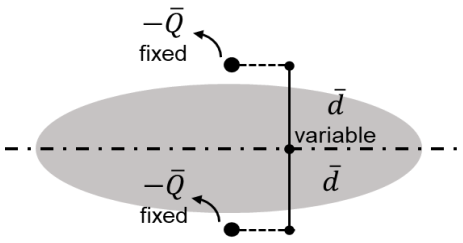
F. Effect of location for concurrent extraction and injection wells	Injection well is located on the plume centerline and one extraction well is positioned laterally at an increasing distance $\underline{d}$, with the pumping rate $\underline{Q}$ fixed at ±30 m^3/d. This scenario includes injection of either GWWEA or GW in separate sub-scenarios (see text).	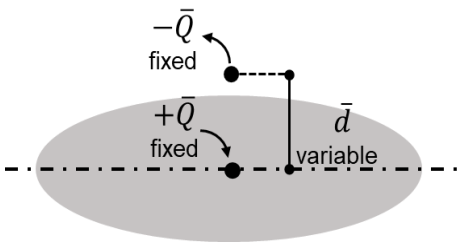

4.2.3 Model development and scenarios

The flow and reactive transport models presented in Section 3.2 were used to create a hypothetical phenol plume using data on the physical aquifer characteristics obtained from previous site investigations conducted by third party consultants (Table 4-1), and research published over the past 25 years (Mayer et al., 2001; Thornton et al., 2001b; Watson et al., 2005). The rationale behind using this approach was not to interpret the actual contamination conditions at the site, but to instead develop a model that is internally coherent and consistent. This enabled a hypothetical but realistic example model to be created, with results that can be extended to other sites with similar characteristic and/or contaminated with coal tar distillate plumes (e.g. Blum et al., 2011).

Figure 4-1 shows a contaminant plume simulated with this model. This is in excellent agreement with plumes produced in other studies at the site using the same dataset (Mayer et al., 2001; Watson et al., 2005), and is similar to the concentration distribution observed in monitoring surveys conducted at the same time (Williams et al., 2001; Thornton et al., 2001b). To create the numerical model, a regional model with local canals and pumping stations was developed based on data from confidential third-party consultant reports. Recharge was estimated from effective infiltration and applied to the water table. Initial simulations revealed that the most important parameters for the transport model are recharge and hydraulic conductivity. These initial simulations also revealed that the groundwater flow in a 1.2 km^2 square area encompassing the plume is steadily east to west, which is supported by site data. Therefore, the original regional flow model was then cropped to a size appropriate for simulating the range of hydraulic gradients observed at the site (horizontal hydraulic gradient of 0.003-0.007). The eastern and western constant head boundary conditions of 103m and 98m, which were acquired from previous groundwater monitoring at the site, were used to simulate the average horizontal hydraulic gradient for the site (0.0042). The north and south boundaries are simulated as general head boundaries with linearly decreasing head from east to west, and the bottom boundary is no flow. The contaminant source consists of DNAPL (coal tar) trapped within shallow groundwater at the site, which was simulated as a single 5x5x5 m^3 cell (the source term is unknown). In order to generate a plume comparable to that observed at the site, the release of phenols from the source was simulated at 1344 mg/d over 70 years. This was determined to give the corresponding concentration distribution in the aquifer, with a maximum dissolved concentration of 25,000 mg/l (similar to the source zone) and total plume mass of 34,000 kg. The source was then assumed to be removed (as per conventional remediation practice) before PAT operations commenced (Cohen et al., 1997). As the magnitude of dispersion is a function of the aquifer dispersivity (Ye et al., 2015), values of this coefficient were taken from previous modelling studies at the site (Table 4-1), which were of the same order as those estimated in other studies (e.g. Cirpka et. al., 1999, 2006; Cupola et al., 2015; Reising, 2018).

Note that the EA concentrations used correspond to those of the background groundwater (Table 4-1). In some of the investigated scenarios, groundwater with this EA composition is injected into the aquifer, with the suffix “GW” to denote the results. In other scenarios, groundwater without EAs (with the suffix “GWWEA”), was injected. Monod parameter values

from previous studies were used for the kinetic reaction component of the model (Mayer et al., 2001; Watson et al., 2005). Based on unpublished calculations of the reaction rates, the most important parameters that are subject to change in space and time are the ED and EA concentrations. The other Monod parameters are constant. See Figure 4-1 for more details.

Six numerical modelling scenarios (experiments) were developed for this study (Table 4-2). Scenario A depicts a longitudinal, vertical cross section of the plume, whereas scenarios B-F depict horizontal cross-sections with wells positioned laterally from the idealised plume centreline and/or on it. The pumping rate ($\bar{Q}$) can be negative (extraction) or positive (injection). The performance of the system in each scenario was compared using ratios of total phenol mass removed (M_{rem}) to initial phenol mass (M_0), M_{rem}/M_0. M_{rem} has two components, M_{bio}, the mass of phenol biodegraded, and M_{ext}, the mass of phenol extracted. Hence, $M_{rem} = M_{bio} + M_{ext}$. Normalizing M_{bio} and M_{ext} to the initial plume mass, M_0, allows the results to be compared directly and shows the relative contribution of mass removal by each process.

For all scenarios except Scenario A the well screen is 5-m long and located approximately 70 mbgl. This pumping depth has the highest aquifer hydraulic conductivity and was selected to allow for higher pumping rates. The wells in each scenario are pumping for a period T of 10 years. The simulations within each scenario are carried out independently to prevent the effects of previous simulations interfering with subsequent results. For all groundwater (suffix GW) injection sub-scenarios, groundwater with a concentration of 9.28 mg/l of oxygen and 105 mg/l of nitrate (aquifer concentration) was injected. For groundwater without EA (suffix GWWEA) injection scenarios, no EAs are injected. Simulations in each scenario were carried out until the value of M_{rem}/M_0 or biodegradation began to decrease. For scenarios where M_{rem}/M_0 and biodegradation did not increase, they were capped at 7 simulations, as this was sufficient to evaluate the trend. In all, 68 simulations were conducted.

The following controlling variables were tested in several scenarios, adjusting each for (i) well locations in the longitudinal and transverse horizontal planes, (ii) pumping rates, (iii) effectiveness of an injection vs extraction well, (iv) impact of increasing the pumping rate for 2 wells, (v) impact of increasing the transverse horizontal distance between 2 pumping wells with a constant pumping rate, and (vi) the impact of an injection and extraction well in the same scenario. The aim of these scenarios was to determine strategies which increase M_{bio}/M_0 while decreasing or minimizing M_{ext}/M_0.

Scenario A investigates the effect of extraction well location along the plume flow path on the enhancement of biodegradation *in situ* (Table 4-2A). A single extraction well located in the plume interior/centreline is tested in 4 simulations which span the length (L) of the plume. Since the plume flow path is diving to recharge, the plume centreline changes with longitudinal distance and the depths of the well screens change accordingly (between 10 and 70 mbgl) for each simulation to keep the well within the plume interior. The variable in this scenario is L (the x location), which begins at the plume front at 200 m, and is increased by 200 m until near the plume source, at 800 m. The well extracts groundwater at -30 m^3/d for 10 years. It is hypothesized that M_{bio}/M_0 and M_{ext}/M_0 will increase as longitudinal distance trends to 800 m.

Scenario B investigates the effect of pumping rate on the enhancement of biodegradation *in situ* (Table 4-2B). The well is consistent for all simulations, located 15m from the plume centreline/interior and at the plume fringe. This scenario has three sub-scenarios: extraction, injection of groundwater without electron acceptors (GWWEA), and injection of groundwater (GW) with the peak concentration of EAs found in the aquifer. The sub-scenarios are labelled as B-Ext, B-GWWEA, and B-GW in Figure 4-4a. For each sub-scenario, the pumping rate of the well is varied from 5 to 100 m^3/d. Seven simulations are run for each sub-scenario. The purpose of having separate groundwater injection scenarios (with and without EAs) is to observe the effect of only plume fringe biodegradation processes, as there is no biodegradation within the plume core when GWWEA is injected. The variable tested is the effect of the pumping rate, the constant well location at the plume fringe and the type of groundwater injected. These are compared with the no-action case, other scenarios, and among the sub-scenarios. The first simulation in Scenario B-Ext is comparable to Scenario A at 800 m, as they have the same pumping rate; the only variable that changes is that the well in Scenario B-Ext is 15 m further away from the plume centreline than in Scenario A at 800 m; thus, the impact of distance can be compared. The difference between pumping at the plume centre vs plume fringe was determined in this comparison. It is hypothesized that M_{bio}/M_0 for Scenario B will increase with pumping rate. M_{ext}/M_0 will increase with pumping rate only for Scenario B-Ext.

Scenario C investigates the effect of lateral well location on the enhancement of biodegradation *in situ* (Table 4-2C). The scenario has three sub-scenarios: extraction, injection of groundwater without electron acceptors (GWWEA), and injection of groundwater (GW) with the peak concentration of EAs found in the aquifer. The sub-scenarios are labelled as C-Ext, C-GWWEA, and C-GW in Figure 4-4a. The purpose of having separate groundwater injection scenarios (with and without EAs) is to compare the effect of plume fringe vs core biodegradation processes, as there is no biodegradation within the plume core when GWWEA is injected. Six simulations are run for each sub-scenario. The only changing variable is the north horizontal transverse distance to the plume interior/centreline, which is varied by 20 m each step and then by 10 m for the final two steps. Since Scenario C starts at the plume centreline (d = 0 m), this specific simulation is directly comparable to Scenario A at 800 m; thus, the impact of varying longitudinal vs lateral distance can be directly compared. It is hypothesized that for Scenario C-Ext, M_{bio}/M_0 will increase and M_{ext}/M_0 will decrease as lateral distance from the plume centreline increases. For Scenario C-GWWEA and C-GW, only M_{bio}/M_0 are expected to increase. Therefore, the relevant comparison between Scenario B-Ext and Scenario A at 800 m is the effect of the change in pumping rate.

Scenario D investigates the effect of variable pumping rate for two extraction wells on the enhancement of biodegradation *in situ* (Table 4-2D). The extraction wells are located 15m north and south of the plume centreline (cumulative 30 m lateral distance). The pumping rate is split between the two wells and is varied from 5 to 100 m^3/d. This scenario is essentially the same as Scenario B-Ext, except with an extra well. The cumulative pumping rate in Scenario D is kept identical to Scenario B-Ext so that the effect of an additional well can be directly compared. It is hypothesized that M_{bio}/M_0 and M_{ext}/M_0 will increase with the pumping rate.

Scenario E investigates the effect of lateral distance between two extraction wells on the enhancement of biodegradation *in situ* (Table 4-2E). This scenario is identical to Scenario D, except that the lateral distance between the two extraction wells changes during each simulation and the cumulative pumping rate is kept constant. The distance between the wells starts at 30 m and is increased by 30 m during successive simulations to a maximum of 90 m. A cumulative pumping rate of -60 m^3/d was chosen, which is comparable to the mid-range pumping rate in Scenario D and Scenario B. It is hypothesized that M_{bio}/M_0 will increase and M_{ext}/M_0 will decrease as the distance between the two wells increases.

Scenario F investigates the effect of lateral distance of a doublet injection and extraction well on the enhancement of biodegradation *in situ* (Table 4-2F). This scenario has two sub-scenarios: extraction combined with injection of groundwater without electron acceptors (GWWEA) and extraction combined with injection of groundwater (GW) with the peak concentration of EAs found in the aquifer. The sub-scenarios are labelled as F-GWWEA and F-GW in Figure 4-4a. The purpose of having separate groundwater injection scenarios (with and without EAs) is to observe the effect of plume fringe vs plume core biodegradation processes, as there is no biodegradation within the plume core when GWWEA is injected. The lateral distance between the injection and extraction well starts at 15m and is increased by 15m with subsequent simulations, to a maximum of 105m. As with Scenario D, the effect of lateral distance in well spacing is investigated. However, this scenario differs in that one well is an injection well, which may increase plume spreading (and therefore biodegradation) to a greater degree due to the divergent flows caused by injection. The pumping rates are kept constant at 30 and -30 m^3/d for the injection and extraction wells, respectively. It is hypothesized that using an injection and extraction well doublet will increase spreading of the plume and enhance M_{bio}/M_0 greater than a scenario in which this is done with two extraction wells, and M_{ext}/M_0 will decrease as the lateral distance between the two wells increases.

An additional experiment was conducted to consider the effect of dispersivity coefficients on mass removal by biodegradation, as a basis to understand the role of dispersion. The dispersivity in all dimensions was changed for three test cases, with a model duration of 10 years. The dispersivity coefficients were estimated using the regression equation from Xu and Eckstein (1995) and data from Gelhar et al., (1992). Each test case is split into a simulation with “no intervention”, in which there are no wells and only intrinsic biodegradation is quantified, and a simulation with groundwater injection at 30 m^3/d with a well located 15m lateral to the plume centreline (same location as Scenario B-GW). In case 1, the dispersivity (meters) is the same as the baseline model (α_x=1, α_y=1e-2, α_z=4e-3). In case 2, the dispersivity is reduced 10x from case 1 (α_x=0.1, α_y=1e-3, α_z=4e-4) and in case 3, the dispersivity is increased 10x from case 1 (α_x=10, α_y=1e-1, α_z=4e-2). Beside the dispersivity coefficients, all other parameters are consistent for all cases (Table 4-1).

4.3 Results and discussion

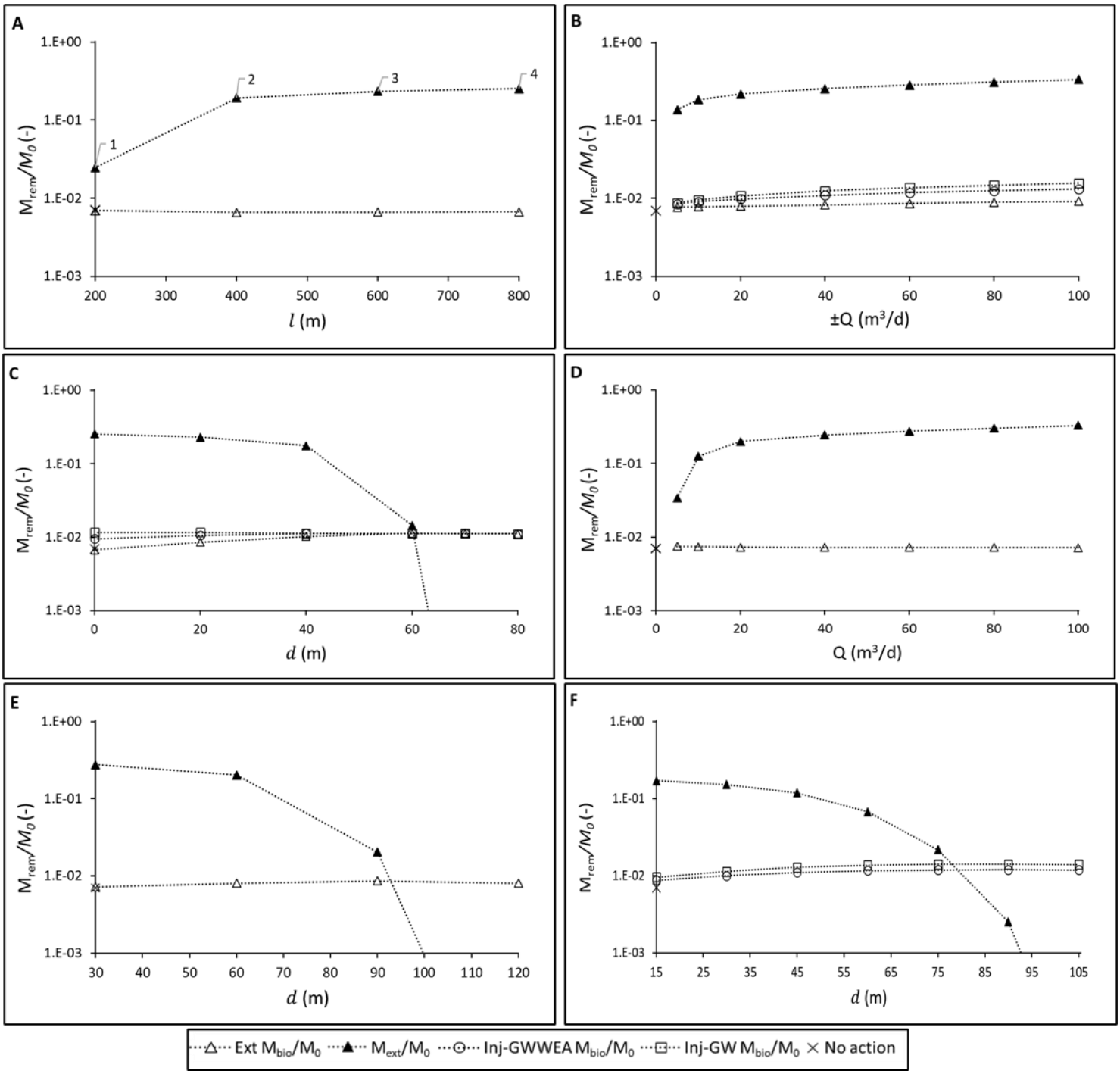

Figure 4-2. Ratios of contaminant mass removed for scenarios A-F. The y-axis is the contaminant mass removed (M_{rem}) by biodegradation *in situ* (M_{bio}) and extraction (M_{ext}), normalised to the initial mass (M_0). For Scenario A, the numbered points correspond to the well locations in Table 4-2, where well 1 is at the front of the plume (200m), downgradient of the source, and well 4 is close to the source (800m). "No action" refers to the initial condition in which NA occurs without PAT intervention.

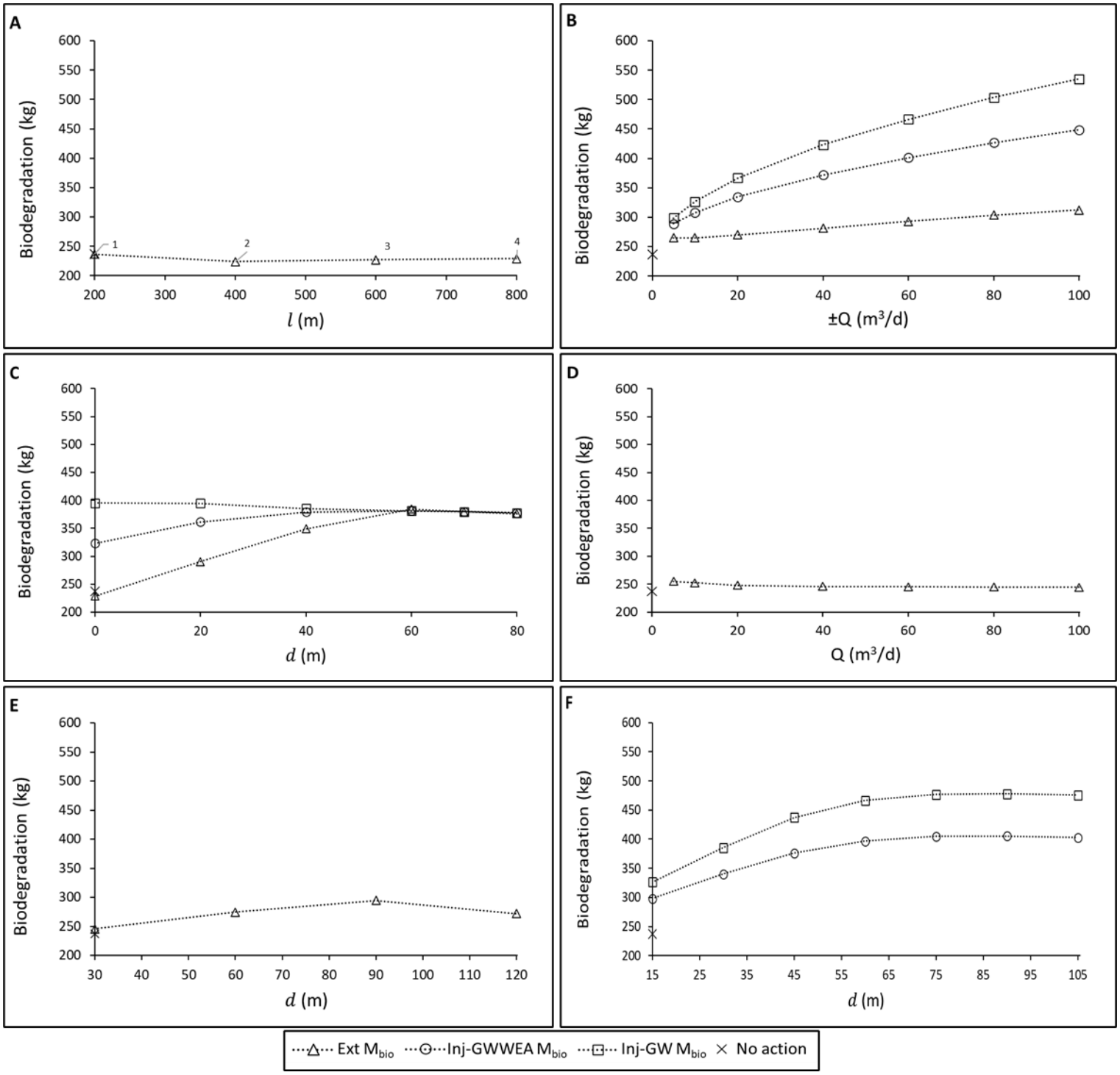

Figure 4-3. Mass removed by biodegradation for scenarios A-F. The x-axis is the variable under consideration for the particular scenario and the y-axis is the mass removed by biodegradation, for the entire model domain over 10 years, in kilograms. GWWEA is injection of groundwater without EAs and GW is injection of groundwater with EAs.

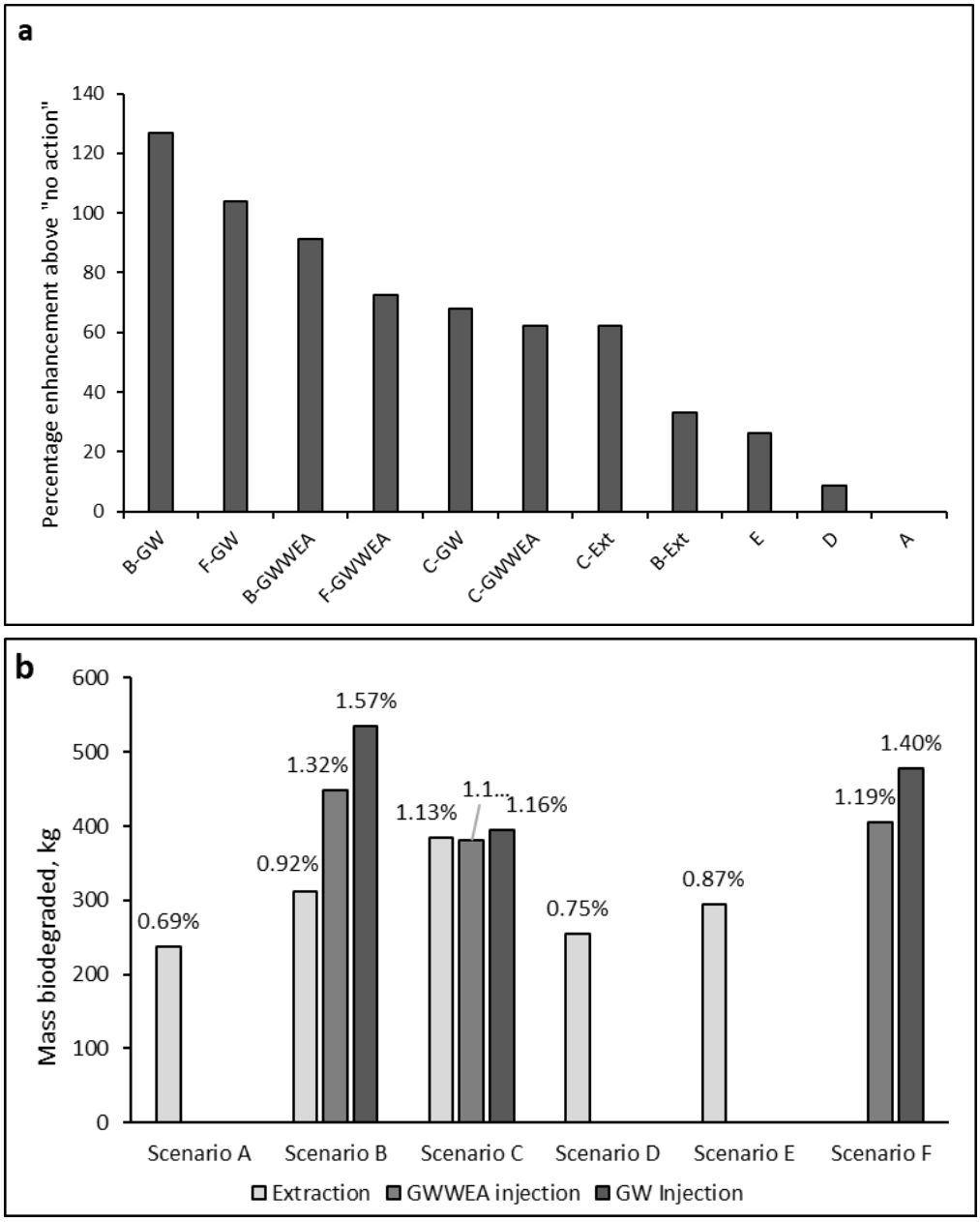

Figure 4-4. (a) Scenarios with respective sub-scenarios ranked by percentage enhancement in biodegradation above “no action”, from highest to lowest. (b) Absolute and percentage of total plume mass biodegraded.

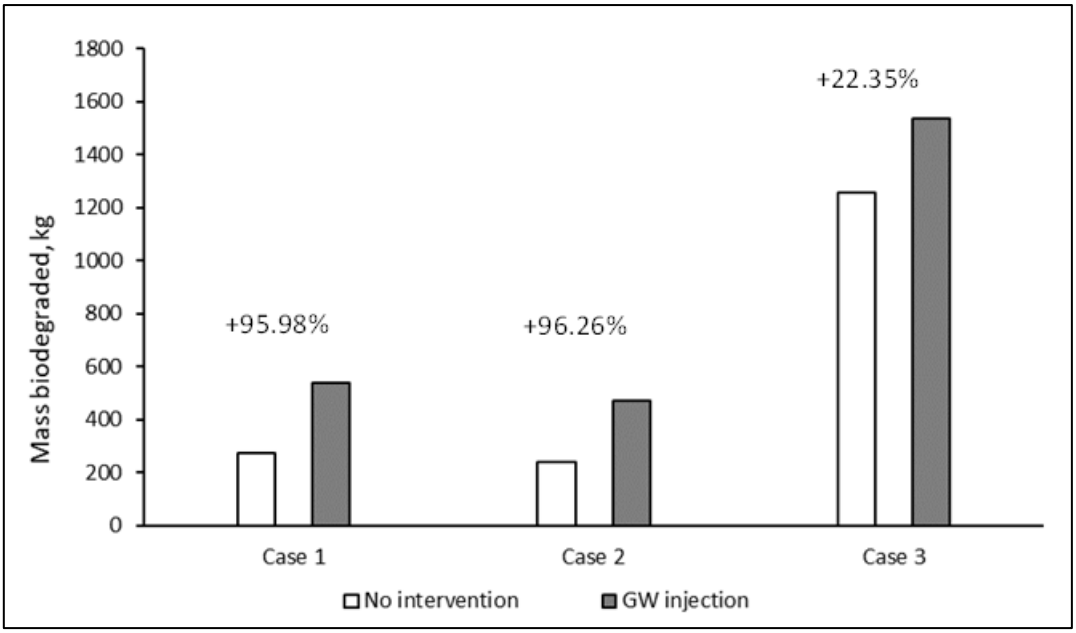

Figure 4-5. Total mass removed by biodegradation for an experiment in which the dispersivity in all dimensions is changed for three test cases, each of which were simulated over 10 years. Each test case is split into a simulation with "no action", in which there are no wells and only intrinsic biodegradation is measured, and a simulation with groundwater injection at 30 m^3/d with a well located 15m lateral to the plume centerline (same location as Scenario B-GW). The percentages show the enhancement of biodegradation above the "no action" case due to GW injection. The dispersivity values are presented at the end of section 4.2.3.

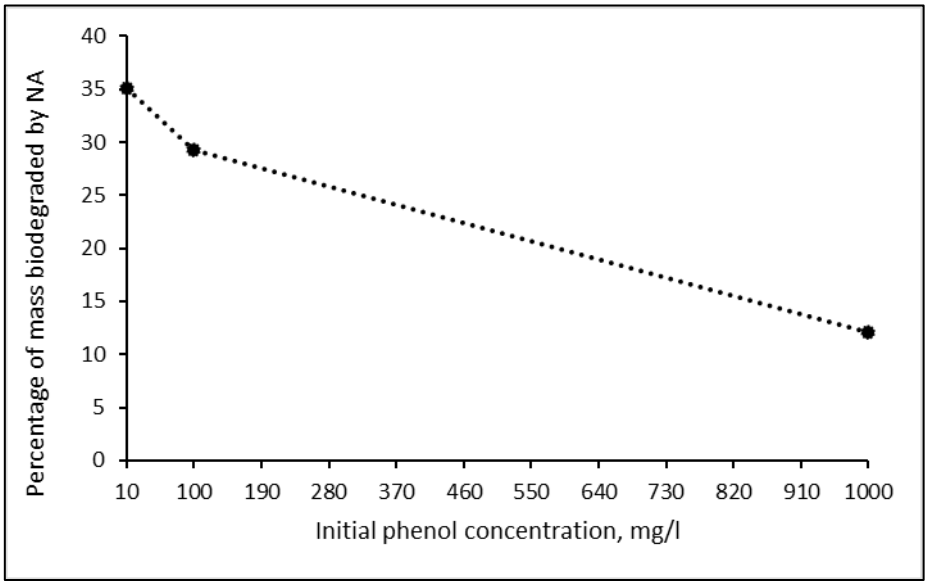

Figure 4-6. Shown above is the relationship between initial phenol concentration and the percentage of total contaminant mass that is degraded by intrinsic NA. No PAT intervention is considered in this case.

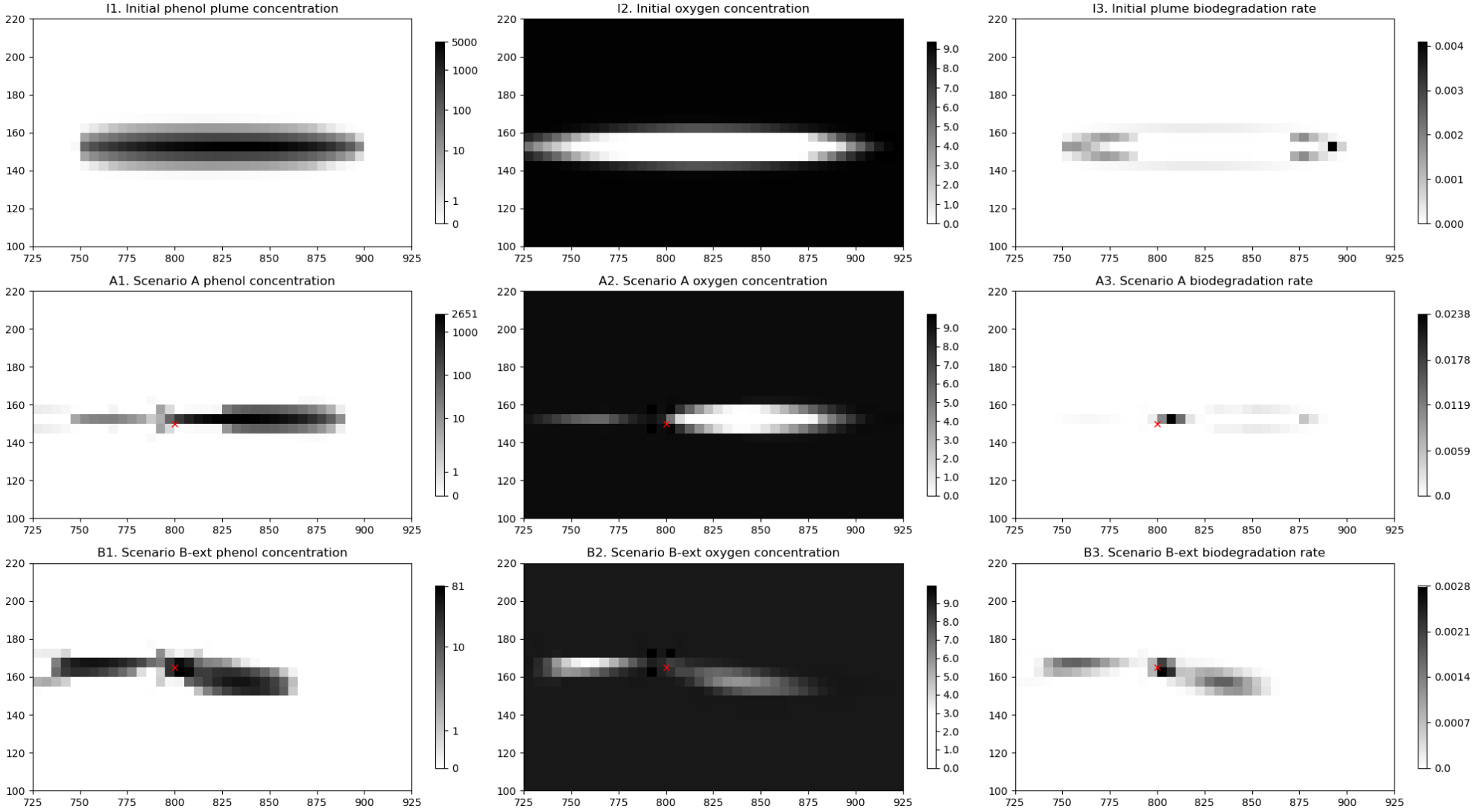
I1. Initial phenol plume concentration
I2. Initial oxygen concentration
I3. Initial plume biodegradation rate
A1. Scenario A phenol concentration
A2. Scenario A oxygen concentration
A3. Scenario A biodegradation rate
B1. Scenario B-ext phenol concentration
B2. Scenario B-ext oxygen concentration
B3. Scenario B-ext biodegradation rate

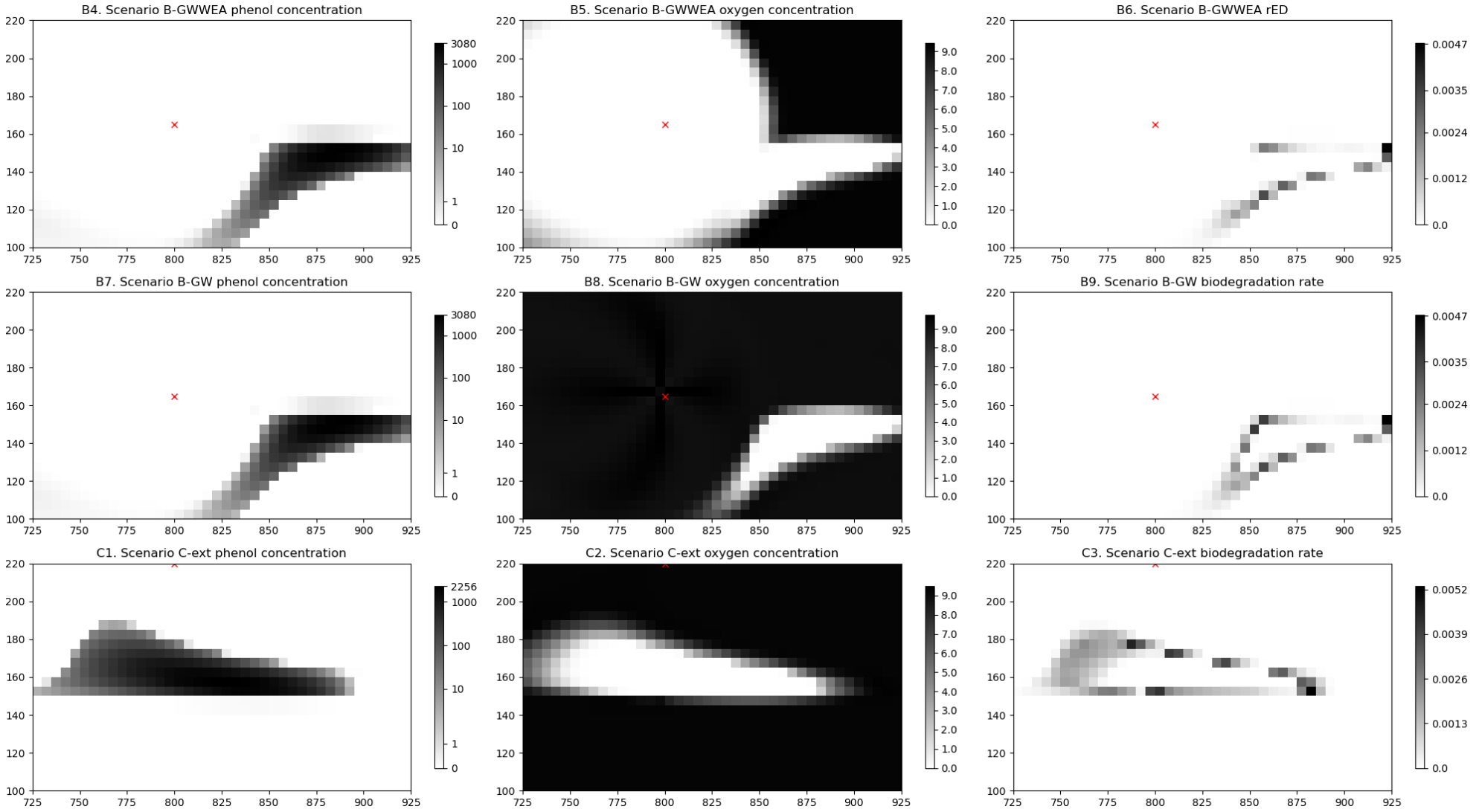
B4. Scenario B-GWWEA phenol concentration
B5. Scenario B-GWWEA oxygen concentration
B6. Scenario B-GWWEA rED
B7. Scenario B-GW phenol concentration
B8. Scenario B-GW oxygen concentration
B9. Scenario B-GW biodegradation rate
C1. Scenario C-ext phenol concentration
C2. Scenario C-ext oxygen concentration
C3. Scenario C-ext biodegradation rate

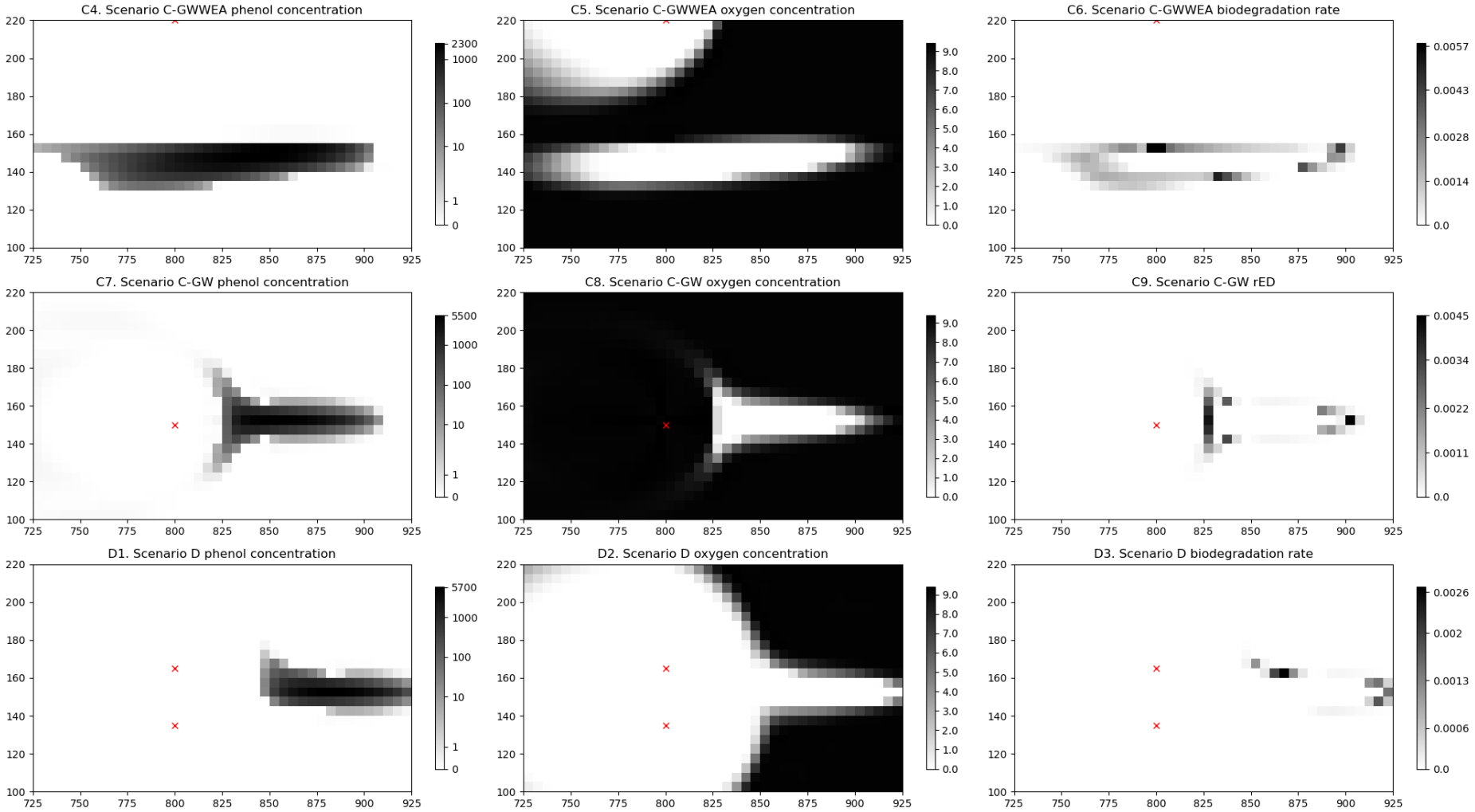
C4. Scenario C-GWWEA phenol concentration
C5. Scenario C-GWWEA oxygen concentration
C6. Scenario C-GWWEA biodegradation rate
C7. Scenario C-GW phenol concentration
C8. Scenario C-GW oxygen concentration
C9. Scenario C-GW rED
D1. Scenario D phenol concentration
D2. Scenario D oxygen concentration
D3. Scenario D biodegradation rate

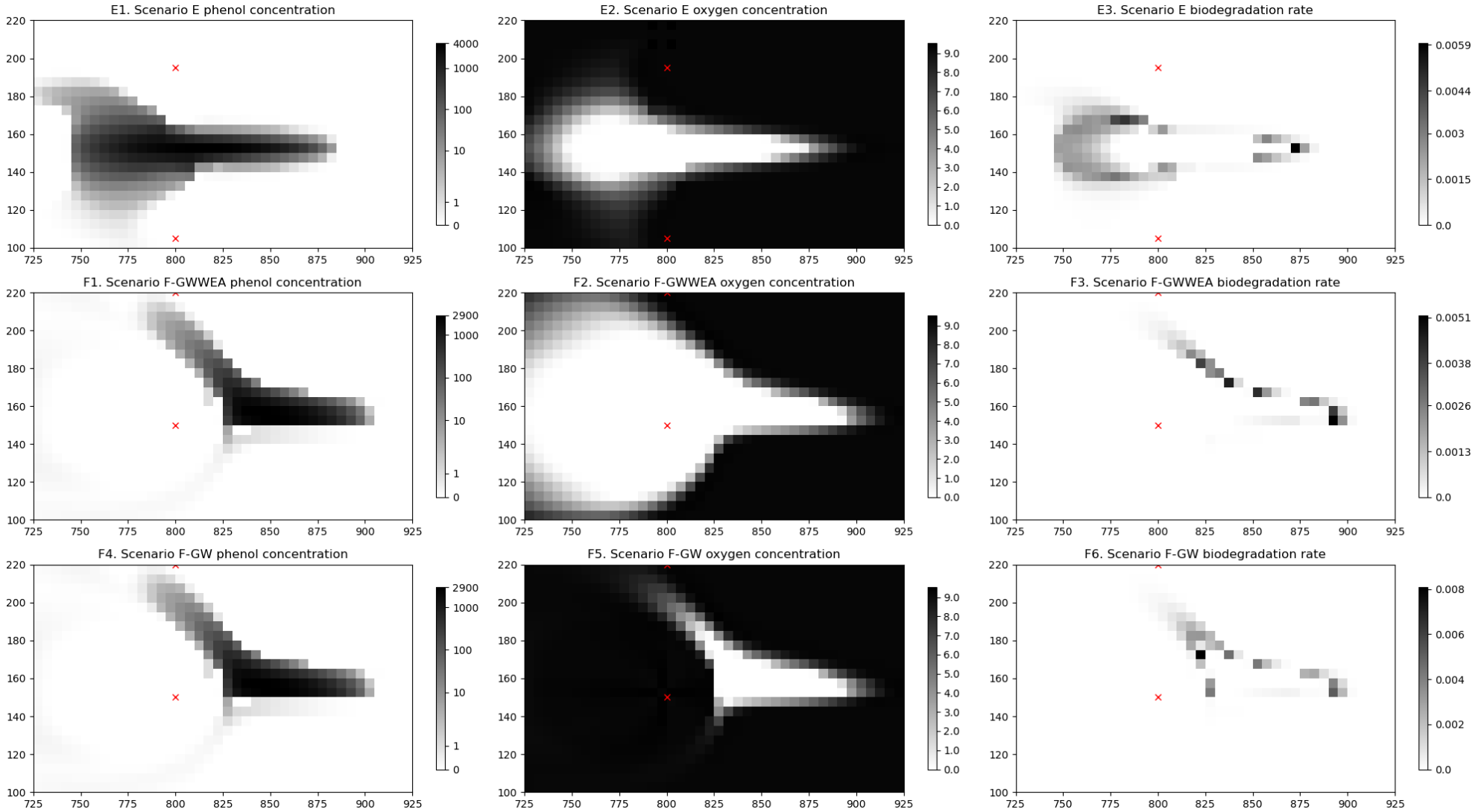

Figure S1. Pixelized concentrations of phenol, oxygen and the biodegradation rate (rED) for each modelling scenario. Concentrations are in units of mg/l and rED is in units of mg/l/d. Each graph is produced at the end of 10 years. For brevity, only the most effective scenario data points have been presented and only 1 layer of the results are shown. For Scenario A, only the simulation at 800m is shown. For Scenario B-Ext, only the simulation at -100 m^3/d is shown. For Scenario C-GW, the most effective simulation is shown, with the injection well at the center of the plume. The red 'x' indicates the location of pumping well(s). The phenol concentrations (left panel) are shown on a symmetrical logarithmic scale, whereas the other graphs are shown on a linear scale.

4.3.1 Overview of scenario analysis

The outputs from the scenario modelling are shown in Figure 4-2 as ratios of M_{bio}/M_0 and M_{ext}/M_0, which are combined under the label M_{rem}/M_0, which represents the proportion of total mass removed by pumping and biodegradation (Section 3.3). M_{bio}/M_0 is calculated and labelled for each well type, including the extraction and injection well. The prefix "Ext" and "Inj" refer to a scenario which has injection and/or extraction wells, respectively. The suffixes GW (groundwater) and GWWEA (groundwater without EAs) are used to distinguish the injection of water with or without EAs, respectively. The M_{rem}/M_0 ratio profiles are reported for $T = 10$ years after the start of the PAT operation, at $t = 0$. The value of M_{bio}/M_0 for "no action" is denoted by the "X" on the y-axis in Figure 4-2, which is a constant value for all panels. This represents 0.69% of the total phenol mass that is biodegraded over 10 years without PAT intervention. As an example, a M_{ext}/M_0 ratio of 0.32 implies that the PAT extraction well removed 32% of the phenol mass. A scenario is considered more effective as the value of M_{bio}/M_0 increases (*i.e.* biodegradation is increased), and more efficient if it also has a lower value of M_{ext}/M_0 (*i.e.* less mass to be sent for treatment is removed). Objectives (a) and (b) are addressed in Scenario A-F, whereas objective (c) is addressed in Scenario F.

Figure 4-3 shows the mass biodegraded (kg) in each scenario, which consists of the same data shown Figure 4-2 before normalization to the initial mass (M_0), to allow observing more detail. Figure 4-4 shows the relative and absolute rankings of all scenarios, with respect to each other and the initial mass. Figure 4-5 shows the results of the dispersion experiment with 3 dispersion test cases: case 1, where dispersion is the same as the values shown in Table 4-1; case 2, where dispersion is decreased by a factor of 10; and case 3, where dispersion is increased by a factor of 10. Except for Figure 4-5, the results for each figure are discussed per scenario, from A-F.

4.3.2 Scenario A

Figure 4-2A shows that the ratio M_{bio}/M_0 remains rather constant, with no significant variation from the no-pumping (no action) case, denoted by the "X" label, which is the same for all graphs. Figure 4-2A also shows that M_{ext}/M_0 increases in the simulations as the well location approaches the plume core (800 m). Figure 4-3A likewise shows that the mass biodegraded remains mostly unchanged, with slightly elevated biodegradation occurring at the plume front (l=200 m). Figure 4-4a shows that Scenario A did not enhance biodegradation above the baseline "no action" and Figure 4-4b shows that Scenario A only biodegraded 0.69% of the total plume mass. The results of Scenario A indicate that changing the longitudinal well location has no significant effect on biodegradation, at least for well locations in the plume interior/centreline. The results also indicate that M_{ext}/M_0 increases with phenol concentration, as the concentration significantly increases from 200 m to 800 m, which is expected.

As the well is placed at the plume centreline, it is less effective at enhancing biodegradation since the EA (O_2 and NO_3) concentrations are depleted within the plume very quickly and most biodegradation occurs at the fringe where the plume and EAs mix. At a selected pumping rate (-30 m^3/d), the area of influence of the well does not extend beyond the plume fringe, which reduces mixing between the ED and EAs. Extraction in the plume interior/centreline does not enhance mixing or transverse spreading, which has been shown to increase reaction rates in

other studies (Rolle et al., 2009; Castro-Alcaca et al., 2012; Sather et al., 2022; 2023). Additionally, groundwater extraction at the plume centre limits biodegradation because the ED is extracted before reacting with the EAs in the background groundwater. These interactions and limitations on biodegradation for this scenario are illustrated in Figure S1-A3, which shows a very weakly developed plume fringe and low biodegradation rate (r_{ED}), even compared with the initial plume condition (Figure S1-I3). This well configuration therefore removes phenol mass with no significant biodegradation due to limited dispersive flux of EAs from the background groundwater. Scenario A did not enhance biodegradation above the baseline condition since the radius of influence of the well is not sufficient to induce significant mixing at the plume fringe. This can be seen in Figure S1-A3, where the biodegradation rate is mainly enhanced near the well. While the biodegradation rate in Figure S1-A3 is larger (greater intensity), the overall area where the biodegradation rate is >0 is lower than the initial condition (Figure S1-I3).

4.3.3 Scenario B

Figure 4-2B shows that the value of M_{bio}/M_o increases with pumping rate for all sub-scenarios, but with a higher contribution to mass removal through biodegradation from the injection sub-scenarios (B-GWWEA and B-GW). Figure 4-2B also shows that M_{ext}/M_0 increases with pumping rate for Scenario B-Ext, as expected. Figure 4-3B shows the mass removed by biodegradation for each sub-scenario in greater detail. Figure 4-4a and 4-4b show that Scenario B-Ext increases M_{bio}/M_o by 50% above "no action" and 0.92% of the plume contaminant mass is biodegraded at the maximum pumping rate. Figure 4-4a and 4-4b show that in the GWWEA injection sub-scenario, M_{bio}/M_o is enhanced by 89% above "no action" and 1.32% of the plume mass is biodegraded at the maximum injection rate. Figure 4-4a and 4-4b show that in the GW injection sub-scenario, M_{bio}/M_o is enhanced by 128% above "no action" and 1.57% of the plume mass is biodegraded at the maximum injection rate. The GWWEA and GW injection sub-scenarios are 44% and 71% more effective at enhancing biodegradation above no action than the Ext sub-scenario, respectively. Due to the injection of EAs, the GW case enhanced biodegradation by 19% relative to the GWWEA case (no EAs present). The results of Scenario B indicate that pumping rate has a significant effect on mass removal by biodegradation, and that injection of groundwater is significantly more effective at enhancing biodegradation than groundwater extraction.

The enhancement of biodegradation resulting from an increased pumping rate is attributable to the following. In general, as the pumping rate increases, the plume is spread over a larger area under the spatially varying velocity field created, which results in enhanced dispersive mixing between the ED and EAs (Rolle et al., 2009; Suk et al., 2021; Sather et al., 2022; 2023). For GWWEA injection, biodegradation (represented by r_{ED}) is only enhanced in a narrow zone at the plume fringe (Figure S1-B6). For GW injection, biodegradation is enhanced both in the plume interior and at the plume fringe, although the EAs will be rapidly consumed within the plume interior, which may result in their complete depletion (Figure S1-B8 and B9). For GW extraction, biodegradation is enhanced near the well where the ED and EA are mixed, and at the plume fringe (Figure S1-B3 and A3). However, since the extraction well removes mass from the system, it does not enhance the biodegradation rate r_{ED} as much as groundwater

injection, where mixing between the ED and EA is more effective and the resultant biodegradation rate is higher (Figure S1-B3 vs B6 and B9).

4.3.4 Scenario C

Figure 4-2C shows that, except for Scenario C-GW, the value of M_{bio}/M_0 increases with lateral distance from the plume centreline/interior up to 60 m, and then appears to stay constant for the remainder of the experiment. Scenario C-GWWEA and C-GW start at a higher value of M_{bio}/M_0 than Scenario C-Ext, but eventually converge to approximately the same value at 60 m. Figure 4-3C shows more detail, in that after 60 m biodegradation for C-Ext and C-GWWEA begins to slightly decrease. Scenario C-GW responds differently to the change in lateral distance than the other sub-scenarios. Figure 4-3C shows that C-GW is most effective in the plume interior/centreline (0 m), and begins to decline, eventually converging to the same value of biodegradation as the other sub-scenarios. Figure 4-4a and 4-4b show that for Scenario C-Ext and GWWEA, M_{bio}/M_o is enhanced by ~62% above "no action" and ~1.13% of the total phenol mass is biodegraded. Figure 4-4a and 4-4b also show that for C-GW, M_{bio}/M_o is enhanced by ~68% above "no action" and 1.16% of total phenol mass is biodegraded. Figure 4-2C and 3C show that, initially, at a distance of 0 m (plume centreline), GW injection is 23% more effective in enhancing biodegradation than GWWEA injection, 73% more effective than C-Ext. In addition, Scenario C-GW is 73% more effective than Scenario A at 800m (Figure 4-2A and 4-3A).

The reason why M_{bio}/M_0 is not enhanced beyond a lateral distance of 60 m is due to the capture zone of the well having a reduced influence on the plume. This is supported by the significant decrease in M_{ext}/M_o that occurs after 40 m, trending to zero after 60 m (Figure 4-2C). Since no ED (phenol) mass is removed, the well increases the value of M_{bio}/M_o (i.e. stimulates biodegradation) by increasing plume spreading and the plume fringe interface as the plume is pulled further away from the center (Sather et al., 2022; 2023).

The initial and final values of phenol concentration, dissolved O_2 concentration and biodegradation rate r_{ED} for the Scenario C-Ext simulation are compared with the initial plume condition in Figure S1, illustrating the dynamic nature of the plume fringe interface and biodegradation under pumping. These simulations and those more generally in Figure S1 show stretching and folding of the plume due to active spreading induced by the arrangement of the PAT system in each scenario, also documented by Piscopo et al. (2013) in a similar study. As the extraction well located lateral to the plume centreline removes contaminant mass, the phenol concentration is decreased and the plume fringe surface area is increased by lateral spreading (SI I1 vs SI C1) of the plume during pumping, allowing greater mixing of dissolved EAs (note the increased O_2 footprint) across the interface (SI I2 vs SI C2). Ultimately, this increases the spatial extent of the interface and rate of biodegradation r_{ED} at the plume fringe compared with the initial condition (SI I3 vs SI C3). By changing the plume flow direction in this way, the reaction front (plume fringe) is aligned perpendicular to the local flow field towards the extraction well. In this case mixing is dominated by longitudinal dispersion in the direction of flow, which is much greater than transverse dispersion, resulting in enhanced biodegradation (Sather et al., 2022; 2023).

With each sub-scenario at their peak performance, GW injection at 0 m is marginally the most effective strategy overall as it significantly enhances biodegradation while reducing mass extraction For example, it is ~2.6% more effective than GWWEA injection or C-Ext at 60 m. Groundwater injection is effective for this enhancement because biodegradation inside the plume is limited by the depletion of available EAs (oxygen and nitrate) and the flux of these EAs into the plume, as induced by the PAT system. These points highlight that while the injection of groundwater at the plume centre can significantly enhance biodegradation compared to injection of EA-depleted groundwater or groundwater extraction at the same location, increasing plume spreading by pumping laterally to the plume is equally important.

4.3.5 Scenario D

Figure 4-2D shows that M_{bio}/M_0 remains mostly constant as the pumping rate is increased for both extraction wells. This is confirmed by Figure 4-3D (enhanced resolution) which shows the absolute contaminant mass biodegraded. The lowest pumping rate of -5 m^3/d resulted in the highest value of M_{bio}/M_0. Figure 4-4a and 4-4b show that Scenario D enhanced mass removal by biodegradation by 8% over the no action case and removed 0.75% of the plume mass (vs 0.69% for "no action"). These results indicate that increasing the pumping rate for two extraction wells located at a constant lateral distance (30 m) has little to no effect on biodegradation.

The results also indicate that extracting groundwater symmetrically from two wells is less effective compared to a single well with similar pumping rate, such as Scenario B-Ext. This is attributed to a decrease in dispersive mixing of EAs within the plume caused by the proximity of the two wells, which have an overlapping radius of influence. This is evidenced by the absence of biodegradation at or near the wells (Figure S1, D3). In Scenario D both the maximum value of the biodegradation rate and area in which biodegradation occurs is reduced (Figure S1, I3 vs D3). In Scenario B, the well promotes dispersive mixing of the background groundwater and plume, increasing the value of M_{bio}/M_o within the well capture region (Figure S1, B3). However, in this dual well configuration (Scenario D), the background groundwater is drawn into the plume margin at each side. At high pumping rates, adequate mixing between the ED and EA does not occur because the phenol mass is excessively removed by the combined action of the two extraction wells, which are located too close together (Figure S1, D1-D3). Also, at low pumping rates, these extraction wells cannot appropriately influence the region between them to the same degree, as the EAs are instead drawn away from the plume toward the extraction well on either side. The performance of this scenario could be improved if the lateral distance between the two wells was greater.

Despite Scenario B having only one well, more contaminant mass was extracted than in Scenario D. This is because the two wells in Scenario D are located 30 m apart, and the pumping rate is split between them (up to -50 m^3/d each), rather than concentrated (-100 m^3/d) in a single cell. The strategy in Scenario D is therefore not effective because biodegradation is limited by the very close spacing of the wells and the contaminant mass extracted is large, implying increased operational costs for subsequent groundwater treatment.

4.3.6 Scenario E

Figure 4-2E shows that M_{bio}/M_0 increases with lateral distance between the two extraction wells. At the first point in Scenario E, M_{bio}/M_0 and "no action" are equal, indicating that at a lateral distance of d=30 m, biodegradation was not enhanced above baseline conditions. Figure 4-2E also shows that the most effective arrangement is for each well to be placed 45m away from the plume centreline (i.e. the distance between them is 90 m). Figure 4-4a and 4-4b show that at this optimal position, 0.9% of the total plume mass was biodegraded compared to the no action case (0.7%), with a maximum enhancement in M_{bio}/M_o of ~24% above "no action". The enhancement in biodegradation is due to the same processes as in Scenario C-Ext and C-GWWEA. As the lateral distance between the extraction wells increases, phenol biodegradation is enhanced by the greater degree of dispersive mixing created by this interaction.

Beyond the 45m distance, the overlap between the capture zone of the two wells and the plume decreases. This is supported by the decrease in M_{ext}/M_o, which indicates that the plume is unaffected by this well arrangement. The value of M_{ext}/M_o decreases after a well separation of 60 m because contaminant concentrations decrease quickly at the plume margin (Thornton et al, 2001a). The extent of biodegradation at the plume fringe is also limited by the supply of organic contaminants to this interface, controlled by the dispersive mixing. Unlike Scenario D, Scenario E enhances plume spreading and mixing because the pumping rates are lower and the wells are further apart, such that the ED and EAs are not removed as rapidly and adequate mixing between the plume and groundwater is possible to support biodegradation. Further analysis shows that this scenario results in significant spreading of the plume and enlargement of the plume fringe between the extraction wells, as shown by the increased footprint of the dissolved O_2 concentration gradient across this interface (Figure S1-E2) and corresponding zone of enhanced biodegradation rate, r_{ED} (Figure S1-E3).

4.3.7 Scenario F

Figure 4-2F shows that the value of M_{bio}/M_o increases with the lateral distance between the extraction and injection wells. For both the GWWEA and GW sub-scenarios, M_{bio}/M_0 reached its highest value at a lateral distance of 90 m, after which it begins to decline.

Figure 4-4a and 4-4b show that 1.2% and 1.4% of the total phenol mass were biodegraded for each sub-scenario, respectively. This is respectively an enhancement of 67% and 100% above "no action" in mass removal by biodegradation (Figure 4-4a). For this arrangement GW injection was ~18% more effective at enhancing biodegradation than GWWEA injection, as shown by the increased mass biodegraded (Figure 4-4a). This difference arises because biodegradation occurs within the plume interior (where the injection well is located) and at the plume fringe (where the extraction well is located) in the GW injection sub-scenario. However, biodegradation only occurs at the plume fringe in the GWWEA sub-scenario, as the latter has no EA suite to support biodegradation directly, and the injected GWWEA simply enhances dispersive mixing without supplementing the EA supply.

After a well separation distance of 90 m, M_{ext}/M_o decreases sharply to zero, as progressively less contaminant mass is extracted, and M_{bio}/M_o begins to decrease, indicating a reduced influence of the well on biodegradation in the plume (Figure 4-2F). Overall, this scenario was

respectively 87% and 62% more effective at enhancing biodegradation than using two concurrent extraction wells, as in Scenario D and E. However, the plume fringe was enhanced much less by the well and pumping arrangement in Scenario F, as opposed to Scenario D (compare Figure S1-F3 and Figure S1-F6 to Figure S1-E3). Nonetheless, the biodegradation rate in Scenario F-GW is generally higher than in Scenario F-GWWEA and Scenario D, which results in higher overall mass removal through biodegradation.

The performance of the combined PAT-NA system in the different scenarios is compared in Figure 4-4 relative to the "no action" case. This shows that groundwater injection in Scenario B-GW was most effective in removing contaminant mass (Figure 4-4a) and enhancing biodegradation (Figure 4-4b) relative to the other scenarios. Over 500 kg of contaminant mass was biodegraded using groundwater injection within Scenario B (Figure 4-4b). The arrangement of pumping wells in this scenario, with a fixed location at the plume fringe and continuous supply of O_2 and NO_3 in the injected groundwater, ensures dispersive mixing at the plume fringe is enhanced and biodegradation is not EA limited. While the mass biodegraded in these scenarios is a modest percentage (ca. 2%) of the overall plume, this simply reflects the significant mass of dissolved contaminant in groundwater at the site; the concentration of phenol is several orders of magnitude higher than the concentration of the EAs. Figure 4-6 shows that when the concentration of phenol and the EAs are of a similar order, biodegradation removes a higher percentage of the overall phenol mass, which would also improve the remediation performance of the scenarios. Moreover, the mass biodegraded also reflects the low value of aquifer transverse dispersivity at this site, which limits dispersive mixing in the plume.

4.4 Effect of dispersion on biodegradation

Figure 4-5 shows a hypothetical experiment which illustrates the effect of dispersion on biodegradation, as assessed by comparing numerical simulations of the contaminant mass biodegraded for different values of the dispersivity coefficients. A 10-fold increase of the dispersivity coefficients (case 3) above the baseline model (case 1) enhances the biodegradation by approximately 360%, whereas a 10-fold decrease (case 2) reduces biodegradation by only 12%, indicating that the original dispersivity value (case 1) is already quite low for a solute plume of that scale (Gelhar et al., 1992; Xu and Eckstein, 1995). GW injection enhances biodegradation by approximately 96% for case 1 and 2, and by 22% for case 3 (Figure 4-5). Higher values of dispersivity coefficients result in greater plume spreading in all dimensions, which increases the dispersive mixing between the ED and EAs, as well as the EA flux into the plume to stimulate biodegradation. This feature is evident in several scenarios (e.g. C and E) from the increased size of the plume fringe interface under pumping, and the corresponding greater spatial development of zones with an increased biodegradation rate (Figure S1). GW injection further enhances biodegradation for the same reason, but with diminishing returns at higher values of the dispersivity coefficients. This is likely due to the plume becoming very dilute in case 3, which reduces the biodegradation rate r_{ED} ; the injection well should be located in a more concentrated region of the plume in order to be more effective.

4.5 Conclusion

This research examined the design of conventional pump and treatment (PAT) systems to increase the *in situ* biodegradation of organic contaminants in groundwater, by addressing potential limitations (electron acceptor supply) on the relevant processes. The aim was to identify the effect of system variables on plume remediation to increase contaminant mass removal by enhancement of biodegradation, as a proof-of-concept evaluation and basis to optimise the system design for best performance. Six scenarios were developed to evaluate the design of the PAT system with these variables, using a 3-D numerical model (MODFLOW and MT3D-USGS) constructed with historical site characterisation data from a chemical manufacturing plant on a UK sandstone aquifer. Using this data, a "synthetic plume" was created in the model to investigate the scenarios in this conceptual analysis. The contaminants in groundwater at the site were all converted into equivalent concentrations of phenol (the predominant contaminant) for the modelling. A Monod formulation was used in the model to simulate the kinetic reactions between phenol and different electron acceptors (dissolved oxygen and nitrate) involved in biodegradation. A 10-year scenario with no active wells and passive natural attenuation was used as a control to compare the additional contribution of biodegradation to mass removal in the groundwater.

The scenario modelling showed that the enhancement of biodegradation depends on the location, number, pumping rate and distance between well location(s) in the PAT scheme. Placing the PAT wells too close together limits biodegradation rates and extraction in the plume interior/centreline is less effective than injection in the same location. Since the extraction well removes contaminant mass from the system, this reduces the overall biodegradation rate r_{ED} in space and time, as this is strongly influenced by phenol concentration. In general, injection enhances plume fringe reactions by increasing dispersive mixing through the creation of divergent flows. As the wells are moved laterally outward from the plume centreline, the mass extracted decreases and mass biodegraded increases. The most effective scenarios are injection of groundwater with electron acceptors at 15m from the plume interior/centreline (scenario B-GW), and injection of groundwater with electron acceptors in the plume centreline combined with an extraction well that is located away from the plume centreline (Scenario F-GW). The PAT system enhances *in situ* biodegradation of contaminants by (i) increasing dispersive mixing between solutes in the plume and background groundwater, and (ii) increasing the flux of dissolved electron acceptors into the plume from the background groundwater in zones (e.g. plume fringe) which have high biodegradation potential. Enhanced mixing also increases contaminant dilution and can remove factors which are inhibitory to biodegradation, such as high contaminant concentrations. The analysis shows that biodegradation was significantly improved with PAT intervention above the "no action" case, with an increase of 100-128% in mass biodegraded. The pumping rate is the most effective (and controllable) intervention to enhance biodegradation, as it increases the EA flux into the plume. Furthermore, groundwater extraction at the plume fringe is the most efficient basis to increase the surface area of this interface and enhance solute mass transfer across it by dispersion.

Future studies should identify how to minimize the diminishing returns observed with multi-well configurations. If the effectiveness of a single well could be multiplied or scaled (Scenario

C-Ext), this could potentially shorten remediation timeframes significantly. The effectiveness of different combinations of EAs in the injected groundwater for biodegradation should also be considered, although this will likely depend on the contaminant mixture in specific cases. Overall, the approach illustrated here offers new opportunities to integrate PAT with natural attenuation as a management strategy at sites where groundwater is contaminated by organic chemicals.

PAGE INTENTIONALLY LEFT BLANK.

Chapter 5

Enhancing in situ biodegradation in groundwater using pump and treat remediation: a modelling analysis of the impact of multiwell configurations on NA.

5.0 Abstract

A remediation approach which uses pump and treatment (PAT) to enhance the biodegradation of organic contaminants by increasing dispersive mixing between plumes and groundwater was evaluated for a phenol-contaminated aquifer, using a reactive transport model which simulates kinetic reactions between an electron donor (ED) in the plume and electron acceptor (EA) in the groundwater. The influence of system design and operation was examined in a series of 10 increasingly complex multiwell modelling scenarios. Previous research determined that diminishing returns occurred when multiple PAT wells were used in the same simulation, as their enhancement of biodegradation was less than the sum of what each of the wells achieved in separate simulations. This research attempts to find methods to reduce the diminishing returns incurred by having multiple wells and to establish a sub-linear relationship between numbers of wells and biodegradation. This chapter also investigates the effect of amendment injection on biodegradation mass and compares it to fringe biodegradation processes. Analysis of this phenomenon discovered a configuration of 4 injection wells which enhanced biodegradation by 520% over no intervention over 10 years.

5.1 Introduction

Groundwater pollution via organic contaminants is a significant problem globally. Remediation timeframes using current technologies are prolonged and expensive. It has been estimated that there are at least 126,000 US sites which will require 110 billion to 127 billion USD to remediate, and about 10% of these sites are unlikely to reach remediation targets within 50-100 years (NRC, 2013).

Pump and treat (PAT) is an effective strategy for remediation at sites with certain conditions, such as homogeneous, permeable, and isotropic sites impacted with contaminants possessing high aqueous solubility (McDade et al., 2013). However, PAT has many limitations and may be unsuitable at remediating sites which have complexities such as physical heterogeneity, anisotropy, low permeability, sorption-desorption processes, and matrix diffusion (McDade et al., 2013; Truex et al., 2017); or sites with contaminants that partition into different phases, such as volatile organic compounds, which form vapours, and non-aqueous phase liquids, which have an immiscible phase with low solubility and mobility and can persist in aquifers (FRTR, 2023). In these instances, PAT systems alone are inadequate to remediate the contaminated site and the technology may instead be implemented for hydraulic containment of the plume to manage risk to downstream receptors. In order to improve the efficacy of remediation, PAT can instead be combined with other technologies such as source removal (excavation), in situ bioremediation or chemical oxidation, surfactants, or air sparging/in situ venting, as determined by the specific site characteristics, such as hydrogeology and contaminant class (Freeze and Cherry, 1999; Truex et al., 2017; NRC, 2013; Fetter et al., 2017; FRTR, 2023).

Natural attenuation (NA) can remediate many classes of contaminants under a wide range of hydrogeological settings. NA can be defined as the combination of physical processes (e.g., advection, dispersion, dilution, and sorption), chemical processes (e.g., ion exchange, precipitation/dissolution, abiotic transformation) and biological processes (e.g., bioaccumulation, and biodegradation (Favas et al., 2016; Wiedemeier et al., 1999)), which can reduce the mobility, bioavailability, toxicity, or concentration to levels that are less harmful to human health and ecosystems (NRC, 2000). Advection transports contaminants downgradient but conserves mass and concentration. Mechanical dispersion occurs as a result of changes in groundwater velocity at the pore scale related to heterogeneity, pore friction, pore size, and tortuosity; it conserves mass but reduces concentration. Of all these NA processes, biodegradation is the only process that reduces both contaminant concentration and mass. This is achieved through microbially mediated redox reactions which transform contaminants into a variety of organic and inorganic compounds. These microbially mediated redox reactions occur between an electron donor (ED) and an electron acceptor (EA); the ED is oxidized, and the EA is reduced. These reactions are typically accentuated on the fringes of the plume, where the concentration of the ED is lower than the plume interior, and the EA concentrations are higher than inside the plume interior, and where poor dispersivity and groundwater velocity limit the mixing of the ED and EA.

NA typically occurs naturally in most contaminant sites without intervention; however, reaction rates may be slow due to the lack of bioavailable EA and the efficacy of biodegradation depends on the site conditions and contaminant. Biodegradation rates in groundwater are reduced when the hydraulic conductivity and dispersivity are low, as this decreases the mixing between the ED (e.g., contaminant) and EA (e.g., oxygen, nitrate) in the groundwater. Where dispersivity, and therefore mixing, between the two interfaces is higher, biodegradation can still be limited by lack of EAs, either due to poor bioavailability or inadequate concentrations.

Monitored natural attenuation (MNA) is the management of NA processes through careful long-term monitoring and data analysis. MNA, if properly managed, can help remediate many classes of contaminants under a wide range of hydrogeological settings (Carey et al., 2000). Since this approach is almost entirely passive, rather than engineered, the costs of MNA are considerably lower than other technologies, such as PAT (Santo and Prosperi, 2022). However, MNA takes longer to remediate sites than other technologies. For this reason, MNA is rarely chosen as the sole remedy for contaminated sites and is enhanced with either bioaugmentation and biostimulation or used in conjunction with other technologies, for example as in situ bioremediation (NAVFAC, 2018; FRTR, 2023). This approach has gained popularity in recent years as it can remediate a site quicker than either MNA or PAT alone, and is often cheaper, as much of the contaminant is transformed or degraded in situ. While in situ remediation strategies such as MNA can be significantly cheaper than ex situ remediation strategies such as PAT, remediation timeframes are significantly longer. Clean up time with MNA varies between 10 to 70 years (McGuire et al., 2004; DoD, 2008).

Alternative technologies may accelerate site remediation. Some studies have found that an in situ bioremediation strategy using amendments may have a better balance between a lower

cost (relative to PAT) but with comparatively shorter remediation timeframes than MNA alone (Khan et al., 2004; Santo and Prosperi, 2022). In situ bioremediation is a combined technology that uses an upgradient injection well to disperse amendments, nutrients, microbes, hydrogen, enzymes, oxygen release compounds, or controlled release materials (CRMs) through the plume in order to induce biostimulation or bioaugmentation which leads to in situ biodegradation of the contaminant (NRC, 2013; Alvarez et al., 2005).

Enhancing the rates of intrinsic NA by injecting chemical amendments such as EAs, EDs, or nutrients needed for microbially mediated TEAPS is a process known as biostimulation (Kao et al., 2016). Bioaugmentation is the addition of specific cultured microbes to stimulate the biodegradation of organic contaminants (Lyon et al., 2013). Typically, a downgradient extraction well is used to promote the flow of the amendment through the plume, rather than remove mass. This increased flow promotes biodegradation to occur or enhances intrinsic biodegradation rates. Sometimes the injection and extraction system are recirculated to improve mixing (Bagtzoglou and Oates, 2007).

Due to the physical and economic limitations of PAT remediation, in situ bioremediation has become a more common approach in recent decades (Fetter et al., 2017). The technology is particularly effective at remediating BTEX, MTBE, and chlorinated solvent plumes (Wiedemeier et al., 1999; Adamson and Newell, 2014; FRTR, 2023). However, mixing between the treatment chemical and the contaminant plume is typically limited (Piscopo et al., 2013). Improving the mixing between the treatment chemical and the contaminant would be highly advantageous in reducing remediation timeframes and overall effectiveness of the bioremediation approach; however, enhancing mixing to achieve these remediation objectives is a relatively new and underexplored area of research. Another limitation of in situ bioremediation is that excess microbial biomass can cause plugging of the aquifer around the injection site (Hazen, 2018). This limitation can possibly be overcome by using CRMs.

CRMs are a type of amendment sometimes used to support in situ bioremediation via the introduction of carbon sources (electron donors), oxygen (electron acceptors), oxidants (to facilitate in redox reactions), which can enhance in situ biodegradation. There are various types of CRMs which differ in their composition and design and thus are used for different situations. These include: “candle” type CRMs which are directly placed in a borehole and release reaction materials slowly; pellet and droplet type CRMs which come in different sizes but are generally smaller than candle type CRMs and can be dispersed in coarser aquifer materials; and gel type CRMs which are injected in liquid form and dissolve quickly, allowing their contents to be released in the groundwater (O’Connor et al., 2018). CRMs release reaction materials for prolonged periods and can be utilized without the need for injection wells and above ground storage tanks (O’Connor et al., 2018).

Combining PAT with chemical amendment injection has been shown in previous research to increase mass biodegradation in situ and thereby reducing the amount of mass that is treated ex situ (Marquis and Dineen, 1994; Park et al., 2007). However, only concentration data, rather than a full mass balance, was reported in these studies, so the contribution of NA to mass removal relative to contaminant dilution and dispersion caused by the injection is

unclear. Also, intrinsic NA was not accounted for in these modelling studies - instead a first order decay rate was used which is independent of the ED and EA concentration. However, previous research has shown that PAT could also enhance in situ intrinsic NA (Jones et al., 2002; Thornton et al., 2014) by enhancing dispersive mixing (Piscopo et al., 2013; LJ Sather 2022; 2023) and mass flux of EAs into the plume.

In cases where a biodegradable plume suffers from low dispersion, amendment with CRMs may enhance mass loss from biodegradation. Since targeted PAT has been shown to enhance intrinsic NA only at the plume fringes, CRM injection with targeted PAT could potentially be combined such that biodegradation rates are enhanced in the plume interior and at the fringes simultaneously (Marquis and Dineen, 1994; Park et al., 2007; Thornton et al., 2014). To the author's knowledge, combining targeted PAT with CRM remediation to also enhance the effects of intrinsic NA has never been attempted.

However, at sites with a biodegradable contaminant and an abundance of EAs, a bioremediation type approach may not be necessary, especially if the limitation on biodegradation rates is physical, such as due to low dispersivity and aquifer hydraulic conductivity (Lerner et al., 2000; Pickup et al., 2000; Williams et al., 2001; Thornton et al., 2001a,b; Jones et al., 2002). Recent studies have shown that PAT targeted at the fringes of a plume can enhance the dispersive mixing of the interface between the plume and groundwater (Thornton et al., 2014). The enhanced dispersive mixing induced by the PAT system resulted in a virtual doubling of the biodegradation rate at the plume fringe. This enhancement in biodegradation is due to an increase in mixing between the contaminant and the uncontaminated groundwater where EAs exist at a higher concentration. This approach effectively enhances the plume fringe biodegradation processes that are naturally occurring, albeit at slower rates (Thornton et al., 2001 a,b).

While Thornton et al., (2014) did not mention plume spreading, other studies have shown that engineered injection and extraction can be used to enhance the advective spreading of plumes in groundwater and thereby increase the mixing between the plume and an amendment chemical (Bagtzoglou and Oates, 2007; Piscopo and Neupauer 2012; 2013; 2014; Sather et al., 2023). While it has been suggested that an engineered injection and extraction approach might enhance NA (Bagtzoglou and Oates, 2007), it has never been investigated.

Thus, if MNA and PAT are combined to enhance biodegradation, it can be possible to improve solute mass removal and lower remediation time scales as well as operational costs. This proposed combined technology differs from an in situ bioremediation approach, in that targeted PAT is used to enhance the intrinsic NA in situ, rather than using amendments. This method may potentially surpass bioremediation in terms of remediation effectiveness and cost, and/or it could be combined with a bioremediation approach to accelerate biodegradation even further. In this chapter, amendment supplementation is compared with intrinsic NA and NA as enhanced by the PAT system.

Using PAT to leverage the benefits of enhancing NA in situ could potentially reduce remediation timeframes and further decrease cost by reducing the amount of mass that is pumped and treated by the PAT system (Thornton et al., 2014). Additionally, actively

enhancing NA using amendments could possibly reduce treatment costs further, by degrading additional mass in situ, reducing the number of extraction wells and treatment instrumentation needed, or both (Marquis and Dineen, 1994; Park et al., 2007; NRC, 2013). Identifying well configurations utilizing PAT and injection to promote mixing and enhance NA further is one way in which this could be achieved (Park et al., 2007; Piscopo et al., 2013).

5.1.2 Relationship to previous chapters

Chapter 4 investigated the effect of PAT design variables, such as flow rate, well locations, and well configuration, as a proof of concept for enhancing NA (biodegradation) using targeted PAT. A preliminary analysis of PAT systems which combines extraction and injection was also investigated. Two types of injection were considered: injection of water without EAs, with the aim of determining the effect of divergent flows on biodegradation as a function of plume fringe processes, and injection of EA-rich water (oxygen and nitrate). The objective of this chapter was to develop a series of modelling scenarios to assess the effectiveness of remediation using NA-enhanced PAT compared with conventional PAT.

Chapter 5 builds upon chapter 4 by extending the investigation of the plume space to identify the pumping locations which enhance biodegradation the most, as the 3D plume has a complex geometry due to aquifer physical heterogeneity and the high vertical gradient component as a result of recharge. This research attempts to find ways to reduce the diminishing returns incurred by having more than 1 well, which was identified as a problem in Chapter 4. The diminishing returns occurred when multiple wells were used in the same simulation, their enhancement of biodegradation was less than the sum of what each of the wells achieved in separate simulations. The goal is to find a sub-linear relationship between numbers of wells and biodegradation, rather than logarithmic. Chapter 5 also investigates the effect of amendment concentration on biodegradation mass and compares it to the fringe biodegradation processes. Since biodegradation rates are low, due to reduced bioavailability, the injection of amendments could be used to introduce EAs to the most contaminated regions of the plume in addition to spreading the plume. In other words, amendment injections may enhance biodegradation by promoting the direct contact between the phenol and the EAs, in addition to enhancing the plume fringe reactions. The objective of this chapter was to examine multiwell scenarios and determine their impact on mass removal and in situ biodegradation, in addition to comparing the impact of different amendments and terminal electron accepting processes.

5.2 Methodology

5.2.1 Study site

Table 5-1. Input parameters used in the scenario modelling.

Flow and transport parameters		**Value**		**Data source**
Effective porosity (-)		0.125[a]		Core samples/geophysical logs[a]
Hydraulic conductivity range, K (m/d)		0.35-1.0[a]		Pumping tests and RFM[c]
Recharge rate (m/d)		8.00e-04[a]		Effective infiltration estimation[b]
Longitudinal dispersivity (m)		1[b]		
Vertical transverse dispersivity (m)		4.00e-03[b]		Tracer tests and numerical modelling
Horizontal transverse dispersivity (m)		1.00e-02[b]		
Grid block size (m^3)		5		Well screen lengths are 5 meters.[a]
Model length, width, and depth (m)		1200x300x255		
		Species		
Biodegradation module parameters	*Phenol*	*Oxygen*	*Nitrate*	
Half saturation constant (mg/l)	-	0.1[b]	0.5[b]	Determined by a mesocosm experiment[b]
Inhibition constant (mg/l)	-	0.9[b]	0.9[b]	
Decay rate (1/T)	-	3.44e-05[b]	3.44e-06[b]	
Yield coefficient (-)	0	2.38[b]	3.69[b]	Reaction stoichiometry
Source concentration (mg/l)	25000	0	0	Groundwater quality monitoring
Background groundwater concentration (mg/l)	0	4.5-9.28[b]	91-105[b]	Groundwater quality monitoring

g. Unpublished data from confidential third-party consultant reports.
h. Values used in previous modelling studies on the site [Watson et al. (2005) and Mayer et al. (2001)].
i. RFM refers to Radial Flow Modelling undertaken by third party consultants.

This field site is a fine-grained, unconfined, fluviatile, sandstone bedrock aquifer located underneath a former coal tar distillation plant. The site has been extensively investigated over 25 years, with studies on the interpretation of groundwater contamination (Williams et al., 2001), redox processes and contaminant biodegradation (Thornton et al., 2001a; 2014; Wu et al., 2006; Baker et al., 2012; Hedbavna et. al., 2016), aquifer stable isotope geochemistry (Spence et al., 2001), aquifer microbiology (Pickup et al., 2001; Elliot et al., 2010; Rizoulis et al., 2013; Mujica-Alarcon et al., 2021), plume mass balance (Thornton et al., 2001b) and reactive transport modelling (Mayer et al., 2001; Watson et al., 2005). The site history, summarised here, is described in detail in Williams et al. (2001).

A mixed plume of phenolic compounds (primarily phenol, cresols and xylenols) extends approximately 700 m down hydraulic gradient of the site, with an estimated width of 150m and depth of 60m (Figure 1). Groundwater flow is westerly, with a pore velocity between 4-11 m/year, and consistent over the history of the plume. Vertical flow due to groundwater recharge is also important (Table 1). Previous investigations have identified a heterogeneous distribution of phenolic compounds and biogeochemical processes responsible for their biodegradation within the plume (Thornton et al, 2001a). The plume is anchored by a NAPL source, with concentrations of individual phenolic compounds (e.g., phenol) reaching 25,000 mg/l. Considering this, and to reduce the complexity of the numerical model, phenol was selected as a representative organic contaminant for the simulations and the concentrations of all other

phenolic compounds were converted into equivalent phenol concentrations. A conceptual model of the plume developed from this analysis and used in the numerical investigations is shown in Figure 5-1.

Previous studies have shown that the phenolic contaminants are biodegraded by several processes; however, most mass loss due to biodegradation (>90%) arises from consumption of oxygen and nitrate in the groundwater (Lerner et al., 2000; Thornton et al., 2001a,b; Mayer et al., 2001; Jones et al., 2002; Watson et al., 2005). For this reason, the modelling scenarios were developed to assess the contribution of these two EAs to biodegradation, as influenced by the PAT system.

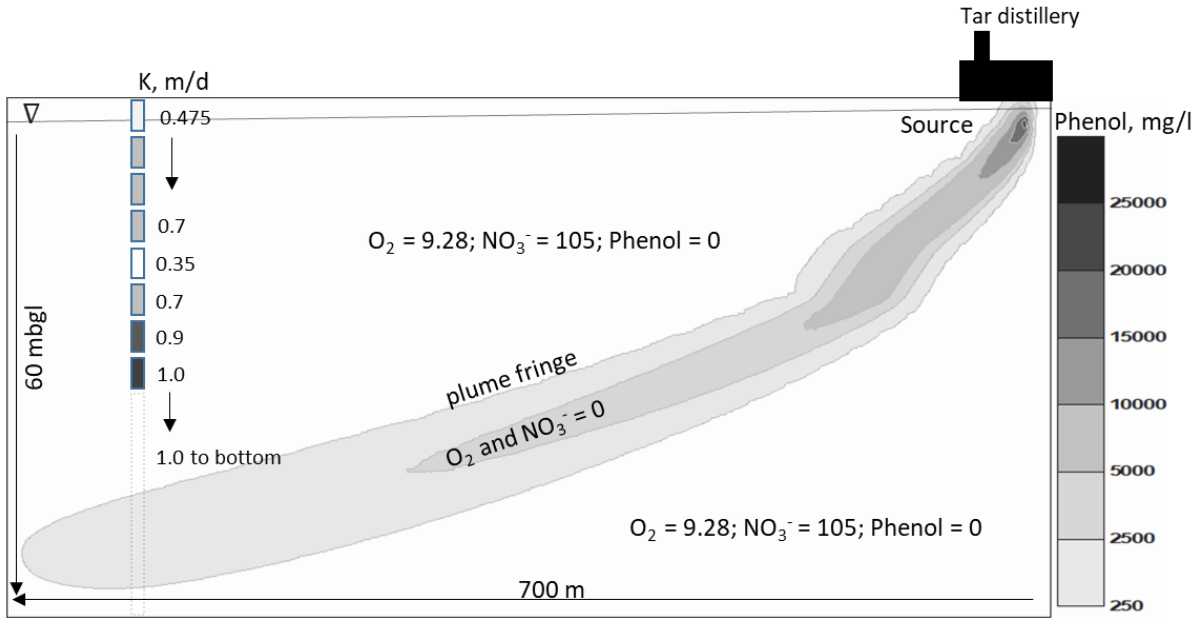

Figure 5-1. Simplified conceptual model of the study plume based on the output from the numerical model. The concentrations shown are in mg/l. The hydraulic conductivity scale indicates that some values are repeated throughout the layered system (Thornton et al., 2001b). Note the concentrations of oxygen and nitrate are below detection in the plume due to biodegradation of the phenols.

5.2.2 Flow and transport model

A 3-D flow and transport model was developed using the input data in Table 4-1. Groundwater flow is governed by the classical PDE:

$$\frac{\partial}{\partial x}\left(K_{xx}\frac{\partial h}{\partial x}\right)+\frac{\partial}{\partial y}\left(K_{yy}\frac{\partial h}{\partial y}\right)+\frac{\partial}{\partial z}\left(K_{zz}\frac{\partial h}{\partial z}\right)+W=S_s\frac{\partial h}{\partial t} \qquad \text{Eq 1}$$

where K_{xx}, K_{yy}, and K_{zz} are hydraulic conductivity along the x, y, and z coordinate axes (L/T); h is the hydraulic head (L); W is a volumetric flux per unit volume representing sources and/or sinks, such as recharge and wells (1/T); S_s is the specific storage of the porous material (1/L); and t is time (T). The model is isotropic ($K_{xx} = K_{yy} = K_{zz}$) and heterogeneous, with hydraulic conductivity generally increasing with depth (Figure 4-1). The groundwater flow system was set to steady state, as the hydraulic heads trend to steady state after ~2 years of pumping.

Equation 1 is solved using MODFLOW-2005 (Harbaugh et al., 2005), based on a finite different grid characterized by 200 columns, 60 rows, and 38 layers, with a grid-block size of 5m × 5m × 5m in the region of the plume. The flow model is by characterized by a constant head boundary condition on the east and west (see Figure 4-1), with groundwater recharge applied to the water table (Table 4-1). Other boundaries are set as "no flow". MODFLOW-2005 calculates the pore velocity field ($\boldsymbol{v} = -\frac{K}{\phi} \cdot \nabla h$, where ϕ is the effective porosity), which is then used in the multispecies reactive contaminant transport simulator MT3D-USGS (Bedekar et al., 2016) to solve a system of coupled partial differential equations, each of which represents the mass continuity for the species simulated:

$$\nabla(\phi \cdot \mathbf{D} \cdot \nabla C_i) - \nabla(\phi \cdot \mathbf{v} \cdot C_i) + \mathrm{q}_{s,i} \cdot C_{s,i} + R_i = \frac{\partial(\phi \cdot C_i)}{\partial t} \quad \text{Eq 2}$$

where C_i is the concentration of species i [M/L^{-3}], **D** is the hydrodynamic dispersion tensor [L^2/T^1], $\mathrm{q}_{s,i}$ [M/L^3] represents the specific discharge for species i, $C_{s,i}$[M/L^3] represents the concentration of sources for species i, and R_i represents the reaction rate of species i [M/L^3/T^1]. In this case, there are three species ($i = 1, 2, 3$), and the term R_i depends on ongoing kinetic reactions occurring between 1 electron donor (ED) and 2 electron acceptors (EAs), simulated using a Monod kinetic model developed by Lu et al. (1999), following approaches used in previous studies (Rolle et al., 2008).

The stoichiometric reactions between phenol (C_6H_6O), which is the ED, and the two EAs, oxygen (O_2) and nitrate (NO_3^-), are described by the following equations:

(a) $C_6H_6O + 7O_2 \rightarrow 6CO_2 + 3H_2O$ Eq 3

(b) $C_6H_6O + \frac{28}{5}NO_3^- + \frac{28}{5}H^+ \rightarrow 6CO_2 + \frac{14}{5}N_2 + \frac{29}{5}H_2O$ Eq 4

Eq 3 and 4 are presented to illustrate the stoichiometry of the reactions which are considered in Eq 6.

The rate of ED biodegradation ($i = 1$ in Eq. 2) is given by (Lu et al., 1999):

$$r_{ED} = \sum_{j=1}^{2} r_{ED,j} = -\left\{\frac{k_{EA_1} \cdot [EA_1]}{K_{EA_1} + [EA_1]} + \frac{k_{EA_2} \cdot [EA_2]}{K_{EA_2} + [EA_2]} \cdot \frac{K_{I,EA_1}}{K_{EA_1} + [EA_1]}\right\} \cdot [ED] \quad \text{Eq 5}$$

where $[ED]$, $[EA_1]$, and $[EA_2]$ represent the concentration of the ED and the two EAs (M/L^3), respectively; k_{EA_1} and k_{EA_2} are first-order decay rate constants for the EAs (1/T); K_{EA_1} and K_{EA_2} are the "half saturation" constants for the EAs (M/L^3); K_{I,EA_1} (M/L^3) is the inhibition constant for the first EA, oxygen, which has the highest Gibbs free energy (Christensen et al., 2000). Correspondingly, the rate of consumption of the two EAs, which affects the concentration of the EAs, ($i = 2, 3$ in Eq. 2) is given by:

$$r_{EA_j} = Y_{EA_j} \cdot r_{ED} \qquad \text{Eq 6}$$

where $Y_{EA_j} (j = 1, 2)$ is the yield coefficient for the EA, that is, the EA mass used per ED unit mass biodegraded, calculated from the stoichiometry in Eqs. 3 and 4 (Table 4-1).

The mass biodegraded is obtained by integration of the rate of ED biodegradation r_{ED} (Eq 5) over the model domain for the remediation period T, that is:

$$M_{bio}(T) = \int_{t=0}^{T} \left[\int_{\Omega} \theta \cdot r_{ED} \cdot d\Omega \right] dt \qquad \text{Eq 7}$$

where Ω represents the 3D model domain, θ (/) is the effective porosity, r_{ED} (M/L^3/T) is the biodegradation rate (Eq 5). This integral is numerically calculated over the model grid and the discretization of the time interval $[0, T]$ adopted in the flow and transport simulation.

5.2.3 Scenario development

Several scenarios were investigated using the MODFLOW-2005 and MT3D-USGS coupled flow and reactive transport model previously developed (Chapter 3 and 4). Most scenarios explore the effect of more than 1 well on the enhancement of in situ NA. Two scenarios involve the use of 3 wells and 4 wells, respectively. Each scenario has several separate simulations. Each scenario is a synthetic experiment investigating a hypothesis.

The 10 modelling scenarios, summarised in Table 5-2, were developed. Most scenarios are located within the same layer and can be easily portrayed with a horizontal cross section (Scenarios 1, 2, 3, 5, and 10). Other scenarios are portrayed with a vertical cross section (Scenarios 4, 6, 9a, and 9b). However, for the remainder of the scenarios (Scenario 7 and 8), which are more complex and 3D, require horizontal and vertical cross sections in order to be better understood and visualized.

The performance of the system in each scenario was compared using ratios of total phenol mass removed (M_{rem}) to initial phenol mass (M_0), M_{rem}/M_0. M_{rem} is split into the two components M_{bio}, that is, the mass of phenol biodegraded, and M_{ext}, that is, the phenol mass extracted. Hence, $M_{rem} = M_{bio} + M_{ext}$. In the case of scenarios involving injection wells. The values of M_{bio} and M_{ext} are normalized to the initial mass so that they can be compared on the same scale.

Table 5-2. Scenarios (1-10) evaluated in 10-year modelling simulations, with respective methodology used (see text for explanation). In scenarios where the wells are moved in 3 dimensions, a plane view and side view are shown.

Scenario	Description	Injection/extraction well layout
Scenario 1. Effect of longitudinally staggering location of dual extraction wells.	Twenty simulations with dual wells placed on plume centerline at a constant lateral distance $\bar{d}$ of 120m (60m north and south of plume center). Longitudinal distance, *l*, is subsequently increased by 190m on successive simulations. Dual well extraction rate is fixed at $\bar{Q}$=-30 m^3/d (-60 m^3/d cumulative).	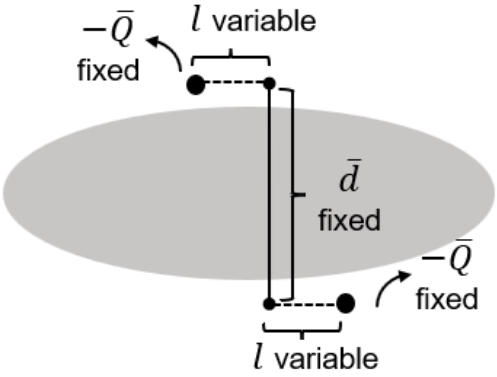
Scenario 2. Effect of triple well where lateral distance is increased, and longitudinal distance remains fixed. Lateral well locations and rates are inherited from Scenario D in Chapter 4.	Four simulations with fixed well longitudinal distance *l* (x direction) and variable lateral distance $\bar{d}$ (y direction). A fixed middle well injects 20 m^3/d and each extraction well pumps -20 m^3/d.	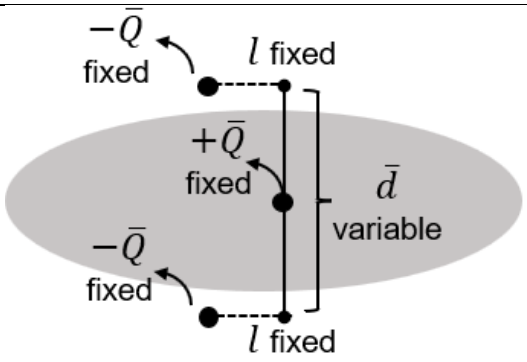
Scenario 3. Effect of triple well where longitudinal distance is increased, and lateral distance remains fixed. Lateral distance is inherited from the final distance in Scenario 2.	Four simulations with well lateral (y direction) location fixed and longitudinal (x direction) location progressively increased. A fixed middle well injects 20 m^3/d and each extraction well pumps -20 m^3/d.	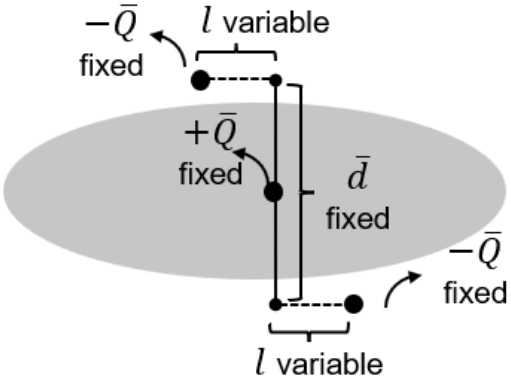
Scenario 4. Effect of longitudinal centerline injection well location.	Six simulations with one injection well placed in the plume centerline/interior. The longitudinal well coordinate, *l*, is progressively increased towards the original contaminant source. Injection of groundwater without EAs at fixed rate of 30 m^3/d.	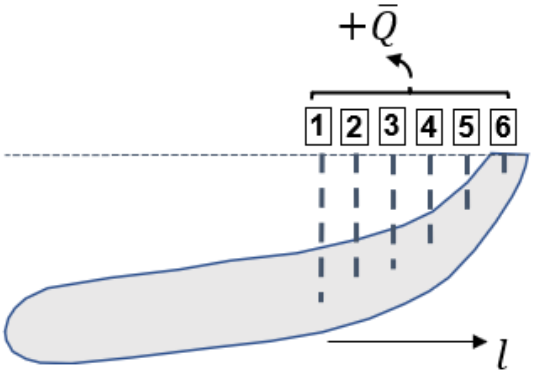

Scenario 5. Effect of injection well at plume center/interior injecting groundwater without EAs at sequentially increasing rates.	Five simulations with an injection well in a fixed location in the plume centerline/interior. Groundwater without EAs is injected to evaluate the effects of fringe processes only. The pumping rate is progressively increased.	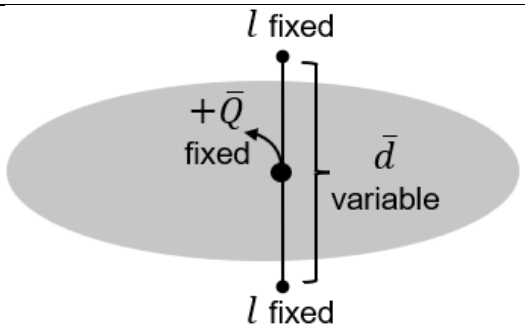
Scenario 6. Effect of injection well injecting amendments in source and extraction well at tip.	Four simulations with one well injecting pure oxygen (50 mg/l) in the source and one extraction well located near the plume front. The wells are aligned along the plume centerline. Injection and extraction rates are progressively increased from ±30 m^3/d to ±100 m^3/d each. Well locations are fixed.	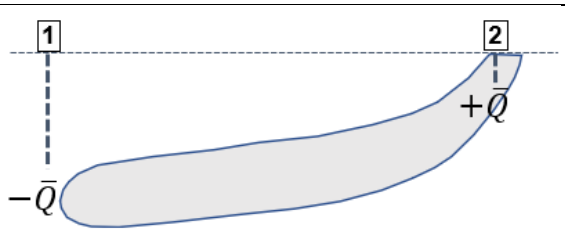
Scenario 7, E1 and E2. Effect of variable location and rates of three wells on biodegradation mass.	Well 2 and 3 are from the "optimal" point (which enhanced biodegradation the most) in Scenario 1. Well 1 is from Scenario A in Chapter 4. Well 2 and 3 are both laterally 60m from the plume centerline and are 100m longitudinally (x direction) apart. This arrangement is essentially the most effective in Scenario 1 with an added extraction well at the front. Each well pumps at -33.3 m^3/d. For E2, the well locations are the same, except the rates are lowered to -20 m^3/d per well.	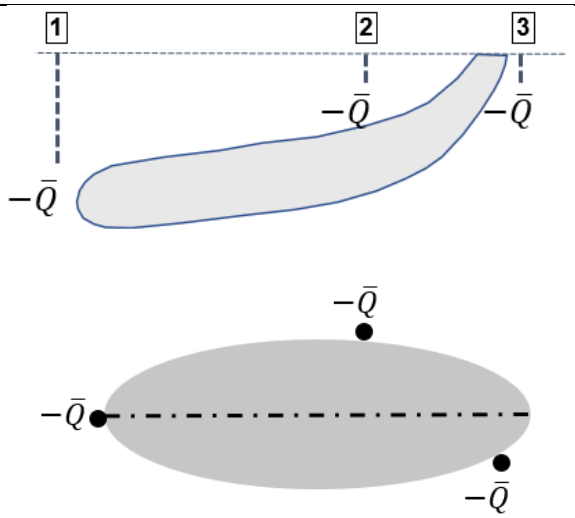

Scenario 7, E3. Effect of variable location and rates of three wells on biodegradation mass.	Well 2 and 3 locations and pumping rates from the previous simulation are used, except for the addition of an injection well between them, in the well centerline/interior. The wells are pumping at $\pm$30 m^3/d. each.	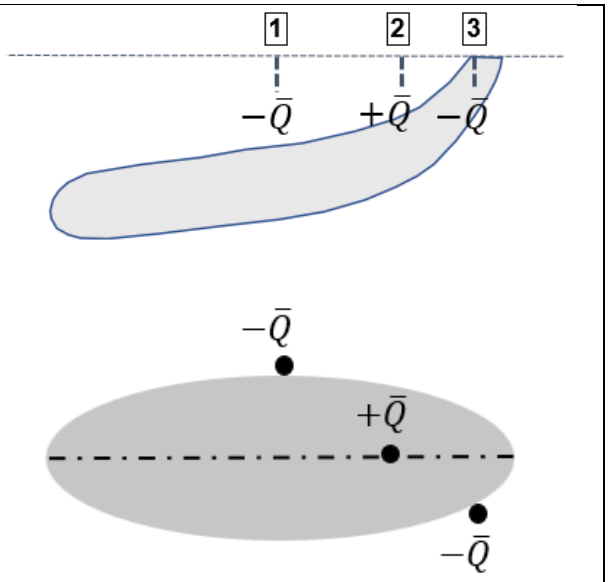
Scenario 7, E4. Effect of variable location and rates of three wells on biodegradation mass.	The same extraction well locations and pumping rates from Scenario 7-E3 are used, except for the addition of an injection well in the plume source. The wells are pumping at $\pm$30 m^3/d each.	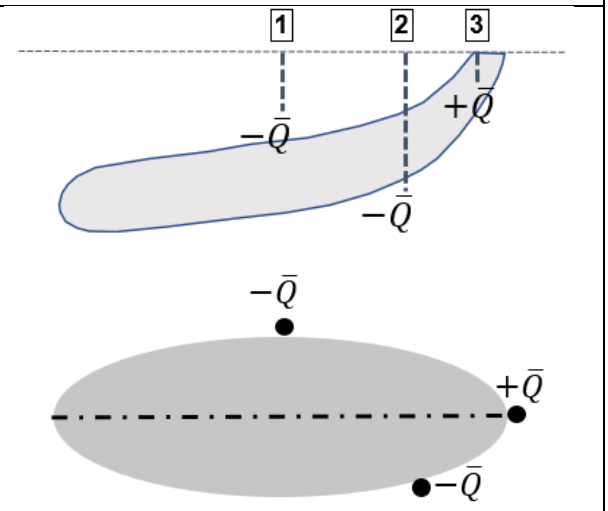
Scenario 7, E5. Effect of variable location and rates of three wells on biodegradation mass.	Well 1 from the Scenario 7-E4 remains the same. Well 2 is moved to the plume centerline and is now injecting. Well 3 remains in the plume source. The wells are pumping at $\pm$30 m^3/d. each.	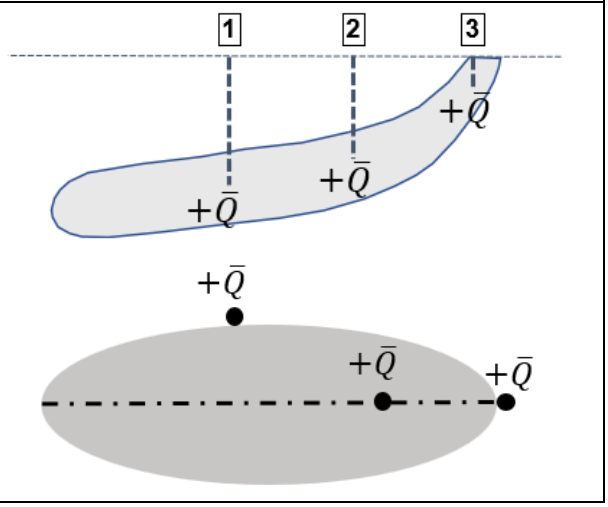

Scenario 7, E6. Effect of variable location and rates of three wells on biodegradation mass.	Each well has been moved to the plume centerline/interior. Well 3 and 2 are longitudinally 95m apart and well 1 and 2 are longitudinally 190m apart.	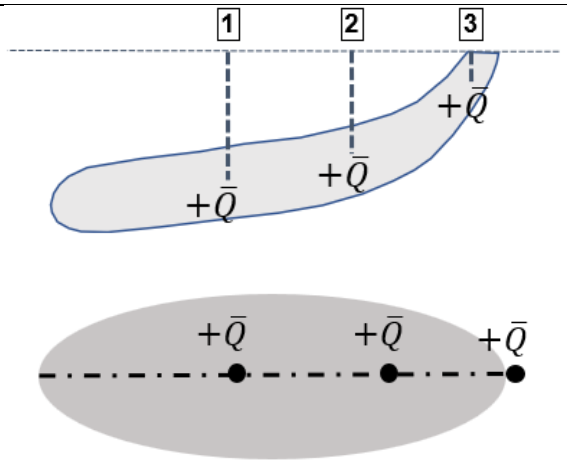
Scenario 8. Effect of constant 4 injection well configuration on biodegradation mass.	This is an attempt to improve the optimal experiment (#5) in Scenario 7. Well 2 is located 60m laterally from the plume centerline. There are 3 experiments where the only changing variable is the pumping rate, which is increased from 20 m^3/d per well to 33.3 m^3/d, terminating at 50 m^3/d per well (cumulative 200 m^3/d).	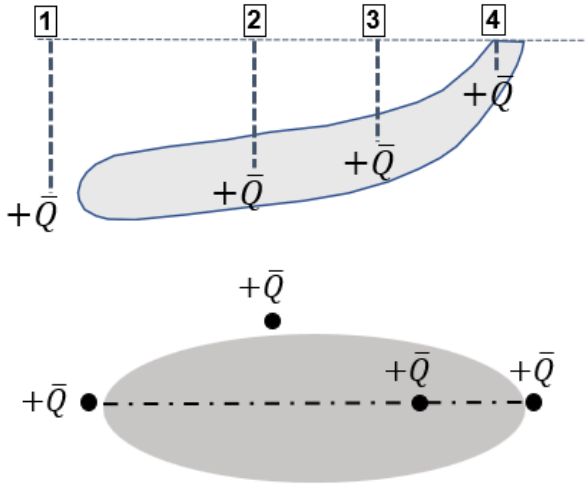
Scenario 9a. Effect of CRM constant concentration on biodegradation mass without pumping.	Sixteen CRMs placed along plume centerline. They are releasing a constant concentration of 9.28 and 105 mg/l of oxygen and nitrate, respectively.	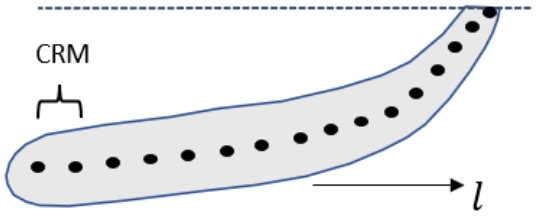
Scenario 9b. Effect of CRM constant concentration on biodegradation mass with injection in source and extraction near plume tip.	Same as the above, except there is extraction near the plume front and injection near the plume back. Pumping rates are ± 30 m^3/d.	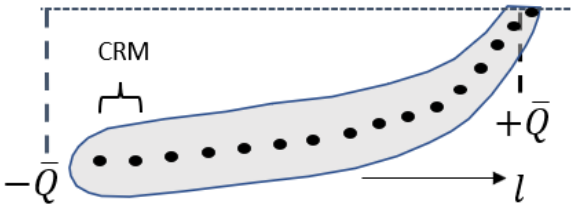
Scenario 10. Effect of different injection well experiments on biodegradation mass.	One injection well located in the plume center/interior, pumping at +30 m^3/d.	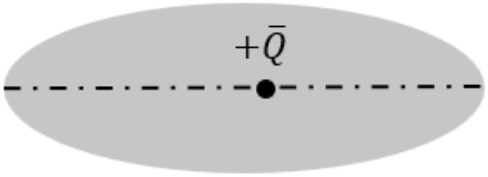

Scenario 1

Scenario 1 explores the effect of dual extraction well longitudinal (x location) on biodegradation mass, with the aim to increase plume spreading and reduce mass extraction (Table 5-2, Scenario 1). The pumping rate for each extraction well is -30 m3/d (cumulative -60 m3/d). The lateral (y location) of the wells is kept constant, 90m apart (each well is 45m from the center of the plume). The depth (z location) of the well remains constant, at layer 14 – the same layer used for the scenarios in Chapter 4. The starting point for the distance measurement is close to the middle of the plume (the plume is 700 m long; middle is 350 m). This scenario is an extension of Scenario A from Chapter 4. The aim is to find an extraction well location that optimizes biodegradation, while keeping the y location (row) constant, as this well orientation creates divergent flows in all directions.

Scenario 2

Scenario 2 investigates the effects of a fixed injection well in the plume centerline and the increase of lateral distance between two extraction wells on the biodegradation mass (Table 5-2, Scenario 2). Scenario 2 builds upon Scenario E in Chapter 4 but increases the complexity. In Scenario E, two extraction wells were placed laterally on either side of the plume centerline and the distance between the wells was progressively increased, while the pumping rate remained constant. The biodegraded mass in Scenario E slightly declines at the end. Scenario 2 uses the best well location (well location which enhanced biodegradation the most) from Scenario E in Chapter 4 as a starting point but adds an additional (injection) well (see Table 5-2, Scenario 2). It was hypothesized that adding an injection well in the center of the plume could increase biodegradation mass further. The injection rate is 20 m^3/d and the extraction rate for each well is -20 m^3/d (20 m^3/d injection, -40 m^3/d extraction). The injection well in Scenario 2 is injecting groundwater without EAs in order to observe the effect of fringe reactive processes only. The wells remain at the same depth as Scenario 1.

Scenario 3

Scenario 3 investigates the effect of a fixed injection well in the plume centerline and the increase of longitudinal distance between two extraction wells on the biodegradation mass. Scenario 3 builds upon Scenario 2 by using the optimal point (which enhanced biodegradation the most) from Scenario 2 as the starting point for Scenario 3. The lateral well location is kept constant (120m apart) while the longitudinal distance (y location) between the wells is increased (Table 5-2, Scenario 3). It is hypothesized that increasing the distance between the wells would improve the spreading and mixing of the plume with EAs, thereby enhancing biodegradation mass. The depth (z location) and all pumping rates remain the same as Scenario 2. The north extraction well is moving west while the south extraction well is moving east. The injection well is injecting groundwater without EAs in order to observe the effect of fringe reactive processes only.

Scenario 4

Scenario 4 investigates the effect of interior (centerline) injection of groundwater without EAs at a fixed rate of 30 m^3/d along the longitudinal axis of the plume (Table 5-2, Scenario 4). For each respective simulation, the wells are moved 20m apart from west to east. As the plume is diving, in order to keep the wells within the plume interior, the depth of the well also increases with distance by 10m each time, from 15m to 60m depth for the final simulation. It is hypothesized that biodegradation will decrease with longitudinal distance, that is, as the well moves from the source (at x=0m) towards the middle of the plume (at x=120m). It is expected that the regions with higher phenol concentration will result in a higher biodegradation mass.

Scenario 5

Scenario 5 investigates the impact of variable pumping rate through an injection well at a fixed location (x=800m on the plume centerline) on biodegradation mass. Groundwater without EAs is being injected in order to measure the effect of only fringe reactive processes. This scenario builds upon Scenario B in Chapter 4, except that the pumping rates are raised further (200-500 m^3/d) to determine whether the trend from Scenario B in Chapter 4 continues. The goal of this scenario is to establish a precedent for how well a single injection well can perform on its own and what the appropriate injection rate would be for other scenarios. This scenario will serve as a control to compare other scenarios with similar pumping rates in order to isolate whether biodegradation is being enhanced primarily by the pumping rate or the well location. The hypothesis is that increasing the pumping rate will result in higher biodegradation. The highest rate in the same aquifer is -4300 m^3/d (Chapter 3, Table 3-2), so the rate could be increased higher, but the goal was to see the trend.

Scenario 6

Scenario 6 uses a well configuration that consists of an injection well at the plume back combined with an extraction well at the plume front, to investigate their combined effect on mass biodegraded. The injection well is injecting pure oxygen at 50 mg/l (Morgan and Watkinson, 1991; Balcke et al., 2009; Greer et al., 2010; Chu et al., 2018), and the pumping rates for both wells are sequentially increased from 60-200 m^3/d (see Table 5-2, Scenario 6). The aim of this scenario is to increase the biodegraded mass by injecting the maximum rate of oxygen possible at the plume back which has the highest concentration of phenol, while extracting at the plume front to spread the amendment through the interior of the plume. At first the extraction well was located too close to the plume front, which removed more mass than expected, so it was moved 30m westward and then the well location was kept constant for the remainder of the scenario. Subsequently, both wells remain stationary while the flow rates are increased. It was hypothesized that a higher flow rate would more effectively spread the amendment downgradient through the plume centerline.

Scenario 7

Scenario 7 builds upon optimal well locations from Scenario 1 and Scenario 3. Scenario 7 has 6 sub-scenarios or experiments (labelled E1, E2…) which investigate the effect of variable

well location and pumping rate for 3 concurrent wells on biodegradation mass (Table 5-2, Scenario 7). The aim is to find a set of 3 wells which multiply the effect of a single well on biodegradation.

The distance between the well locations for Scenario 7 were chosen in order to avoid stagnant zones caused by the wells being too close together, which can prevent mixing and therefore prevent reactions from occurring effectively.

Previous scenarios have demonstrated that using additional wells does not always outperform a single well, even when the pumping rates remain the same. Moreover, when/if they do outperform a single well, the increase is nonlinear. In the next few paragraphs, the design of Scenario 7 is discussed in more detail.

For Scenario 7, experiment 1 (E1), the same extraction well locations from the optimal point (x=100m) from Scenario 1 are used in conjunction with an extraction well at the plume front (Table 5-2, Scenario 7, E1). It is hypothesized that these wells are far enough so that they accelerate mixing and that the well at the plume front will enhance spreading throughout the entire plume. This is achieved by enhancing the spreading caused by longitudinal dispersion (when a well is used to spread the plume laterally, transverse dispersion plays a role in enhancing biodegradation, but most of the enhancement comes from longitudinal dispersion). The rates of each extraction well are -33.3 m^3/d (cumulative -100 m^3/d).

For Scenario 7, experiment 2 (E2), the same wells as E1 are used but the pumping rates are decreased by 40% (-20 m^3/d each; cumulative -60 m^3/d) to observe the impact that pumping rate has for this configuration (Table 5-2, Scenario 7, E2). It is hypothesized that the lower pumping rate will result in a lower mass extraction and mass biodegradation.

For Scenario 7, experiment 3 (E3), it also uses the same extraction wells from Scenario 1, but there is now an injection well near the plume center (x=890), which is the optimal injection well from Scenario 4 (Table 5-2, Scenario 7, E3). It is hypothesized that this well placement will enhance biodegradation greater than experiment 1. The pumping rates for the dual extraction wells and the injection well are -33.3, -33.3, and 33.3 m^3/d, respectively.

For Scenario 7, experiment 4 (E4), the dual well configurations and pumping rates are the same as E3, except the injection well is now placed in the plume back, as in Scenario 4 (Table 5-2, Scenario 7, E4). It is hypothesized that this new injection well placement will result in an enhancement in biodegradation mass.

For Scenario 7, experiment 5 (E5), there are 3 injection wells, with one located in the plume back, one downgradient from the plume back, and one lateral to the plume centerline, on the plume fringe (Table 5-2, Scenario 7, E5). Each well is injecting water without EAs in order to understand the effect of plume fringe processes only. The pumping rates are 33.3 m^3/d each (cumulative 100 m^3/d). It was hypothesized these injection wells would enhance biodegradation greater than the previous experiments.

For Scenario 7, experiment 6 (E6), all of the conditions are the same as experiment 5, but the injection well at the plume fringe is moved to the plume centerline (Table 5-2, Scenario 7, E6). The effect of injection well placement fully within the centerline of the plume was investigated to determine the effect on biodegradation mass. It was hypothesized that injection fully within the plume centerline would enhance biodegradation mass more than experiment 5.

Scenario 8

Scenario 8 builds upon the best experiment (experiment 5) from Scenario 7 and adds an additional well (Table 5-2, Scenario 8). This scenario is an attempt to find a well configuration with a multiplicative relationship between the number of wells and biodegradation. It was hypothesized that if the effects of a single well in Scenario C-ext in Chapter 4 could be multiplied, then biodegradation could be significantly enhanced.

Scenario 8 investigates the effect of 4 fixed location injection wells on biodegradation. The scenario is split into 3 experiments where only pumping rate is sequentially increased. For experiment 1, 2, and 3, the pumping rates are 20, 33.3, and 50 m^3/d for each well, for a cumulative rate of 80, 133, and 200 m^3/d, respectively. Each experiment is split into two parts: A and B. For part A, the injection wells are injecting water without EAs. For part B, amendments of pure oxygen and nitrate at 50 and 105 mg/l, respectively, are injected. For part A, only fringe reactions are occurring as the groundwater that is being injected has no EAs; for part B, both interior reactions and fringe reactions are occurring as the groundwater that is being injected contains EAs, which is causing the plume to spread and react with the EAs in the groundwater.

Scenario 9

Scenario 9 is split into two closed linked experiments labelled 9a and 9b. Scenario 9a measures the effect of controlled release materials (CRMs) on biodegradation mass by simulating 16 evenly spaced CRM cells of constant concentration aligned in a transect along the plume centerline. The CRM cell is meant to simulate a well candle type amendment which could feasibly release a constant concentration of EAs for a prolonged period (O'Connor et al., 2018). Each CRM cell is located 50 meters apart, and the Z location is changing to keep the CRM in the plume centerline, for a total transect length of 800 meters. The CRMs release 9.28 and 105 mg/l of oxygen and nitrate, respectively, they flow along the hydraulic gradient for 10 years (Table 5-2, Scenario 9a). There are no wells present in scenario 9a as it is used as a control with which to compare scenario 9b, in order to determine if PAT combined with CRMs can enhance NA. Scenario 9a is also compared with the baseline biodegradation mass over 10 years.

Scenario 9b combines Scenario 9a and Scenario 6: The same CRM cells from 9a are kept, but with a well configuration added. Well locations and initial pumping rates are the same as Scenario 6, consisting of an injection well at the plume back combined with an extraction well at the plume front, to investigate their combined effect on mass biodegraded. The

injection and extraction wells are at fixed locations and are pumping at 30 and -30 m^3/d, respectively. Scenario 9b is directly compared to Scenario 9a and Scenario 6.

Scenario 10

Scenario 10 investigates the effect of interior injection of various amendments at the plume centerline on mass biodegraded for 7 experiments (Table 5-2, Scenario 10). In each experiment, a single fixed injection well is located at the center of the plume with a pumping rate of 30 m^3/d.

Scenario 10 compares the effect of injection of the following amendments: (i) injection of 105 mg/l of nitrate while oxygen is 0 mg/l; (ii) the injection of oxygen at 9.28 mg/l while nitrate at 0 mg/l; (iii) the combined effect oxygen and nitrate at 9.28 and 105 mg/l, respectively; (iv) injection of nitrate at 230 mg/l, with oxygen is 0 mg/l; (v) injection of oxygen at 50 mg/l, with nitrate at 0 mg/l; (vi) the combined effect of nitrate and oxygen at 230 mg/l and 50 mg/l, respectively; Scenario 6 at the its point of highest biodegradation enhancement; and Scenario 9a and 9b. The reason for the design of these experiments is to isolate the relative effect of different terminal electron accepting processes on biodegradation *in situ*.

Scenario 10 compares the injection of amendments with the results from Scenario 6 at its initial pumping rate, Scenario 9a, and Scenario 9b. The pumping rates for Scenario 6 and Scenario 9b are -30 m^3/d and 30 m^3/d, so that they are comparable. The injection of pure oxygen is being simulated, which can feasibly reach concentrations of 50 mg/l at high pressures present in aquifers and has been tested and simulated in several field and modelling studies to date (Morgan and Watkinson, 1991; Balcke et al., 2009; Greer et al., 2010; Chu et al., 2018).

5.3 Results and discussion

Figure 5-2 shows the results of the scenarios 1-8 with regards to the ratios of $M_{rem}/M_{0.}$ The black triangles represent the ratio of mass extracted, M_{ext}/M_0 and the open circles represent the ratio of mass biodegraded, $M_{bio}/M_{0,}$ which are both normalized to the initial mass. Scenario 7 and 8

Figure 5-3 shows the biodegradation mass results for scenarios 1-8. These graphs are essentially enhanced images of $M_{bio}/M_{0,}$ so that the differences in biodegradation can be more easily compared.

Figure 5-4 shows the results for Scenario 9a, 9b, and 10.

The baseline mass degraded by intrinsic NA, without PAT intervention, over 10 years is 237 kg, which is the control on which the various scenarios presented here are compared. If a scenario increases biodegradation above the baseline (higher than 237 kg), then biodegradation mass is considered to be enhanced. Consequently, the y axis in Figure 5-3 begins at 237 kg.

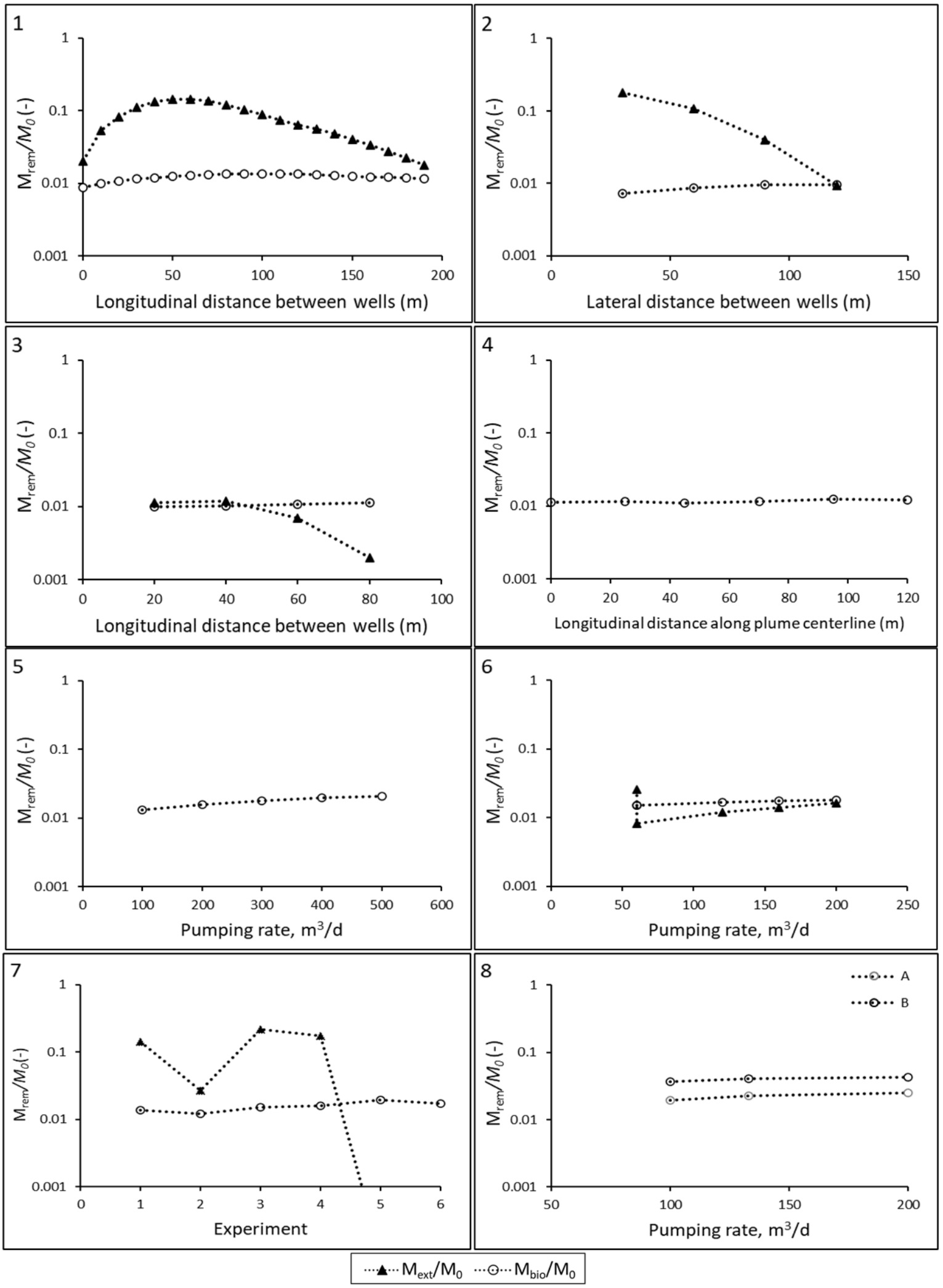

Figure 5-2. Presented above are the ratios of mass removal and the mass biodegraded for scenarios 1-8. The y-axis is the value of contaminant mass removed by biodegradation in situ (M_{bio}) and extraction (M_{ext}), normalised to the initial mass (M_0). The scenarios depicted above follow the same order as Table 5-2.

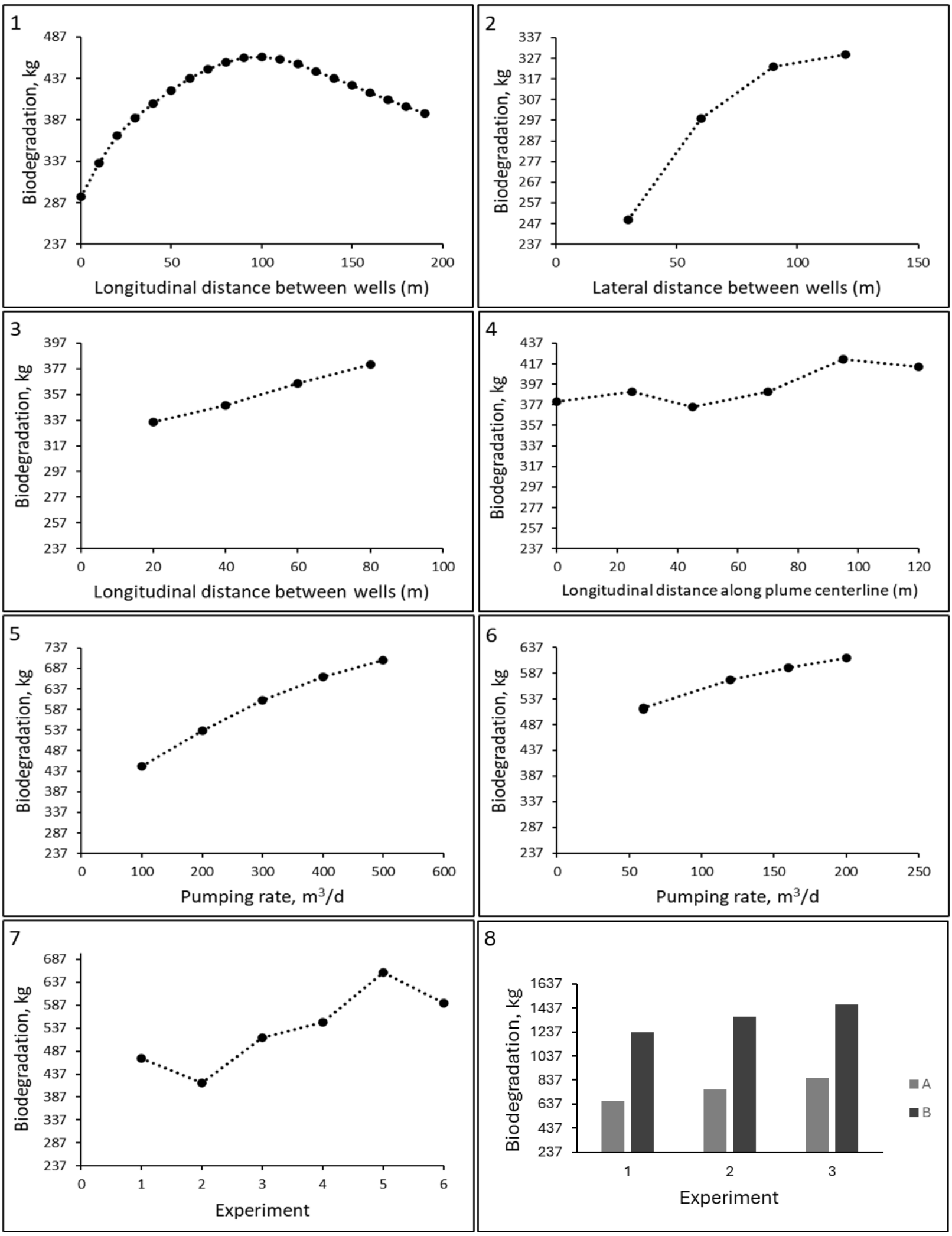

Figure 5-3. Presented above are the values of mass biodegraded for scenarios 1-8. The y-axis shows the biodegradation mass in kilograms while the x-axis shows the variable under consideration for the particular scenario. The scenarios depicted above follow the same order as Table 5-2. The y-axis begins at 237 kg as that is the baseline (no intervention) biodegradation mass over 10 years on which the performance of these scenarios are compared.

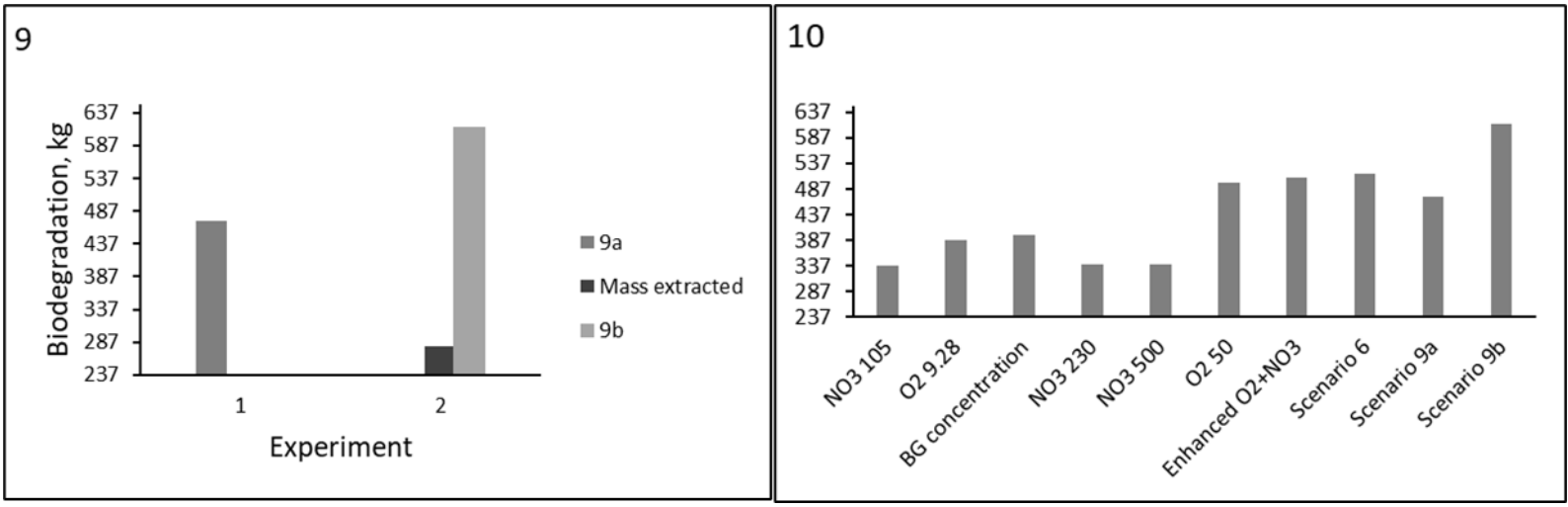

Figure 5-4. Scenario 9 and 10 are presented above. Scenario 10 compares a series of groundwater injection and amendment injection scenarios. Scenario 5, 9a, and 9b are also compared here.

Scenario 1

Figure 5-2, 1 and Figure 5-3, 2 show that as the longitudinal distance between the extraction wells increases up to 100m, so does the mass biodegraded. At 100m, biodegradation was enhanced by 89% above the baseline due to spreading induced by the extraction wells. After 100m, biodegradation mass then declines, due to the influence of the wells on the plume decreasing. Conversely, mass extracted peaks at 50m distance (14.4% of total plume mass) and then steadily declines up to 200m distance (1.7% of total plume mass). Mass extraction decreases by 40% between 50m and 100m. The difference in biodegradation between 100m and 200m is 15%, but there is an 80% difference in mass extracted. The data in this scenario could be useful if the remediation goal is to find a compromise between mass extraction and *in situ* biodegradation, given that the plume is allowed to spread.

Scenario 2

Figure 5-2, 2 shows that the biodegraded mass increases with lateral distance and mass extracted declines with lateral distance. Figure 5-3, 2 shows the results of the biodegradation mass, with diminishing returns in the mass biodegraded beginning after 90m, due to the decreased influence of the extraction wells on the plume. At 120m distance, biodegradation is enhanced by 38% over the baseline and 11.5% over Scenario E in Chapter 4. Over 120m, mass extracted decreases by 94.8%. Increasing the lateral distance further would result in an additional decrease in mass extraction but may not increase biodegradation further by much, if at all.

Scenario 3

Figure 5-2, 3 shows that the biodegraded mass increases with longitudinal distance. Figure 5-3, 3 shows the results of the biodegradation mass. The enhancement in biodegradation above the baseline is 60%. The enhancement in biodegradation over Scenario 2 is approximately 15%, which is insignificant. Additionally, using this well configuration results in a reduction

in mass extracted up to 78%. The overall reduction in mass extracted from the first data point in Scenario 2 to the final data point in Scenario 3 is 98.89%. Moving the wells in this way enhances biodegradation while reducing the mass extracted by the extraction wells. However, the trend of biodegradation mass increasing with longitudinal distance between the wells would not persist much longer, as the results of Scenario 1 indicate.

Scenario 4

Figure 5-2, 4 and 5-3, 4 show that biodegradation mass generally increases with increasing distance from the plume source. Biodegradation was enhanced by 77% above the baseline at the optimal point, which occurred at x=90m. Injecting further from the source results in the highest biodegraded mass.

These results were unexpected, as they are directly the opposite of what was hypothesized. The reason why the optimal point occurred at 90m is due to physical heterogeneity – at this location, the hydraulic conductivity is 30% of the maximum K (see Table 5-1 for range of K values). In a cross-sectional view, transverse vertical dispersivity is enhanced as the plume flows through the lower K zone as induced by the hydraulic gradient. Injection causes additional plume spreading which is enhanced by the aquifer heterogeneity. However, the change in biodegradation within the scenario is 15% at most.

Scenario 5

Figure 5-2, 5 and and Figure 5-3, 5 show that biodegraded mass increased with pumping rate. Biodegradation was enhanced by 195% above the baseline (Figure 5-3, 5). Biodegradation responds well to injection rate due to injection causing strong divergent flows which enhance plume spreading in all dimensions and therefore enhance dispersive mixing of the plume with groundwater.

Scenario 6

Figure 5-2, 6 and Figure 5-3, 6 show that biodegradation increases as a result of the combination of the increase in pumping rate and the injection of pure oxygen at 50 mg/l. Biodegradation was enhanced by 168% over the baseline. However, there is only a 20% increase in biodegradation while there is a 233% increase in pumping rate. This pumping rate increase also resulted in a significant increase (97%) in the mass extracted (Figure 5-2, 6). Consequently, increasing the pumping rate in this scenario is not efficient or significant at enhancing biodegradation *in situ* and it is not recommended. Moreover, Scenario 6 was unsuccessful at spreading the amendment throughout the entirety of the plume due to the low groundwater velocity in the aquifer; a period longer than 10 years is required to spread the amendment throughout the plume centerline or the hydraulic gradient in the plume area would need to be hydraulically eliminated using an injection well at the plume front and an extraction well at the plume back, which is impractical for such a large plume.

Scenario 7

Figure 5-2, 7 and Figure 5-3, 7 show the results for the performance ratios and biodegradation mass, respectively, for Scenario 7.

Scenario 7, experiment 1 enhanced biodegradation mass by 98.52% over the baseline. Experiment 1 enhanced biodegradation 5% more than a single injection well (Scenario B-GW in Chapter 4) at the same rate (100 m^3/d), despite having the advantage of enhancing the biodegradation rate in several regions of the plume at once. However, it did perform 50% and 93% better at enhancing biodegradation than a single (compared to Scenario B-ext) and double extraction well (compared to Scenario D), respectively, at the same rate. Experiment 1 extracted 60% more mass than Scenario 1, while only enhancing biodegradation by 1.51% more than Scenario 1. Also, the overall pumping rate is 40% higher, there is an extra well, and significantly more mass was extracted. Consequently, this experiment did not improve on Scenario 1. The reason why this experiment did not have an improvement over Scenario 1 is due to the additional extraction well at the plume front. This well mainly extracted additional mass while barely enhancing the biodegradation rate, due to a combination of the low phenol concentration found at and near the plume front and the contribution of only longitudinal dispersion to plume mixing in this case.

Experiment 2 enhanced the mass biodegraded by 75.97% over the baseline. Experiment 2 performed 11.27% worse and extracted 81% less mass than experiment 1. The reduction in biodegraded mass was expected, but the significant drop in mass extracted was not. There was an approximate 80% drop in mass extracted per 40% decrease in pumping rate. This experiment may not have enhanced the in-situ biodegradation mass, but it did reduce the mass that must be treated ex situ, which may be desirable for plume management.

Experiment 3 enhanced the mass biodegraded by 117.48% over the baseline. Experiment 3 performed 9.65% more effectively than experiment 1. While the placement of the injection well did enhance biodegradation as expected, it also significantly increased the mass extracted by 708%, by increasing the recovery of the plume by one of the extraction wells, which is undesirable, as the goal is to biodegrade the plume *in situ*.

Experiment 4 enhanced the mass biodegraded by 131.61% over the baseline and by 6.4% compared with experiment 3. The placement of the injection well at the source rather than the center reduced the mass extracted by 19.55% compared to E3 (Figure 5-3, 7).

Experiment 5 enhanced the mass biodegraded by 177.81% over the baseline and by 20% over experiment 4. Since only injection wells were used for this experiment, there is no mass extraction. The injection wells cause more pronounced plume spreading and mixing, which further increases the biodegradation rate, and therefore the mass biodegraded.

Experiment 6 enhanced the mass biodegraded by 149.47% over the baseline but performed 10% worse at enhancing the mass biodegraded than experiment 5. The reason is due to one of the injection wells being moved from its lateral location outside the plume to within the plume centerline. It was expected that injection in the interior/centerline would enhance biodegradation more than injection at the fringe/laterally, since the plume is more concentrated at this location and would evenly spread in all directions, as opposed to being spread mostly laterally. Injection lateral to the plume causes spreading in the transverse direction, which then spreads longitudinally due to the direction of the advective flow path and the effects of longitudinal dispersion.

In summary, the best performing experiment of Scenario 7 was experiment 5 (E5), which enhanced the mass biodegraded by 177.81% over the baseline. The increase in biodegradation from E1 to E5 is 40%, which was achieved by only changing the location of the wells, and from extraction to injection. The overall rate of groundwater being moved (absolute value of pumping rate) between the two experiments is the same. E5 also extracted no mass, in contrast to other scenarios, which would reduce the treatment cost. This scenario illustrates the importance of well location and well type (injection or extraction) on the contaminant mass biodegraded.

Scenario 8

Part A - injection of groundwater without EAs

Figure 5-3, 8 shows that Scenario 8, experiment 1A enhanced biodegradation by 178.69% over the baseline. The pumping rate for each well is 20 m^3/d (cumulative 80m^3/d). This experiment biodegraded essentially the same amount of mass as experiment 5 (optimal point of highest biodegradation mass) in Scenario 7, despite this scenario having an additional well. This diminishing returns in performance is a combination of the additional (4^{th}) injection being in a suboptimal location (plume front) and the pumping rates at the laterally placed wells being too low to cause the desired plume spreading.

Scenario 8, experiment 2 uses the same well locations as experiment 1 but increases the pumping rates by 66.5% (from 20 to 33.3 m^3/d per well). Figure 5-3, 8 shows that experiment 2A enhanced biodegradation by 220.22% over the baseline. This increase in pumping rate resulted in a 14.91% enhancement from 1A.

Experiment 2A uses the same well configuration pumping rate for each well as Experiment 5 in Scenario 7, except with 1 additional injection well added (Table 5-2, Scenario 7, E5 and Scenario 8). The difference in biodegradation between Scenario 7-E5 and Scenario 8, experiment 2A is only 15% despite a 33% increase in cumulative pumping rate, due to the additional injection well.

Scenario 8, experiment 3 uses the same well locations as the previous two experiments, but pumping rate is increased an additional 50.15% (from 33.3 to 50 m^3/d per well – cumulative 200 m^3/d). Figure 5-3, 8 shows that experiment 3A enhanced biodegradation by 258.54% over the baseline. This is a 11.96% increase in biodegradation mass from 2A.

Part B - injection of groundwater with amendments

Scenario 8, experiment 1B enhanced biodegradation by 421.13% over the baseline (Figure 5-3, 8). It is an 87.12% enhancement from 1A. Injecting amendments with an enhanced concentration of oxygen at 50 mg/l is enough to nearly double the mass biodegraded with respect to 1A.

Scenario 8, experiment 2B (amendment injection) enhanced biodegradation by 475.55% over the baseline (Figure 5-3, 8). It is a 79.73% improvement from 2A.

Figure 5-3, 8 shows that experiment 3B enhanced biodegradation by 518.10% over the baseline. It is a 72.38% improvement from 3A. 3B enhanced biodegradation by 7.33% over 2B, which is insignificant. Overall, experiment 3B biodegraded 3.4% of total plume mass over 10 years, which is close to the estimated 2-5% that has previously been biodegraded over 50 years of natural attenuation (Lerner et al., 2000; Thornton et al., 2001b).

Figure 5-3, 8 shows that for the 4 injection wells, pumping rate does not cause a significant difference. There is only a difference in biodegradation of 30% between 1A and 3A despite an increase in pumping rate of 150%. The difference in biodegradation between 1B and 3B is ~20% despite an increase in pumping rate of 150%. This in general illustrates the diminishing returns in enhancement of biodegradation that are incurred from using more than one well.

However, there is a significant difference in biodegradation between part A and part B due to the injection of pure oxygen at 50 mg/l. This enhancement is due to a more favorable stoichiometric ratio of mass between oxygen and phenol. This shows that these diminishing returns can be surmounted by using injected amendments.

Scenario 8 also illustrates the importance of mixing the plume interior with amendments. Fringe reactive processes combined with plume interior reactive processes – e.g., high concentration of ED mixing with a high concentration of EA – play an important role in enhancing biodegradation. Injecting amendments in the plume interior is so effective due to direct mixing of EAs and phenol at their highest concentration, in conjunction with spreading enhanced reactions; whereas, when groundwater without EAs in injected in the center of the plume, there is no enhancement of biodegradation rate near the well – there is only enhancement of biodegradation rate at the fringes. Conversely, injecting amendments in the center of the plume causes enhancement of biodegradation rate near the well, in the plume interior, and at the fringes – i.e., everywhere the ED and EA come into contact. Consequently, at least in this context, injection wells are more effective at enhancing biodegradation rates and mass biodegraded than extraction wells.

Scenario 9

Figure 5-4, 9 shows that the biodegraded mass is significantly enhanced (99%) over the baseline by the CRM amendments without pumping intervention. However, with pumping, biodegradation is enhanced by 159%. There is a 30% increase in biodegradation between 9a and 9b; consequently, most of the biodegradation mass is a result of the CRMs, and the PAT intervention is not further enhancing biodegradation as much as expected.

Scenario 9b also performed 18.76% more effectively than Scenario 6 at the same pumping rate, which is essentially the same scenario without the CRMs (see Table 5-2, Scenario 6 and Scenario 9a and 9b for comparison). This is despite the CRMs releasing lower concentrations of EAs than the direct amendment injection in the source that Scenario 6 employs. The 16 CRMs spread EAs more effectively through the plume than injection with a single well alone.

Scenario 10

Figure 5-4, 10 shows that oxygen is the most effective EA, as the k-max term is 10 times higher than that for nitrate (Table 5-1), and even increasing the injected nitrate concentration by 375% has no additional effect on biodegradation mass, due to the inhibition constant (Table 5-1). The most effective experiment was the injection of oxygen 50 mg/l and nitrate 230 mg/l, which enhanced biodegradation by 114%, of which nitrate only contributed 2.4%. The most effective amendment experiment enhanced biodegradation by 20% over Scenario 9b, which indicates that amendment injection at these concentrations is effective.

As Scenario 6 showed, the combined effect of injecting oxygen at 50 mg/l concentration in the source and extracting at the plume front is only slightly more effective (1.57%) at enhancing the mass biodegraded when compared with simply injecting a combination of oxygen 50 mg/l and nitrate 230 mg/l without pumping. This result implies that the extraction well in Scenario 6 is not enhancing biodegradation. The results would be different if aerobic respiration were not formulated to inhibit denitrification and if the k-max term for nitrate were higher. In that respect, the denitrification results for Scenario 10 are site specific and may differ at other sites.

5.4 Conclusion

The 10 scenarios in this chapter aimed to find ways to reduce the “diminishing returns” incurred by having multiple wells in operation as demonstrated in Chapter 4. These diminishing returns occurred whenever multiple wells were used in the same simulation; their enhancement of biodegradation was less than the sum of what each of the wells achieved in separate simulations. This chapter attempted to address this aim by simulating different multiwell configurations, pumping rates, amendment injections, and well types (injection or extraction).

However, this chapter failed to find a configuration with a linear relationship between a higher number of wells and biodegradation mass. For example, despite Scenario 2 and 3 having an additional well than Scenario 1, they were not more effective at enhancing NA. Diminishing returns were still occurring between well number and biodegradation mass, pumping rate and biodegradation mass, and amendment injection and biodegradation mass; the relationship remained sub-linear and logarithmic. It is concluded that concurrently using multiple wells of any type does not necessarily increase mixing or spreading to enhance biodegradation more effectively than a single well. However, experiments in Scenario 7 succeeded in enhancing degradation by 40% and mass extracted was reduced by only changing the well location and well type while keeping the pumping rate the same. This illustrates that specific location of the well and the well type is an important factor when designing a multiwell PAT configuration with the aim of enhancing in situ NA.

Overall, injection wells were found to be far more effective than extraction at enhancing biodegradation. This is due to the divergent flows induced in 3 dimensions by the injection wells which increase the dispersive mixing of the plume and the uncontaminated groundwater (Marquis and Dineen, 1994; Jones et al., 2002). Injection of EAs and amendments further enhanced biodegradation due to an increase in the stoichiometric ratio between the ED and EA and specific reactions in the plume interior between the ED and EA; whereas injection of

groundwater without EAs did not enhance reactions in the plume interior - only on the plume fringes, where mixing occurs.

This chapter also aimed to investigate multiwell scenarios with the injection of amendments and determine their impact on mass removal and in situ biodegradation. This was explored by simulating different amendment scenarios with varying levels of oxygen or nitrate and investigating whether multiple injection or extraction wells could enhance their influence on biodegradation. Scenario 9b was most effective at enhancing biodegradation, compared to no intervention over 10 years. Despite Scenario 6 injecting higher concentrations of EAs in the highest concentrated region of the plume, the EAs were more evenly spread throughout the entire plume in Scenario 9b, which led to this enhancement. Injecting oxygen at 50 mg/l and nitrate at 230 mg/l was only marginally more effective than injecting 50 mg/l of oxygen alone due to the inhibition term used in the Monod formulation. This is a site specific finding as aerobic respiration would likely simultaneously occur with denitrification at other sites (Wiedermeier et al., 1999).

While changing well layouts, well types (injection vs extraction), amendment injection, and amendment with CRMs resulted in significantly enhanced biodegradation, there were still diminishing returns incurred. This is due to limitations such as limited mixing between the ED and EAs, low aquifer mechanical dispersion, order of magnitude higher ED concentration, intrinsically slow reaction kinetics, and stagnation zones in between wells (Cunningham et al., 2004). Future studies could examine ways to overcome these limitations by enhancing mixing between the ED and EA further. The mixing and low dispersion limitations could be realistically overcome by employing time variant recirculating or oscillating wells that are commonly employed in in situ bioremediation studies (Bagtzoglou and Oates, 2007; Zhang et al., 2009; Piscopo et al., 2013; Sather et al., 2022; 2023).

Overall, these trial-and-error methods, with the qualitative comparison of well configurations and biodegradation mass show that there is significant potential for optimization of these operational variables such as well location, pumping rates, number of wells, and amendment type and concentration. In the future, the application of mathematical optimization could possibly be applied to advance the research for which this chapter has laid the foundation.

Finally, while Scenario 7, E5 and Scenario 8 significantly enhanced biodegradation, these are hypothetical scenarios aimed at exploring the science and are not meant to remediate a field site. In reality, these injection wells would need to be bounded by extraction wells to manage the contaminant plume size and contain it within the site. These more practical applications are considered in the subsequent chapter, where the lessons learned from Chapters 3, 4, and 5 are used to create more practical scenarios that aim to remediate a hypothetical field site.

PAGE INTENTIONALLY LEFT BLANK.

Chapter 6

Enhancing in situ biodegradation in groundwater using multiwell pump and treat remediation: operational cost analysis for longer term remediation scenarios.

6.0 Abstract

A remediation approach which uses pump and treatment (PAT) to enhance the biodegradation of organic contaminants by increasing dispersive mixing between plumes and groundwater was evaluated for a phenol-contaminated aquifer, using a reactive transport model which simulates kinetic reactions between an electron donor (ED) in the plume and electron acceptor (EA) in the groundwater. This research explores a series of 6 scenarios aimed at enhancing in situ biodegradation as much as possible by using combinations of injection and extraction wells, in order to reduce the total cost of remediation. These scenarios were simulated with the constraint that they reach the remediation target of 90% of contaminant mass removed, through combination of biodegradation and mass extraction, within 60 years. Each scenario used slightly different well locations, pumping rates, well types (injection vs extraction) and one scenario included temporally varying side to side injection and extraction. Scenarios which enhanced biodegradation, and thus, cost reduction through biodegradation the most, required significantly more time to reach the remediation target compared to conventional PAT. The arguably best performing scenario enhanced biodegradation by 285%, degraded 15% of total phenol mass, and reduced the cost of remediation by $66,000, but incurred $85,000 in electricity costs and $540,000 in treatment costs over 40 years. It was determined that this approach examined in this study was limited by the concentration of the contaminant, which is orders of magnitude higher than the concentration of the oxidants, in addition to the slow biodegradation kinetics. However, this framework may remediate contaminants that are more readily biodegradable under aerobic conditions, such as BTEX.

6.1 Introduction

Groundwater pollution via organic contaminants is a significant problem globally. Remediation timeframes using current technologies are prolonged and expensive. It has been estimated that there are at least 126,000 US sites which will require 110 billion to 127 billion USD to remediate, and about 10% of these sites are unlikely to reach remediation targets within 50-100 years (NRC, 2013).

Pump and treat (PAT) is an effective strategy for remediation at sites with certain conditions, such as homogeneous, permeable, and isotropic sites impacted with contaminants possessing high aqueous solubility (McDade et al., 2013). However, PAT has many limitations and may be unsuitable at remediating sites which have complexities such as physical heterogeneity, anisotropy, low permeability, sorption-desorption processes, and matrix diffusion (McDade et al., 2013; Truex et al., 2017); or sites with contaminants that partition into different phases, such as volatile organic compounds, which form vapours, and non-aqueous phase liquids, which have an immiscible phase with low solubility and mobility and can persist in aquifers (FRTR, 2023). In these instances, PAT systems alone are inadequate to remediate the contaminated site and the technology may instead be implemented for hydraulic

containment of the plume to manage risk to downstream receptors. In order to improve the efficacy of remediation, PAT can instead be combined with other technologies such as source removal (excavation), in situ bioremediation or chemical oxidation, surfactants, air sparging/in situ venting, as determined by the specific site characteristics, such as hydrogeology and contaminant class (Freeze and Cherry, 1999; Truex et al., 2017; NRC, 2013; Fetter et al., 2017; FRTR, 2023).

Natural attenuation (NA) is the combination of physical, chemical, and biological processes which attenuate contaminant concentrations through the processes of advection, hydrodynamic or mechanical dispersion, sorption, dilution via recharge, volatilization, biodegradation, and abiotic/chemical degradation (Wiedemeier 1996; 1999; NRC, 2000; Scow and Hicks, 2005; Rivett and Thornton, 2008).

NA can remediate many classes of contaminants under a wide range of hydrogeological settings. NA can be defined as the combination of physical processes (e.g., advection, dispersion, dilution, and sorption), chemical processes (e.g., ion exchange, precipitation/dissolution, abiotic transformation) and biological processes (e.g., bioaccumulation, and biodegradation (Favas et al., 2016; Wiedemeier et al., 1999)), which can reduce the mobility, bioavailability, toxicity, or concentration to levels that are less harmful to human health and ecosystems (NRC, 2000). Advection transports contaminants downgradient but conserves mass and concentration. Mechanical dispersion occurs as a result of changes in groundwater velocity at the pore scale related to heterogeneity, pore friction, pore size, and tortuosity; it conserves mass but reduces concentration. Of all these NA processes, biodegradation is the only process that reduces both contaminant concentration and mass. This is achieved through microbially mediated redox reactions which transform contaminants into a variety of organic and inorganic compounds. These microbially mediated redox reactions occur between an electron donor (ED) and an electron acceptor (EA); the ED is oxidized, and the EA is reduced. These reactions are typically accentuated on the fringes of the plume, where the concentration of the ED is lower than the plume interior, and the EA concentrations are higher than inside the plume interior, and where poor dispersivity and groundwater velocity limit the mixing of the ED and EA.

NA typically occurs naturally in most contaminant sites without intervention; however, reaction rates may be slow due to the lack of bioavailable EA and the efficacy of biodegradation depends on the site conditions and contaminant. Biodegradation rates in groundwater are reduced when the hydraulic conductivity and dispersivity are low, as this decreases the mixing between the ED (e.g., contaminant) and EA (e.g., oxygen, nitrate) in the groundwater. Where dispersivity, and therefore mixing, between the two interfaces is higher, biodegradation can still be limited by lack of EAs, either due to poor bioavailability or inadequate concentrations.

The planned and managed utilization of natural attenuation processes to remediate contaminated aquifers is known as monitored natural attenuation (MNA). It requires comprehensive monitoring and analysis to determine if natural attenuation is occurring in the

aquifer, requiring lines of evidence such as reduced concentration along the flow path, presence of biogeochemical indicators/markers, microbiological analysis, microcosm analysis, and so on (Rivett and Thornton, 2008; Illman and Alvarez, 2009). MNA is a risk-based remediation method, wherein the combined effect of naturally occurring physical, chemical and biological processes, such as sorption, dispersion, and biodegradation, are used to treat contaminants in situ (Wiedemeier et al., 1999). MNA, if properly managed, can help remediate many classes of contaminants under a wide range of hydrogeological settings (Carey et al., 2000). Since this approach is almost entirely passive, rather than engineered, the costs of MNA are considerably lower than other technologies, such as PAT (Santo and Prosperi, 2022).

However, MNA has complications and limitations. MNA is limited by pore velocity, mechanical dispersion, and kinetic biodegradation rates as influenced by the contaminant type, the EA availability, and the capability of the microbial community of using the EAs to degrade the contaminant. MNA on its own, without enhancement, is capable of biodegrading many types of organic contaminants in both aerobic and anaerobic conditions, but typically takes a substantial period of time, from >8 years to >800 years, depending on the type of contaminant, the mass of the plume, and the attenuation rate (Santo and Prosperi, 2022; Thornton et al., 2001a; DoD, 2008; FRTR, 2023). For this reason, MNA is typically only used to remediate certain parts of a plume, certain contaminants within a mixed plume, or at the end of a treatment protocol once the primary technologies, such as source removal and PAT, have reduced the contaminant concentration to a level at which MNA is able to achieve remediation to required standards (NRC, 2013; Adamson and Newell, 2014; Truex et al., 2017).

However, some of the limitations of MNA could potentially be reduced with intervention. When EA availability is high, transport processes are more important to biodegradation (Thornton et al., 2001 a,b; Harrison et al., 2001). If mixing can be increased, then it will accelerate biodegradation rates by enhancing the respiration reactions that are already occurring at the plume fringe (Bagtzoglou and Oates, 2007; Castro-Alcaca, 2012; Piscopo et al., 2013; Thornton et al., 2014). However, if EA availability is low, increasing EA availability with amendments would be more important (Kao et al., 2016). If both EA availability and dispersion are low, then both mixing, and EA concentrations would need to be enhanced (Lerner et al., 2000; Jones et al., 2002; Thornton et al., 2014).

Recent studies have shown that PAT targeted at the fringes of a plume can enhance the dispersive mixing of the interface between the plume and groundwater (Thornton et al., 2014). The enhanced dispersive mixing induced by the PAT system resulted in a virtual doubling of the biodegradation rate at the plume fringe. This enhancement in biodegradation is due to an increase in mixing between the contaminant and the uncontaminated groundwater where EAs exist at a higher concentration. This approach effectively enhances the plume fringe biodegradation processes that are naturally occurring, albeit at slower rates (Thornton et al., 2001 a,b).

While Thornton et al. (2014) did not mention plume spreading, it is expected that the PAT system considered in their study enhanced NA through this phenomenon. Similarly, studies have shown that engineered injection and extraction can be used to enhance the advective spreading of plumes in groundwater and thereby increase the mixing between the plume and an amendment chemical (Bagtzoglou and Oates, 2007; Piscopo and Neupauer 2012; 2013; 2014; Sather et al., 2023). While it has been suggested that this approach might enhance NA, it has never been investigated.

Thus, if MNA and PAT are combined to enhance biodegradation, it can be possible to improve solute mass removal and lower remediation time scales as well as operational costs. This proposed combined technology differs from an in situ bioremediation approach, in that targeted PAT is used to enhance the intrinsic NA in situ, rather than using amendments. This method may potentially surpass bioremediation in terms of remediation effectiveness and cost, and/or it could be combined with a bioremediation approach to accelerate biodegradation even further.

Remediation costs are also an important consideration. In situ remediation strategies tend to have a much lower cost than other technologies such as PAT, which can cost millions (US EPA, 2001; Khan et al., 2004). For example, on average, in situ chemical oxidation remediation costs a total of $220,000, whereas in situ bioremediation of MTBE contaminated sites can cost between $100,000 to $700,000, with a median of $125,000 (US EPA, 2001c; US EPA, 2005). Overall, MNA typically is one of the lowest cost technologies available, with a median capital cost of $100,000 and a median operating cost of $25,000 per year (McGuire et al., 2004; DoD, 2008; Santo and Prosperi, 2022).

In a PAT treatment train, contaminants such as phenol can be remediated ex situ by a variety of processes such as pyrolysis, distillation, separation, and adsorption. Phenol is only slightly volatile, so a stripping tower system would likely have low efficacy (Hamdaoui and Naffrechoux, 2007; FRTR, 2023). Phenol has fair sorptability on activated carbon therefore granular activated carbon system could hypothetically remediate phenol up to concentrations of 4000 mg/l (Gundogdu et al., 2012; Hamdaoui and Naffrechoux, 2007). Previously an optimization and cost framework was developed for a joint PAT and GAC treatment system (Culver et al., 1999). GAC has generally low capital, operating costs, and low labor requirements compared to other ex situ treatment methods (US EPA, 2005). The operating cost of sites that use granular activated carbon (GAC) only range between $2 to $12 per 3.78 m^3 (Khan et al., 2004). However, operating cost is dependent on the size of the treatment system; the larger the size, the lower the operating cost. Phenol adsorption onto GAC is 0.2 kg/kg (Gundogdu et al., 2012; Hamdaoui and Naffrechoux, 2007); for example, it would take 5 kg of GAC to remove 1 kg of phenol.

While in situ remediation strategies such as MNA can be significantly cheaper than ex situ remediation strategies such as PAT, remediation timeframes are significantly longer. There is a compromise between short remediation timeframes and incurring higher upfront costs; or remediating the site more slowly and having the costs spread over a longer period with

variable savings from NA (Fetter et al, 2017). Alternatively, some studies have found that an in situ bioremediation strategy using amendments may have a better balance between a lower cost (relative to PAT) but with comparatively shorter remediation timeframes than MNA alone (Santo and Prosperi, 2022).

However, because MNA has such a low operational cost comparative to other remediation methods, designing remediation systems incorporating biodegradation to reduce the overall cost has been gaining momentum in research (Butler et al., 1995; NRC, 2000; NRC, 2013). For example, a study by the US Department of Defence (2008) found that a source area remediation strategy combined with MNA to remediate a TCE and naphthalene plume could lead to estimated savings of $100,000 per year. Furthermore, incorporating a combined MNA and source removal remediation strategy at >200 similar sites could result in >$20,000,000 in savings (DoD, 2008). However, the timeframe of this strategy is long, requiring 50 years for the TCE plume and 70 years for the naphthalene plume to be remediated using these strategies. This contrasts with the relatively short remediation timeframes of relatively higher cost remediation strategies, such as in situ bioremediation or in situ chemical oxidation (Khan et al., 2004).

Using PAT to leverage the benefits of enhancing NA in situ could potentially reduce remediation timeframes and further decrease cost by reducing the amount of mass that is pumped and treated by the PAT system (Thornton et al., 2014). Additionally, actively enhancing NA using amendments could possibly reduce treatment costs further, by degrading additional mass in situ, reducing the number of extraction wells and treatment instrumentation needed, or both (Marquis and Dineen, 1994; Park et al., 2007; NRC, 2013). Identifying well configurations utilizing PAT and injection to promote mixing and enhance NA further is one way in which this could be achieved (Park et al., 2007; Piscopo et al., 2013).

6.1.2 Relationship to previous chapters

Chapter 4 investigated the effect of PAT design variables, such as flow rate, well locations, and well configuration, as a proof of concept for enhancing NA (biodegradation) using targeted PAT. A preliminary analysis of PAT systems which combines extraction and injection was also investigated. Two types of injection were considered: injection of water without EAs, with the aim of determining the effect of divergent flows on biodegradation as a function of plume fringe processes, and injection of EA-rich water (oxygen and nitrate). The objective of this chapter was to develop a series of modelling scenarios to assess the effectiveness of remediation using NA-enhanced PAT compared with conventional PAT.

Chapter 5 builds upon chapter 4 by extending the investigation of the plume space to identify the pumping locations which enhance biodegradation the most, as the 3D plume has a complex geometry due to aquifer physical heterogeneity and the high vertical gradient component as a result of recharge. This research attempts to find ways to reduce the diminishing returns incurred by having more than 1 well, which was identified as a problem in Chapter 4. The diminishing returns occurred when multiple wells were used in the same

simulation, their enhancement of biodegradation was less than the sum of what each of the wells achieved in separate simulations. The goal is to find a sub-linear relationship between numbers of wells and biodegradation, rather than logarithmic. Chapter 5 also investigates the effect of amendment concentration on biodegradation mass and compares it to the fringe biodegradation processes. As the reduced bioavailability of the plume results in low biodegradation rates, the injection of amendments could be used to introduce EAs to the most contaminated regions of the plume in addition to spreading the plume. This promotes the direct contact between the phenol and the EAs, in addition to enhancing the plume fringe reactions. The objective of this chapter was to examine multiwell scenarios and determine their impact on mass removal and in situ biodegradation, in addition to comparing the impact of different amendments and terminal electron accepting processes.

6.1.3 Chapter 6 aims and objectives

This chapter (6) builds upon chapters 4 and 5 by applying the lessons learned to complete the third objective of this thesis, which is to establish whether a well configuration (injection and extraction wells) can be used to enhance NA can be in situ to reduce the operational cost of PAT for the remediation of organic contaminants. Based on the model simulations presented in chapter 4, 5, and preliminary simulations for this chapter which are not shown, it has been determined that this will be a challenge due to the aquifer properties, geometry of the plume, the large phenol mass, and slow reaction kinetics.

The specific objectives are (a) to remediate 90% of the plume through combinations of extraction and biodegradation within 60 years, with the residual to be remediated by NA only; (b) design and simulate an assortment of modelling scenarios with the aim of enhancing in situ biodegradation using combinations of multiple extraction and injection wells; (c) and establish whether the enhancement of NA *in situ* can reduce the operational cost of PAT for the remediation of organic contaminants. Fundamentally, the aim is to achieve these objectives in the context of a more realistic remediation target, which precludes some of the hypothetical well configurations and scenarios used in the previous chapters.

The purpose of the 60 year remediation period is to compare modelling scenarios which may reach the 90% remediation target at different times, as it is understood from previous modelling scenarios that a PAT system designed to enhance biodegradation will require more time to reach the remediation target than a conventional PAT system with the extraction located in the plume interior/centerline. There are 6 modelling scenarios in all, which use between 7 to 16 wells. The majority of modelling scenarios include 3 downgradient hydraulic containment wells to stop the plume growing in length and leaving the model through the western boundary. The pumping rate for all scenarios depends on the location of the well within the aquifer. If the pumping well is located in the upper layers of the aquifer where the hydraulic conductivity is lower, then the pumping rate is no higher than ±30 m^3/d.
For each scenario, the amount of mass removed via biodegradation is analyzed, the time taken to reach 90% of contaminant solute mass removal, and the operational cost, which includes energy and treatment. All simulations in all scenarios will then be cross-compared

and ranked by operational cost, remediation efficiency and effectiveness compared to a conventional PAT system. Capital cost is not taken into account, as optimization is beyond the scope of this thesis.

Methodology

The methodology is divided into the following components: conceptual site model and model background information; flow and transport model methodology; and cost model methodology.

6.2.1 Study site

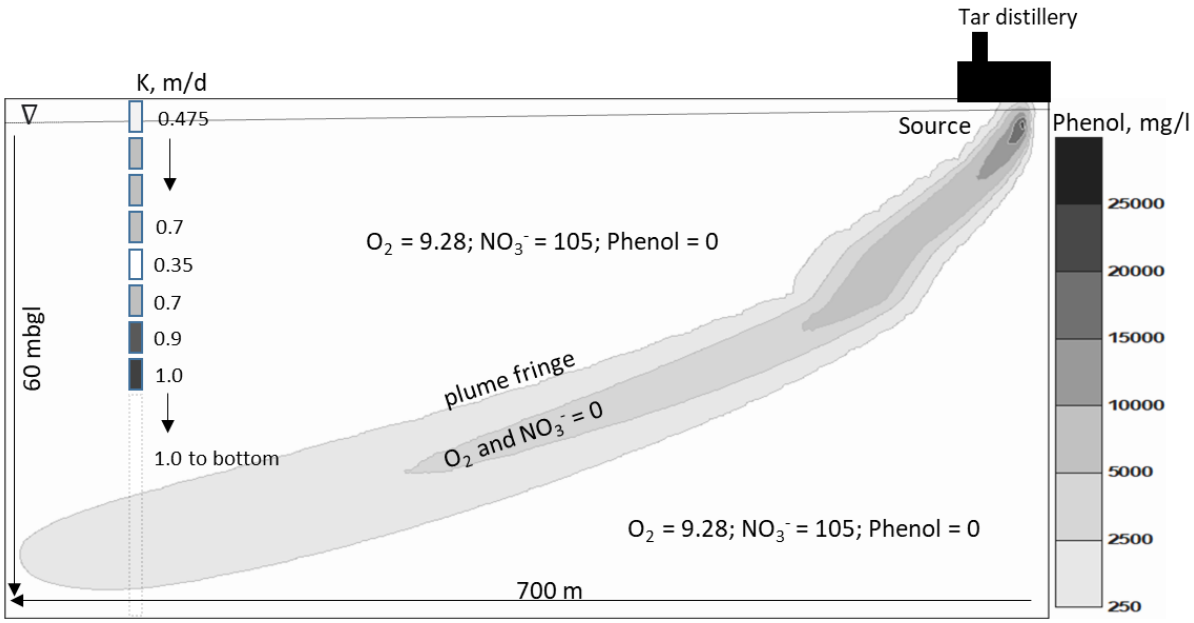

Figure 6-1. Schematic of plume concentration envelope based on groundwater chemistry and numerical simulation of site data. The concentrations shown are in mg/l. The hydraulic conductivity scale indicates that some values repeat throughout the layered system (Thornton et al., 2001b). Note that the concentrations of oxygen and nitrate are below detection in the plume due to biodegradation of the phenolic compounds. Note the vertical exaggeration of the depth scale.

This field site is a fine-grained, unconfined, fluviatile, sandstone bedrock aquifer located underneath a former coal tar distillation plant. The site has been extensively investigated over 25 years, with studies on the interpretation of groundwater contamination (Williams et al., 2001), redox processes and contaminant biodegradation (Thornton et al., 2001a; 2014; Wu et al., 2006; Baker et al., 2012; Hedbavna et. al., 2016), aquifer stable isotope geochemistry (Spence et al., 2001), aquifer microbiology (Pickup et al., 2001; Elliot et al., 2010; Rizoulis et al., 2013; Mujica-Alarcon et al., 2021), plume mass balance (Thornton et al., 2001b) and reactive transport modelling (Mayer et al., 2001; Watson et al., 2005). The site history, summarised here, is described in detail in Williams et al. (2001).

A mixed plume of phenolic compounds (primarily phenol, cresols and xylenols) extends approximately 700 m down hydraulic gradient of the site, with an estimated width of 150m and depth of 60m (Figure 6-1).

Table 6-1. Input parameters used in the scenario modelling.

Flow and transport parameters		Value		Data source
Effective porosity (-)		0.125[a]		Core samples/geophysical logs[a]
Hydraulic conductivity range, K (m/d)		0.35-1.0[a]		Pumping tests and RFM[c]
Recharge rate (m/d)		8.00e-04[a]		Effective infiltration estimation[b]
Longitudinal dispersivity (m)		1[b]		
Vertical transverse dispersivity (m)		4.00e-03[b]		Tracer tests and numerical modelling
Horizontal transverse dispersivity (m)		1.00e-02[b]		
Grid block size (m^3)		5		Well screen lengths are 5 meters.[a]
Model length, width, and depth (m)		1200x300x255		
		Species		
Biodegradation module parameters	*Phenol*	*Oxygen*	*Nitrate*	
Half saturation constant (mg/l)	-	0.1[b]	0.5[b]	Determined by a mesocosm experiment[b]
Inhibition constant (mg/l)	-	0.9[b]	0.9[b]	
Decay rate (1/T)	-	3.44e-05[b]	3.44e-06[b]	
Yield coefficient (-)	0	2.38[b]	3.69[b]	Reaction stoichiometry
Source concentration (mg/l)	25000	0	0	Groundwater quality monitoring
Background groundwater concentration (mg/l)	0	4.5-9.28[b]	91-105[b]	Groundwater quality monitoring

j. Unpublished data from confidential third-party consultant reports.
k. Values used in previous modelling studies on the site [Watson et al. (2005) and Mayer et al. (2001)].
l. RFM refers to Radial Flow Modelling undertaken by third party consultants.

Groundwater flow is westerly, with a pore velocity between 4-11 m/year, and consistent over the history of the plume. Vertical flow due to groundwater recharge is also important (Table 6-1). Previous investigations have identified a heterogeneous distribution of phenolic compounds and biogeochemical processes responsible for their biodegradation within the plume (Thornton et al, 2001a). The plume is anchored by a NAPL source, with concentrations of individual phenolic compounds (e.g., phenol) reaching 25,000 mg/l. Considering this, and to reduce the complexity of the numerical model, phenol was selected as a representative organic contaminant for the simulations and the concentrations of all other phenolic compounds were converted into equivalent phenol concentrations. A conceptual model of the plume developed from this analysis and used in the numerical investigations is shown in Figure 6-1.

Previous studies have shown that the phenolic contaminants are biodegraded by several processes; however, most mass loss due to biodegradation (>90%) arises from consumption of oxygen and nitrate in the groundwater (Lerner et al., 2000; Thornton et al., 2001a,b; Mayer et al., 2001; Jones et al., 2002; Watson et al., 2005). For this reason, the modelling scenarios were developed to assess the contribution of these two EAs to biodegradation, as influenced by the PAT system.

6.2.2 Flow and transport model

A 3-D flow and transport model was developed using the input data in Table 6-1. Groundwater flow is governed by the classical PDE:

$$\frac{\partial}{\partial x}\left(K_{xx}\frac{\partial h}{\partial x}\right)+\frac{\partial}{\partial y}\left(K_{yy}\frac{\partial h}{\partial y}\right)+\frac{\partial}{\partial z}\left(K_{zz}\frac{\partial h}{\partial z}\right)+W=S_s\frac{\partial h}{\partial t} \quad \text{Eq 1}$$

where K_{xx}, K_{yy}, and K_{zz} are hydraulic conductivity along the x, y, and z coordinate axes (L/T); h is the hydraulic head (L); W is a volumetric flux per unit volume representing sources and/or

sinks, such as recharge and wells (1/T); S_s is the specific storage of the porous material (1/L); and *t* is time (T). The model is isotropic ($K_{xx} = K_{yy} = K_{zz}$) and heterogeneous, with hydraulic conductivity generally increasing with depth (Figure 6-1). The groundwater flow system was set to steady state, as the hydraulic heads trend to steady state after ~2 years of pumping. Equation 1 is solved using MODFLOW-2005 (Harbaugh et al., 2005), based on a finite different grid characterized by 200 columns, 60 rows, and 38 layers, with a grid-block size of 5m × 5m × 5m in the region of the plume. The flow model is by characterized by a constant head boundary condition on the east and west (see Figure 6-1), with groundwater recharge applied to the water table (Table 6-1). Other boundaries are set as "no flow". MODFLOW-2005 calculates the pore velocity field ($\boldsymbol{v} = -\frac{K}{\phi} \cdot \nabla h$, where ϕ is the effective porosity), which is then used in the multispecies reactive contaminant transport simulator MT3D-USGS (Bedekar et al., 2016) to solve a system of coupled partial differential equations, each of which represents the mass continuity for the species simulated:

$$\nabla(\phi \cdot \mathbf{D} \cdot \nabla C_i) - \nabla(\phi \cdot \mathbf{v} \cdot C_i) + \mathrm{q}_{s,i} \cdot C_{s,i} + R_i = \frac{\partial(\phi \cdot C_i)}{\partial t} \quad \text{Eq 2}$$

where C_i is the concentration of species i [M/L^{-3}], **D** is the hydrodynamic dispersion tensor [L^2/T^1], $\mathrm{q}_{s,i}$ [M/L^3] represents the specific discharge for species i, $C_{s,i}$[M/L^3] represents the concentration of sources for species i, and R_i represents the reaction rate of species i [M/L^3/T^1]. In this case, there are three species ($i = 1, 2, 3$), and the term R_i depends on ongoing kinetic reactions occurring between 1 electron donor (ED) and 2 electron acceptors (EAs), simulated using a Monod kinetic model developed by Lu et al. (1999), following approaches used in previous studies (Rolle et al., 2008).

The stoichiometric reactions between phenol (C_6H_6O), which is the ED, and the two EAs, oxygen (O_2) and nitrate (NO_3^-), are described by the following equations:

(a) $C_6H_6O + 7O_2 \rightarrow 6CO_2 + 3H_2O$ Eq 3

(b) $C_6H_6O + \frac{28}{5}NO_3^- + \frac{28}{5}H^+ \rightarrow 6CO_2 + \frac{14}{5}N_2 + \frac{29}{5}H_2O$ Eq 4

Eq 3 and 4 are presented to illustrate the stoichiometry of the reactions which are considered in Eq 6.

The rate of ED biodegradation ($i = 1$ in Eq. 2) is given by (Lu et al., 1999):

$$r_{ED} = \sum_{j=1}^{2} r_{ED,j} = -\left\{\frac{k_{EA_1} \cdot [EA_1]}{K_{EA_1} + [EA_1]} + \frac{k_{EA_2} \cdot [EA_2]}{K_{EA_2} + [EA_2]} \cdot \frac{K_{I,EA_1}}{K_{EA_1} + [EA_1]}\right\} \cdot [ED] \quad \text{Eq 5}$$

where $[ED]$, $[EA_1]$, and $[EA_2]$ represent the concentration of the ED and the two EAs (M/L^3), respectively; k_{EA_1} and k_{EA_2} are first-order decay rate constants for the EAs (1/T); K_{EA_1} and K_{EA_2} are the half saturation constants for the EAs (M/L^3); K_{I,EA_1} (M/L^3) is the inhibition constant for the first EA, oxygen, which has the highest Gibbs free energy (Christensen et al., 2000). Correspondingly, the rate of consumption of the two EAs, which affects the concentration of the EAs, ($i = 2, 3$ in Eq. 2) is given by:

$$r_{EA_j} = Y_{EA_j} \cdot r_{ED} \qquad \text{Eq 6}$$

where $Y_{EA_j} (j = 1, 2)$ is the yield coefficient for the EA, that is, the EA mass used per ED unit mass biodegraded, calculated from the stoichiometry in Eqs. 3 and 4 (Table 6-1).

The mass biodegraded is obtained by integration of the rate of ED biodegradation r_{ED} (Eq 5) over the model domain for the remediation period T, with the following equation:

$$M_{bio}(T) = \int_{t=0}^{T} \left[\int_{\Omega} \theta \cdot r_{ED} \cdot d\Omega \right] dt \qquad \text{Eq 7}$$

where Ω represents the 3D model domain, θ (/) is the effective porosity, r_{ED} (M/L^3/T) is the biodegradation rate (Eq 5). This integral is numerically calculated over the model grid and the discretization of the time interval $[0, T]$ adopted in the flow and transport simulation.

6.2.3 Methodology for the operational cost model

This section presents a cost model (Culver et al., 1988) which estimates the PAT operational cost, which is the pumping electricity cost combined with GAC treatment system cost, over the remediation period *p*, of 60 years. The operational cost is determined by the number of wells, the screen locations, the extraction/injection schedule, the concentration extracted by the wells over time, the total dynamic head, and the time required to reach the remediation target. This cost model is used to test the hypothesis of whether enhancing *in situ* biodegradation can reduce remediation costs and is used to rank the modelling scenarios.

The operational cost, in $USD, for each scenario in Chapter 6 is calculated using the following equation (Culver et al., 1998):

$$Operational\ Cost = G_{pump,p} + G_{GAC,p} \qquad \text{Eq 8}$$

where $G_{pump,p}$ is the PAT system electricity cost and $G_{GAC,p}$ is the operational cost for the granular activated carbon (GAC) treatment system.

As Eq 8 states, the operational cost is the sum of the electricity cost for the pumping wells and the cost of the GAC. The electricity cost is calculated using the following equation:

$$G_{pump,p} = \sum_{k=1}^{N_{tp}} \rho \cdot g \cdot Q_{ik} \cdot (Z_h - h_{ik}) \cdot \frac{S_p}{\varepsilon} \cdot \Delta t_k \quad \text{Eq 9}$$

where ρ is the density of water (M/L^3), g is acceleration due to gravity (L/T^2), Q_{ik} is the well i volumetric flow rate at time step k (L^3/T), Z_h is the elevation of the ground surface (L), h_{ik} is the hydraulic head in the well at time step k (L), S_p is the cost of electricity per kilowatt-hour (\$/M*L^2/T^2), ε is the efficiency of the submersible pump (/), and Δt_k is the length of the time period k (T). The $(Z_h - h_{ik})$ term is the total dynamic head.

The pressure head Z_h needed by the GAC adsorber is 3 meters above ground surface (108 meters), assuming the height of the GAC tank inlet is 3 meters. For the injection wells, the pressure head Z_h is calculated from the ground surface (105 meters). The submersible pump efficiency ε is assumed to be 80%. The electricity cost per kilowatt-hour S_p is assumed to be 0.34 \$USD/kWh.

The GAC treatment cost is primarily determined by the amount of phenol mass that is removed by the extraction wells, the mass of carbon required to adsorb (remove) the mass of the contaminant, $CURC_p$, and the cost per unit, S_c, of the carbon. $G_{GAC,p}$ is calculated as:

$$G_{GAC,p} = \sum_{k=1}^{N_{tp}} \frac{S_c}{CURC_p} \cdot C_k \cdot Q_{Tk} \cdot \Delta t_k \quad \text{Eq 10}$$

where S_c is the carbon cost coefficient (\$/M), $CURC_p$ is the constant carbon use rate per mass of concentration (M/M), C_k is the weighted average influent concentration to the adsorbers (M/L^3), Q_{Tk} is the total volumetric flow rate for time step k (L^3/T), and Δt_k is the time step length at period k (T).

The GAC treatment cost is in \$USD and it is estimated that GAC costs \$4/kg, by applying the value used in Culver et a., 1998, adjusted for inflation to 2020 prices, assuming 2% inflation per year. It is recognized that is a simplification of the GAC price, which will vary depending on the market value. The constant carbon use rate per mass of concentration $CURC_p$ is 0.2 kg/kg of phenol (Hamdaoui and Naffrechoux, 2007; Gundogdu et al., 2012).

Q_{Tk}, the total groundwater volume extracted, is calculated as:

$$Q_{Tk} = \sum_{i=1}^{m} Q_{ik} \quad \text{Eq 11}$$

where Q_{ik} is the well i volumetric flow rate at time step k (L^3/T).

C_k is the weighted average influent concentration sent to the adsorbers, which varies over time and is calculated as:

$$C_k = \frac{\sum_{i=1}^{m} C_{ik} \cdot Q_i}{Q_{Tk}} \quad \text{Eq 12}$$

where C_{ik} is the concentration of the extracted groundwater from well i (M/L^3) at time-step k.

The flow and transport model developed in the previous section is used to calculate variables such as the total dynamic head, volume of groundwater extracted, the concentration of groundwater extracted, and the mass extracted, for well *i*, required by the cost model.

6.2.3 Key uncertainties and sensitivities in the operational cost model

The pressure head Z_h needed by the GAC tank is uncertain. This would affect the total dynamic head term. The dynamic head term is particularly important to Eq. 9 as most of the other variables are constant or can be controlled, such as the pumping rate. Higher pumping rates will increase the electricity cost due to increased drawdown.

The cost S_p of electricity per kilowatt-hour is assumed to be 0.34 $/kWh. The electricity cost inflation rate is estimated from energy indices from 1990 to 2019 (UK Office of National Statistics, 2024), where the average inflation is 4%, which is twice as fast as the idealized market inflation rate of 2%. With a constant inflation factor of 1.04, the price could reach $1.7/kWh by the year 2080, the end of the hypothetical remediation period for this study. This would significantly alter the pumping electricity cost in Eq. 9. However, it is impossible to know with certainty.

Additionally, the efficiency ε of well submersible pump is unknown. It is assumed to be 80%, as the efficiency of submersible pumps have improved since 1998 (Bordeasu et al., 2022).

The constant carbon use rate per mass of concentration, $CURC_p$, is a simplification from Culver et al., (1998), as the empirical coefficients for the Freundlich isotherm are unknown. This value of $CURC_p$ used for this study is derived from Langmuir adsorption experiments of phenol onto GAC (Hamdaoui and Naffrechoux, 2007; Gundogdu et al., 2012). However, there is uncertainty in this value, as it varies depending on the isotherm model used (Langmuir or Freundlich), and it is also dependent on phenol influent concentration, temperature, and the particle size of the adsorbent (Hamdaoui and Naffrechoux, 2007; Gundogdu et al., 2012). The adsorption values in the literature have been cited as high as 0.3 kg/kg, but to maintain a conservative approach, a value of 0.2 kg/kg was assumed.

The overall GAC treatment cost model is sensitive to mass of the contaminant extracted, the cost S_c, and the value of $CURC_p$. Lower values of $CURC_p$would significantly increase the cost of GAC remediation, whereas higher values of $CURC_p$would reduce the cost. The $\frac{S_c}{CURC_p}$ term is the most sensitive term in Eq. 10, as the total groundwater volume extracted and influent concentrations can be controlled, to a degree, but this term cannot.

The cost S_c of GAC per kilogram is assumed to be \$4/kg. The cost of GAC/kg over time is unknown. The cost of GAC might be cyclical. It has cycled between \$1.84 and \$2.35 from 2019-2024, but the source is dubious (businessanalytiq.com, 2024).

Since the pumping rates are relatively low in a thick unconfined aquifer and the phenol mass is substantial, the GAC treatment cost is significantly higher than the pumping electricity cost.

Modelling financial markets is not the aim of this research. The cost function, approximately at present value, is merely used to rank PAT scenarios and to test the hypothesis of whether NA could aid in meeting remediation objectives while reducing the cost.

6.2.3 Model development and scenarios

The flow and reactive transport models presented were used to create a hypothetical phenol plume using data on the physical aquifer characteristics obtained from previous site investigations conducted by third party consultants (Table 6-1), and research published over the past 25 years (Mayer et al., 2001; Thornton et al., 2001b; Watson et al., 2005). The rationale behind using this approach was not to interpret the actual contamination conditions at the site, but to instead develop a model that is internally coherent and consistent. This enabled a hypothetical but realistic example model to be created, with results that can be extended to other sites with similar characteristic and/or contaminated with coal tar distillate plumes (e.g. Blum et al., 2011).

Figure 6-1 shows a contaminant plume simulated with this model. This is in excellent agreement with plumes produced in other studies at the site using the same dataset (Mayer et al., 2001; Watson et al., 2005), and is similar to the concentration distribution observed in monitoring surveys conducted at the same time (Williams et al., 2001; Thornton et al., 2001b). To create the numerical model, a regional model with local canals and pumping stations was developed based on data from confidential third-party consultant reports. Recharge was estimated from effective infiltration and applied to the water table. Initial simulations revealed that the most important parameters for the transport model are recharge and hydraulic conductivity. These initial simulations also revealed that the groundwater flow in a 1.2 km^2 square area encompassing the plume is steadily east to west, which is supported by site data. Therefore, the original regional flow model was then cropped to a size appropriate for simulating the range of hydraulic gradients observed at the site (horizontal hydraulic gradient of 0.003-0.007). The eastern and western constant head boundary conditions of 103m and 98m, which were acquired from previous groundwater monitoring at the site, were used to simulate the average horizontal hydraulic gradient for the site (0.0042). The north and south boundaries are simulated as general head boundaries with linearly decreasing head from east to west, and the bottom boundary is no flow. The contaminant source consists of DNAPL (coal tar) trapped within shallow groundwater at the site, which was simulated as a single 5x5x5 m^3 cell (the source term is unknown). In order to generate a plume comparable to that observed at the site, the release of phenols from the source was simulated at 1344 mg/d over 70 years. This was

determined to give the corresponding concentration distribution in the aquifer, with a maximum dissolved concentration of 25,000 mg/l (similar to the source zone) and total plume mass of 34,000 kg. The source was then assumed to be removed (as per conventional remediation practice) before PAT operations commenced (Cohen et al., 1997). As the magnitude of dispersion is a function of the aquifer dispersivity (Ye et al., 2015), values of this coefficient were taken from previous modelling studies at the site (Table 6-1), which were of the same order as those estimated in other studies (e.g. Cirpka et. al., 1999, 2006; Cupola et al., 2015; Reising, 2018).

Besides the scenarios developed for this study, numerous preliminary experiments were run to determine the minimum number of wells needed for plume control and containment. Scenarios with interior extraction (wells oriented along plume centerline) achieved remediation targets more quickly and with fewer wells than scenarios with exterior extraction. It was determined that for exterior extraction scenarios - which would enhance biodegradation - require 7 wells at a minimum in order to meet the remediation target within 60 years. This is due in part to the large size of the plume and slow biodegradation rates. Preliminary experiments also investigated remediating the plume within 40 years, but this was only possible for conventional PAT scenarios, with extraction wells in the plume interior.

The six modelling scenarios, summarised in Table 6-2, were developed. The initial plume is first shown to provide a perspective for the location of the wells in the 6 modelling scenarios. For all scenarios, except Scenario 1, there are 3 downgradient containment wells which are constantly extracting groundwater. The GAC operational cost and pumping electricity costs are calculated for each well at each time period for each scenario. The total operational cost is the sum of the GAC operational cost and the pumping electricity cost. The mass biodegraded over time is calculated for each scenario, over the entire model domain (Eq 7). The mass extracted is then calculated for each well.

The cost reduction from biodegradation is calculated by using the biodegradation mass as an input for Eq 9; the reasoning behind this is since the mass reduced by biodegradation is mass that would otherwise have to be extracted in order to meet the remediation target of 90% within 60 years; therefore, it is a cost reduction or saving.

For scenarios 3-6, the wells in the middle are injection wells. Their aim is to spread the plume while injecting groundwater containing dissolved EAs, which increases the mixing between the ED and EA. In general, the injection rates are much lower than the extraction rates, in order to maintain plume control and water mass balance.

Scenario 1

Scenario 1 aims to remediate the plume as quickly as possible by using targeted PAT at the highly concentrated regions of the plume (Table 6-2, Scenario 1). It has 7 extraction wells situated in the plume interior/centerline and a constant cumulative pumping rate of -170 m^3/d. The individual extraction rates vary between -10 m^3/d in the upper layers and -30 m^3/d in the lower layers. This scenario is intended to simulate a conventional PAT approach, with the aim of remediating the plume as quickly as possible.

Scenario 2

Scenario 2 aims to use interior injection of groundwater to spread and remediate the plume. There are 7 wells in total (Table 6-2, Scenario 2). As preliminary experiments showed that plume management was impossible with injection wells only, 3 downgradient containment wells were implemented to keep the plume contained while 4 interior injection wells were used to spread the plume. Wells 1-4 inject groundwater with 9.28 and 105 mg/l of oxygen and nitrate, respectively, for 15 years at low rates. Wells 5-7 extract at -50 m^3/d each for the duration of the remediation period. To prevent the uncontrolled expansion of the plume, the injection wells all switch to extraction after 15 years, and continue extracting until the end of the remediation period. The pumping rates for the individual wells vary between ±5 m^3/d and ±30 m^3/d, depending on well location, and time period. The cumulative injection and extraction rates are 75 and -225 m^3/d , respectively.

Scenario 3

Scenario 3 aims to use interior injection and exterior extraction wells to spread the plume while keeping it contained (Table 6-2. Scenario 3). There are 10 wells in total: 4 exterior extraction wells pumping -40 m^3/d each to spread the plume, 3 interior injection wells injecting groundwater (10 m^3/d each), and 3 containment wells (-30 m^3/d each). The cumulative injection and extraction rates are 30 m^3/d and -250 m^3/d. This scenario differs from Scenario 3 in that it has 3 additional wells, the well locations are different, the cumulative pumping rate is higher, and Scenario 3 has a constant pumping rate.

Scenario 4

Scenario 4 aims to build upon Scenario 3 by further increasing the spreading of the plume in the vertical dimension, using alternating injection and extraction in the plume interior (Table 6-2, Scenario 4). In order to maintain control of the plume, Scenario 4 uses a variable pumping rate, there are 10 wells in total. The downgradient containment wells 8-10 are injecting groundwater for 10 years (30 m^3/d each), then start extracting for the remainder of the remediation period (-30 m^3/d each). Well 5 and 7 in the plume interior each follow the same pattern of extraction and injection: extracts (-30m^3/d) for 15 years, injects groundwater for 5 years (30 m^3/d), and then extracts (-30 m^3/d) for the remainder of the remediation period. The exterior extraction wells are always pumping at -60m^3/d.

The cumulative injection and extraction rates are 100 m^3/d and -300 m^3/d for 10 years. After 10 years, the injection rate is between 0 and 30 m^3/d and the extraction rate is between -370 and -400 m^3/d, for the remainder of the simulation.

Scenario 5

Scenario 5 uses the same well configuration as Scenario 4 (Table 6-2, Scenario 5). However, scenario 5 uses a transient flow model and implements temporally varying pumping rates to explore if this enhances plume spreading and therefore biodegradation (Jones et al., 2002). All of the wells on the north and south side of the plume are sequentially alternating between injection (60m^3/d) and extraction (-60m^3/d) every 5 years for the entire duration of the remediation period. The 2 interior wells are also sequentially pumping, alternating between injection (30m^3/d) and extractions (-30 m^3/d) every 5 years. The 3 downgradient containment

wells are all pumping at -30 m^3/d throughout the remediation period. The cumulative injection and extraction rates are 150 and -250 m^3/d for 60 years.

Scenario 6

Scenario 6 aims to use fixed rate interior injection wells and exterior extraction wells to spread the plume as much as possible while also keeping it contained and under control (Table 6-2, Scenario 6). There are 16 wells in total. This scenario differs from the other scenarios in that the 3 downgradient containment wells are simulated as fully screened over 28 layers and are pumping at -60m^3/d each, with the aim to spread the plume vertically and horizontally, as well as reducing mass extraction. There are 4 interior injection wells each pumping at 10 m^3/d, aligned with 8 exterior extraction wells pumping between -30 and -40 m^3/d, each, depending on the layer. Scenario 6 has constant cumulative injection and extraction rates of 50 and -460 m^3/d, respectively.

For all scenarios relatively low to moderate pumping rates (as compared to pumping rates in the region and in previous studies) were chosen, to reduce drawdowns (Jones et al., 2002; unpublished data). Using lower pumping rates also reduces the likelihood of the radii of influences of wells overlapping and limiting dispersive mixing between the plume and the EAs, as discussed in Chapter 4. For all scenarios that utilize injection, the wells are injecting groundwater containing EAs, oxygen and nitrate, at 9.28 and 105 mg/l, respectively, which are the background concentrations found in the aquifer.

Table 6-2. Scenarios (1-6) evaluated in 60-year modelling simulations, with respective methodology used (see text for explanation). The perspective is a plane view.

Scenario	Description	Injection/extraction well layout
Scenario 1.	A single simulation with 7 fixed extraction wells placed on plume centerline. Cumulative extraction rate is 170 m^3/d.	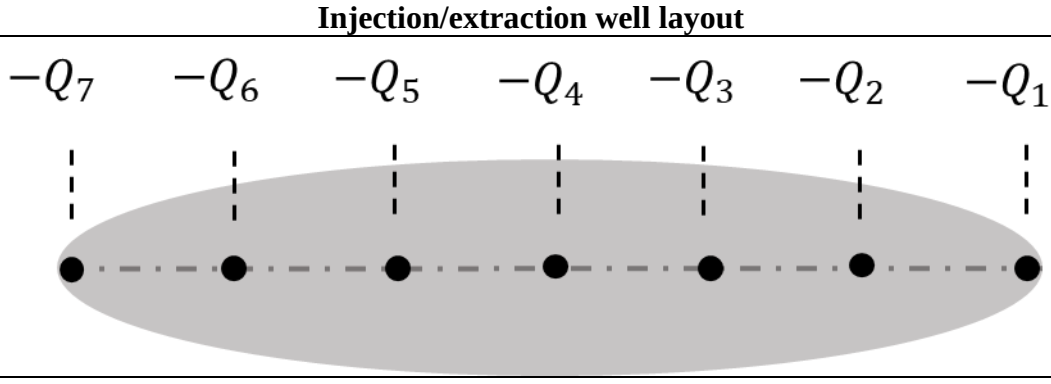
Scenario 2.	A single simulation with 7 fixed extraction and injection wells. The cumulative injection rate is 75 m^3/d. Cumulative extraction rate is -225 m^3/d.	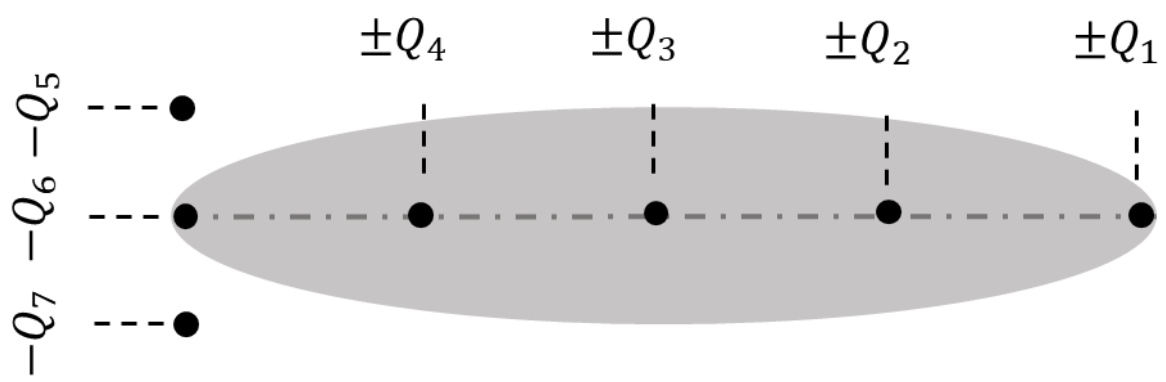
Scenario 3.	A single simulation with 10 fixed extraction and injection wells. The cumulative injection rate is 30 m^3/d. Cumulative extraction rate is -250 m^3/d.	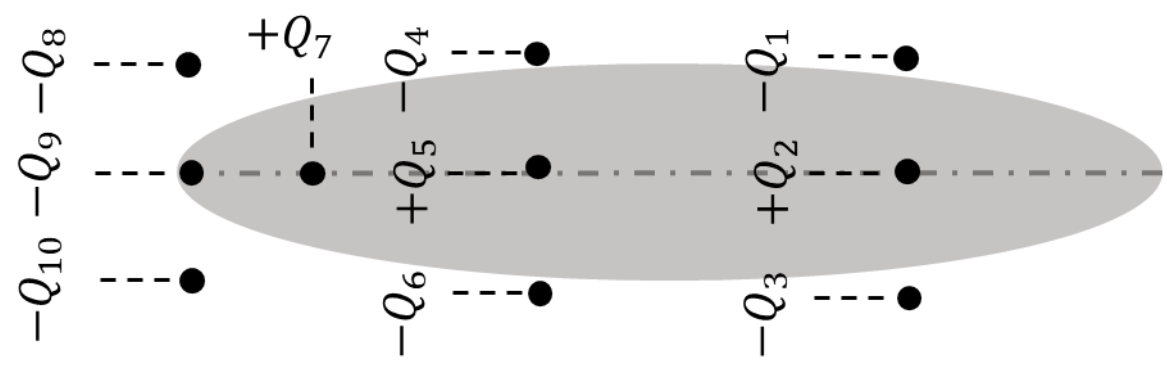
Scenario 4.	A single simulation with 10 fixed extraction and injection wells. Cumulative injection rate is 100 m^3/d. Cumulative extraction rate is -400 m^3/d.	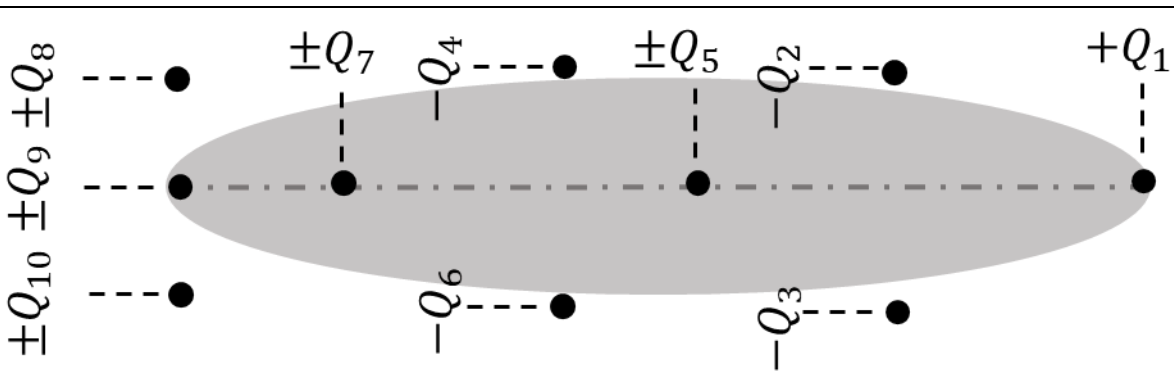
Scenario 5.	A single simulation with 10 fixed extraction and injection wells. Cumulative extraction rate is 190 m^3/d. Cumulative injection rate is -280 m^3/d. Note that well 2-7 are temporally varying.	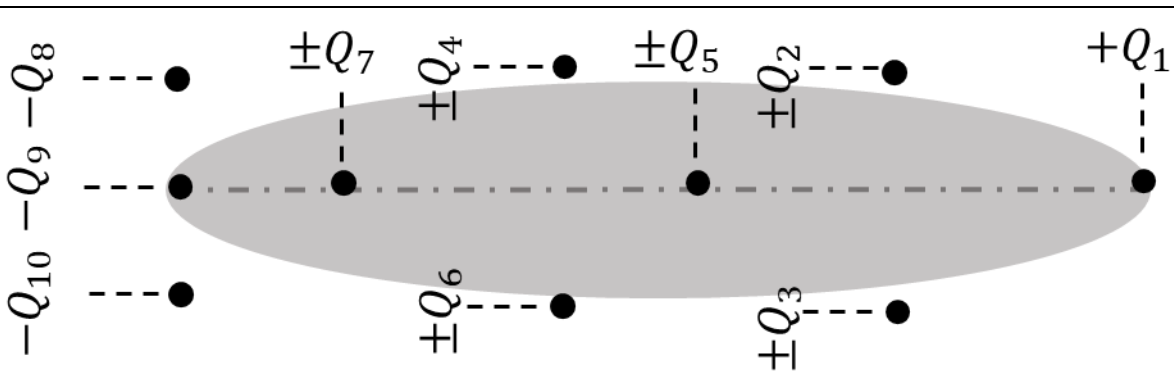
Scenario 6.	A single simulation with 16 constant extraction and injection wells. Cumulative injection rate is 100 m^3/d. Cumulative extraction rate is -460 m^3/d.	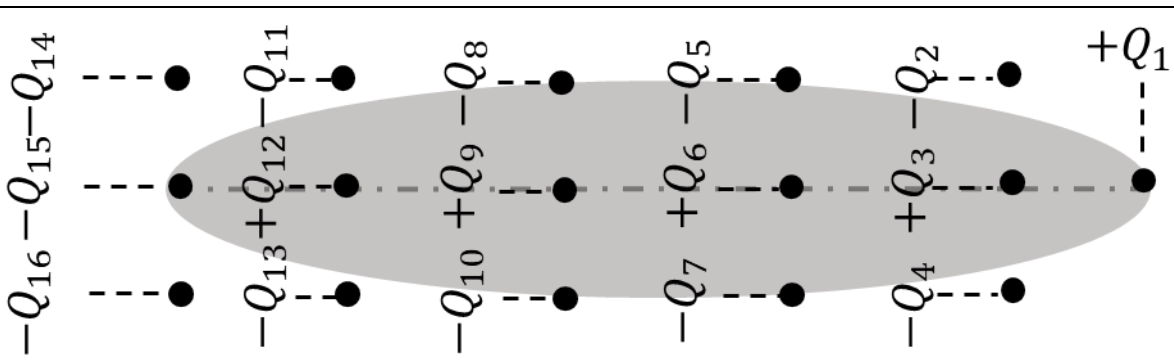

6.3 Results and discussion

The results of the scenario modelling with regards to mass removal and cost are shown below.

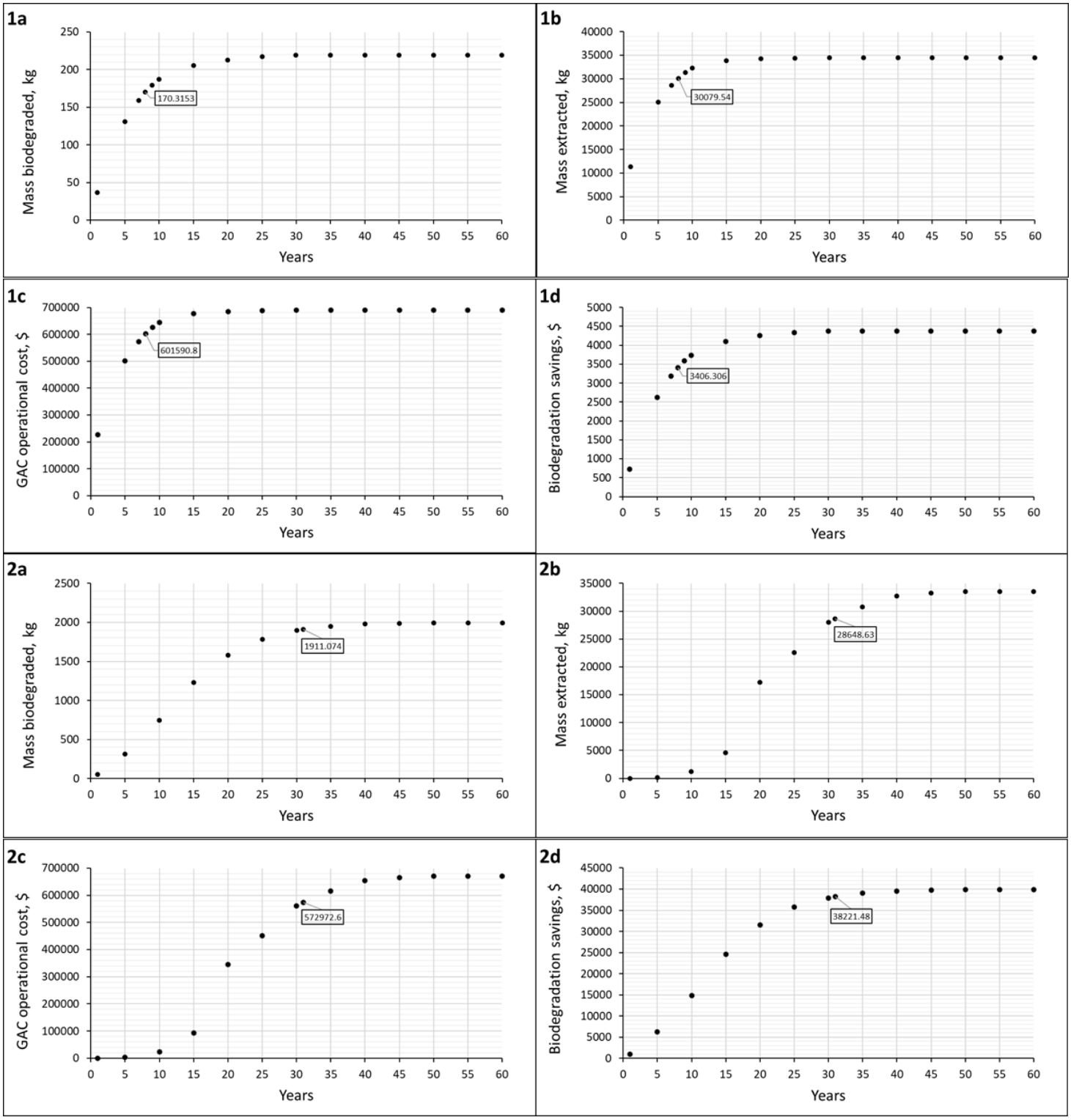

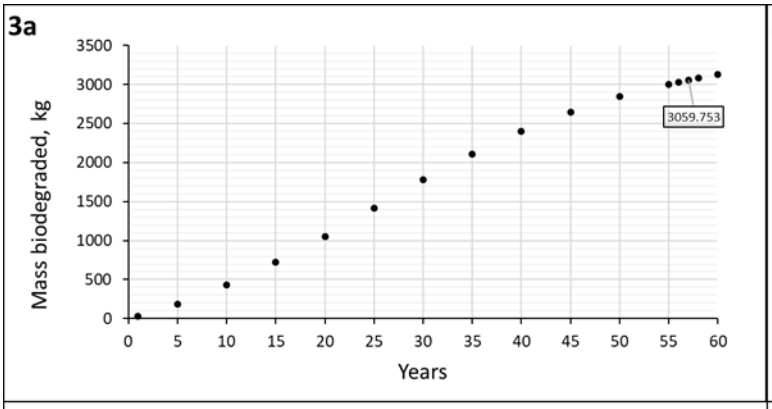
3a
Mass biodegraded, kg
Years
3059.753

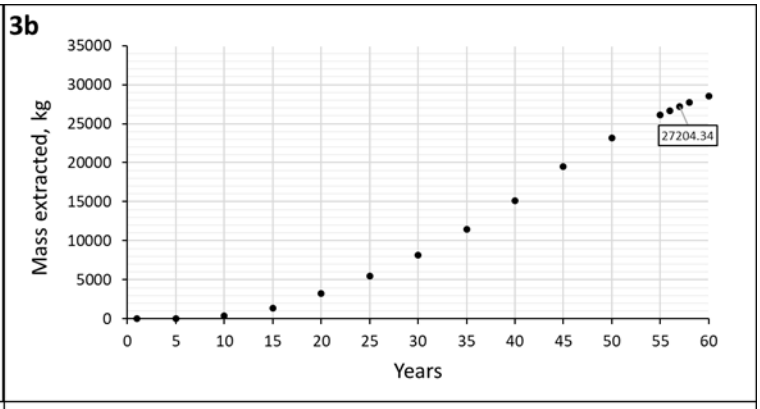
3b
Mass extracted, kg
Years
27204.34

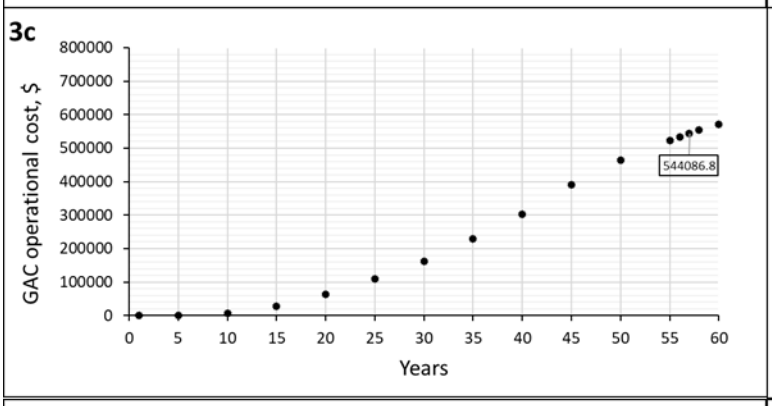
3c
GAC operational cost, $
Years
544086.8

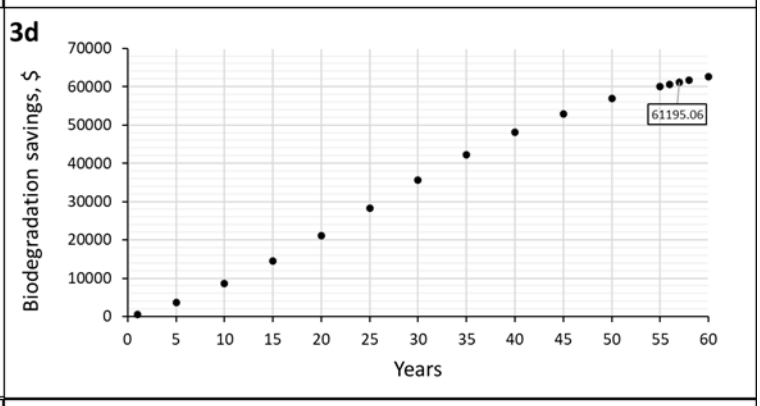
3d
Biodegradation savings, $
Years
61195.06

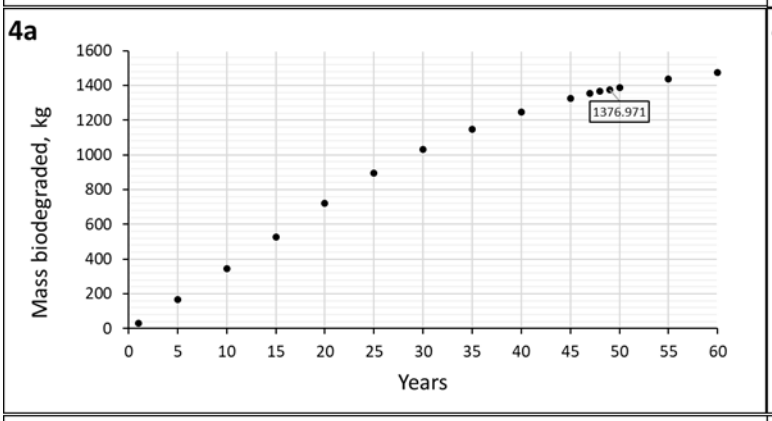
4a
Mass biodegraded, kg
Years
1376.971

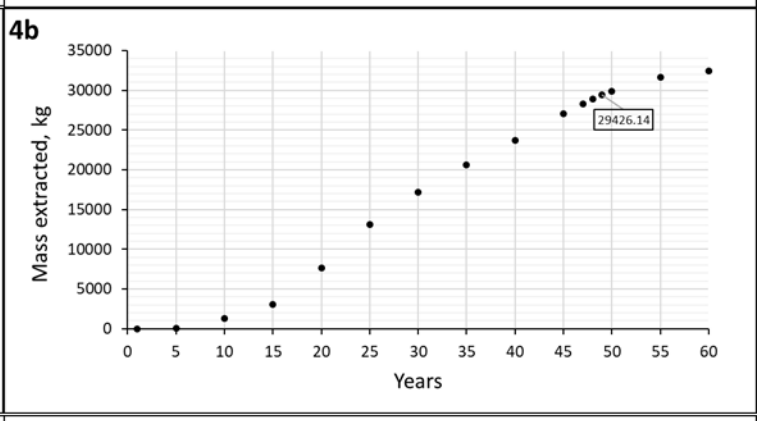
4b
Mass extracted, kg
Years
29426.14

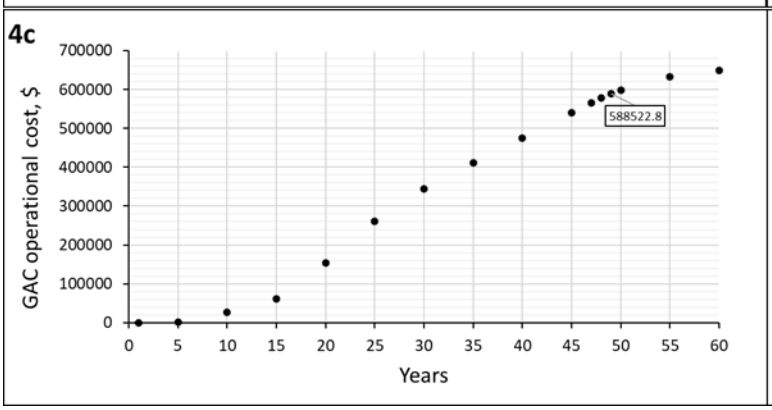
4c
GAC operational cost, $
Years
588522.8

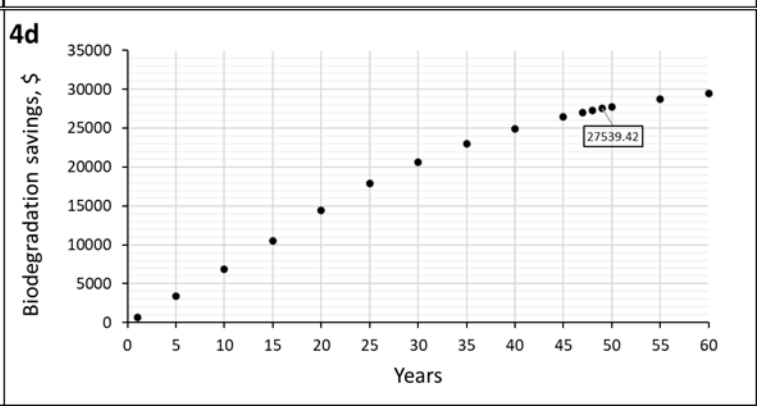
4d
Biodegradation savings, $
Years
27539.42

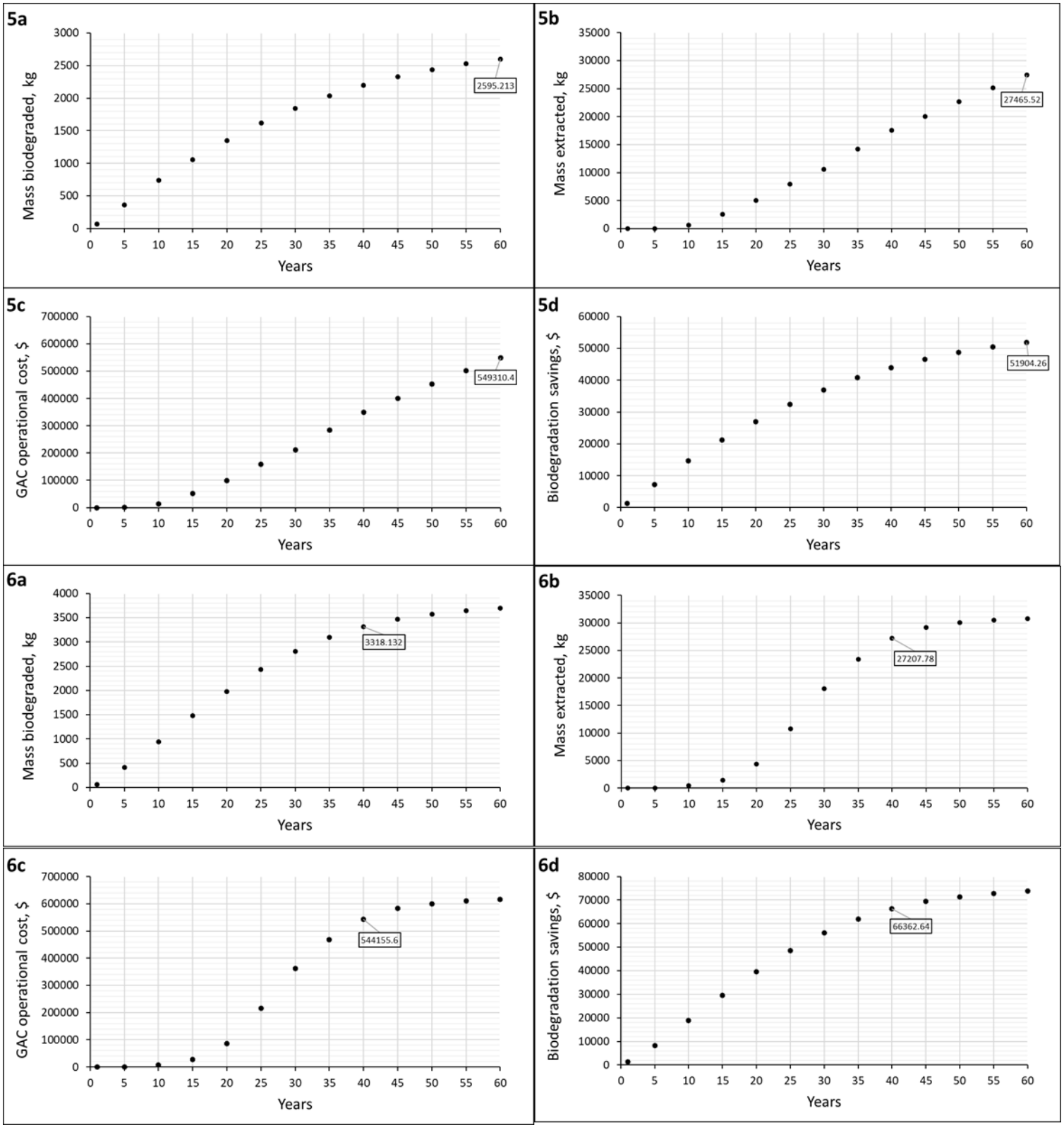

Figure 6-2. Values of mass removal for scenarios 1-6. The cost units are in $USD. The scenarios depicted above follow the same order as Table 6-2. The values in the boxes indicate the value when the remediation target of 90% mass reduction is reached.

Table 6-3. Results summarized from Figure 6-2.

Scenario	Number of wells	Total injection rate (m^3/d)	Total extraction rate (m^3/d)	Intrinsic NA at remediation target (kg)	Mass biodegraded at remediation target (kg)	Percent enhancement in NA	Mass extracted at remediation target (kg)	Time to reach target (years)	Total GAC operational cost, present value ($)	Total pumping electricity cost, present value ($)	Total savings from biodegradation, present value ($)	Total cost, present value ($)	Cost per cubic meter of treated groundwater ($/$m^3$)
1	7	0	170	188	170	-10%	30,079	8	601,591	4,670	3,406	606,261	446
2	7	75	-225	738	1,911	160%	28,648	31	572,973	27,748	38,222	600,721	86
3	10	30	-250	1,348	3,085	130%	27,693	58	553,861	68,964	61,698	622,825	43
4	10	100	-400	1,190	1,377	16%	29,426	49	588,523	82,432	27,540	670,955	34
5	10	120	-280	1,380	2,595	88%	28,065	60	561,310	106,371	51,904	667,681	40
6	16	50	-460	1,000	3,856	285%	27,000	40	540,019	85,286	66,362	625,305	34

The baseline biodegradation mass for intrinsic NA over 60 years is 1380 kg. Through NA alone, without intervention, it would take approximately 1300 years for the contaminant plume to degrade. This hypothetical scenario could not be allowed to happen, as it would reach receptors in 200 years. This scenario is for comparison purposes in order to assess the performance of the PAT system with regards to mass removal through physical extraction and through enhanced in situ biodegradation.

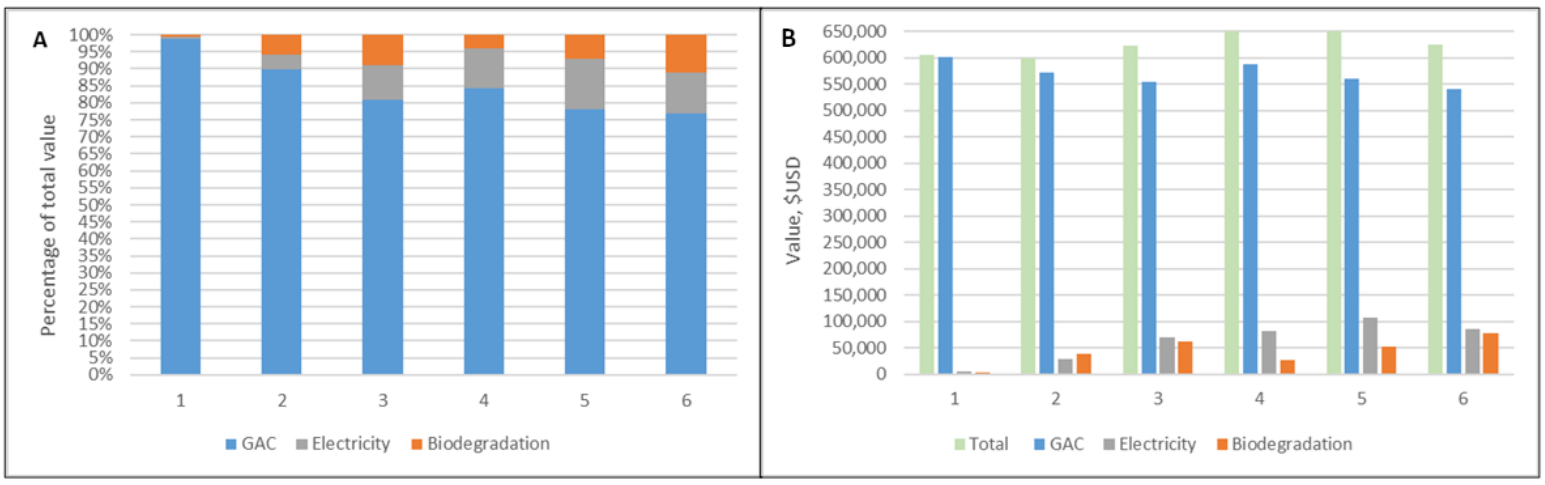

Figure 6-3. Shown above are the (a) stacked percentages of total GAC operational cost, total electricity pumping cost, and cost reduction from biodegradation, and (b) the values of each of the former in $USD. The x axis number corresponds to the scenario.

Scenario 1

The aim of Scenario 1 was to remediate the plume quickly by placing extraction wells inside the centerline of the plume. The effect on situ biodegradation was measured. It was expected that biodegradation would not be enhanced much since the wells are doing the opposite of spreading the plume – they are causing it to bottleneck to the well screen. This is achieved with 7 wells and a constant cumulative pumping rate of 170 m^3/d.

Graphs 1a to 1d (Figure 6-2) show the results of Scenario 1 (Table 6-2). Scenario 1 reaches the remediation target of 90% mass reduction (through biodegradation and mass extracted) in 8 years (see Table 6-3). Graph 1a (Figure 6-2) shows that 170kg of contaminant mass is biodegraded over the 8 years required to reach the remediation target. As Scenario 1 did not enhance biodegradation, this value is slightly less (-10%) than the mass biodegraded by no intervention over the same time period (Table 6-3). This is due to the location of the PAT wells within the plume interior, which inhibits the dispersive mixing between the contaminant and the EAs. This finding is supported by the reaction rate results of Scenario A in Chapter 4. Graph 1b (Figure 6-2) shows that >30,000 kg of contaminant mass is extracted by the PAT wells. For both graph 1a and 1b (Figure 6-2), the mass biodegraded and mass extracted increase over time until they reach an asymptotic limit once the PAT system has removed all of the contaminant mass. Graph 1c (Figure 6-2) shows the GAC operational cost over time for the PAT system, which amounts to >$600,000 over the remediation period. Graph 1d (Figure 6-2) shows the cost reduction from in situ NA, which amounts to $3,400 over the remediation period, almost covering the PAT electricity cost of $4,670 (see Table 6-3). Due to the low pumping rates, number of wells, and short remediation period (8 years), the total electricity cost for Scenario 1 is significantly lower than the electricity cost for the other scenarios (Table 6-3).

Scenario 2

The aim of Scenario 2 was to induce spreading by injecting with 4 wells in the plume centerline for as long as possible while maintaining hydraulic control – which was determined to be 15 years – before switching all the wells entirely to extraction for the remainder of the remediation period.

Graph 2a through 2d (Figure 6-2) shows the results of Scenario 2 (Table 6-2). Scenario 2 reaches the remediation target of 90% mass reduction (through biodegradation and mass extracted) in 31 years (see Table 6-3). Graph 2a shows that 1900 kg of contaminant mass is biodegraded over the remediation period. This induction of spreading from the well injection resulted in a significantly higher biodegradation mass than NA at the same time period (160%) and very significantly higher than Scenario 1 (1000%) but required much longer to reach the remediation target (275% longer or 22 years). Graph 2b (Figure 6-2) shows that >28,000 kg of contaminant mass is extracted by the PAT system over the remediation period. Graph 2c (Figure 6-2) shows the GAC operational cost over time for the PAT system, which amounts to $570,000 over the remediation period. Graph 2d (Figure 6-2) shows the cost reduction from the enhancement of in situ NA, which amounts to $38,000. This is a significant

increase compared to Scenario 1, but with a <10% reduction in total cost. The total pumping electricity cost for Scenario 2 is $27,750, which is significantly higher than Scenario 1 due to the higher pumping rates and the longer remediation period.

Scenario 3

The aim of Scenario 3 is to laterally (transverse horizontally) spread the plume by utilizing 3 interior injection wells, each of which are bounded by 2 exterior extraction wells (see Table 6-2, Scenario 3). However, while these exterior extraction wells contribute to spreading the plume (being located approximately 80 m north and south of the plume centreline), – they also keep it contained and ultimately extract contaminant mass, but to a lesser degree than the wells in Scenario 1. Most of the plume mass is being extracted by the downgradient containment wells, which is why the remediation period is longer than the other scenarios (see Table 6-3).

Graph 3a through 3d (Figure 6-2) shows the results of Scenario 3 (Table 6-2). Scenario 3 reaches the remediation target of 90% mass reduction (through biodegradation and mass extracted) in 58 years (see Table 6-3). Scenario 3 significantly enhanced biodegradation (130%) over NA during the same period; however, this enhancement is less than Scenario 2 (Table 6-3). Graph 3a (Figure 6-2) shows that 3,000 kg of contaminant mass is biodegraded over the remediation period. Graph 3b shows that >$27,000 of contaminant mass is extracted by the PAT system over the remediation period. Graph 3c (Figure 6-2) shows the GAC operational cost over time for the PAT system, which amounts to $544,000 over the remediation period. Graph 3d (Figure 6-2) shows the cost reduction from in situ NA, which amounts to $61,000 over the remediation period. The total electricity pumping cost for Scenario 3 is $68,964, which is due to the pumping rates (higher number of wells contributes to this) and the longer remediation period.

Scenario 4

The aim of Scenario 4 was to spread the plume vertically (transverse vertically) and laterally (transverse horizontally) by utilizing exterior extraction wells and injection wells situated above the plume.

Graph 4a (Figure 6-2) through 4d shows the results of Scenario 4 (Table 6-2). Scenario 4 reaches the remediation target of 90% mass reduction (through biodegradation and mass extracted) in 49 years (see Table 6-3). Graph 4a (Figure 6-2) shows that 1376kg of contaminant mass is biodegraded over the remediation period. Scenario 3 only enhanced biodegradation by 16% over NA during the same remediation period, which is low compared to the other scenarios (lowest after Scenario 1- see Table 6-3). Graph 4b (Figure 6-2) shows that >29,000 kg of contaminant mass is extracted by the PAT system over the remediation period. Graph 4c (Figure 6-2) shows the GAC operational cost over time for the PAT system, which amounts to $588,000 over the remediation period. Graph 4d (Figure 6-2) shows the cost reduction from in situ NA, which amounts to $27,000 over the remediation period. The total electricity pumping cost for Scenario 4 is $82,432, which is due to the pumping rates (higher number of wells contributes to this) and the long remediation period.

The strategy of spreading the plume in the vertical dimension did not work as well as spreading in the horizontal dimension, such as in Scenario 3, due to a significantly lower vertical aquifer dispersivity (see Table 6-1). This scenario also took significantly longer than Scenario 2 and the corresponding mass biodegraded was much lower. Consequently, there is no trade-off between longer remediation time and higher biodegradation, and therefore higher cost reduction. The PAT system strategy implemented in this scenario is therefore not recommended. This was the most expensive scenario, at $671,000 (see Table 6-3). This is due to this scenario having the second highest GAC cost and a higher (third highest) electricity cost.

Scenario 5

Scenario 5 uses the same well configuration as Scenario 4. The main difference is that Scenario 5 makes use of temporally varying pumping rates. Scenario 5 has a variable pumping rate. The wells on the north and south side of the plume are alternating between injection and extraction every 5 years for 20 years. Afterwards, the pumping rates remain constant for the duration of the 60 year simulation.

Graph 5a through 5d (Figure 6-2) shows the results of Scenario 5 (Table 6-2). Scenario 5 reaches the remediation target of 90% mass reduction (through biodegradation and mass extracted) in 60 years (see Table 6-3). Graph 5a (Figure 6-2) shows that 2600kg of contaminant mass is biodegraded over the remediation period. Scenario 3 enhanced biodegradation by 88% over NA during the same remediation period. Graph 5b (Figure 6-2) shows that >27,000kg of contaminant mass is extracted by the PAT system over the remediation period. Graph 5c (Figure 6-2) shows the GAC operational cost over time for the PAT system, which amounts to $549,000 over the remediation period. Graph 5d (Figure 6-2) shows the cost reduction from in situ NA, which amounts to $51,000 over the remediation period. The total electricity pumping cost for Scenario 5 is $106,371, which is the highest electricity cost of all scenarios. This high electricity cost is due to the higher pumping rates and due to the cumulative pumping rate being -400 m^3/d for 40 years, after the time variant side-to-side injection and extraction for the first 20 years have ceased. This scenario also has the wells with the highest singular extraction rates of any well used in this study, which causes a larger drawdown, which causes the high electricity cost.

Although Scenario 5 reaches the remediation 11 years later than Scenario 4, and therefore their end results are not directly comparable, Scenario 5 still biodegrades significantly more mass within the same timeframe as Scenario 4 – ~2500kg compared to 1377kg, an enhancement of 82%. However, this comes with the caveat that this significant enhancement in biodegradation incurred a significantly higher electricity cost.

There is potential that this scenario could be optimized in order to reduce the electricity cost or modified in some way to still reap the benefits of enhanced NA. This scenario would be even more effective if the hydraulic gradient could be eliminated or at least reduced, which would allow the plume to stay in the aquifer longer and be remediated in situ. This could be achieved with hydraulic containment wells injecting downgradient of the plume and extracting upgradient of the plume, which is a typical approach for in situ bioremediation

studies (Bagtzoglou and Oates, 2007; Piscopo et al., 2013). If the plume could be entirely remediated in situ then it would eliminate the GAC treatment costs, which even with inflation, would still likely be higher than the pumping electricity costs over the remediation period.

Scenario 6

Scenario 6 aims to use interior injection wells and exterior extraction wells to spread the plume as much as possible while also keeping it contained and under control. This scenario differs from Scenario 3 and 2 in that it uses 3 fully screened downgradient extraction wells, with the aim to spread the plume vertically and horizontally, as well as reducing the reduce of mass extraction.

Graph 6a through 6d (Figure 6-2) shows the results of Scenario 6 (Table 6-2). Scenario 6 reaches the remediation target of 90% mass reduction (through biodegradation and mass extracted) in 40 years (see Table 6-3). Graph 6a (Figure 6-2) shows that 3800kg of contaminant mass is biodegraded over the remediation period. Scenario 3 significantly enhances biodegradation by 285% more than NA over the same period. Graph 6b (Figure 6-2) shows that 27,000kg of contaminant mass is extracted by the PAT system over the remediation period. Graph 6c (Figure 6-2) shows the GAC operational cost over time for the PAT system, which amounts to $544,000 over the remediation period. Graph 6d (Figure 6-2) shows the cost reduction from in situ NA, which amounts to $66,000 over the remediation period, which is not significantly more than Scenario 3, but this is achieved 20 years earlier than Scenario 3. The total electricity pumping cost is $85,286, which is second only to Scenario 5. The high electricity cost is due to the number of wells being higher than any other scenario (16 wells), the cumulative drawdown, and a long remediation period.

The containment wells in Scenario 6 has smaller drawdowns due to the 3 downgradient extraction wells having smaller extraction rates per layer and therefore are exerting smaller changes in hydraulic gradient and therefore velocity near each screen.

Figure 6-3 shows the stacked percentages of GAC operational cost, pumping electricity cost, and the cost reduction from biodegradation, and each of these values are compared. As expected, GAC operational cost is far more expensive than electricity cost. The electricity cost was higher than expected, but it is at most, approximately ~15% of the total cost. At most, the cost reduction from biodegradation saves nearly 15% of the total remediation cost, but electricity cost is higher than the cost reduction from biodegradation. In the case of Scenario 4 and 5, the electricity cost is significantly higher than the cost reduction from biodegradation (>200% and >100%). Only Scenario 2 has a higher cost reduction from biodegradation than electricity cost. Figure 6-3 also shows the cost of treated groundwater per cubic meter ($/m^3). The cost is significantly higher than literature values (Khan et al., 2004), which could be due to the inflated GAC cost per kg that was chosen for this study ($/kg), the high phenol mass, and the value of $CURC_p$ that was used.

Scenarios 1 and 2 were able to achieve 100% remediation of the contaminant plume; all of the other scenarios achieved 90%. Scenarios 2, 3, 4, 5, and 6 had significant enhances in

biodegradation. Scenario 1 did not enhance biodegradation, which was expected, as the wells were placed directly in the plume interior. For Scenarios 1, 3, and 6, the cost reduction from biodegradation covered 75-90% of the electricity cost, whereas Scenario 2 covered 140%. Only Scenario 4 and 5 had significantly higher electricity costs than cost reduction from biodegradation.

In summary, the ranking by total GAC operational cost (high to low) is as follows: Scenario 1, 4, 2, 5, 3, 6. The ranking by total electricity cost (high to low) is as follows: Scenario 5, 6, 4, 3, 2, 1. The ranking by total cost reduction from biodegradation (high to low) is as follows: Scenario 6, 3, 5, 2, 4, 1. The ranking by total cost (high to low): Scenario 4, 5, 6, 3, 1, 2. The ranking by time required to reach remediation target (high to low) is as follows: Scenario 5, 3, 4, 6, 2, 1.

There is no clear optimal strategy or well configuration. The total cost for all scenarios is between $600,000 and $671,000. This is little more than a 10% difference. The cost reduction from biodegradation did not result in significant savings, but the cost savings could potentially cover the cost of electricity.

Scenario 4 is the most expensive scenario and does not enhance biodegradation as much as the other scenarios. Its methodology over spreading a thin plume over a vertical dimension with low vertical dispersion is not recommended.

Scenario 5 is an improvement over Scenario 4, but still requires further improvement. Scenario 5 is the same as Scenario 4 – the well pumping rates are simply temporally varying. This modification resulted in a >80% enhancement in mass biodegraded over the same time period. However, this came at additional cost incurred by the higher pumping rates which resulted in higher drawdowns and therefore a higher electricity cost. This scenario could possibly be optimized further.

Scenario 6 is the 3rd most expensive scenario overall but has the lowest GAC expense and the highest cost reduction from biodegradation. Since the difference among the GAC operational cost is not very large, the electricity cost is what places this scenario in the upper mid-range for total cost. Considering this, Scenario 6 could likely be improved by altering the pumping rates, well locations, or number of wells in order to reduce the electricity cost.

Scenario 2 has the lowest total cost due to having the second lowest electricity cost and having a mid range GAC operational cost. It is the only scenario for which the cost reduction from biodegradation was greater than the total pumping electricity cost. This is due to the smaller number of wells (7), reaching the remediation target in 30 years (half of total allowed remediation time), and the biodegradation enhancement from injecting for 15 years. However, in practice, this strategy of injecting for such a prolonged period is risky, as the plume could grow to an uncontrolled size, migrate offsite, or flow into regions with low hydraulic conductivity.

Scenario 3 has the 2nd lowest GAC operational cost and consequently the 2nd highest cost reduction from biodegradation and is mid-range on total cost and electricity cost. The cost reduction from biodegradation nearly covers the electricity cost.

Scenario 1 has the second lowest total cost. However, this is considering only the operational cost of both GAC and electricity for the pumping wells – capital and installation costs are not considered. Extracting >30,000kg of phenol in only 8 years would result in a massive capital cost. It would require, at the very least, 150,000kg of GAC. According to Culver et al., 1998, GAC treatment units can hold 9,000kg of GAC each, so it would require at least 17 GAC units to get started. The capital costs would be lower for other scenarios but would still be significant and likely higher than the operational cost.

6.4 Conclusion

This chapter presented a series of 6 scenarios aimed at enhancing in situ biodegradation as much as possible by using combinations of injection and extraction wells, in order to reduce the total cost of remediation. These scenarios were simulated with the constraint that they reach the remediation target of 90% of contaminant mass removed, through combination of biodegradation and mass extraction, within 60 years. Each scenario used slightly different well locations, pumping rates, and one scenario included temporally varying pumping rates. Scenarios which enhanced biodegradation, and thus, cost reduction through biodegradation the most, required significantly more time to reach the remediation target compared to conventional PAT. This is expected, as the plume must remain in situ in order to be remediated through NA.

However, there is no clear optimal strategy or well configuration. The cost reduction from biodegradation did not result in significant savings, but it could potentially cover the cost of electricity, with the cost reduction from biodegradation exceeding the electricity cost for only Scenario 2. The largest enhancement of in situ biodegradation was Scenario 6 (285%), which biodegraded nearly 15% of total contaminant mass, which resulted in $66,362 in savings over 40 years. This large enhancement in NA occurred despite the slow kinetics and low dispersivity coefficients – the first order biodegradation rates are 10^{-5} to 10^{-6}, depending on the EA, which are orders of magnitude lower than reported values for phenol and related organic compounds, such as BTEX (Watson et al., 2005; Wiedemeier et al., 1996; 1999; Lu et al., 1999). However, the overall enhancements in biodegradation were much less than expected, based on the results of 4 concurrent injection wells administering EAs from Chapter 5. The high performance seen in 10 years could not be sustained at the longer time scales in Chapter 6 due to the physical properties of the aquifer, the plume geometry, and the constraints of the remediation goals which were to keep the plume controlled and contained.

Another contributing factor to the long remediation time is the high concentration of phenol, which is orders of magnitude higher than the concentration of the EAs. As shown previously in Chapter 4, if the phenol concentration were closer to the same order, it would be significantly more biodegradable and the remediation period and total operational cost would be drastically reduced. The only way to practically reduce the concentration of phenol is by spreading the plume, which will cause dilution and increase the biodegradation rate at the fringes. However, there are numerical and practical constraints with this, as the model grid would need to be larger, increasing computational cost. In practice, spreading the plume over a very wide area is risky and likely illegal in many jurisdictions, as the plume could migrate

offsite, get trapped in low permeability zones, or there could be some anisotropy that causes the plume to migrate in an uncontrolled and unexpected manner. The likely optimal way to solve this problem is to employ a time varying oscillating injection and extraction scheme after the hydraulic gradient has been eliminated, in order to more effectively mix the plume and keep it managed and controlled for a prolonged period.

As outlined in the discussion, there is still potential to improve upon the methodology presented here. If the biodegradation rates could be increased, then the contaminant might be able to be remediated more quickly than 60 years, and it could further reduce the cost of remediation. Regardless, the methodology presented in this chapter might be suitable for further enhancing the biodegradation of BTEX compounds, or other compounds with comparatively fast kinetics and/or low concentrations which are degraded through an aerobic pathway.

PAGE INTENTIONALLY LEFT BLANK.

Chapter 7

7.0 Conclusion

As much of the world relies on groundwater for much of their potable water and irrigation requirements, ensuring that these resources are safe to use is essential. However, there are a large number of deep plumes in consolidated aquifers, such as the one present at the site used in this thesis, where there are few realistic remedial options other than PAT, in situ bioremediation, surfactant enhanced remediation, and in situ chemical oxidation. As the hydraulic conductivity value of the site in question is too low for surfactant enhanced remediation to be applicable and in situ chemical oxidation was ruled out due to the demonstrated evidence of NA occurring at the site, it was speculated by previous research whether NA could be enhanced by targeted PAT. If possible, enhancing PAT with NA could be a more environmentally sustainable option with the potential for reduced upfront costs of remediation. Additionally, it was considered that using targeted PAT to enhance in situ NA could potentially eliminate the need for an in situ bioremediation approach and result in less ex-situ remediation requirements which could reduce the overall cost of remediation.

Ultimately, this thesis aimed to develop a conceptual remedial framework which integrates PAT with NA to improve remediation performance by considering operational variables and analysis of mass transport processes which limit biodegradation. This goal was broken down into a few stages; first, to examine whether PAT can be used to enhance NA in situ, and what mechanisms are responsible for this enhancement. These findings were then built upon to examine more complicated scenarios utilizing multiple wells, exploring the effects of both injection and extraction with the aim to enhance in situ NA even further. Finally, more complex multiwell configurations with between 7 and 16 wells were designed with the aim of trying to remediate 90% of the plume within 60 years. A cost function was employed only for this chapter to address the research question of whether NA-enhanced PAT can be used to reduce overall operational cost of remediation.

The first step involved developing a 3D advective-dispersive-reactive solute transport model using MODFLOW-2005 and MT3D-USGS, which was constructed with historical site characterisation data from a chemical manufacturing plant on a UK sandstone aquifer. This would act as a simulation framework to evaluate scenarios' biodegradation performance for the integrated PAT and NA system. Using the framework, a series of modelling scenarios were developed to assess the remediation effectiveness of NA-enhanced PAT compared with conventional PAT. This aim was intended to address the lack of research relaying the effects of using PAT to enhance in situ intrinsic NA, and the lack of research exploring the mechanisms behind these enhancements in depth. Using this data, a synthetic plume was created in the model to investigate the scenarios in this conceptual analysis. The contaminants in groundwater at the site were all converted into equivalent concentrations of phenol (the predominant contaminant) for the modelling. A Monod formulation was used in the model to simulate the kinetic reactions between phenol and different electron acceptors (dissolved oxygen and nitrate) involved in biodegradation reactions.

7.1 Research findings

Chapters 3 and 4

Chapter 3 compared the numerical accuracy of a coarse grid model (5x5x5 m3) and a fine grid model (2.5x2.5x2.5 m3). It was determined that the coarse grid plume is approximately 20 meters longer and 10 meters thicker than the fine grid plume and the plume width is unchanged. The plume size increase that is induced by numerical dispersion results in a more concentrated plume and more mass that is biodegraded (a difference of +30%) over 70 years of plume generation. For the fine grid model, a trial and error analysis was undertaken to determine which values of dispersivity produce a plume of similar thickness, length, concentration, and biodegradation mass as the coarse grid model. The result was that the fine grid model requires an l of 1.4 m (+40%) and an z of 2 cm (+400%). In the coarse model there is numerical dispersion which is causing the plume to be reduced in concentration and increased in size. However, this issue is not that significant, as the plume simply has higher dispersion than intended for an almost entirely advection driven plume. Despite the fact that the numerical dispersion is inflating the biodegradation mass, the values in Chapters 4 and 5 are still within the established 1-5% of total plume mass that is biodegraded over the lifetime of the plume (Thornton et al., 2001a,b; Williams et al., 2001; Mayer et al., 2001; Watson et al., 2005).

In Chapter 4, there is an experiment with varying values of dispersivity coefficients which show that increasing the dispersivity coefficient significantly enhances biodegradation, as expected. While the TVD method may not be completely eliminating numerical dispersion, it is significantly reducing it considering a Peclet constraint of 2. Other methods that could be used to eliminate numerical dispersion to conduct a quantitative analysis such as parallel computing on a high performance computing cluster or particle tracking. However, the particle tracking method in MT3D-USGS, the method of characteristics, is not mass conservative, which would lead to errors when calculating the total mass biodegraded (Zheng and Bennett, 2002). A novel particle tracking method would instead need to be used in order to include kinetic biodegradation reactions and calculate the total mass biodegraded.

Chapter 4 showed that, in general, extraction wells in the plume centerline/interior decrease the area of the fringe region, and mainly increase biodegradation near the well itself, which was not addressed or discussed in Thornton et al., (2014). However, the 2D experiment in Chapter 3 did show that an extraction well in the plume centerline/interior does increase the flux of EAs into the plume itself, mirrored by the findings of Thornton et al., (2014).

The first experiments in Chapter 4 aimed to use the framework to investigate the effect of PAT design variables, such as flow rate, well locations, and well configuration, as a proof of concept for enhancing NA (biodegradation) using targeted PAT. The impact of each variable was measured by integrating the biodegradation rate in space and time and comparing it to the baseline biodegradation mass (no intervention) over the same time period.

The scenario modelling showed that the enhancement of biodegradation depends on the location, number of wells, pumping rate and distance between well location(s) in the PAT

scheme. Placing the PAT wells too close together limits biodegradation rates and extraction in the plume interior/centreline is less effective than injection in the same location. Since the extraction well removes contaminant mass from the system, this reduces the overall biodegradation rate in space and time, as this is strongly influenced by phenol concentration. In general, injection enhances plume fringe reactions by increasing dispersive mixing through the creation of divergent flows. As the wells are moved laterally outward from the plume centreline, the mass extracted decreases and mass biodegraded increases. The results of this determined that natural attenuation, as defined by dispersion, dilution, and biodegradation, was significantly increased (130% above intrinsic NA in the same timescale), and the plume concentration was significantly reduced.

The PAT system enhances *in situ* biodegradation of contaminants by (i) increasing dispersive mixing between solutes in the plume and background groundwater, and (ii) increasing the flux of dissolved electron acceptors into the plume from the background groundwater in zones (e.g. plume fringe) which have high biodegradation potential. Enhanced mixing also increases contaminant dilution and can remove factors which are inhibitory to biodegradation, such as high contaminant concentrations.

The variables which enhanced biodegradation were identified as injection or extraction rate, injection with or without amendments, lateral and longitudinal distance of the well from the plume center, and distance between wells in dual-well configurations. The most effective scenario in chapter 4 was scenario B-GW where groundwater containing electron acceptors was injected 15 meters from the plume center. It was determined that injection in the plume interior was more effective than injection or extraction at the plume fringe. It was also determined that enhancing transverse mechanical dispersion also enhances biodegradation significantly more than enhancing longitudinal hydrodynamic dispersion alone; as established in Chapter 4, where transverse PAT (scenario C-ext) was significantly more effective and enhancing NA than PAT at the plume front (scenario A). Therefore, inferring from the above, spreading the plume in the horizontal transverse direction essentially increases the mechanical dispersion, and significantly reduces concentration and significantly enhances biodegradation mass. The biodegradation rates were slow, but it was thought that they could still be enhanced further by including more wells and reducing the diminishing returns incurred by using more than 1 well.

Chapter 5

Chapter 5 built upon chapter 4 by extending the investigation of the plume space to identify the pumping locations which enhance biodegradation the most. This research attempted to find ways to reduce the diminishing returns incurred when multiple wells were used in the same simulation, where their enhancement of biodegradation was less than the sum of what each of the wells achieved in separate simulations. The goal was to find a sub-linear relationship between numbers of wells and biodegradation, rather than logarithmic.

Chapter 5 also aimed to address the lack of research investigating whether injections of dissolved EAs can be combined with a targeted PAT system with the goal of further

augmenting biodegradation. Another goal of using amendments was to investigate the effect of amendment concentration on biodegradation mass compared to the mass removal by intrinsic fringe biodegradation processes, as the naturally-occurring biodegradation at the plume fringe has not been taken into account in previous research (Marquis and Dineen, 1994; Park et al., 2007). Since reduced bioavailability in the concentrated areas of the plume results in low rates of biodegradation, amendment injections enhance biodegradation by promoting the direct contact between the phenol and the EAs, in addition to enhancing the plume fringe reactions. The final objective of this chapter was to examine multiwell scenarios and determine their impact on mass removal and in situ biodegradation, in addition to comparing the impact of different amendment types and concentrations.

The multiwell scenarios were built through trial and error. Eventually a 4 well injection scenario was discovered which enhanced biodegradation by 520% above intrinsic NA over the same time period. As expected, injection of electron acceptors not only enhanced mass biodegraded inside the plume, but increases fringe reaction processes (Chapter 5, Scenario 8). Chapter 5 discovered that denitrification is a small contributor to the overall biodegradation rate due to the inhibition (K_i) term and due to the K_{max} term being one order of magnitude lower than that of oxygen. The only situation in which biodegradation rate via nitrate rivals that of oxygen is when the injected nitrate concentration is 500 mg/l or greater. CRMs involving injection in the plume back and extraction at the plume front enhanced NA more than injection of oxygen and nitrate at 50 and 500 mg/l, respectively. This is despite the concentrations of the CRMs being much lower – at 9.28 and 105, for oxygen and nitrate, respectively. The CRMs effectively spread the concentration of EAs around the plume. Some experiments in chapter 5 (Scenario 3 and Scenario 7) succeeded in enhancing mass removal from biodegradation whilst simultaneously reducing the mass extracted.

However, this chapter failed to find a configuration with a linear relationship between a higher number of wells and biodegradation mass. For example, despite Scenario 2 and 3 having an additional well, they were not more effective at enhancing NA more than the single well in Scenario 1. Diminishing returns were still occurring between well number and biodegradation mass, pumping rate and biodegradation mass, and amendment injection and biodegradation mass; the relationship remained sub-linear and logarithmic. It is concluded that concurrently using multiple wells of any type does not necessarily increase mixing or spreading to enhance biodegradation more effectively than a single well. However, experiments in Scenario 7 succeeded in enhancing degradation by 40% and mass extracted was reduced by only changing the well location and well type while keeping the pumping rate the same. This illustrates that specific location of the well and the well type is an important factor when designing a multiwell PAT configuration with the aim of enhancing in situ NA. While dual extraction wells located too close together transversely and longitudinally do not enhance biodegradation, it was found that increasing the radius and the longitudinal distance between wells resulted in a significant enhancement in biodegradation.

Overall, injection wells were found to be far more effective than extraction at enhancing biodegradation. This is due to the divergent flows induced in 3 dimensions by the injection

wells which increase the dispersive mixing of the plume and the uncontaminated groundwater (Marquis and Dineen, 1994; Jones et al., 2002). Injection of EAs and amendments further enhanced biodegradation due to an increase in the stoichiometric ratio between the ED and EA and specific reactions in the plume interior between the ED and EA; whereas injection of groundwater without EAs did not enhance reactions in the plume interior - only on the plume fringes, where mixing occurs.

Chapter 6

In addition to building upon the previous findings and exploring them in more depth, chapter 6 aimed to establish whether it is possible to enhance NA *in situ* enough to reduce the operational cost of PAT for the remediation of organic contaminants. It also aimed to investigate which multi-well configurations and mechanisms contribute most to the enhancement of NA *in situ*.

A series of modelling scenarios was developed with the goal of remediating 90% of the plume through a combination of both mass extraction and biodegradation within 60 years. The purpose of the 60 year remediation period is to compare modelling scenarios which may reach the 90% remediation target at different times, as it is understood from previous modelling scenarios that a PAT system designed to enhance biodegradation will require more time to reach the remediation target than a conventional PAT system with the extraction located in the plume interior/centerline. To achieve this, more wells were required – 4 interior wells were used, combined with 3 downgradient PAT wells to prevent the plume from enlarging and becoming unmanageable. This basic scheme of 7 wells was modified according to the scenario, with some scenarios having 10 wells and others having 16. Taking into account the lessons learned from chapters 4 and 5, the modelling scenarios for chapter 6 aimed at spreading the plume as much as possible with injection wells, while keeping it contained on all sides with extraction wells. The injection wells also administered EAs at concentrations of 9.28 and 105 mg/l for oxygen and nitrate, respectively. A conventional PAT modelling scenario was designed as a control on which the other scenarios were to be compared. Through the modelling scenarios, it was discovered that due to low sorption, fair permeability, no diffusion, and high aqueous solubility, the entire plume can be remediated fairly quickly (<10 years) but will likely have a higher upfront capital cost and the subsequent savings from biodegradation are low ($4k). Biodegradation for the conventional PAT scenario was lower than intrinsic NA over the same period. However, for most other scenarios, biodegradation mass was significantly enhanced as compared to intrinsic NA over the remediation period, with the best performing scenario enhancing biodegradation by 285% (Chapter 6, Scenario 6).

However, if the plume is remediated more slowly, then the upfront costs would likely be lower and there are more savings ($40k-60k) from biodegradation. Savings are approximately 10 times higher by remediating the plume slower, as opposed to extracting it in 10 years. However, longer the remediation periods incurred a higher electricity cost. In most cases, the cost reduction from biodegradation did not cover the total electricity cost from pumping,

except in one scenario (Chapter 6, Scenario 2). Transient side to side alternating injection and extraction (Chapter 6, Scenario 5) biodegraded more mass than the same scenario which employed constant pumping rates; however, this enhancement in biodegradation incurred an additional electricity cost. It is possible that this transient alternating injection and extraction scenario could be enhanced further in order to keep the enhancement of biodegradation while reducing the electricity cost. In summary, the best performing scenario removed approximately 15% of total contaminant mass, which was much less than expected, based on the results of 4 concurrent injection wells administering EAs from Chapter 5. The high performance seen in 10 years could not be sustained at the longer time scales in Chapter 6 due to the physical properties of the aquifer, such as the diagonal flowpath, low hydraulic conductivity, low dispersivity, and the plume geometry. The aquifer also becomes oxidant limited due to the high concentration of phenol and the kinetics, which further contributes to the poor performance of scenarios aiming to enhance biodegradation, as 1 unit of phenol requires 3 units of oxygen to be removed by biodegradation. In order to prevent the oxidant limitations, the plume would need to be spread over a much larger area, which is impractical. The oxidant limitations could be further addressed by injecting increased concentrations of EAs.

Even if the plume could have been forced to remain in situ indefinitely through the use of injection wells downgradient and extraction wells upgradient to induce a stagnant hydraulic gradient in the vicinity of the plume, the low dispersivity values combined with the slow kinetics would result in a significantly long timescale for full plume remediation through biodegradation (600+ years), given that the biodegradation rates remain constant. Therefore, it is concluded that in addition to the complex plume geometry and low values of dispersivity, the slow kinetics are the main limiting factor. Of all the biodegradation rate parameters, the k_{max} rate is the most limiting; it is on order of 10^{-5} to 10^{-6} (1/T) for respiration via oxygen and nitrate, respectively. It is several orders of magnitude lower than the typical k_{max} rates published in the literature for benzene and phenol (Nielsen et al., 1995; Weidemeier et al., 1996; Jones et al., 2002; Watson et al., 2005).

7.3 Implications and further research

The findings of this thesis would suggest that there are significant barriers to achieving the objectives for enhancing intrinsic NA in situ to reduce the remediation timeframes and operational cost over a conventional PAT remediation strategy. However, the methodology implemented in this thesis could potentially be combined with an in situ bioremediation approach to remediate the site to a higher standard. There is a scientific and technical basis to integrate conventional PAT remediation schemes with NA to improve overall remediation performance in aquifers contaminated with oxidizable organic contaminants. There is an opportunity to enhance the performance beyond what was possible with either technology separately. This also translates to an improved basis to reduce cost of remediation by using these approaches, following the work on the cost benefit analysis. The limitations are the dispersivity of the aquifer and the kinetics of the reactions, both of which are not easily determined. The aquifer properties such as dispersivity and heterogeneity, the aquifer

hydrogeology (recharge, specific discharge, hydraulic conductivity, isotropy/anisotropy), and plume dimensions which are dependent on these aquifer properties.

To achieve the above, it is necessary to develop the site characterization in order to obtain appropriate input terms for the transport model and biodegradation model. The aquifer hydrogeology and hydraulics must be known in detail, and site microbiology, biogeochemistry, and aquifer contamination status must be well understood. If there is not already an established MNA scheme, then it would need to be known what the appropriate kinetic biodegradation parameters for the contaminant of concern and its biodegradation pathway are. It would also need to be known what the appropriate redox conditions are in order to determine the appropriate amendments to include.

While changing well layouts, well types (injection vs extraction), amendment injection, and amendment with CRMs resulted in significantly enhanced biodegradation, there were still diminishing returns incurred. This is due to limitations such as limited mixing between the ED and EAs, low aquifer mechanical dispersion, order of magnitude higher ED concentration, intrinsically slow reaction kinetics, and stagnation zones in between wells (Cunningham et al., 2004). Future studies could examine ways to overcome these limitations by enhancing mixing between the ED and EA further. The mixing and low dispersion limitations could be realistically overcome by employing time variant recirculating or oscillating wells that are commonly employed in in situ bioremediation studies (Bagtzoglou and Oates, 2007; Zhang et al., 2009; Piscopo et al., 2013; Sather et al., 2022; 2023).

Another contributing factor to the long remediation times in Chapter 6 is the high concentration of phenol, which is orders of magnitude higher than the concentration of the EAs. As shown previously in Chapter 4, if the phenol concentration were closer to the same order, it would be significantly more biodegradable, and the remediation period and total operational cost would be drastically reduced. The only way to practically reduce the concentration of phenol is by spreading the plume, which will cause dilution and increase the biodegradation rate at the fringes. However, there are numerical and practical constraints with this, as the model grid would need to be larger, increasing computational cost. In practice, spreading the plume over a very wide area is risky and likely illegal in many jurisdictions, as the plume could migrate offsite, get trapped in low permeability zones, or there could be some anisotropy that causes the plume to migrate in an uncontrolled and unexpected manner. The likely optimal way to solve this problem is to employ a time varying oscillating injection and extraction scheme after the hydraulic gradient has been eliminated, in order to more effectively mix the plume and keep it managed and controlled for a prolonged period.

Also, the application of mathematical optimization could possibly be applied to advance the research presented in this thesis by finding optimal well placements which maximize biodegradation. Maximizing biodegradation inherently requires that less mass is removed by the extraction wells, so it would also reduce the treatment cost - hence, the two objectives are not competing. However, the objective of optimizing biodegradation and the objective of minimizing overall remediation period would compete and would therefore require a tradeoff

analysis, with the decision maker to decide the optimal decision. This is because enhancing biodegradation in situ takes longer than conventional PAT - at least for fairly homogeneous aquifers with a highly mobile aqueous phase contaminant, such as what was used in this thesis. Moreover, as the effect of multiwell scenarios on biodegradation is still sublinear, it is unclear if maximizing biodegradaton would also increase electricity costs - it would need to be investigated whether these are competing objectives in future optimization research.

In a few studies (Thornton et al., 2014; Pickup et al., 2001; Lerner et al., 2000; Watson et al., 2005, Nielsen et al., 1995), it was determined that the k_{max} rate for phenol is both dependent on scale and on the concentration of phenol itself. A high phenol concentration severely limits the k_{max} rate by several orders of magnitude, whereas a low phenol concentration increases the k_{max} rate by several orders of magnitude (Wiedemeier et al., 1996; 1999; Nielsen et al., 1995). Phenol typically has a k_{max} rate similar to benzene, which is in the range of 10^{-1} to 10^{-3}, although some studies have found that k_{max} rates are grossly overestimated (Nielsen et al., 1995). A relationship between k_{max} and concentration of the contaminant needs to be established in order to utilize this in the model to more accurately simulate what is happening in situ, such as in the case with Thornton et al., 2014, where the reduction in phenol concentration by the PAT system contributed to the increase of biodegradation rate. This relationship between k_{max} and the concentration of the contaminant could be explored using a simulation code or program which allows kinetic parameters that vary in time and space. Ideally the simulation code would have a mechanism that allows for the k_{max} rate to dynamically change based on the concentration of the contaminant (the ED), which was observed by Thornton et al., (2014).

Alternatively, different amendments could be investigated, such as cometabolic enzymes (Hazen, 2018) in addition to a different simulation code which has a more complete in situ biodegradation kinetic model. Cometabolic remediation processes are used for chlorinated solvents; some enzymes can degrade over 100 different organic contaminants (Hazen, 2018). This could be used in a more complete in situ bioremediation simulator in order to enhance in situ biodegradation of contaminants.

In addition, future research could be directed towards using the pump and treat system package in MT3D-USGS may be able to be used out of the box (as opposed to implementing a custom simulation code) in order to simulate recirculating injection and extraction wells, similar to those used by Bagtzoglou and Oates, 2007, and similar to those used in practical field applications (FRTR, 2023). This simulated system of recirculating wells may be able to achieve higher mixing between the ED and EA, and thereby significantly increase biodegradation rates (rED).

The framework was developed with the aim of having the potential to be adapted to different scenarios and therefore needed to be accessible and reproducible without the need of custom simulators and expensive computing or software packages. For this reason, the model was developed using MODFLOW-2005 and MT3D-USGS and using data from abundant previous research on the study site. The final reactive flow and transport model employed

420,000 to 2.2 million cells, depending on discretization. Implementing more wells or utilizing a pumping rate resulted in higher transport steps and therefore resulted in much longer run times and a higher computational demand. This problem could potentially be addressed by using a simulation code which allows multithreading on a Unix cluster. Additionally, the kinetic reaction package in MT3D-USGS could not simulate kinetic reaction parameters that vary in time and space – only constants. This could likely be addressed by using a different simulation code. However, this would be outside the scope of this research as it would compromise the goal to keep the framework accessible and reproducible.

As outlined in the discussion, there is still potential to improve upon the methodology presented in this thesis. If the biodegradation rates could be increased, then the contaminant might be able to be remediated more quickly than 60 years, and it could further reduce the cost of remediation. Regardless, the methodology presented in this thesis might be suitable for further enhancing the biodegradation of BTEX compounds, or other compounds with comparatively fast kinetics and/or low concentrations which are degraded through an aerobic pathway.

References

Adamson, D.T., and C.J. Newell. 2014. Frequently Asked Questions about Monitored Natural Attenuation in Groundwater. ESTCP Project ER-201211. Environmental Security and Technology Certification Program, Arlington, Virginia.

Ahmadi, H., Kilanehei, F. and Nazari-Sharabian, M., 2021. Impact of pumping rate on contaminant transport in Groundwater—A numerical study. *Hydrology*, *8*(3), p.103.

Alvarez, P.J. and Illman, W.A., 2005. Bioremediation and natural attenuation: process fundamentals and mathematical models.

Antelmi, M., Francesca Renoldi, F. and Alberti, L. (2020). Analytical and numerical methods for a preliminary assessment of the remediation time of pump and treat systems. Water 2020, 12(10), 2850; https://doi.org/10.3390/w12102850.

Bagtzoglou, A. C., and Oates. P. M. (2007). Chaotic advection and enhanced groundwater remediation. Journal of Materials in Civil Engineering, 19, 75-83.

Baker, K. Bottrell, S. H., Thornton, S. F., Peel, K. and Spence, M. J. (2012). Effect of contaminant concentration on in-situ bacterial sulphate reduction and methanogenesis in a phenol-contaminated aquifer. Applied Geochemistry, 27, 2010-2018.

Balcke, G.U., Paschke, H., Vogt, C. and Schirmer, M., 2009. Pulsed gas injection: a minimum effort approach for enhanced natural attenuation of chlorobenzene in contaminated groundwater. *Environmental pollution*, *157*(7), pp.2011-2018.

Bau, D.A. and Mayer, A.S., 2006. Stochastic management of pump-and-treat strategies using surrogate functions. *Advances in water resources*, *29*(12), pp.1901-1917.

Baú, D.A. and Mayer, A.S., 2008. Optimal design of pump-and-treat systems under uncertain hydraulic conductivity and plume distribution. *Journal of contaminant hydrology*, *100*(1-2), pp.30-46.

Bauer, R.D., Maloszewski, P., Zhang, Y., Meckenstock, R.U. and Griebler, C., 2008. Mixing-controlled biodegradation in a toluene plume—results from two-dimensional laboratory experiments. *Journal of Contaminant Hydrology*, *96*(1-4), pp.150-168.

Bauer, R. D., Rolle, M., Bauer, S., Eberhardt, C., Grathwohl, P., Kolditz, O., Meckenstock, R. U. and Griebler, C. (2009). Enhanced biodegradation by hydraulic heterogeneities in petroleum hydrocarbon plumes. Journal of Contaminant Hydrology, 105, 56-68.

Bayer, P., Finkel, M. and Teutsch, G. (2004). Combining pump-and-treat and physical barriers for contaminant plume control. Ground Water, 42, 42, 856-867.

Bedekar, V., Morway, E. D., Langevin, C. D. and Tonkin, M. J. (2016). MT3D-USGS version 1: A US Geological Survey release of MT3DMS updated with new and expanded transport capabilities for use with MODFLOW. Techniques and Methods 6-A53.

Blum, P., Sagner, A., Tiehm, A., Martus, P., Wendel, T. and Grathwohl, P. (2011). Importance of heterocylic aromatic compounds in monitored natural attenuation for coal tar contaminated aquifers: A review. Journal of Contaminant Hydrology, 126, 181-194.

Bordeașu, D., Proștean, O., Filip, I., Drăgan, F. and Vașar, C., 2022. Modelling, Simulation and Controlling of a Multi-Pump System with Water Storage Powered by a Fluctuating and Intermittent Power Source. *Mathematics*, *10*(21), p.4019.

Broholm, K., Nilsson, B., Sidle, R.C., Arvin, E. Transport and biodegradation of creosote compounds in clayey till, a field experiment. *J. Contam. Hydrol*. 41 (2000). (3–4), 239–260.

Burnett, R.D. and Frind, E.O., 1987. Simulation of contaminant transport in three dimensions: 1. The alternating direction Galerkin technique. *Water Resources Research*, *23*(4), pp.683-694.

Butler, W.A. and Bartlett, C.L., 1995. Taking advantage of natural biodegradation.

Carey, M.A., Finnamore, J.R., Morrey, M.J. and Marsland, P.A., 2000. Guidance on the assessment and monitoring of natural attentuation of contaminants in groundwater. *R and D Publication-Environment Agency*.

Castro-Alcalá, E., Fernàndez-Garcia, D., Carrera, J. and Bolster, D., 2012. Visualization of mixing processes in a heterogeneous sand box aquifer. *Environmental science & technology*, *46*(6), pp.3228-3235.

Chapelle, F.H., McMahon, P.B., Dubrovsky, N.M., Fujii, R.F., Oaksford, E.T. and Vroblesky, D.A., 1995. Deducing the distribution of terminal electron-accepting processes in hydrologically diverse groundwater systems. *Water Resources Research*, *31*(2), pp.359-371.

Chiogna, G., Eberhardt, C., Grathwohl, P., Cirpka, O.A. and Rolle, M., 2010. Evidence of compound-dependent hydrodynamic and mechanical transverse dispersion by multitracer laboratory experiments. *Environmental science & technology*, *44*(2), pp.688-693.

Christensen, T. H., Bjerg, P. L., Banwart, S. A., Jakobsen, R., Heron, G. and Albrechtsen, H-J. (2000). Characterization of redox conditions in groundwater contaminant plumes: Journal of Contaminant Hydrology Journal of Contaminant Hydrology, 45, 165-241.

Cirpka, O. A., Frind, E. O. and Helmig, R. (1999). Numerical simulation of biodegradation controlled by transverse mixing. Journal of Contaminant Hydrology, 40, 159−182.

Cirpka, O. A., Olsson, A., Ju, Q., Rahman, A. R. and Grathwohl, P. (2006). Determination of transverse dispersion coefficients from reactive plume length. Ground Water, 44, 212–221.

Cohen, R. M., Mercer, J. W., Greenwald, R. M. and Beljin, M. S. (1997). Design guidelines for conventional pump-and-treat systems. Ground Water Issue. EPA/540/S-97/504

CRC CARE (2019). Technology Guide: Groundwater – pump and treat, National Remediation Framework, CRC for Contamination Assessment and Remediation of the Environment, Newcastle, Australia. pp.39.

Culver, T.B. and Shenk, G.W., 1998. Dynamic optimal ground water remediation by granular activated carbon. *Journal of Water Resources Planning and Management*, *124*(1), pp.59-64.

Cunningham, J.A., Hoelen, T.P., Hopkins, G.D., Lebrón, C.A. and Reinhard, M., 2004. Hydraulics of recirculating well pairs for ground water remediation. *Ground Water*, *42*(6), pp.880-889.

Cupola, F., Tandaa, M. G. and Zaninia, A. (2015). Laboratory estimation of dispersivity coefficients. Procedia Environmental Sciences, 25, 74-81.

Devlin, J.F. and Barker, J.F., 1996. Field investigation of nutrient pulse mixing in an in situ biostimulation experiment. *Water Resources Research*, *32*(9), pp.2869-2877.

Eckert, D., Massimo, R. and Cirpka, O. A. (2012). Numerical simulation of isotope fractionation in steady-state bioreactive transport controlled by transverse mixing. Journal of Contaminant Hydrology, 140, 95-106. 10.1016/j.jconhyd.2012.08.010

Eckert, D., Kürzinger, P., Bauer, R., Griebler, C. and Cirpka, O. A. (2015). Fringe-controlled biodegradation under dynamic conditions: Quasi 2-D flow-through experiments and reactive-transport modeling. Journal of Contaminant Hydrology, 172, 100-111.

Elliott, D. R., Scholes, J. D., Thornton, S. F., Rizoulis, A., Banwart, S. A. and Rolfe, S. A. (2010). Dynamic changes in microbial community structure and function in phenol-degrading microcosms from a contaminated aquifer. FEMS Microbial Ecology, 71, 247-259.

Favas, P.J., Pratas, J., Paul, M.S., Sarkar, S.K. and Prasad, M.N.V., 2016. Phytofiltration of metal (loid)-contaminated water: The potential of native aquatic plants. *Phytoremediation: Management of Environmental Contaminants, Volume 3*, pp.305-343.

Freeze, R.A. and Gorelick, S.M., 1999. Convergence of stochastic optimization and decision analysis in the engineering design of aquifer remediation. *Groundwater*, *37*(6), pp.934-954.

FRTR. 2023. “Enhanced Aerobic Remediation” Technology Screening Matrix. n/d. https://www.frtr.gov/matrix/.

FRTR. 2023. “Pump and Treat” Technology Screening Matrix. n/d. https://www.frtr.gov/matrix/.

FRTR. 2023. “Water Treatment Technologies” Technology Screening Matrix. n/d. https://www.frtr.gov/matrix/.

FRTR. 2023. Monitored Natural Attenuation” Technology Screening Matrix. n/d. https://www.frtr.gov/matrix/.

Gelhar, L.W., Welty, C. and Rehfeldt, K.R. (1992). A critical review of data on field-scale dispersion in aquifers. Water Resources Research, 28, 1955-1974.

Greer, K.D., Molson, J.W., Barker, J.F., Thomson, N.R. and Donaldson, C.R., 2010. High-pressure injection of dissolved oxygen for hydrocarbon remediation in a fractured dolostone aquifer. *Journal of contaminant hydrology*, *118*(1-2), pp.13-26.

Gundogdu, A., Duran, C., Senturk, H.B., Soylak, M., Ozdes, D., Serencam, H. and Imamoglu, M., 2012. Adsorption of phenol from aqueous solution on a low-cost activated carbon produced from tea industry waste: equilibrium, kinetic, and thermodynamic study. *Journal of Chemical & Engineering Data*, *57*(10), pp.2733-2743.

Guo, Z. and Brusseau, M.L., 2017. The impact of well-field configuration and permeability heterogeneity on contaminant mass removal and plume persistence. *Journal of hazardous materials*, *333*, pp.109-115.

Guo, Z., Brusseau, M. L. and Fogg, G. E. (2019). Determining the long-term operational performance of pump and treat and the possibility of closure for a large TCE plume. Journal of Hazardous Materials, 365, 796–803. doi: 10.1016/j.jhazmat.2018.11.057.

Hamdaoui, O. and Naffrechoux, E., 2007. Modeling of adsorption isotherms of phenol and chlorophenols onto granular activated carbon: Part I. Two-parameter models and equations allowing determination of thermodynamic parameters. *Journal of hazardous materials*, *147*(1-2), pp.381-394.

Harbaugh, A.W. (2005). MODFLOW-2005, the US Geological Survey modular ground-water model: the ground-water flow process.

Harbaugh, A.W., Langevin, C.D., Hughes, J.D., Niswonger, R.N., and Konikow, L. F., 2017, MODFLOW-2005 version 1.12.00, the U.S. Geological Survey modular groundwater model: U.S. Geological Survey Software Release, 03 February 2017, http://dx.doi.org/10.5066/F7RF5S7G

Hazen, T.C. (2018). Cometabolic Bioremediation. In: Steffan, R. (eds) Consequences of Microbial Interactions with Hydrocarbons, Oils, and Lipids: Biodegradation and Bioremediation. Handbook of Hydrocarbon and Lipid Microbiology. Springer, Cham.

Hedbavna, P., Rolfe, S.A., Huang, W.E. & Thornton, S.F. (2016). Biodegradation of phenolic compounds and their metabolites in contaminated groundwater using microbial fuel cells. *Bioresource Technology*, 200, 426-434.

Hess, A., Zarda, B., Hahn, D., Häner, A.N.D.R.E.A.S., Stax, D., Höhener, P. and Zeyer, J., 1997. In situ analysis of denitrifying toluene-and m-xylene-degrading bacteria in a diesel fuel-contaminated laboratory aquifer column. *Applied and environmental microbiology*, *63*(6), pp.2136-2141.

Huang, W., Lerner, D.N., Smith, C.C. and Thornton, S.F., 2000. 1-Tracer Studies for Modelling Dispersion, Transport, Existing Contamination and Protection Measures-Non-reactive solute dispersion in Triassic sandstone: Laboratory simulation and an application. *IAHS Publications-Series of Proceedings and Reports-Intern Assoc Hydrological Sciences*, *262*, pp.127-134.

Hudak, P.F., 2018. Variable-component, energy-efficient technology for groundwater remediation. *Environmental Practice*, *20*(1), pp.16-22.

Illman, W.A. and Alvarez, P.J., 2009. Performance assessment of bioremediation and natural attenuation. *Critical Reviews in Environmental Science and Technology*, *39*(4), pp.209-270.

Jones, I., Lerner, D. N. and Thornton, S. F. (2002). A modelling feasibility study of hydraulic manipulation: A groundwater restoration concept for reluctant contaminant plumes. In *GQ2001: Natural and Enhanced Restoration of Groundwater Pollution*, Sheffield, U.K., 16-21 June 2001. (eds, Thornton, S.F & Oswald, S.O.), IAHS Publ. No. 275, 525-532.

Kao, C.M., Liao, H.Y., Chien, C.C., Tseng, Y.K., Tang, P., Lin, C.E. and Chen, S.C., 2016. The change of microbial community from chlorinated solvent-contaminated groundwater after biostimulation using the metagenome analysis. *Journal of hazardous materials*, *302*, pp.144-150.

Karunanidhi, D., Subramani, T., Roy, P.D. and Li, H., 2021. Impact of groundwater contamination on human health. *Environmental Geochemistry and Health*, *43*, pp.643-647.

Kent, B. and Mosquera, G.C.B., 2001. Remediation of NAPL-contaminated aquifers: Is the cure worth the cost? *Journal of Environmental Science and Health, Part A*, *36*(8), pp.1559-1569.

Khan, F.I., Husain, T. and Hejazi, R., 2004. An overview and analysis of site remediation technologies. *Journal of environmental management*, *71*(2), pp.95-122.

Krembs, F.J., Siegrist, R.L., Crimi, M.L., Furrer, R.F. and Petri, B.G., 2010. ISCO for groundwater remediation: analysis of field applications and performance. *Groundwater Monitoring & Remediation*, *30*(4), pp.42-53.

Lahvis, M.A., Baehr, A.L. and Baker, R.J., 2004. Evaluation of volatilization as a natural attenuation pathway for MTBE. Groundwater, 42(2), pp.258-267.

Lemming, G., Hauschild, M.Z. and Bjerg, P.L., 2010. Life cycle assessment of soil and groundwater remediation technologies: literature review. *The International Journal of Life Cycle Assessment*, *15*, pp.115-127.

Lerner, D. N., Thornton, S. F., Spence, M. J., Banwart, S. A., Bottrell, S. H., Higgo, J. J., Mallinson, H. E. H., Pickup, R. W. and Williams, G. M. (2000). Ineffective natural attenuation of degradable organic compounds in a phenol-contaminated aquifer. Ground Water, 38, 922-928.

Li, P., Karunanidhi, D., Subramani, T. and Srinivasamoorthy, K., 2021. Sources and consequences of groundwater contamination. *Archives of environmental contamination and toxicology*, *80*, pp.1-10.

Liang, M., Liang, H., Rao, Z. and Xu, D., 2020. Occurrence of polycyclic aromatic hydrocarbons in groundwater from rural areas in eastern China: spatial distribution, source apportionment and health cancer risk assessment. *Chemosphere*, *259*, p.127534.

Lu, G., T.P. Clement, C. Zheng, and T.H. Wiedemeier. "Natural attenuation of BTEX compounds: Model development and field-scale application." *Groundwater* 37, no. 5 (1999): 707-717.

Luciano, Antonella, Giuseppe Mancini, Vincenzo Torretta, and Paolo Viotti. "An empirical model for the evaluation of the dissolution rate from a DNAPL-contaminated area." *Environmental Science and Pollution Research* 25, no. 34 (2018): 33992-34004.

Lyon, D.Y. and Vogel, T.M., 2013. Bioaugmentation for groundwater remediation: an overview. *Bioaugmentation for groundwater remediation*, pp.1-37.

Mackay, D. M. and Cherry, J. A. (1989). Groundwater contamination: pump-and-treat remediation. Environmental Science and Technology, 23, 630–636. https://doi.org/10.1021/es00064a001

Marquis S.A. Jr., and D. Dineen. "Comparison between pump and treat, biorestoration, and biorestoration/pump and treat combined: Lessons from computer modeling." *Groundwater Monitoring & Remediation* 14, no. 2 (1994): 105-119.

Mayer, K. U., Benner, S. G., Frind, E. O. Thornton, S. F. and D. N. Lerner. D. N. (2001). Reactive transport modeling of processes controlling the distribution and natural attenuation of phenolic compounds in a deep sandstone aquifer. Journal of Contaminant Hydrology, 53, 341-368.

Mays, D.C. and Neupauer, R.M., 2012. Plume spreading in groundwater by stretching and folding. *Water Resources Research*, *48*(7).

McCarty, P.L., Goltz, M.N., Hopkins, G.D., Dolan, M.E., Allan, J.P., Kawakami, B.T. and Carrothers, T.J., 1998. Full-scale evaluation of in situ cometabolic degradation of trichloroethylene in groundwater through toluene injection. *Environmental Science & Technology*, *32*(1), pp.88-100.

McDade, J. M., Kulkarni, P.R., Seyedabbasi, M. A., Newell, C. J., Gandhi, D., Gallinatti, J. D., Cocianni, V. and Ferguson, D. J. (2013). Matrix diffusion modeling applied to long-term pump-and-treat Data: 1. Method development. Remediation Journal, 23, 71-91.

McGuire, T.M., Newell, C.J., Looney, B.B., Vangelas, K.M. and Sink, C.H., 2004. Historical analysis of monitored natural attenuation: A survey of 191 chlorinated solvent sites and 45 solvent plumes. *Remediation Journal: The Journal of Environmental Cleanup Costs, Technologies & Techniques*, *15*(1), pp.99-112.

Meckenstock, R. U., Elsner, M., Griebler, G., Lueders, T., Stumpp, C., Aamand, J., Agathos, S. N., Albrechtsen, H-J., Bastiaens, L., Bjerg, P. L., Boon, N., Dejonghe, W., Huang, W. E., Schmidt, S. I., Smolders, E., Sørensen, S. R., Springael, D. and van Breukelen, B. (2015). Biodegradation: Updating the concepts of control for microbial cleanup in contaminated aquifers. Environmental Science and Technology, 49, 7073−7081. http://dx.doi.org/10.1021/acs.est.5b00715.

Morgan, P. and Watkinson, R.J., 1992. Factors limiting the supply and efficiency of nutrient and oxygen supplements for the in situ biotreatment of contaminated soil and groundwater. *Water Research*, *26*(1), pp.73-78.

Mujica-Alarcon, J. F., Thornton, S. F. and Rolfe, S. A. (2021). Long-term dynamic changes in attached and planktonic microbial communities in a contaminated aquifer. Environmental Pollution, 277, 116765, https://doi.org/10.1016/j.envpol.2021.116765

National Research Council (2013). Alternatives for managing the nation's complex contaminated groundwater sites. The National Academies Press, pp.408.

National Research Council, 2000. *Natural attenuation for groundwater remediation*.

NAVFAC. 2003. Groundwater Pump and Treat Systems. NFESC Special Publication SP-2429-ENV, Feb. 2003.

NAVFAC (2018). Advances in the state of practice for enhanced in situ bioremediation. TR-NAVFAC EXWC-EV-1806. February.

Neupauer, R.M., Meiss, J.D. and Mays, D.C., 2014. Chaotic advection and reaction during engineered injection and extraction in heterogeneous porous media. *Water Resources Research*, *50*(2), pp.1433-1447.

Neupauer, R. M., Sather, L. J., Mays, D. C., Crimaldi, J. P. and Roth, E. J. (2020). Contributions of pore-scale mixing and mechanical dispersion to reaction during active spreading by radial groundwater flow. Water Resources Research, 56, e2019WR026276. doi.org/10.1029/2019WR026276.

O'Connor, D., Hou, D., Ok, Y.S., Song, Y., Sarmah, A.K., Li, X. and Tack, F.M., 2018. Sustainable in situ remediation of recalcitrant organic pollutants in groundwater with controlled release materials: A review. *Journal of Controlled Release*, *283*, pp.200-213.

Park, D.K., Ko, N.Y. and Lee, K.K., 2007. Optimal groundwater remediation design considering effects of natural attenuation processes: pumping strategy with enhanced-natural-attenuation. *Geosciences Journal*, *11*, pp.377-385.

Pickup, R. W., Rhodes, G., Alamillo, M. L., Mallinson, H. E. H., Thornton, S. F. and Lerner, D. N. (2001). Microbiological analysis of multilevel borehole samples from a contaminated groundwater system Journal of Contaminant Hydrology, 53, 269-284.

Piscopo, A.N., Neupauer, R.M. and Mays, D.C., 2011. Contrasting advective spreading and dispersive mixing. In *World environmental and water resources congress 2011: Bearing knowledge for sustainability* (pp. 954-961).

Piscopo, A. N., Neupauer, R. M. and Mays, D. C. (2013). Engineered injection and extraction to enhance reaction for improved in situ remediation. Water Resources Research, 49, 3618-3625.

R. L. Satkin and P. B. Bedient. 1988. Effectiveness of various aquifer restoration schemes under variable hydrogeologic conditions. *Groundwater* 26:488–498.

Rahman, M.A., Jose, S.C., Nowak, W. and Cirpka, O.A., 2005. Experiments on vertical transverse mixing in a large-scale heterogeneous model aquifer. *Journal of contaminant hydrology*, *80*(3-4), pp.130-148.

Rawe, J., Hodge, V., Acheson, C.M., Lutes, C. and Liles, D., 2006. In situ and ex situ biodegradation technologies for remediation of contaminated sites [engineering issue.

Reising, L. J. (2018). Effects of active and passive spreading on mixing and reaction during groundwater remediation by engineered injection and extraction. PhD thesis. University of Colorado, pp. 119.

Rivett, M.O. and Thornton, S.F., 2008, December. Monitored natural attenuation of organic contaminants in groundwater: principles and application. In *Proceedings of the Institution of Civil Engineers-Water Management* (Vol. 161, No. 6, pp. 381-392). Thomas Telford Ltd.

Rizoulis, A., Elliott, D. R., Rolfe, S. A., Thornton, S. F., Banwart, S. A., Pickup, R. W. and Scholes, J. S. (2013). Diversity of planktonic and attached bacterial communities in a phenol-contaminated sandstone aquifer. Microbial Ecology, 66, 84-95.

Rolle, M., Clement, T. P., Sethi, R. and Di Molfetta, A. (2008). A kinetic approach for simulating redox-controlled fringe and core biodegradation processes in groundwater: model development and application to a landfill site in Piedmont, Italy. Hydrological Processes, 22, 4905-4921. 10.1002/hyp.7113.

Sather, L. J., Neupauer, R. M., Mays, D. C., Crimaldi, J. P. and Roth, E. J. (2022). Active spreading: Hydraulics for enhancing groundwater remediation. Journal of Hydrologic Engineering, 27, p.04022007.

Sather, L. J., Roth, E. J., Neupauer, R. M., Crimaldi, J. P. and Mays, D. C. (2023). Experiments and simulations on plume spreading by engineered injection and extraction in refractive index matched porous media. Water Resources Research, 59, p.e2022WR032943.

Scow, K.M. and Hicks, K.A., 2005. Natural attenuation and enhanced bioremediation of organic contaminants in groundwater. *Current Opinion in Biotechnology*, *16*(3), pp.246-253.

Speight, J. G. (2020). Natural water remediation. Butterworth-Heinemann, Elsevier, pp.394.

Spence, M. J., Bottrell, S., Thornton, S. F. and Lerner, D. N. (2001) Isotopic modelling of the significance of sulphate reduction for phenol attenuation in a polluted aquifer Journal of Contaminant Hydrology, 53, 285-304.

Spence, M. J., Bottrell, S. H., Thornton, S. F., Richnow, H. and Spence, K. H. (2005). Hydrochemical and isotopic effects associated with fuel biodegradation pathways in a chalk aquifer. J. of Contaminant Hydrology, 79, 67-88.

Suk, H. Chen, J-S., Park, E. Han, W. S. and Kihm, Y. H. (2021). Numerical evaluation of the performance of injection/extraction well pair operation strategies with temporally variable injection/pumping rates. Journal of Hydrology, 598, 126494. https://doi.org/10.1016/j.jhydrol.2021.126494

Suthersan, S., Killenbeck, E., Potter, S., Divine, C. and LeFrancois, M. (2015). Resurgence of pump and treat solutions: Directed groundwater recirculation. Groundwater Monitoring and Remediation, 35, 2, 23-29.

Thornton, S. F., Baker, K. M., Bottrell, S. H., Rolfe, S. A., McNamee, P., Forrest, F., Duffield, P., Wilson, R. D., Fairburn, A. W. and Cieslak, L. A. (2014). Enhancement of *in situ* biodegradation of organic compounds in groundwater by targeted pump and treat intervention. Applied geochemistry, 48, 28-40.

Thornton, S. F., Quigley, S., Spence, M. J., Banwart, S. A., Bottrell, S. and Lerner, D. N. (2001a). Processes controlling the distribution and natural attenuation of dissolved phenolic compounds in a deep sandstone aquifer. Journal of Contaminant Hydrology, 53, 233-267.

Thornton, S. F., Lerner, D. N., and Banwart. S. A. (2001b). Assessing the natural attenuation of organic contaminants in aquifers using plume-scale electron and carbon balances: model development with analysis of uncertainty and parameter sensitivity. Journal of Contaminant Hydrology, 53, 199-232.

Thornton, S. F., Bottrell, S. H., Spence, K. S., Pickup, R., Spence, M. J., Shah, N., Mallinson, H. E. H. M. and Richnow, H. H. (2011). Assessment of MTBE biodegradation in contaminated groundwater using ^{13}C and ^{14}C analysis: Field and laboratory microcosm studies. Applied Geochemistry, 26, 828-837.

Thornton, S.F., Baker, K.M., Bottrell, S.H., Rolfe, S.A., McNamee, P., Forrest, F., Duffield, P., Wilson, R.D., Fairburn, A.W. and Cieslak, L.A., (2014). Enhancement of in situ biodegradation of organic compounds in groundwater by targeted pump and treat intervention. *Applied geochemistry*, *48*, pp.28-40.

Truex, M., Johnson, C., Macbeth, T., Becker, D., Lynch, K., Giaudrone, D., Frantz, A. and Lee, H. (2017). Performance assessment of pump-and-treat systems. Groundwater Monitoring and Remediation, 37, 3, 28-44.

Tuxen, N., Albrechtsen, H.-J., Bjerg, P. L. (2006). Identification of a reactive fringe zone at a landfill leachate plume fringe using high-resolution sampling and incubation techniques. J. Contam. Hydrol. 85, 179–194.

USDoD, 1998. Evaluation of DoD waste site groundwater pump-and-treat operations. Report No. 98-090. U.S. Department of Defense. pp. 68.

US DoD, 2008. ESTCP Cost and Performance Report. US Department of Defense. Publication # DoD ER-0436, Washington, DC.

US EPA, 1997. Design Guidelines for Conventional Pump and Treat Systems. US Environmental Protection Agency. Publication # EPA/540/S-97/504, Washington, DC.

US EPA, 2001a. Cost Analyses for Selected Groundwater Cleanup Projects: Pump and Treat Systems and Permeable Reactive Barriers. US Environmental Protection Agency. Publication # EPA 542-R-00-013, Washington, DC.

US EPA, 2001b. Groundwater Pump and Treat Systems: Summary of Selected Cost and Performance Information at Superfund-financed Sites. US Environmental Protection Agency. Publication # EPA 542-R-01-021b, Washington, DC.

US EPA, 2001c. Remediation Technology Cost Compendium – Year 2000. US Environmental Protection Agency. Publication # EPA-542-R-01-009, Washington, DC.

US EPA, 2004a. Technologies for Treating MtBE and Other Fuel Oxygenates. US Environmental Protection Agency. Publication # EPA 542-R-04-009, Washington, DC.

US EPA, 2004b. Cleaning Up the Nation's Waste Sites: Markets and Technology Trends. US Environmental Protection Agency. Publication # EPA 542-R-04-015, Washington, DC.

US EPA, 2005. Cost-Effective Design of Pump and Treat Systems. US Environmental Protection Agency. Publication # EPA 542-R-05-008, Washington, DC.

US EPA, 2006. In Situ and Ex Situ Biodegradation Technologies for Remediation of Contaminated Sites. US Environmental Protection Agency. Publication # EPA/625/R-06/015, Washington, DC.

US EPA, 2007. Treatment Technologies for Site Cleanup: Annual Status Report. US Environmental Protection Agency. Publication # EPA-542-R-07-012, Washington, DC.

US EPA, 2013. Superfund Remedy Report, 14th Edition. US Environmental Protection Agency. Publication # EPA 542-R-13-016, Washington, DC.

USEPA (1990). Basics of pump-and-treat ground-water remediation technology. EPA/600/8-90/003, pp.66.

USEPA (1996). Pump-and-treat ground-water remediation: A guide for decision makers and practitioners. EPA/625/R-95/005, pp. 91.

USEPA (1997). Design guidelines for conventional pump-and-treat systems. EPA/540/S-97/504.

USEPA (2021). Green remediation best management practices: Pump and treat systems. Office of Land and Emergency Management, EPA 542-F-21-029., pp 6.

Watson, I. A., Oswald, S.E., Banwart, S.A., Crouch, R.S. and Thornton, S.F. (2005). Modeling the dynamics of fermentation and respiratory processes in a groundwater plume of phenolic contaminants interpreted from laboratory-to field-scale. Environmental Science and Technology 39, 8829-8839.

Werth, C. J., Cirpka, O. A. and Grathwohl, P. (2006). Enhanced mixing and reaction through flow focusing in heterogeneous porous media. Water Resources Research, 42, https://doi.org/10.1029/2005WR004511.

Wiedemeier, T.H., Wilson, J.T., Kampbell, D.H., Miller, R.N. and Hansen, J.E., 1995. Technical Protocol for Implementing Intrinsic Remediation with Long-Term Monitoring for Natural Attenuation of Fuel Contamination Dissolved in Groundwater. Volume II.

Wiedemeier, T. H., Rifai, H. S., C. Newell, C.J., and Wilson. J.T. (1999). Natural attenuation of fuels and chlorinated solvents in the subsurface. John Wiley & Sons

Williams, G. M., Pickup, R. W., Thornton, S. F., Lerner, D. N., Mallinson, H. E. H., Moore, Y. and White, C. (2001). Biogeochemical characterisation of a coal-tar distillate plume J. of Contaminant Hydrology, 53, 175-198.

Wu, Y., Lerner, D. N., Banwart, S. A., Thornton, S. F. and Pickup, R. W. (2006). Persistence of fermentative process to phenolic toxicity in ground water. J. Environmental Quality, 35, 2021-2025.

Xie, B., Qin, J., Wang, S., Li, X., Sun, H. and Chen, W., 2020. Adsorption of phenol on commercial activated carbons: modelling and interpretation. *International Journal of Environmental Research and Public Health*, *17*(3), p.789.

Xu, M. and Eckstein, Y. (1995). Use of weighted least-squares method in evaluation of the relationship between dispersivity and field scale. Groundwater, 33, 905-908.

Xu, T., Ye, Y., Zhang, Y. and Xie, Y. (2018). Recent advances in experimental studies of steady-state dilution and reactive mixing in saturated porous media. Water, 11(1), 3 https://doi.org/10.3390/w11010003.

Ye, Y., Chiogna, G., Cirpka, O. A., Grathwohl, P. and Rolle, M. (2015). Enhancement of plume dilution in two-dimensional and three-dimensional porous media by flow focusing in high-permeability inclusions. Water Resources Research, 51, doi:10.1002/2015WR016962.

Ye, Y., Zhang, Y., Lu, C., Xie, Y. and Luo, J. (2021). Effective chemical delivery through multi-screen wells to enhance mixing and reaction of solute plumes in porous media. Water Resources Research, 57, e2020WR028551. doi.org/10.1029/2020WR028551.

Zhang, P., DeVries, S.L., Dathe, A. and Bagtzoglou, A.C., 2009. Enhanced mixing and plume containment in porous media under time-dependent oscillatory flow. *Environmental science & technology*, *43*(16), pp.6283-6288.

Zheng, Chunmiao, and Wang, P. Patrick. (1999). "MT3DMS: A modular three-dimensional multispecies transport model for simulation of advection, dispersion, and chemical reactions of contaminants in groundwater systems; documentation and user's guide," Contract Report SERDP-99-1, U.S. Army Engineer Research and Development Center, Vicksburg, MS.